PB 277 944

REPORT NO.
UCB/EERC-77/23
AUGUST 1977

EARTHQUAKE ENGINEERING RESEARCH CENTER

EARTHQUAKE SIMULATION TESTS OF A NINE STORY STEEL FRAME WITH COLUMNS ALLOWED TO UPLIFT

by

ARTHUR A. HUCKELBRIDGE

Report to Sponsors:
American Iron and Steel Institute
National Science Foundation

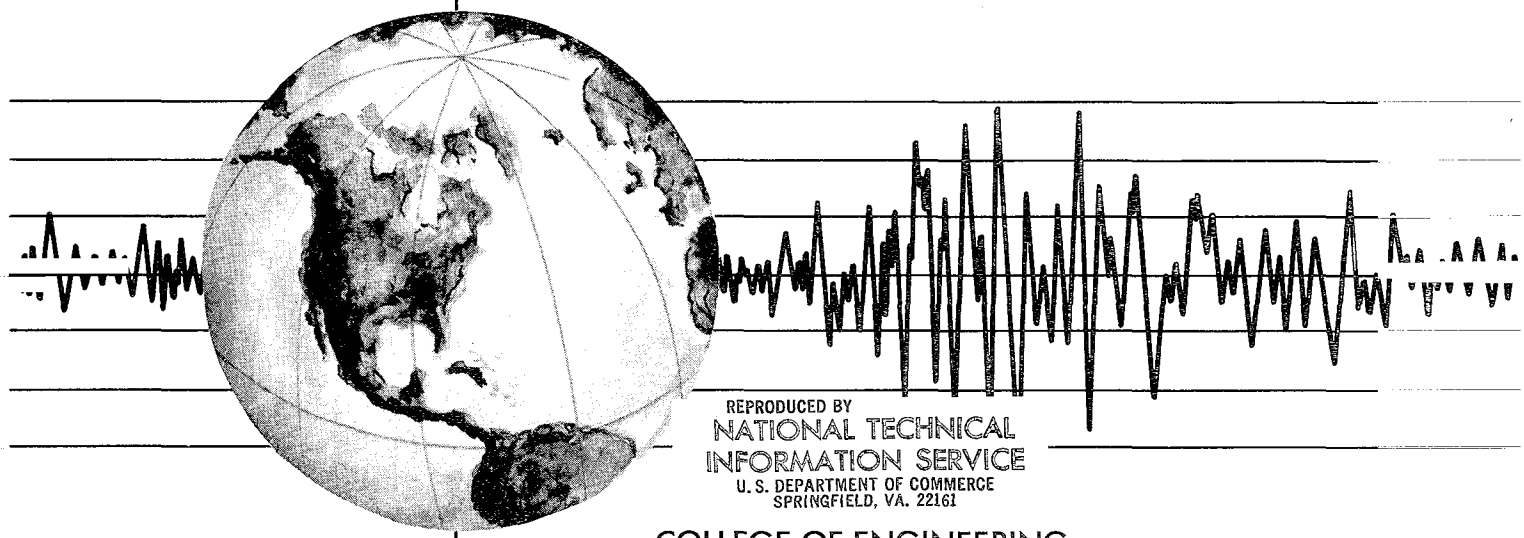

COLLEGE OF ENGINEERING

UNIVERSITY OF CALIFORNIA · Berkeley, California

EARTHQUAKE SIMULATION TESTS OF A NINE STORY STEEL FRAME WITH COLUMNS ALLOWED TO UPLIFT

by

Arthur A. Huckelbridge Jr.

Report to

American Iron and Steel Institute

and

National Science Foundation

UCB/EERC-77/23
Earthquake Engineering Research Center
College of Engineering
University of California
Berkeley, California

August 1977

ABSTRACT

The computed lateral loading imposed on a structure during a major earthquake will often produce an overturning moment in excess of the dead-weight overturning resistance of the system. Assuming that no supplementary anchorage capacity is provided, this condition implies a transient uplift of the structure from its foundation. Linear structural dynamic analysis techniques are not capable of treating this type of highly nonlinear response.

This thesis presents experimental and analytical response data for a model nine-story building frame under seismic excitation, both with and without supplementary anchorage of the columns provided. The experimental work was carried out on the shaking table of the U. C. Berkeley Earthquake Simulator Laboratory. Appreciable amounts of column uplift were observed in the tests for which column uplift was permitted, with significant reductions in the lateral loading, when compared to the fixed base response.

An analytical technique employing bilinear foundation support elements with zero tensile capacity and stiffness in the upward direction is shown to predict the uplifting response with excellent accuracy. Analytical predictions of the nonlinear fixed base response, employing concentrated bilinear plastic hinges are also shown to be very accurate for the levels of nonlinearity encountered.

From the results of this study, it appears that intentionally designing uplifting capability into prototype structures in regions of high seismicity would be both rational and economical. The lateral loading and/or ductility requirements under severe seismic excitation could be significantly lowered, resulting in potential cost savings for

the superstructure system. In addition, there is a potential cost saving in the substructure system through eliminating the necessity of providing tensile capacity to resist high overturning moments.

ACKNOWLEDGEMENTS

The research described in this report was supported by the American Iron and Steel Institute Project 177, and a National Science Foundation Grant, ENV76-04262; both sources of support are gratefully acknowledged. The author is also grateful for the financial support received under the educational benefits program of the Veterans Administration, which made the pursuit of a graduate degree a possibility.

The author would like to thank Professor Graham Powell and his students for developing a very usable nonlinear program, DRAIN-2D, utilized extensively in the analytical portion of this research. The University of California, Berkeley, Earthquake Engineering Research Center and the Computer Center of the Berkeley campus provided excellent facilities for carrying out this research program.

A special acknowledgement is due Professor Ray W. Clough for his guidance throughout the work described in this report, but especially for having the kind of faith in his students that allows a great deal of independent thought and development. The author would also like to thank Professor Graham Powell and Professor Bruce Bolt for their careful review of the manuscript of this thesis.

The many daily details of experimental work, sometimes tedious but always essential, could not have been carried out with the assistance of many individuals in the Earthquake Simulator Laboratory and elsewhere. Particular credit is due Mr. David Steere, whose meticulous efforts in instrument calibration and operation of the shaking table itself made a successful test program possible.

The manuscript of this report was expertly typed by Ms. Renée Dayce

and Ms. Shirley Edwards; numerous figures were prepared by Mr. Larry Bell.

Lastly, but most sincerely, the author would like to acknowledge the loyalty, encouragement, and endurance of his wife, Bev, and their sons, Brett and Craig. Their support gave this research program a purpose and meaning beyond its mere academic value.

This report is essentially the same as the thesis submitted to the Graduate Division of the University of California, Berkeley, in partial satisfaction of the requirements for the degree of Doctor of Engineering.

TABLE OF CONTENTS

1. INTRODUCTION

1.A. The Overturning Effect in Seismic Response

A structure subjected to an earthquake develops lateral forces resulting from its own inertia resisting the accelerations applied to its foundation. The product of each of these lateral forces by its respective lever arm produces an overturning moment at the base of the structure. Complications arise in the analysis of the structure when this computed overturning moment exceeds the assumed capacity of the structural system.

The traditional building code approach to the seismic resistive design of structures is characterized by the use of an equivalent static lateral load. The overturning effect of this equivalent load is intended to be resisted entirely by the dead weight of the structure and/or supplementary anchorage. In the past, relatively small lateral loads were specified as the design loading condition, and overturning was rarely a major consideration.

Since the structural failures associated with the 1971 San Fernando earthquake, however, there has been a trend among building code committees toward a more conservative seismic resistive design philosophy. Dynamic analyses, based on linear elastic structural theory, or static analyses using higher lateral load coefficients, are now required for many structures. Either of these analytical methods results in a greater computed overturning effect, and may lead to the necessity of incorporating expensive anchorage systems into the foundation designs of some structures.

As an example of this situation, consider the requirements of

Article 23, Title 17 of the State of California Administrative Code, which governs the safety of construction of hospitals. The equivalent static analysis provisions of this code lead to a computed base shear as high as 1/4 of the total weight of the structure. Assuming a dynamic first mode shape linearly increasing with height, the magnitude of base shear results in a supplementary anchorage requirement for any structure with a height to width ratio greater than 3.

A base shear equal to 1/4 the weight of the system, is not an unrealistically high value. Assuming the same mode shape mentioned above, this corresponds to an elastic pseudoacceleration response value of 1/3 g. For a damping ratio of 10%, the 1940 N-S El Centro ground motion, for example, gives an elastic pseudoacceleration response level greater than 1/3 g for all structures with a period less than 1 second, and an elastic pseudoacceleration response level around 2/3 g for structures with a period less than 0.5 seconds.

Although somewhat simplified, this discussion points out that the overturning effect is a legitimate concern of the structural designer. In order to be effectively treated it needs to be rationally considered, not ignored. A rational treatment, however, does not imply blindly following code provisions when more effective solutions are available.

1.B. Implications of Allowing Column Uplift

When the dynamic behavior of a structural system is taken into account, it is obvious that a computed dynamic overturning moment in excess of the capacity of the system does not imply imminent toppling or collapse of the structure. Rather, there will occur some type of transient uplifting of the "tension" columns from the foundation,

providing a type of structural fuse limiting the resisting overturning moment.

The dynamic response of an uplifting system is highly nonlinear in nature, however, with drastic stiffness changes occurring at instants when column bases separate from, or return to, the foundation. Moreover, these changes in stiffness occur at instants of relatively high velocity, resulting in potential analytical complications due to impact phenomena. Thus the analysis of this uplifting behavior requires more sophisticated treatment than the standard linear dynamic, or equivalent static analysis.

Preliminary experimental and analytical studies on a single bay three-story structure at the University of California Earthquake Simulator showed very promising results for this simple uplifting system (2). Lateral loads imposed on the system were considerably reduced by allowing column uplift to occur, and analytical results correlated well with the experimental data. Analytical studies by Beck and Skinner (1) and Meek (5) have shown similar promising results.

1.C. Objectives and Scope of the Thesis

As a consequence of the results mentioned above, it was decided that an experimental and analytical program extending the research to the behavior of a more complex structural system should be carried out. The objectives of this study were

(1) Observe experimentally the uplifting behavior of this more complex system, and extrapolate the performance to that which might be expected of a realistic prototype system.

(2) Compare this uplifting behavior to the more conventional fixed-base behavior resulting from similar ground motion excitation.

(3) Evaluate current nonlinear analytical techniques for predicting the uplifting behavior of a complex structural system.

(4) Evaluate current nonlinear analytical techniques for predicting the behavior of a complex fixed-base structural sytem subjected to intense ground motion.

(5) Evaluate the desirability and feasibility of including uplifting capability into the design of prototype structural systems.

This study encompassed the design of a suitable test structure, its instrumentation and testing, reduction of test data, and correlation of analytical results to that test data. Due to limitations of the test facility and in the interest of economy in analytical work, the study was intended to be 2-dimensional in nature. It was felt, however, that such a study would be adequate to meet the stated objectives.

This report presents the results of the study from the design of the model through the final analytical correlation. Conclusions are drawn concerning all the stated objectives.

2. TEST FACILITY

2.A. Earthquake Simulator

The experimental portion of this investigation was carried out at the Earthquake Simulator Laboratory, located on the Richmond Field Station of the University of California, Berkeley. The main dynamic test facility is a 20' x 20' shaking table with its associated control equipment, described by Rea and Penzien (7). The shaking table and control room are shown in Fig. 2.A.1.

Basically the table is a 20' x 20' x 1', essentially rigid, prestressed concrete slab. It is independently driven vertically and in one direction horizontally by servo-controlled actuators. The 100^{k} dead weight of the table, plus the payload it carries, is supported by differential air pressure during operation, thus relieving the vertical actuators of any static load-carrying function.

The control signals for the two degrees of freedom are in the form of analog displacement time histories on magnetic tape, obtained normally through a double integration of acceleration time histories. The repeatability of table motion has been demonstrated to be quite good.

The limits of table motion for a zero payload condition are shown in Fig. 2.A.2. The displacement limits result from the actuator strokes; the velocity limits result from oil pumping capacity; the acceleration limits result from actuator force capacities and the oil column resonance of the drive system. With a payload on the table, the acceleration limits will be somewhat lower; the other limits are not appreciably affected.

2.B. Data Acquisition

The data acquisition system, centered on a NOVA 1200 minicomputer equipped with a Diablo 31 magnetic disk unit, is capable of discretely sampling up to 128 data channels at rates up to 100 samples/sec/channel. Transducer signals, in analog form, pass through a NEFF system 620 Analog-Digital processor. The digitized data are then temporarily stored on the magnetic disk before being transferred to tape by a Wang 9 track magnetic tape drive for permanent storage.

Limited data reduction can be carried out on the minicomputer, but the bulk of detailed data reduction is carried out on the Berkeley campus CDC 6400 computer system. In order to be compatible with the CDC system, a conversion to 7 track magnetic tape form must be performed on the data. Once reduced to a desired form, the data are generally converted to a graphical display utilizing a Calcomp plotting system on the Berkeley campus.

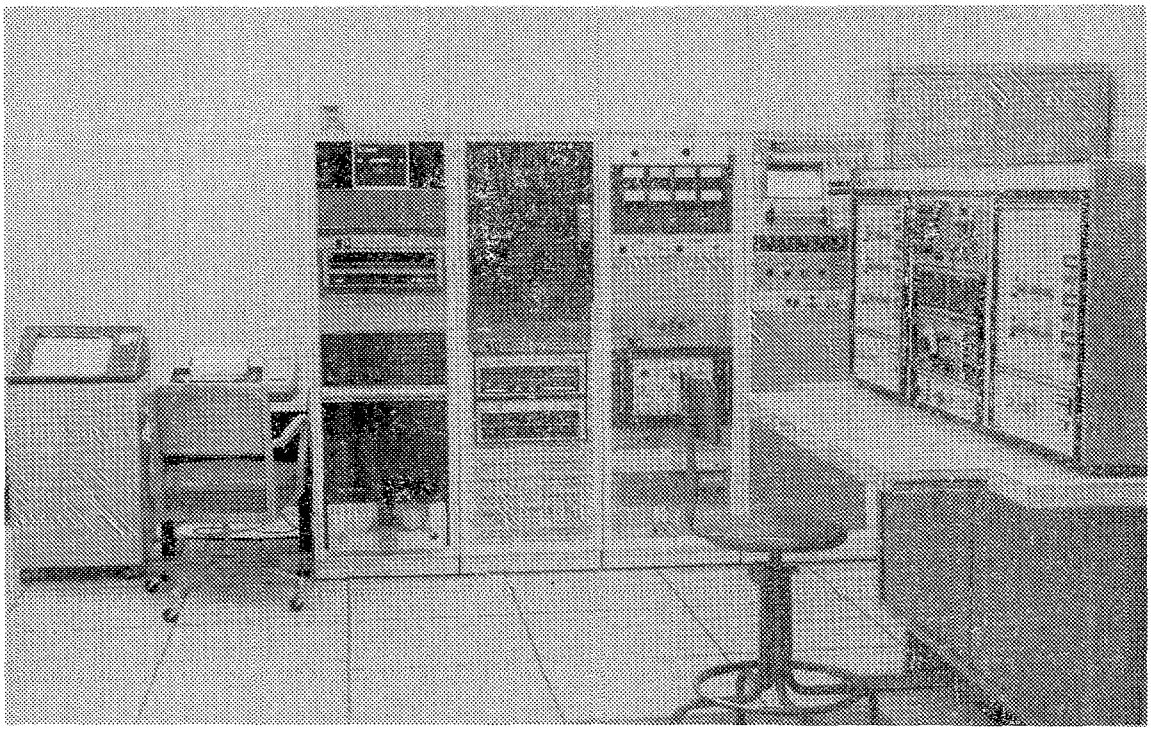

a. Control Room

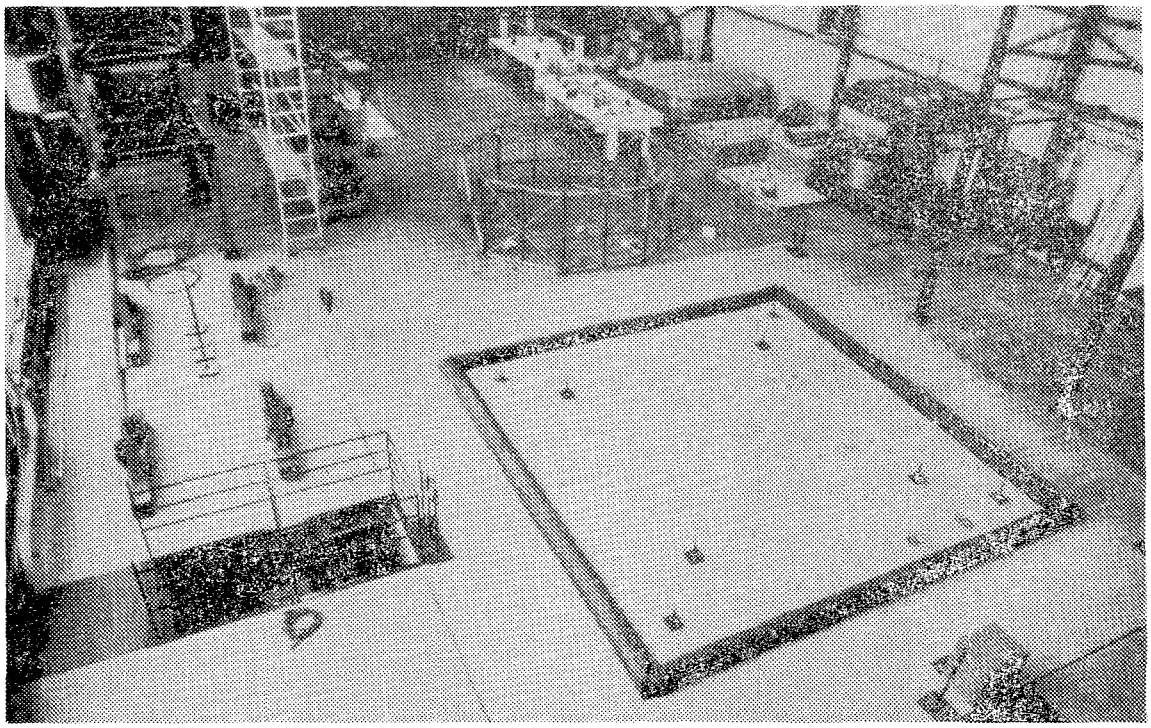

b. Shaking Table

Fig. 2.A.1 Test Facility

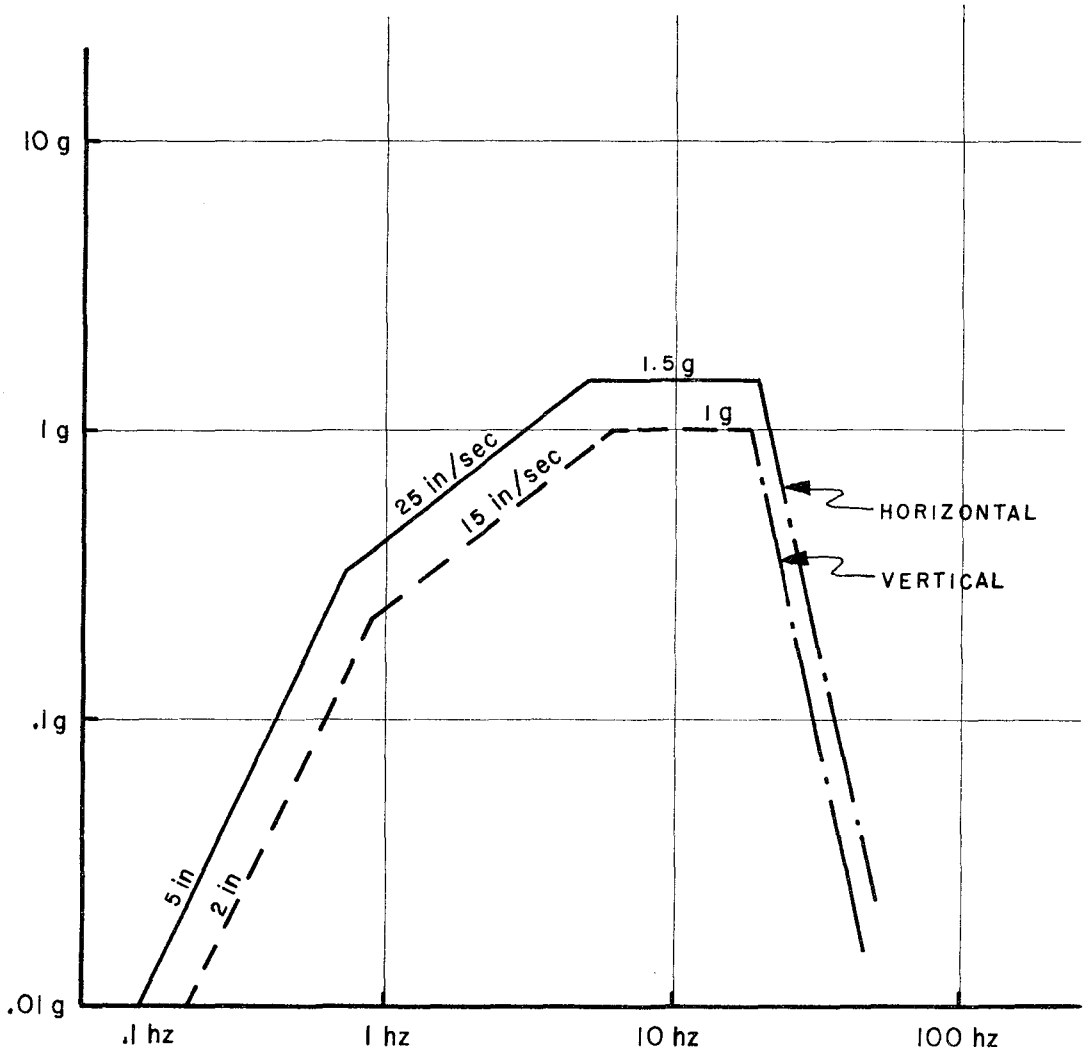

Fig. 2.A.2 Shaking Table Motion Limits

3. THE TEST STRUCTURE

3.A. Design Criteria

As a means of meeting the stated objectives, it was decided that the experimental investigation should consider the seismic response of a multiple-bay, multi-story steel moment frame allowed to uplift. It was intended the study should represent the behavior of a realistic prototype structure, but not that a reduced scale study of any particular prototype should be undertaken.

The physical size and capacity of the shaking table were the primary design constraints encountered. These limits were a 20' x 20' plan dimension, a 31' - 10" vertical clearance to the overhead crane bridge, a 10-ton lifting capacity for the crane itself, and a payload limit of approximately 100^{k} for the shaking table. In addition, actuator capacities limited the structural response to roughly 100^{k} base shear and 1700 k-ft overturning moment.

3.B. Preliminary Design

The first design decision was to fit 3 bays onto the 20' table length. This decision fixed the prototype/model scale ratio to a value around 3 for realistic bay widths. The overhead clearance, combined with a reasonable model story height, then limited the vertical layout to 9 floors of approximately 3' each. Since the study was intended to be 2-dimensional in nature, the lateral dimension was rather arbitrarily chosen as 6' to give adequate stability and to match lines of tie-down points on the table. This dimension did correspond roughly, however, to the appropriate bay dimensions of reasonable prototype designs.

The next major decision was to fabricate the frame from readily available rolled A36 wide flange sections. The smallest reasonable sections available were W4 x 13 and W6 x 8.5 for the columns and girders, respectively.

The design payload limit of 100^{k} for the table indicated a maximum floor weight of about 11^{k}. For an 18' x 6' floor plan, this value indicated a total unit floor load of slightly over 100 psf for both model and prototype, which did not seem unreasonable.

The first trial design examined was that shown in Fig. 3.B.1. The in-plane floor bracing at each level was sufficient to produce an essentially rigid diaphragm behavior. The eccentric K-bracing in the lateral direction, provided only in the end panels, provided lateral and torsional stiffness. It was considered that eventually the frame would be tested in the lateral direction also, and this bracing configuration was chosen with such a test program in mind. The weights of 4^{k} and 2^{k} to be provided in the exterior and interior bays, respectively, were selected to make maximum usage of existing 4^{k} concrete weights in the simulator laboratory. The outer bay weights were shifted inward, however, so as to produce static column axial loads equivalent to a uniform weight distribution on each floor.

Uplift Behavior

From previous experience with the earthquake simulator facility, it was realized from the onset that there would be a considerable amount of structure-table interaction, particularly in the pitching mode. This phenomenon was accounted for analytically by including the shaking table compliance in the mathematical model as a spring-mass foundation system with rotational and vertical degrees of freedom, as

shown in Fig. 3.B.2.

The static moment distribution on the frame is shown in Fig. 3.B.3. The concrete block weights were all point supported on the girders. As can be seen, the static moments were very low; even the largest static moments were less than 10% of the plastic moments of the sections.

An insight into the structural behavior of the frame can be gained by examining its pseudostatic 1st mode behavior. If a monotonically increasing load pattern is applied, corresponding to the nearly triangular 1st mode shape, a plot of base shear vs 9th floor displacement can be constructed analytically as shown in Fig. 3.B.4.

In the first portion of the load curve, up to a base shear around 24^k, all four columns of each frame are in contact with the foundation; the 1st mode period in this range is around .50 sec. In the upper portion of this range there is a transition to the next range of behavior, that in which one column has uplifted. This transition is not particularly sharp because, as the axial force in the 1st column approaches zero, its moment restraint is gradually lost.

In the 2nd portion of the load curve, up to around 40^k base shear, one column has uplifted and the 1st mode period has increased to about .59 sec. Near the upper portion of this range there is again a transition to the next range, in which two columns have separated from the foundation. Again the transition is gradual because of the loss of moment restraint.

In the 3rd portion of the load curve, up to slightly under 50^k base shear, 2 columns have uplifted, and the 1st mode period has increased to about .78 sec. At about the same time that the 3rd column uplifts, however, the 4th column reaches its moment capacity at its

base, and there is a transition to nearly rigid body rotation about the plastic hinge at that column base. The period for rigid body rotation is, of course, infinite; strain hardening would actually preclude true rigid body rotation, however, until very large displacements were reached.

For reasonable displacement amplitudes, the unloading curve, neglecting the relatively small amount of energy dissipation which might occur in the 4th column plastic hinge, would essentially retrace the loading curve, i.e., a nonlinear pseudoelastic system.

For the linear behavior preceding any uplift response, the first 6 calculated mode shapes and periods are shown in Fig. 3.B.5. The 1st mode period is, understandably, very sensitive to the shaking table compliance; a rigid support condition would lower this period by about 20%. The higher modes were not nearly so sensitive, however, to the pitching compliance.

One nonlinear dynamic analysis was performed on the preliminary design in order to estimate the amount of uplift that might conceivably occur. The excitation used was a previously recorded test accelerogram based on the 1940 El Centro ground motion. The signal was amplified in intensity to produce a peak acceleration of .67 g, and was time scaled (speeded up) by a factor of 1.732 to account for the reduced scale of the model.

The uplift motions resulting from this preliminary analysis are shown in Fig. 3.B.6. As shown, the amplitude of uplift motion predicted was slightly less than 1/2", with a number of cycles occurring. All moments predicted were less than the section plastic moments, and the base shear and overturning were well within the capacity of the

shaking table.

Based on this predicted behavior, column base "mechanism" to permit uplift, shown in Fig. 3.B.7, was conceived and designed. The 1/4" flexure plate provides a shear connection to prevent the column from "walking" off the foundation, but readily accommodates relatively large uplift motions with very little restraint. The impact pads serve their nominal purpose, and also provide a column moment restraint so long as to the column foot is in full contact with the pads. The pads themselves were fabricated from 1/2" thick, 50 durometer hardness neoprene, bonded to 1/4" steel plates on both the top and bottom surfaces.

Fixed Base Behavior

It was planned that tests on the frame would be conducted also in the conventional fixed base support condition. Physically, the change was to be accomplished by removing the impact pads and bolting the baseplates solidly to the foundation.

A linear static first mode response spectrum analysis was therefore carried out for this fixed base condition, using the same ground motion mentioned previously. The resulting seismic moment distribution is shown in Fig. 3.B.8. These moments were greater than the section plastic moments of the interior girders up through the 6th floor; in the 1st floor the computed moments are about twice the section plastic moments of both the columns and girders.

From this linear analysis, it would seem that some nonlinear material behavior could be expected in the fixed base condition. One factor which might limit the extent of nonlinear response for the fixed base case, however, was the overturning capacity of the shaking table. The loading case considered produced an overturning moment

greater than the specified table limit of 1700 k-ft. The anticipated nonlinear behavior of the frame would reduce the overturning response, however, from the value predicted by the linear analysis.

In order to develop the anticipated moments, it was necessary to reinforce the joint panel zones of the structure. This was accomplished by welding doubler plates on the exterior panel zone faces, as indicated in Fig. 3.B.9.

3.C. Final Design

From the preliminary design analyses, it appeared that the model would perform satisfactorily in dynamic testing. Detail fabrication drawings were prepared and fabrication was carried out in the Richmond Field Station machine shop. Specific construction details are shown in Figs. 3.C.1 and 3.C.2. Final assembly of the model was performed on the Earthquake Simulator Laboratory floor area and a coat of rust-preventative primer was applied to the structure. Coupon test results from the steel sections used in the fabrication are shown in Appendix A. As indicated, actual yield stresses vary considerably from the nominal values.

The completed structure is shown on the shaking table in Fig. 3.C.3 and the column base detail is shown in Fig. 3.C.4.

3.D. Prototype Considerations

Even though the test structure is not a model of any particular prototype, it can be considered a fairly realistic representation of this category of steel frame structures. Using laws of similitude and the prototype/model scale ratio of 3, it is possible to extrapolate from the test structure to obtain prototype results. The prototype/model similitude ratios are given in Table 3.D.1.

The prototype girder thus has a depth of 18" and a moment of inertia of 1199 in^4; the prototype column has an area of 34 in^2, a depth of 12" and a moment of inertia of 915 in^4. These hypothetical sections actually correspond fairly closely to W18x77 and W12x106 sections, respectively. The prototype weight/floor is about 100^k, and the prototype first mode period is .87 seconds, assuming a scaled foundation compliance.

Applying the standard UCB seismic formula, V = ZKCW, with Z = 1 and K = .67 for a ductile frame, produces a base shear of 31.5^k. When the corresponding lateral loading is applied and the structure analyzed, the maximum bending stress is around 3 ksi, a very low level.

If the current California hospital code, described in Title 17, is applied using the required K factor of 3.0, the maximum bending stress is about 13 ksi, still well below an economical design level.

The point should be made here, however, that the test structure was only lightly loaded. The static forces were almost negligible, and since there was only one bay in the lateral direction, the horizontal load per bent was lower than would be the case with multiple bays laterally. This structure cannot be classed as slender, either; the height/width ratio was only about 1.5 in the direction of excitation.

Although the hypothetical prototype structure, according to even "conservative" building codes, would not require any special provisions for overturning moment, the preliminary dynamic nonlinear analysis of the model has demonstrated that column uplift would occur during a moderate, very credible, earthquake. If such behavior is to be expected for even structures as "stocky" as the test model, it would certainly seem reasonable to realistically consider the implications of that behavior.

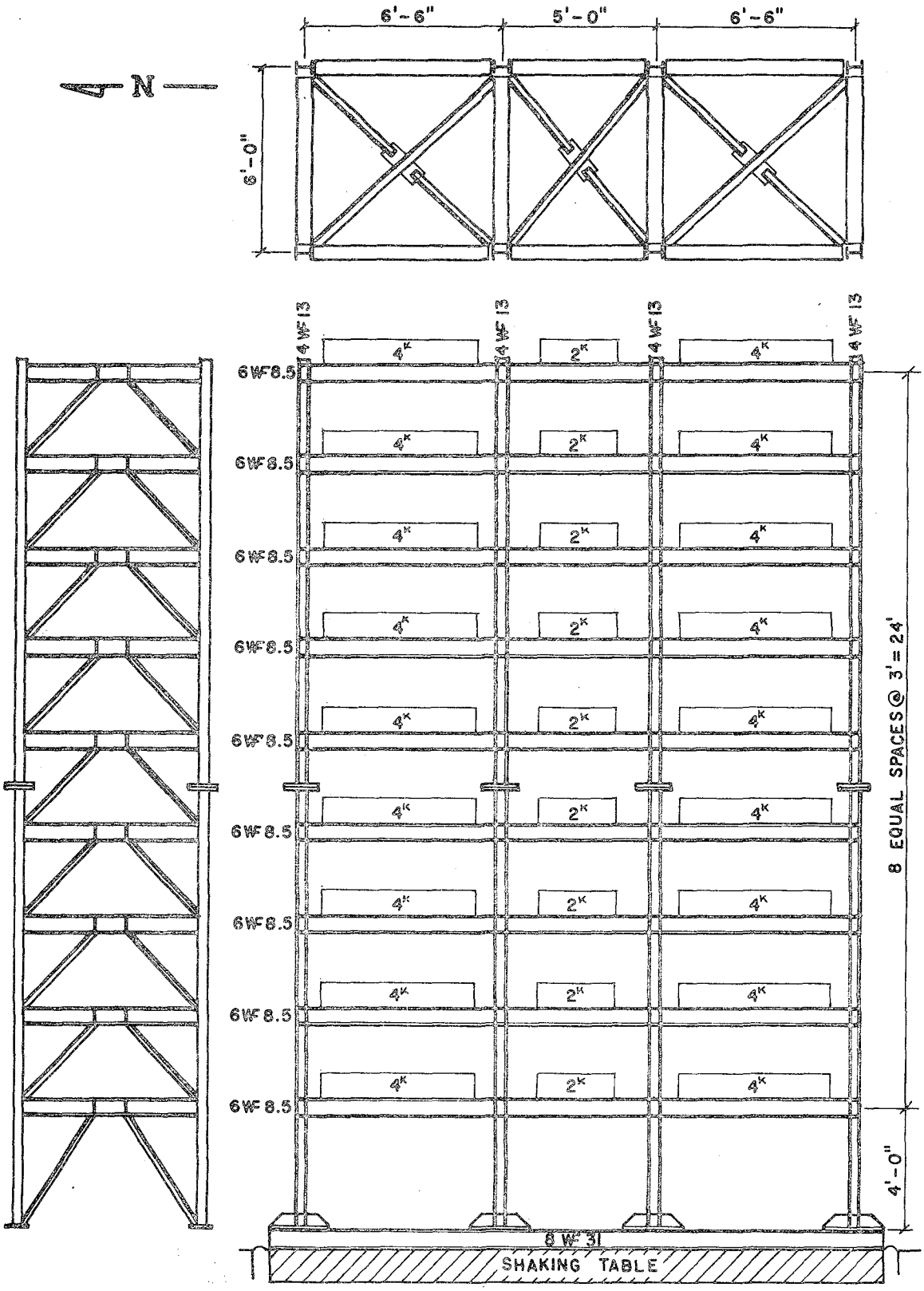

9 STORY STEEL TEST FRAME

Fig. 3.B.1 Preliminary 9 Story Model Design

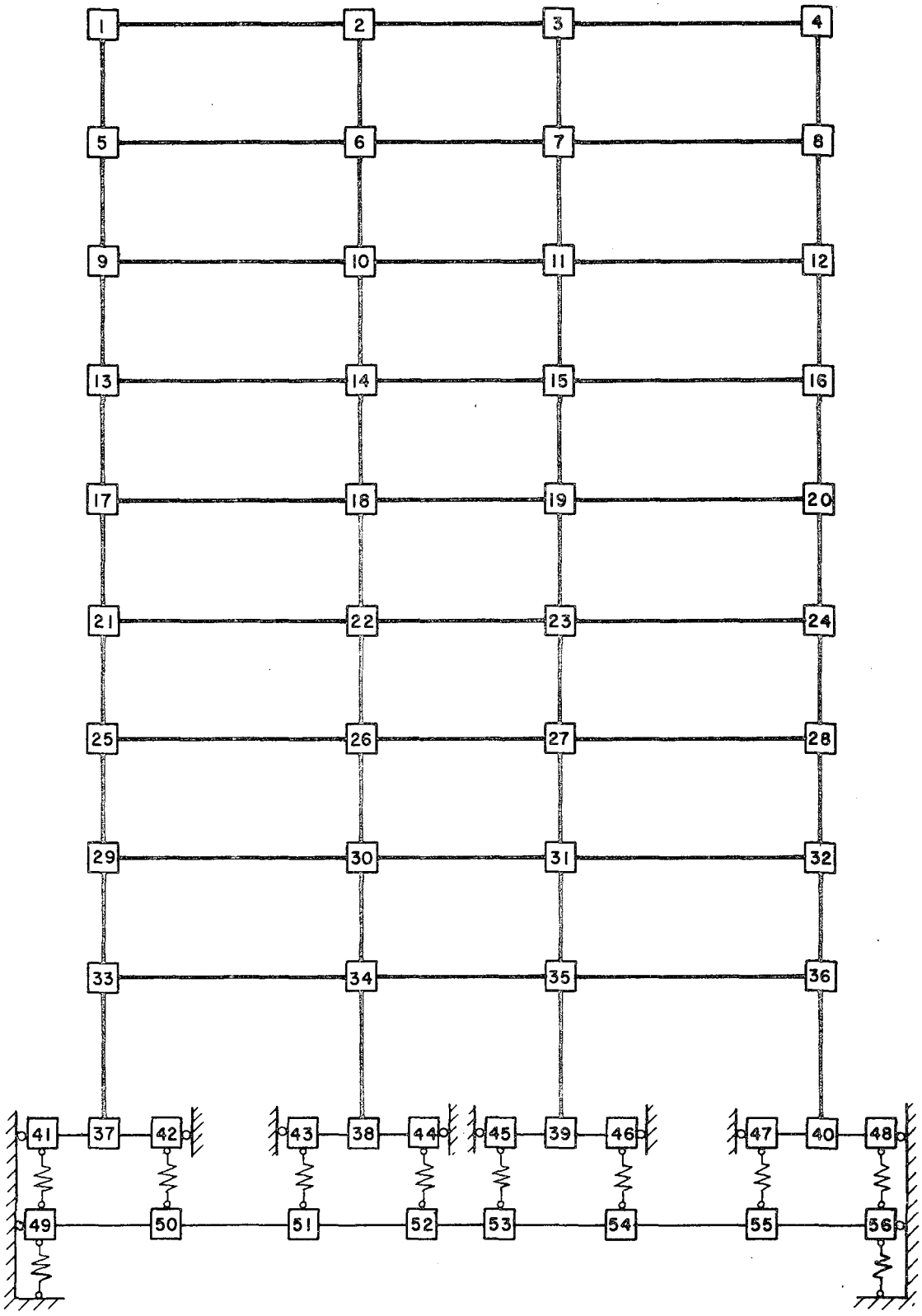

Fig. 3.B.2 Analytical Model

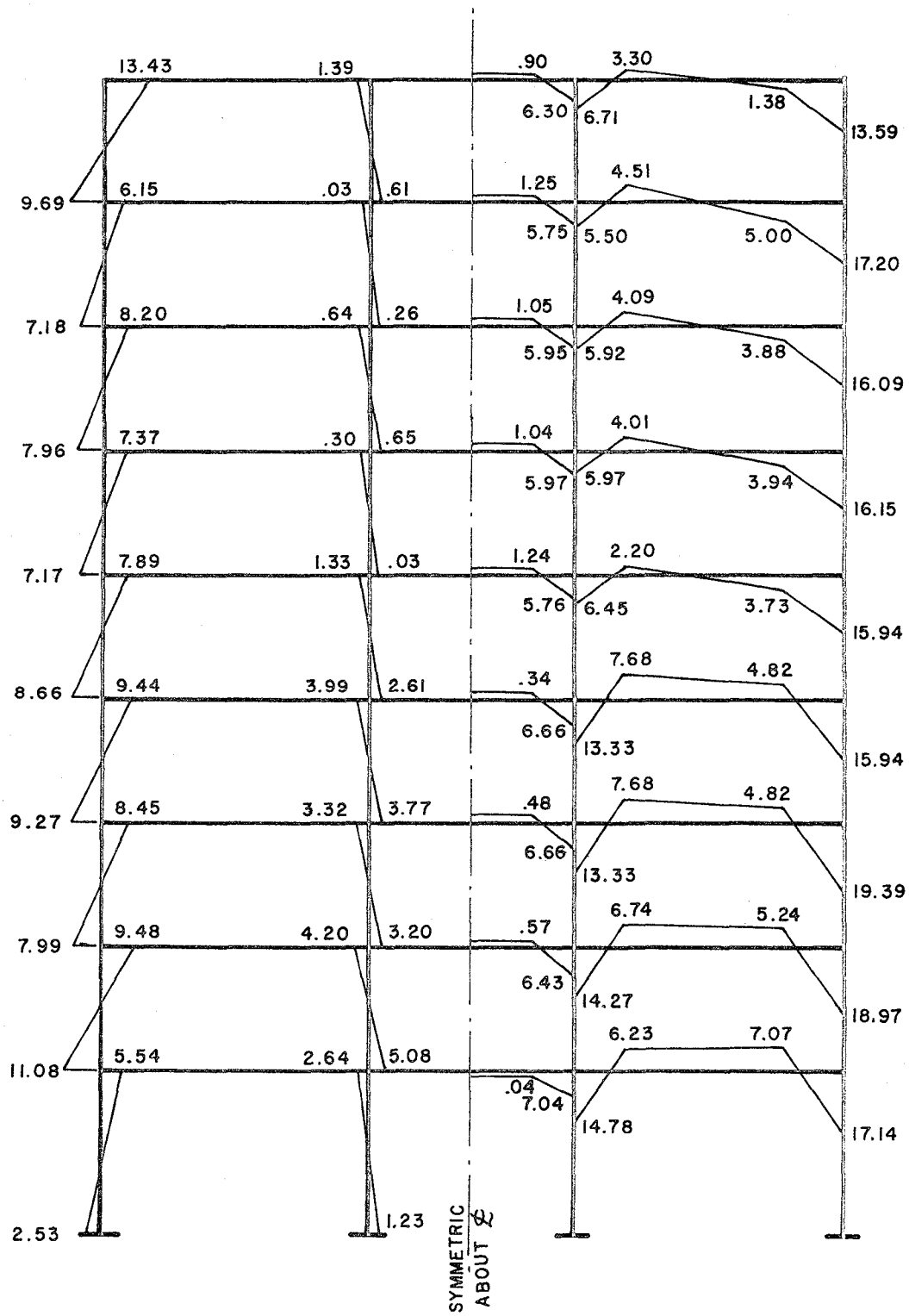

Fig. 3.B.3 Static Moment Distribution (KIP-IN)

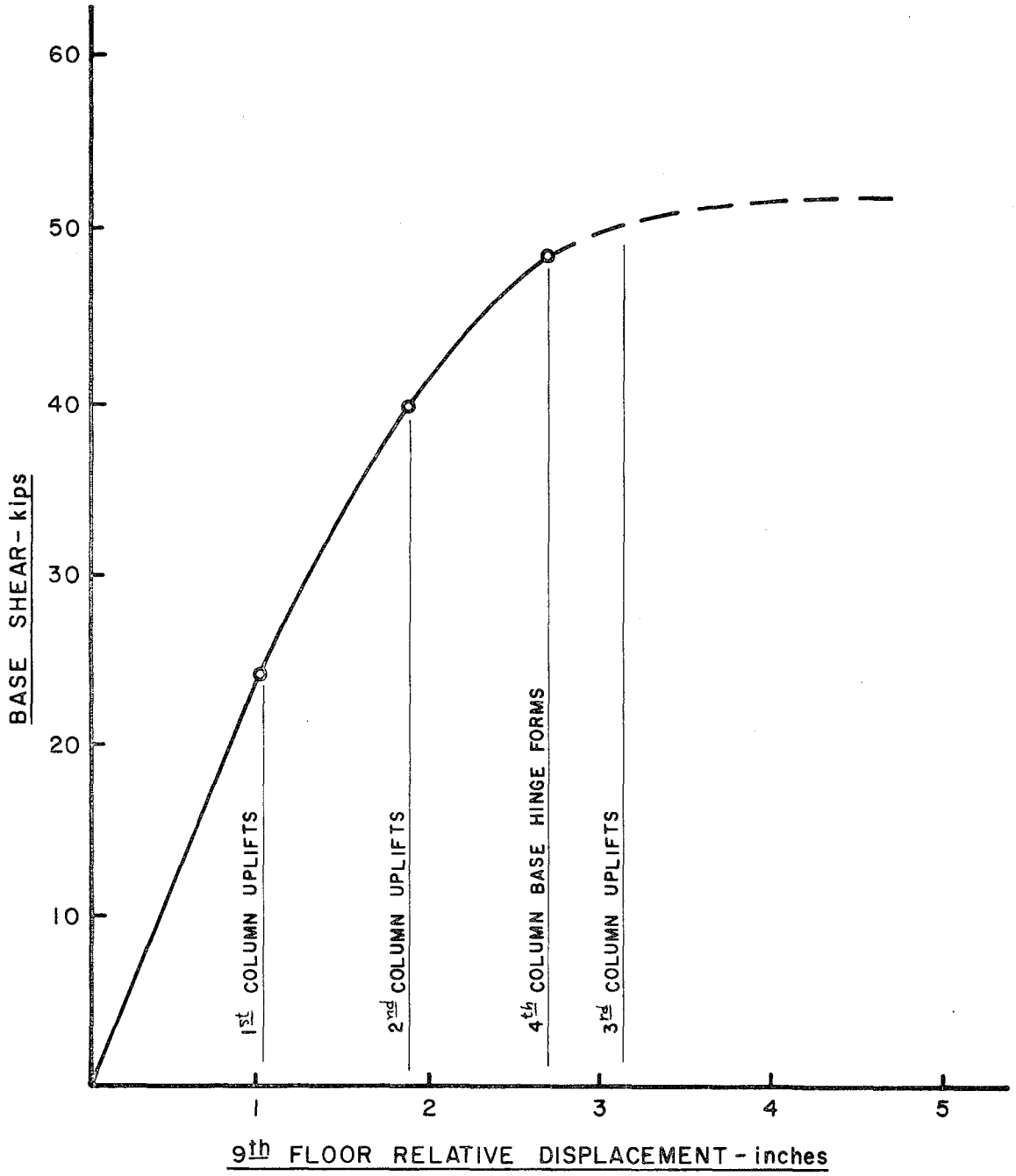

Fig. 3.B.4 Base Shear vs 9th Floor Displacement - 1st Mode Load Pattern Pseudo-Static Behavior

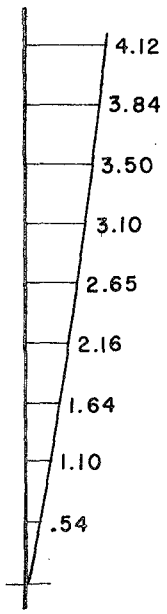

T_1 = .50 sec.

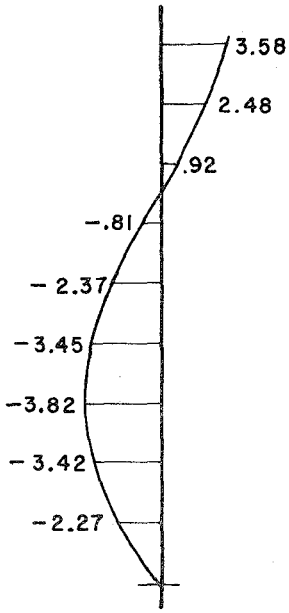

T_2 = .135 sec.

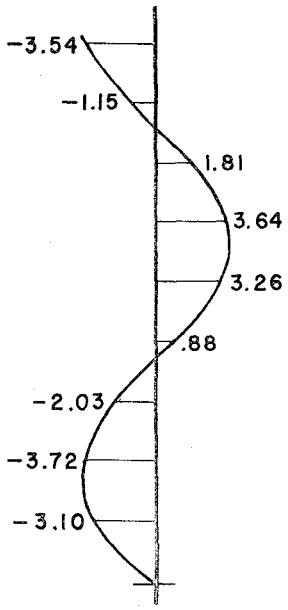

T_3 = .073 sec.

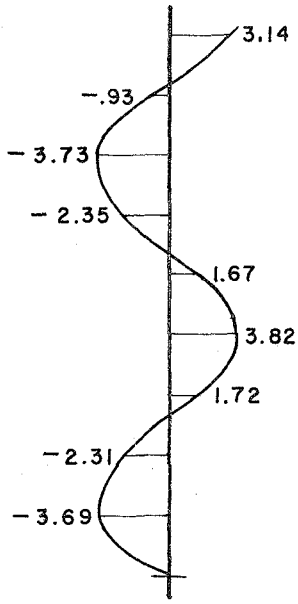

T_4 = .050 sec.

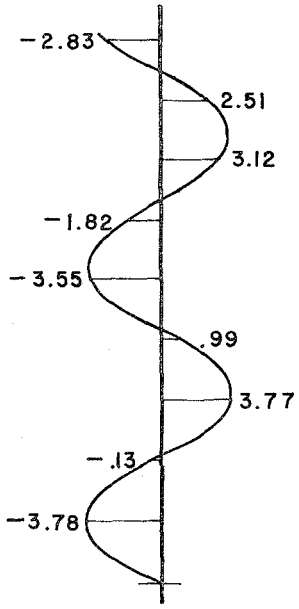

T_5 = .035 sec.

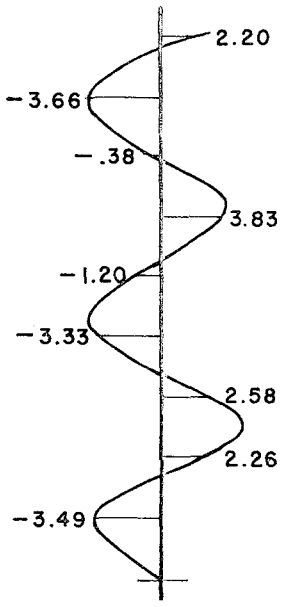

T_6 = .027 sec.

Fig. 3.B.5 Calculated Periods and Mode Shapes

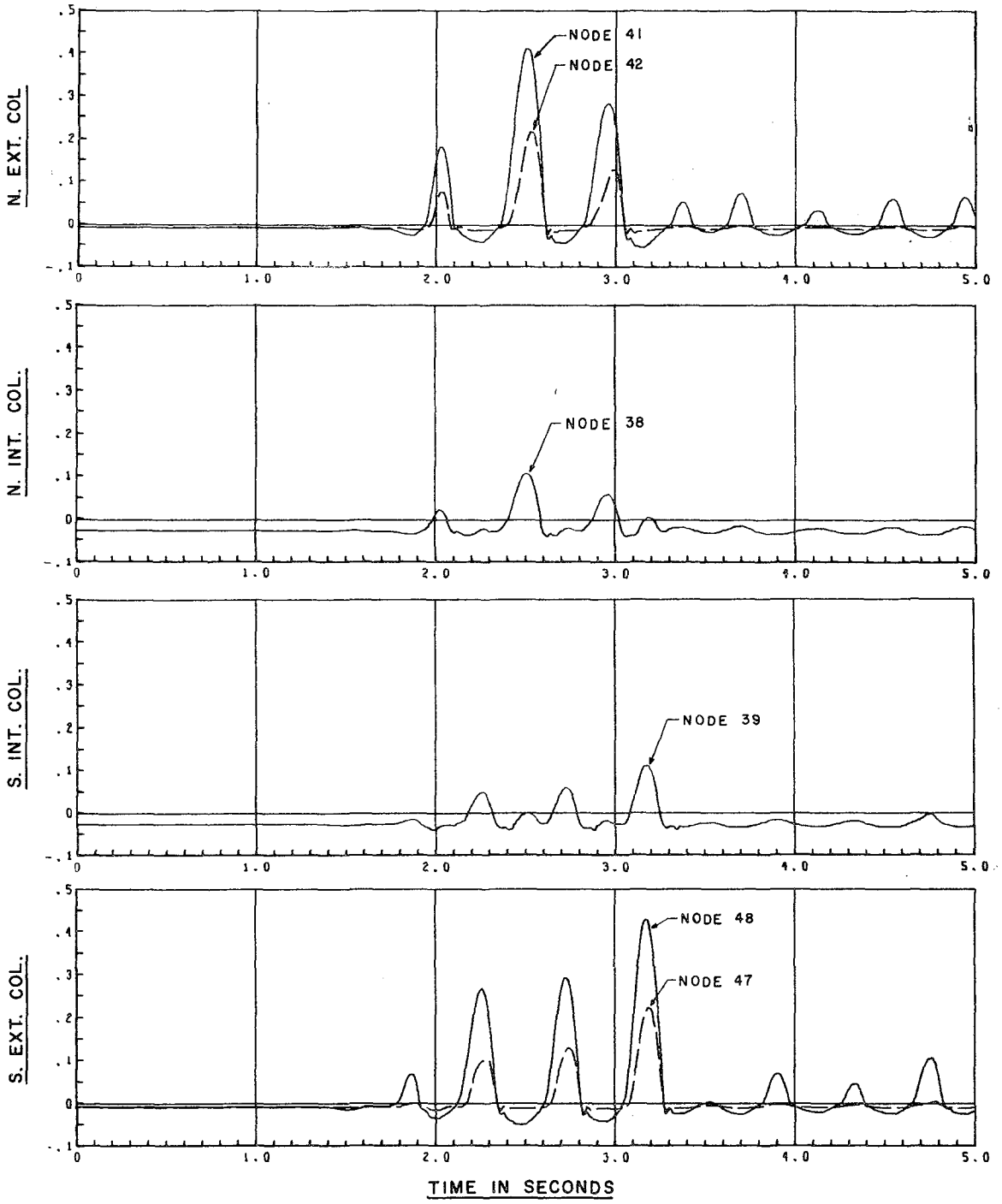

Fig. 3.B.6 Predicted Uplift Response to Time Scaled El Centro (.67g)

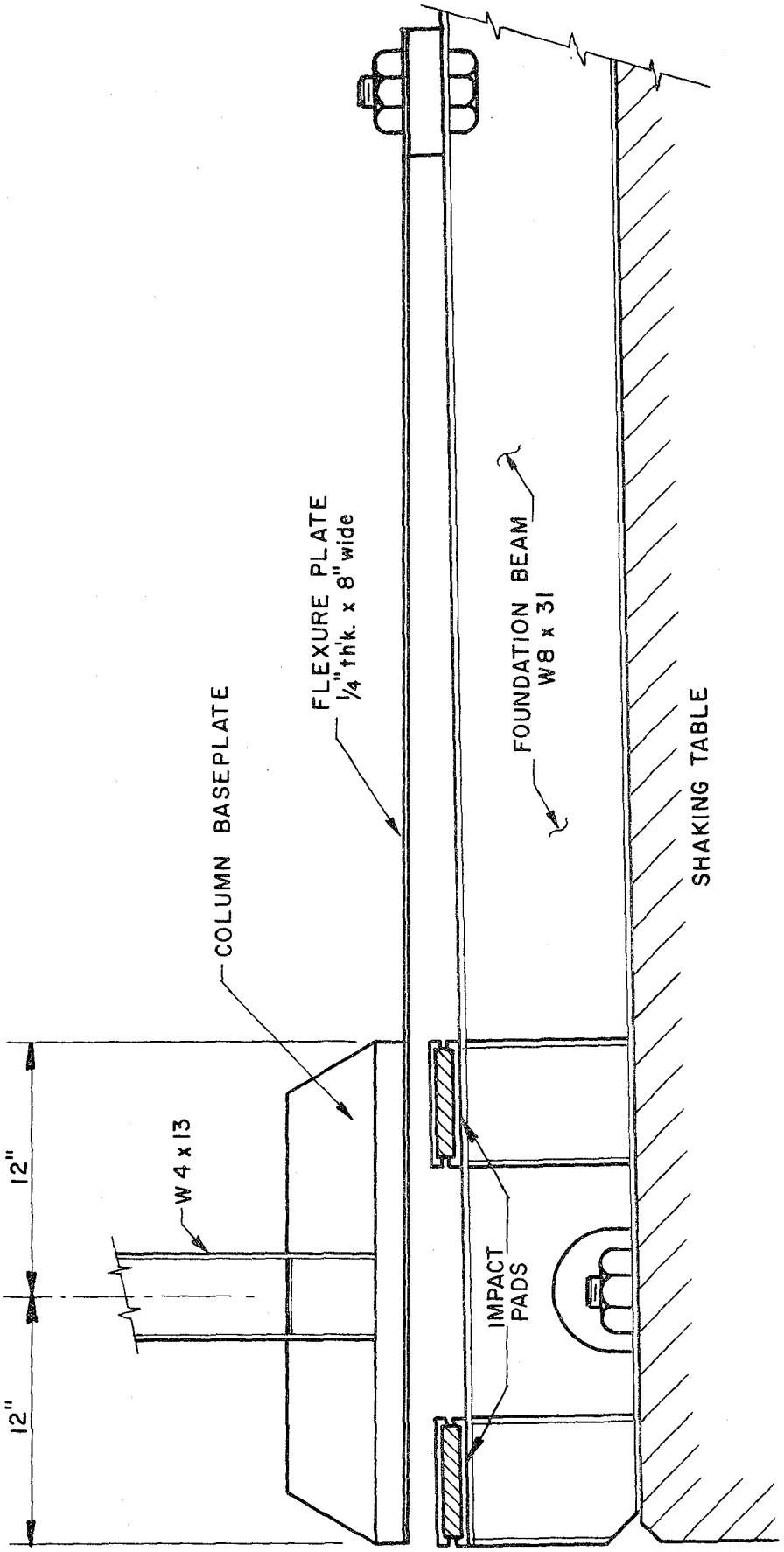

Fig. 3.B.7 Uplifting Column Base Detail

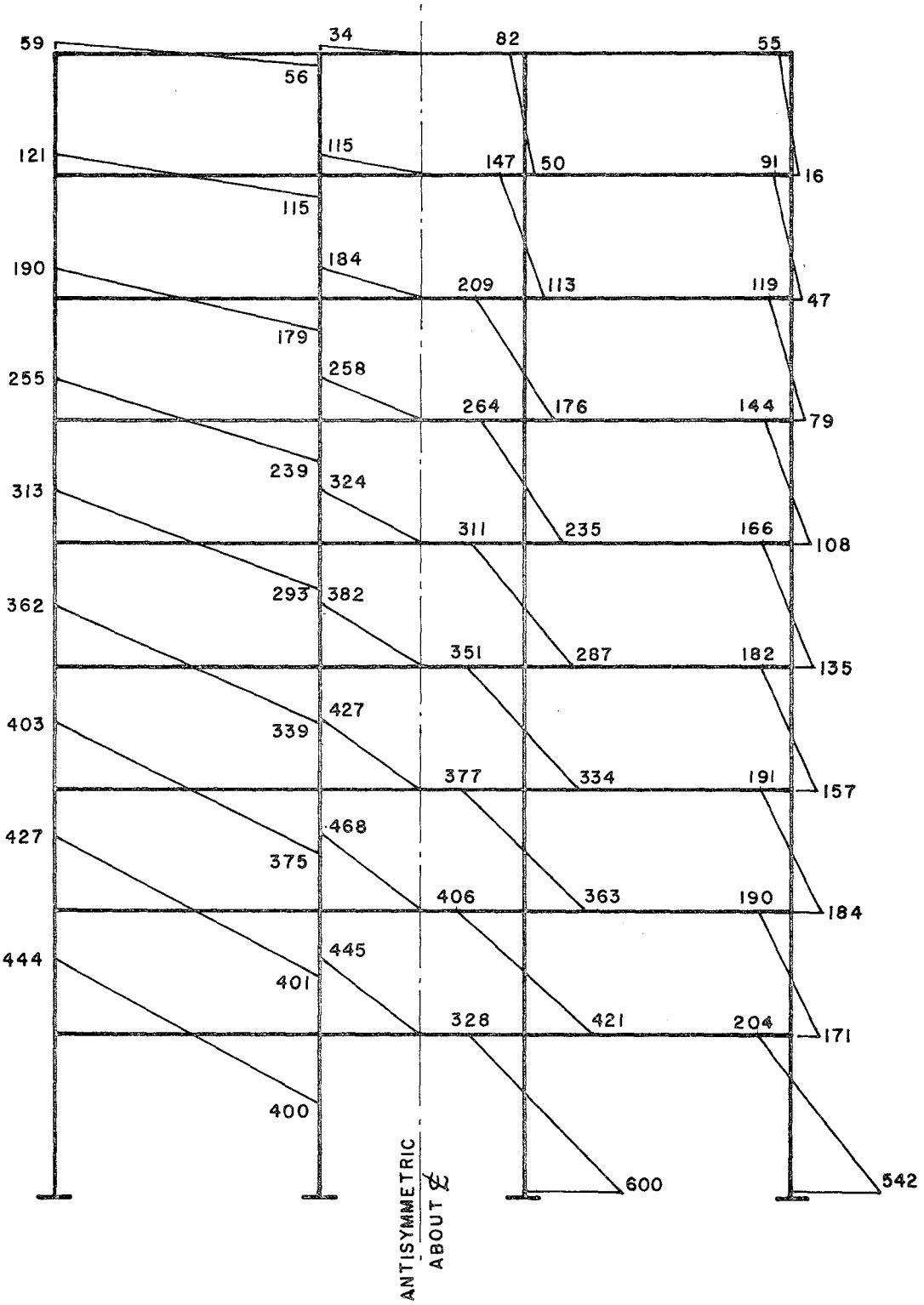

Fig. 3.B.8 Fixed Base Linear Moment Distribution by Response Spectra (KIP-IN)

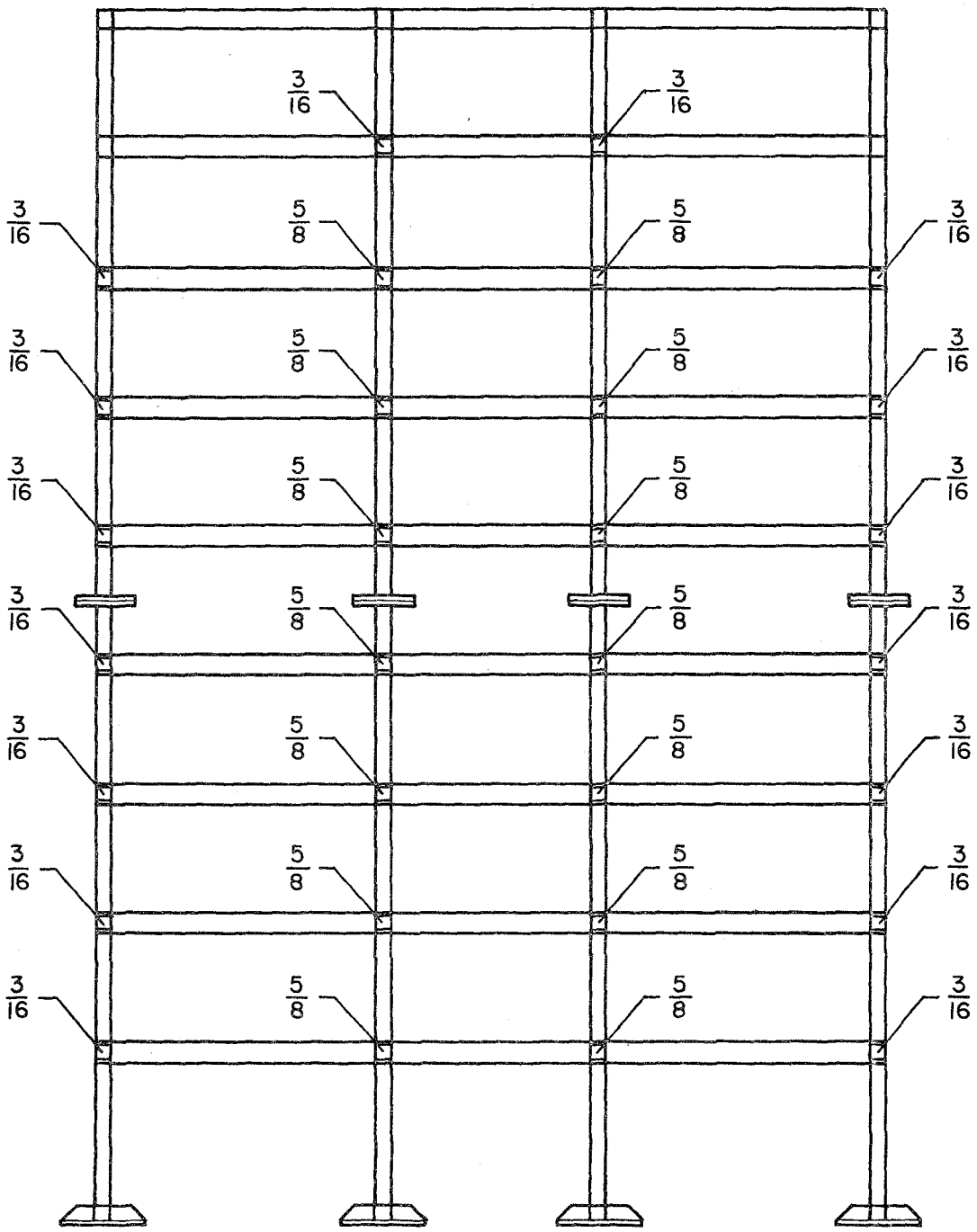

Fig. 3.B.9 Panel Zone Doubler Plate Thicknesses

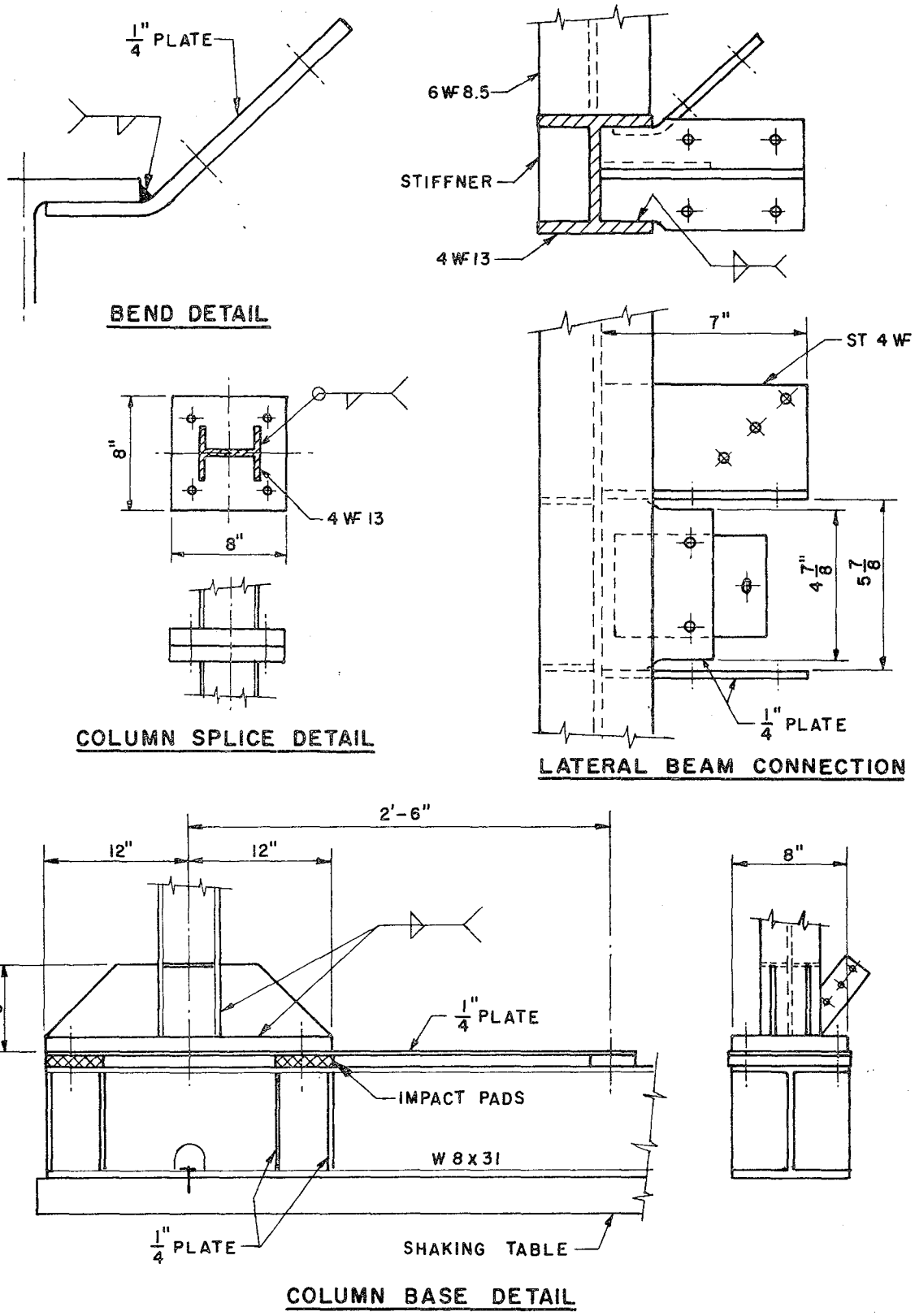

Fig. 3.C.1 Frame Construction Details

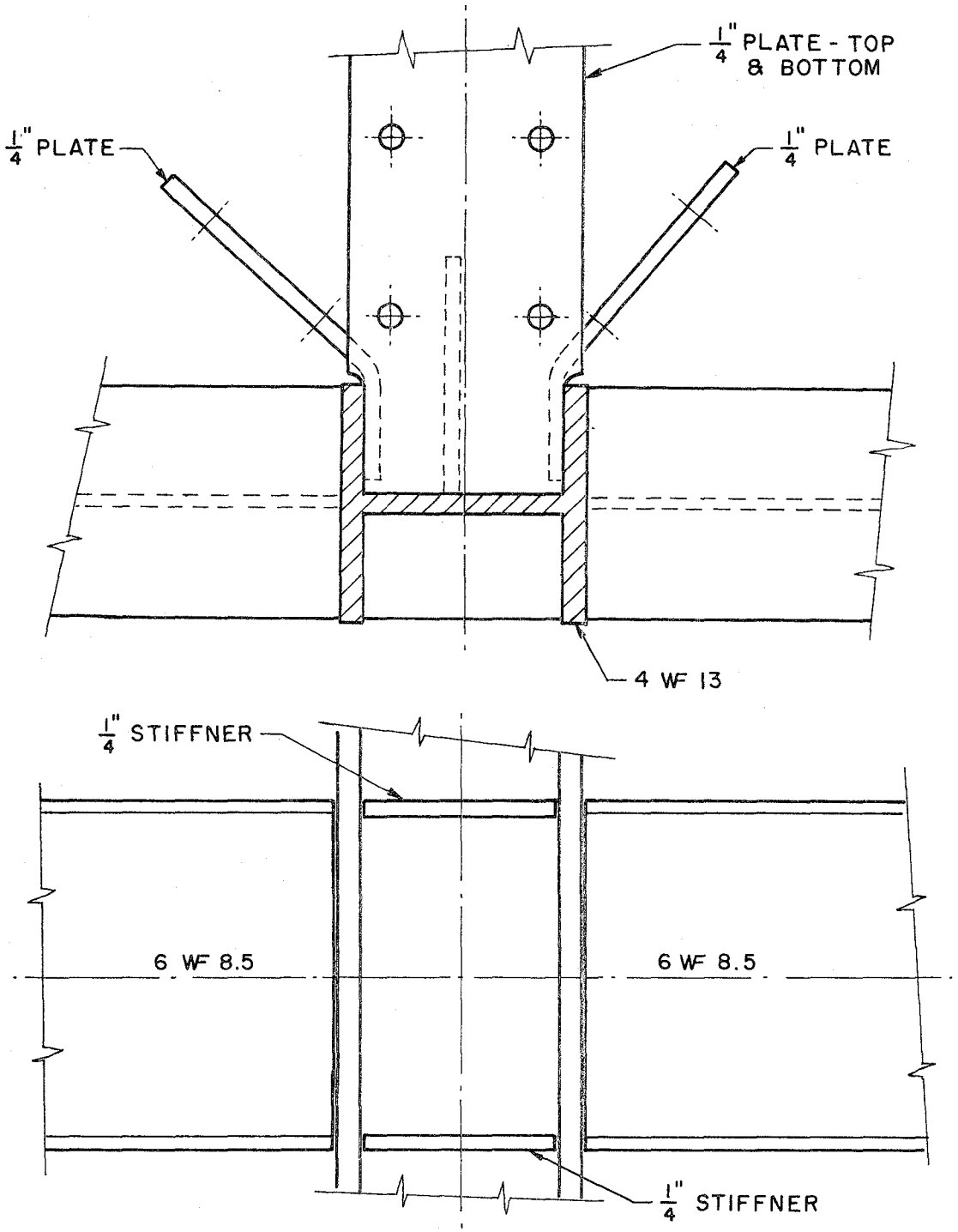

MOMENT CONNECTION DETAIL

Fig. 3.C.2 Frame Construction Details

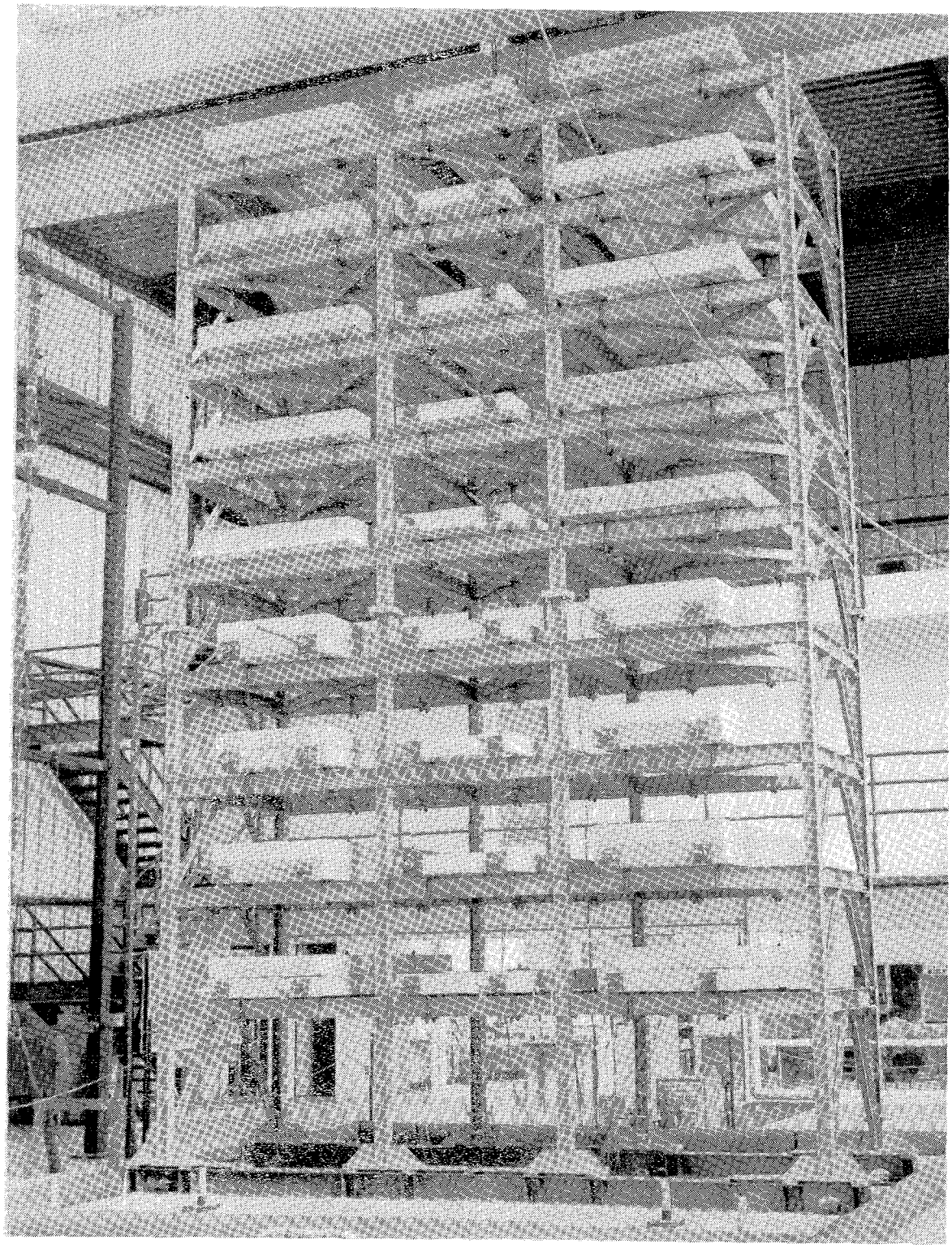

Fig. 3.C.3 Completed Model on Shaking Table

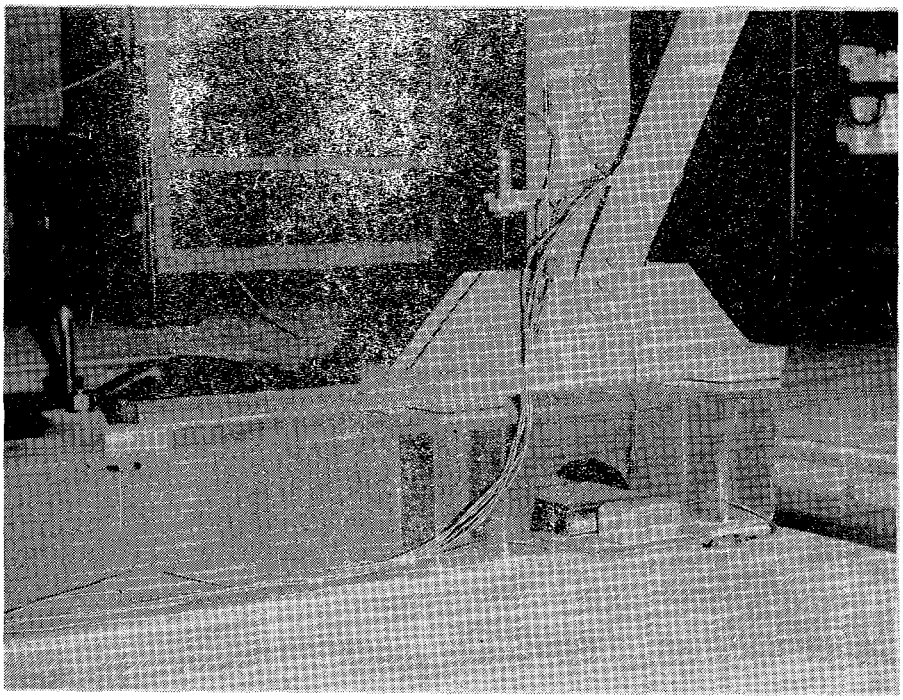

a. Exterior Column

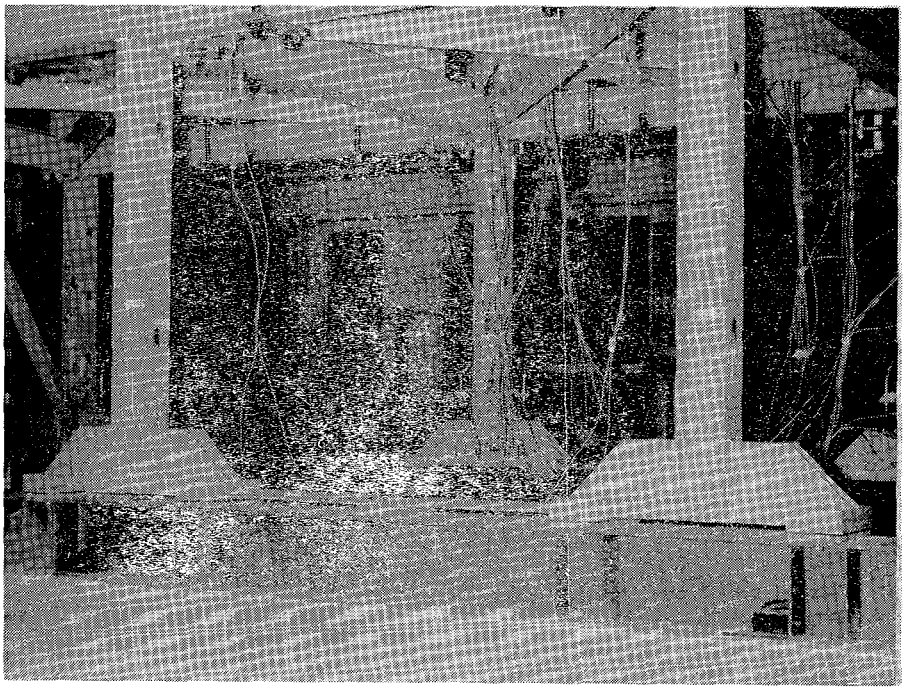

b. Interior Columns

Fig. 3.C.4 Column Base Details

PARAMETER	PROTOTYPE/MODEL RATIO
length	3
area	9
time	1.732
mass	9
acceleration	1
force	9
moment	27
stress	1
strain	1
moment of inertia	81
section modulus	27
displacement	3

Table 3.D.1 Similitude Ratios

4. INSTRUMENTATION

As mentioned in Chapter 2, the Earthquake Simulator data acquisition system has a capability of recording 128 channels of dynamic test data. Of these 128, it was determined to devote 28 channels to monitoring table parameters, leaving 100 channels available for the test structure. In addition, due to circuitry limitations in the analog data processing equipment, the maximum number of strain gage channels which could be conditioned was 56.

The main response parameters of interest were floor accelerations, floor displacements, uplift displacements, and local member forces and deformations. The measurement of these quantities will be discussed individually. A listing of all data channels is given in Appendix B.

4.A. Acceleration Measurement

Accelerations in the longitudinal direction were measured at every floor; lateral accelerations at the two ends of the frame were measured at the 9th floor. The longitudinal accelerometers were mounted at the center of each central bay weight.

Two accelerometer types were utilized in testing. One was the Kistler model 305T non-pendulous, force balance servo accelerometer, with a Kistler model 515T servo-amplifier attached. The second type was the Statham model A39TCb-5-500 resistive bridge accelerometer. The latter utilized strain gage conditioning circuits, reducing the actual number of strain gage channels available to 49. Both types of accelerometers were set to give a data range of $\pm$ 5 g.

4.B. Displacement Measurement

The longitudinal displacements of every floor were monitored using Houston Scientific model 1800-30A linear potentiometers mounted on a reference frame off the shaking table. The range of these instruments is ± 15 in.

The uplift displacements of all 4 columns on the west column line and the two end columns on the east column line were monitored using Houston Scientific model 1800-15A linear potentiometers, mounted on the shaking table as shown in Fig. 3.C.4a. The data range of these instruments is ± 7.5 in.

4.C. Force Measurement

All local member axial forces, shear and moments were derived from strain gages located in the elastic regions of the various members. Axial strains were obtained by measuring the average strain for two gages placed on opposite faces of a section. Flexural strains were obtained by measuring the differential strain for two gages placed similarly. Knowing the flexural strains, hence the moments, at two points on a member allows the computation of the member shear, assuming a straight line moment distribution within any member. All derived forces were based on nominal section properties and a modulus of 29600 ksi for structural steel.

The locations of axial strain gage stations are shown in Fig. 4.C.1. The locations of elastic flexural strain gage stations are shown in Fig. 4.C.2. These gages were all Micro-Measurement model EA-06-250BG-120, option L.

4.D. Local Deformation Measurement

Since forces beyond the elastic limits of certain members were anticipated in the base-fixed testing condition, it was decided to monitor local deformations of the most critical members. Based on preliminary analyses, it appeared that the most likely members to instrument were the first floor columns and the first floor interior girder.

Two types of local deformations were measured, both within what can be considered the plastic hinge regions at the member ends. One type of measurement was the post-yield flexural strain; the other type was the average member curvature, measured over a gage length equal to the section depth.

The post-yield strain gage stations are shown in Fig. 4.D.1. Again, these measurements were made by differencing gages located on opposite faces of the section. The gages employed were Tokyo Sokki Kenkyujo, models YL-10, and YL-20.

Average curvatures were measured by pairs of Sanborn model 7DCDT-500 displacement transducers mounted in frames as shown in Fig. 4.D.2. The DCDT's have a travel range of $\pm$ 0.5 in. The distance between the opposed pairs of DCDT's is 10 in. The locations of the average curvature measurement stations are shown in Fig. 4.D.4.

In addition, the rotations of the ends of the 1st floor interior girder were measured utilizing pairs of DCDT's mounted on a pinned-end reference beam as shown in Fig. 4.D.3. The supports for the reference beam bearings were welded to the joint panel zones. This instrumentation was previously described by Clough and Li (3).

4.E. Data Noise Levels

As an indication of the various instrument resolutions, Appendix C shows envelope data values of a "noise" reading, i.e., no dynamic response occurring, taken with the shaking table fully pressurized and ready for operation. As shown, the noise levels were very low, on the order of 0.01% to 0.5% of the expected dynamic data ranges.

The accuracy of experimental data should thus be very good; of course reduced data derived from the original measurements can only be as good as the assumptions involved in the derivation. A good example of such a potential error is the discrepancy between actual section properties and the nominal section properties used to arrive at force quantities based on strain gage data.

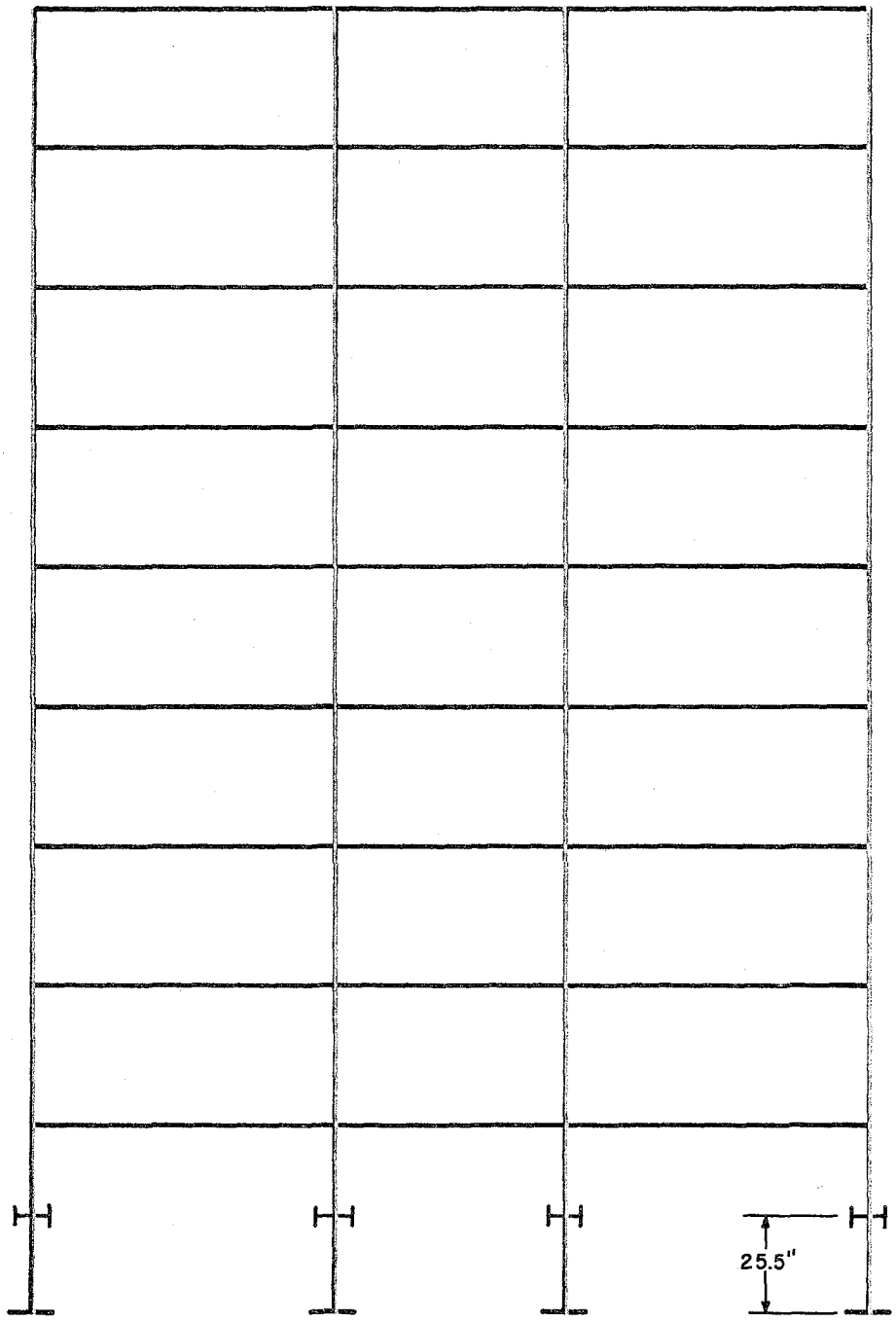

Fig. 4.C.1 Axial Strain Gage Stations

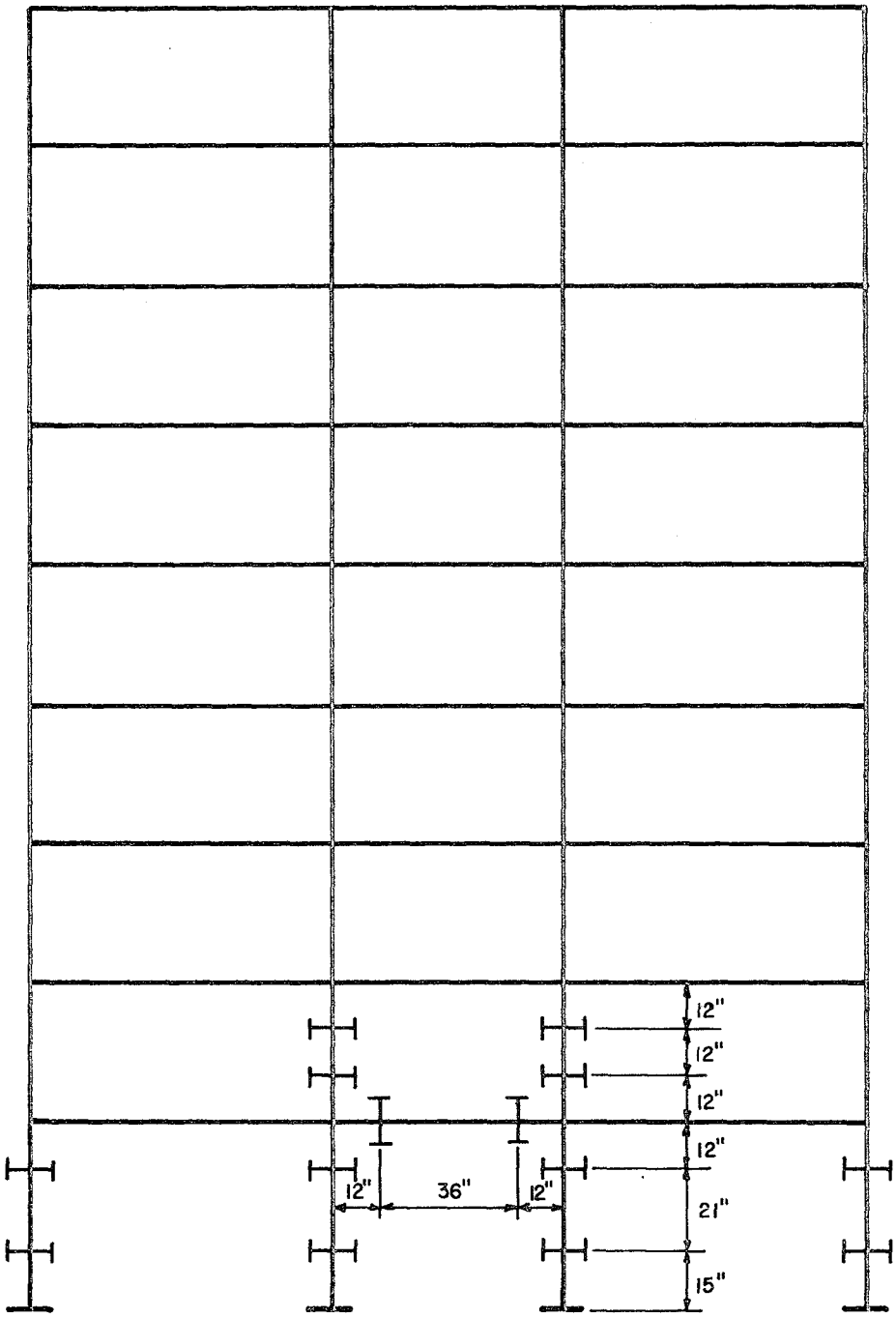

Fig. 4.C.2 Elastic Flexural Strain Gage Stations

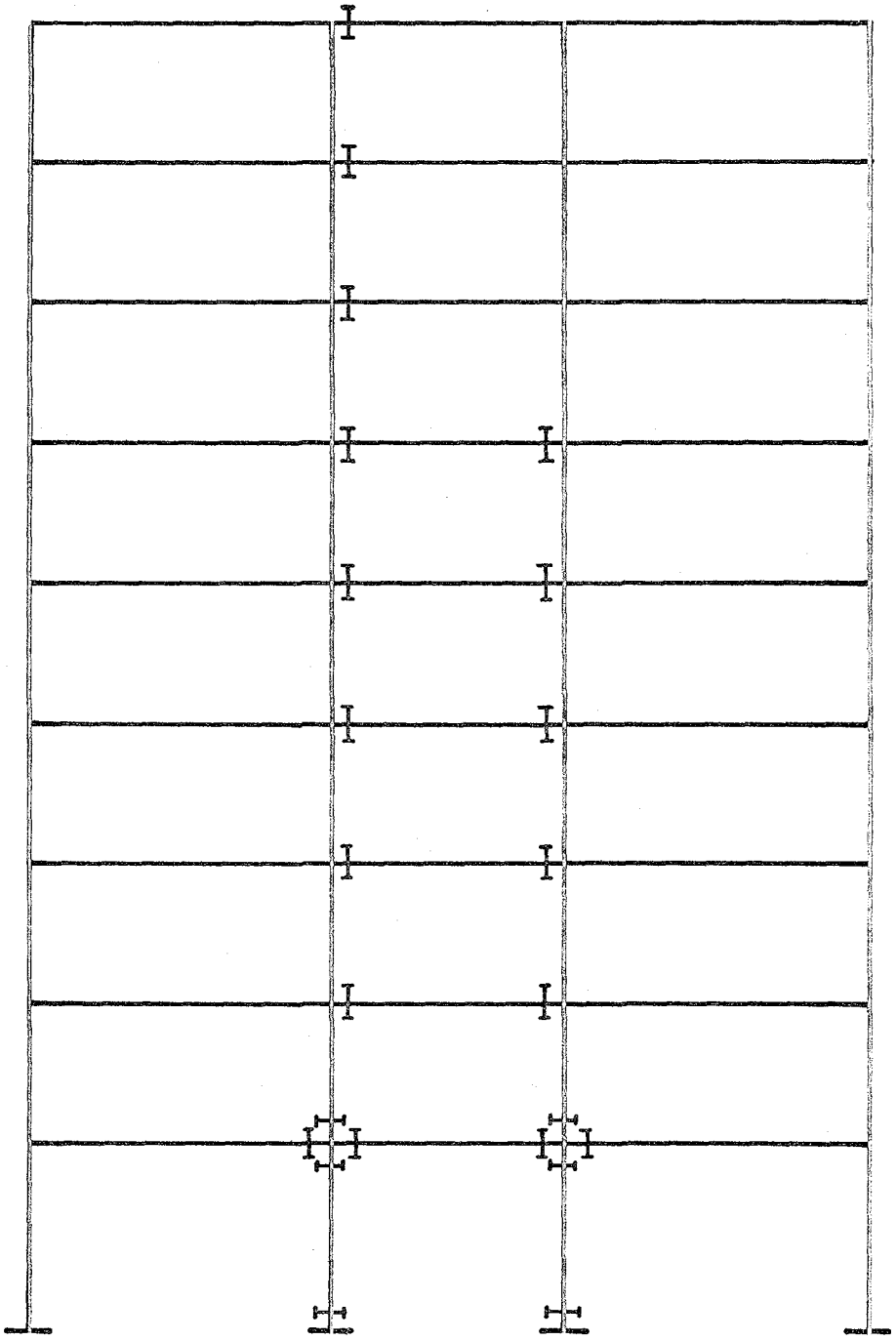

Fig. 4.D.1 Post Yield Flexural Strain Gage Stations

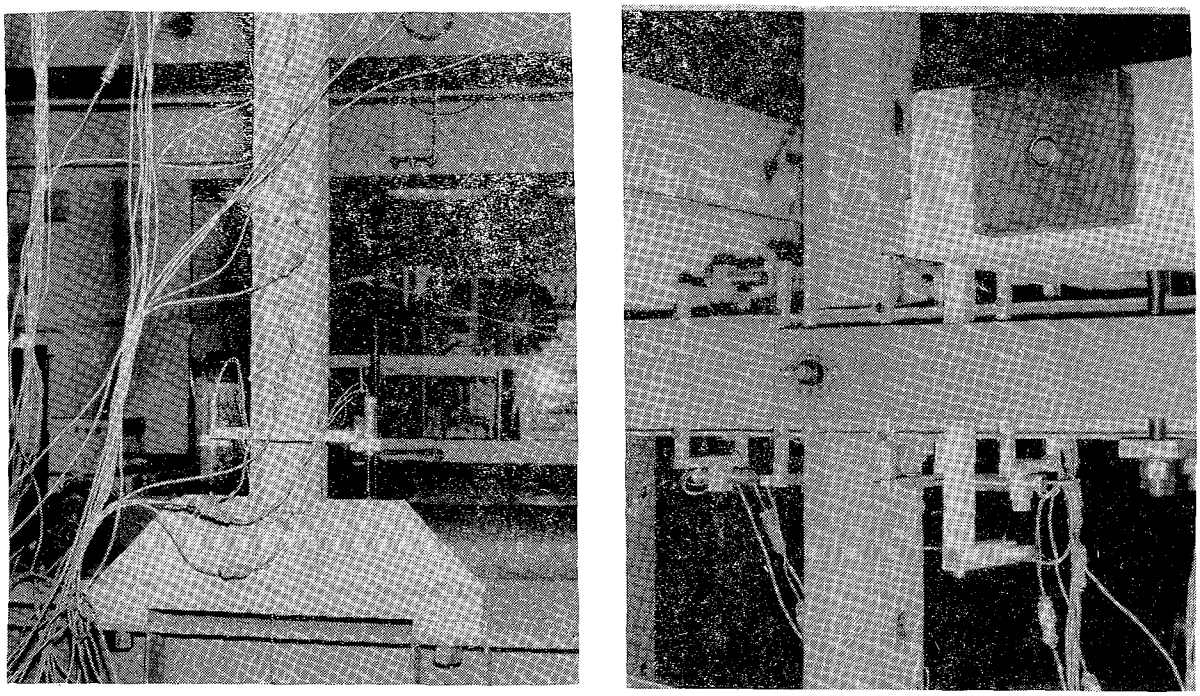

a. Column

b. Girder

Fig. 4.D.2 Local Curvature Measurement

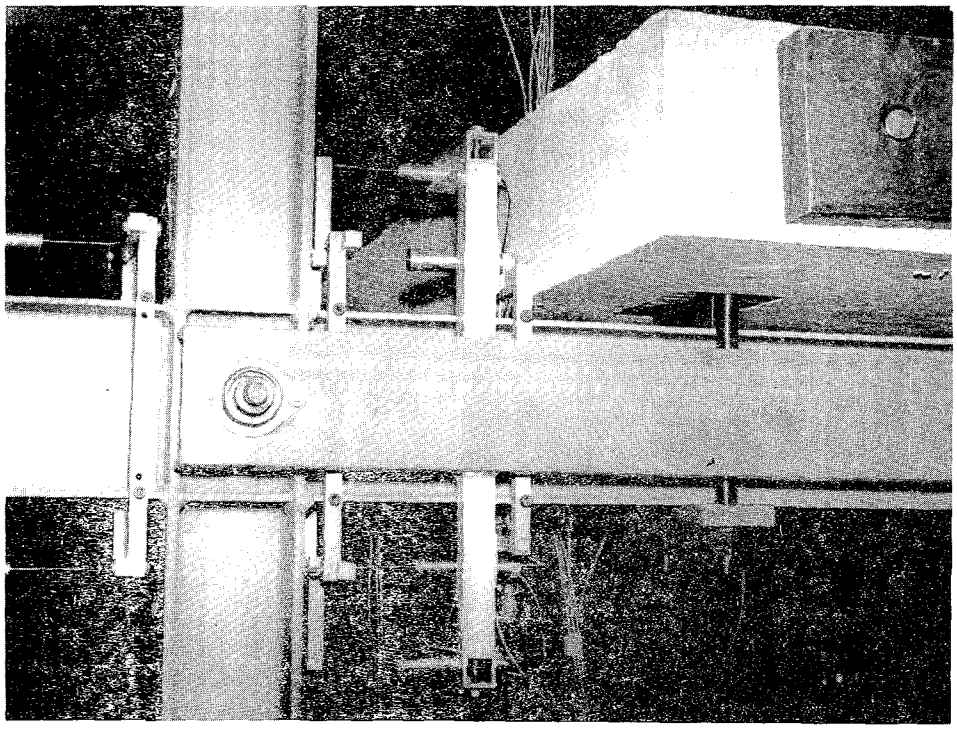

Fig. 4.D.3 Joint Rotation Measurement

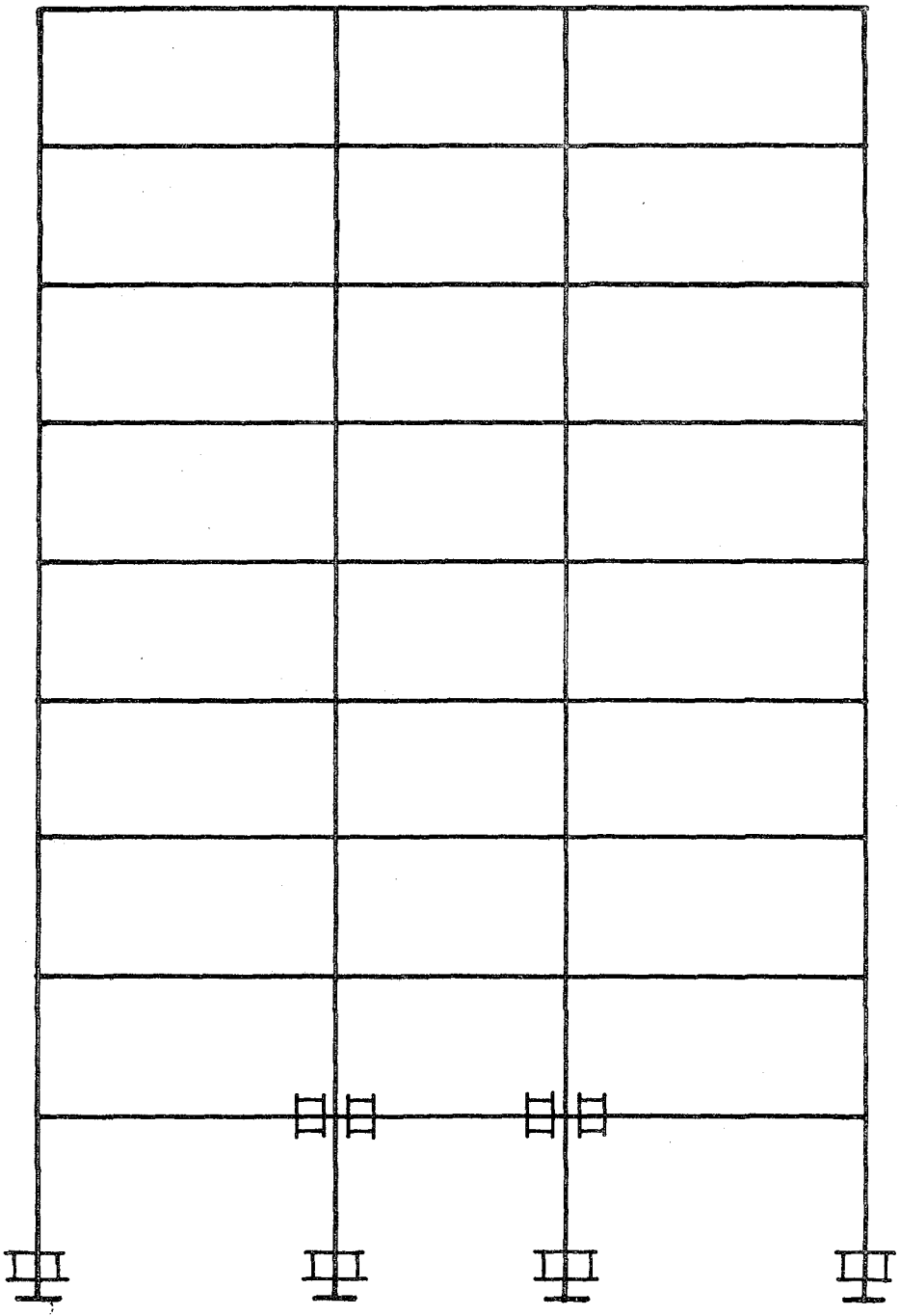

Fig. 4.D.4 Average Curvature Measurement Stations

5. TEST PROGRAM

5.A. Testing Sequence

As previously mentioned, it was decided for comparative reasons, to conduct tests in both the uplifting and base fixed conditions. Due to the fact that higher strains were anticipated for the base fixed case, these tests were conducted last chronologically, in case any damage to the test structure did occur.

For each base condition of the structure, tests generally proceeded sequentially from low to high intensity for a given source signal. Again this was done for obvious safety reasons.

5.B. Ground Motions

As this study was deterministic in nature, rather than probabilistic, it was necessary for reasons of time and economy to select a small number of ground motions to use as input signals to the shaking table. It was considered desirable, however, to investigate the response of the system to more than one type of earthquake input, with regard to frequency content and signal duration.

The two basic ground motions chosen as input signals were the 1940 El Centro N-S and the 1971 Pacoima Dam S 74 W records. Due to the scale of the test model, the input signals were time scaled (speeded up) by a factor of 1.73 from the field recorded signals in order to maintain similitude, as discussed in Chapter 3. Both input motions were employed at a wide range of intensities, up to the extreme limits of the shaking table capabilities.

It should be mentioned that the very low frequency components of the earthquake records are not represented in the test signals. In

order to keep displacements within the limits of the shaking table at relatively high levels of acceleration, the lower frequencies were filtered out as required. These frequencies are subject to the greatest digitization and base line errors, and their elimination is not significant for the purposes of these tests.

The El Centro record has long been utilized in earthquake engineering as a standard for seismic performance. This motion has a frequency content spread over a rather large range of interest to structural engineers. The Pacoima record is of a much shorter duration, and has a frequency content more concentrated in the higher frequency range. Particularly for nonlinear softening systems with initial natural frequencies near that of the first mode of the test model (2 hz), the Pacoima record is extremely effective in exciting a strong response.

In Appendix D, a list is given of the entire set of dynamic tests performed; brief descriptions and comments are presented for each test. The data from this entire set of tests were permanently stored on 9-track magnetic tape.

Of the total number of 67 tests performed on the test model, 7 were selected for detailed data reduction. Of these 7 tests, 4 were conducted in the uplifting base condition and 3 were conducted in the fixed base condition. In selecting tests for detailed reduction, emphasis was placed on those having the great intensities, as the model exhibited the most extensive nonlinear behavior in these tests. Table acceleration and displacement time histories, along with the corresponding response spectra are shown in Figs. 5.B.1 through 5.B.8. The response spectra for each test were obtained using a program developed by Nigam and Jennings (6). The spectral coordinates were computed at

the following period intervals:

.10 - .30 @ .025 sec intervals
.30 - 1.0 @ .050 sec intervals
1.0 - 3.0 @ 0.25 sec intervals
3.0 - 5.0 @ 0.50 sec intervals

The seven tests discussed in this report are referred to by the following mnemonics:

1) 1.73*EC Span 050 Uplift
2) 1.73*EC Span 300 Uplift
3) 1.73*EC Span 300/300 Uplift
4) 1.73*PAC Span 200 Uplift
5) 1.73*EC Span 050 Fixed Base
6) 1.73*EC Span 300 Fixed Base
7) 1.73*PAC Span 250 Fixed Base

The number 1.73 refers to the time scaling factor. EC refers to the El Centro source signal; PAC refers to the Pacoima Dam source signal. The second number indicates the "span setting", the control console setting which governs the intensity of the motion. The table displacement is approximately linearly proportional to this factor. In the 3rd test, the two span setting numbers refers to the fact that the independent vertical component of ground motion was included for this test. (The vertical component was not included for the remainder of the tests.) The uplifting and fixed base descriptions are self-explanatory.

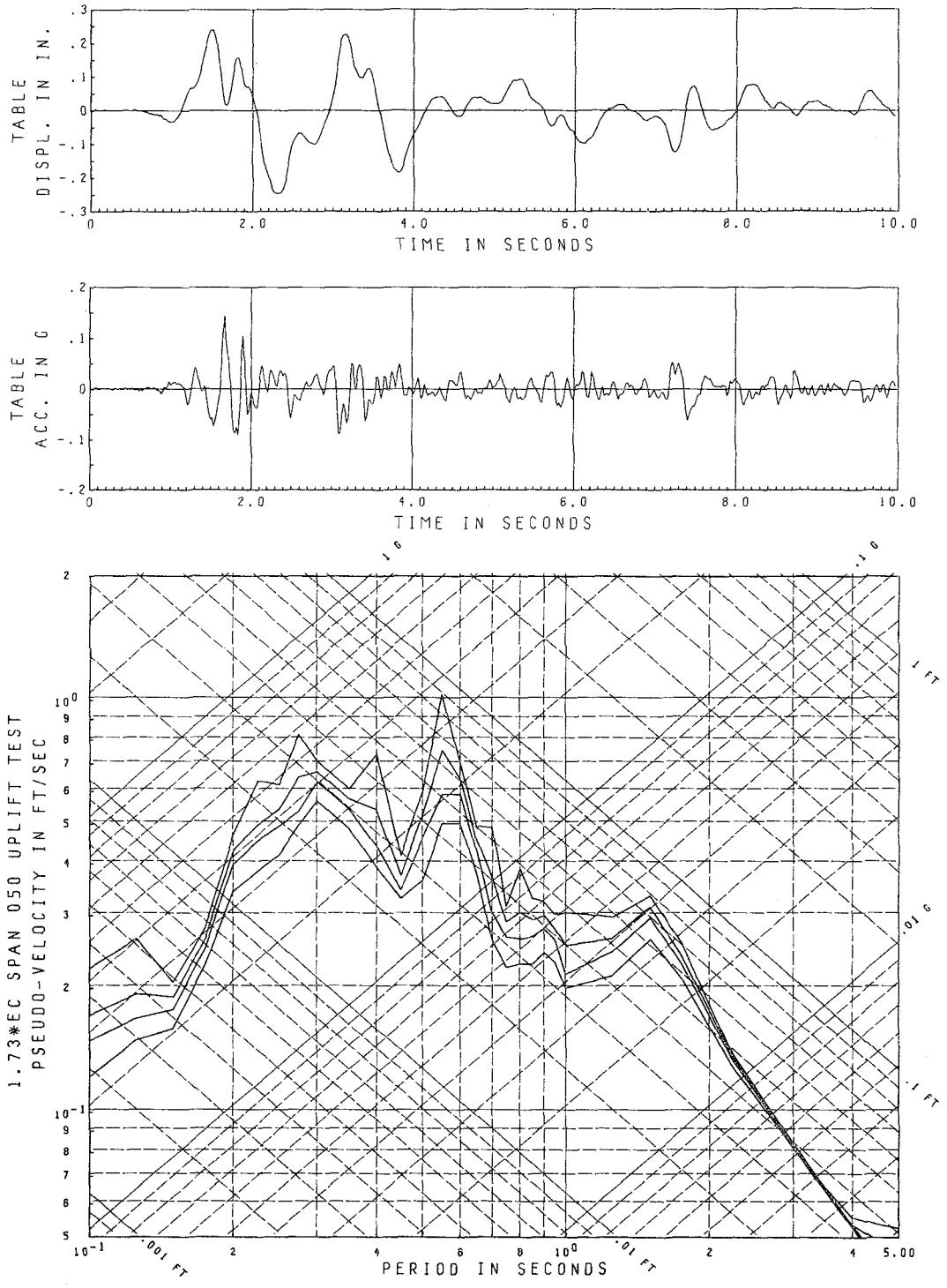

Fig. 5.B.1 1.73*EC Span 050 Horizontal Table Motion Uplift Test

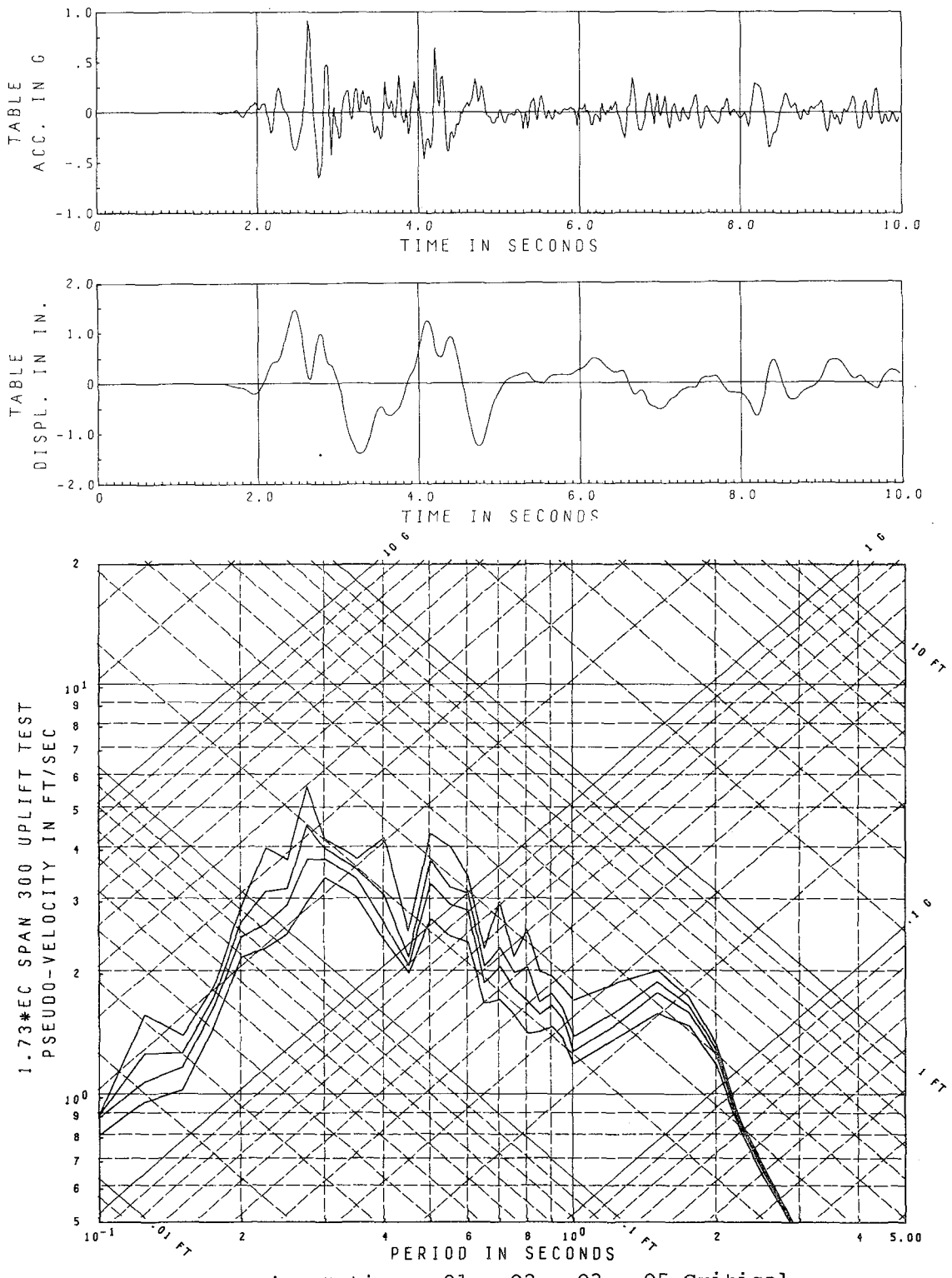

Damping Ratio = .01, .02, .03, .05 Critical

Fig. 5.B.2 1.73*EC Span 300 Horizontal Table Motion Uplift Test

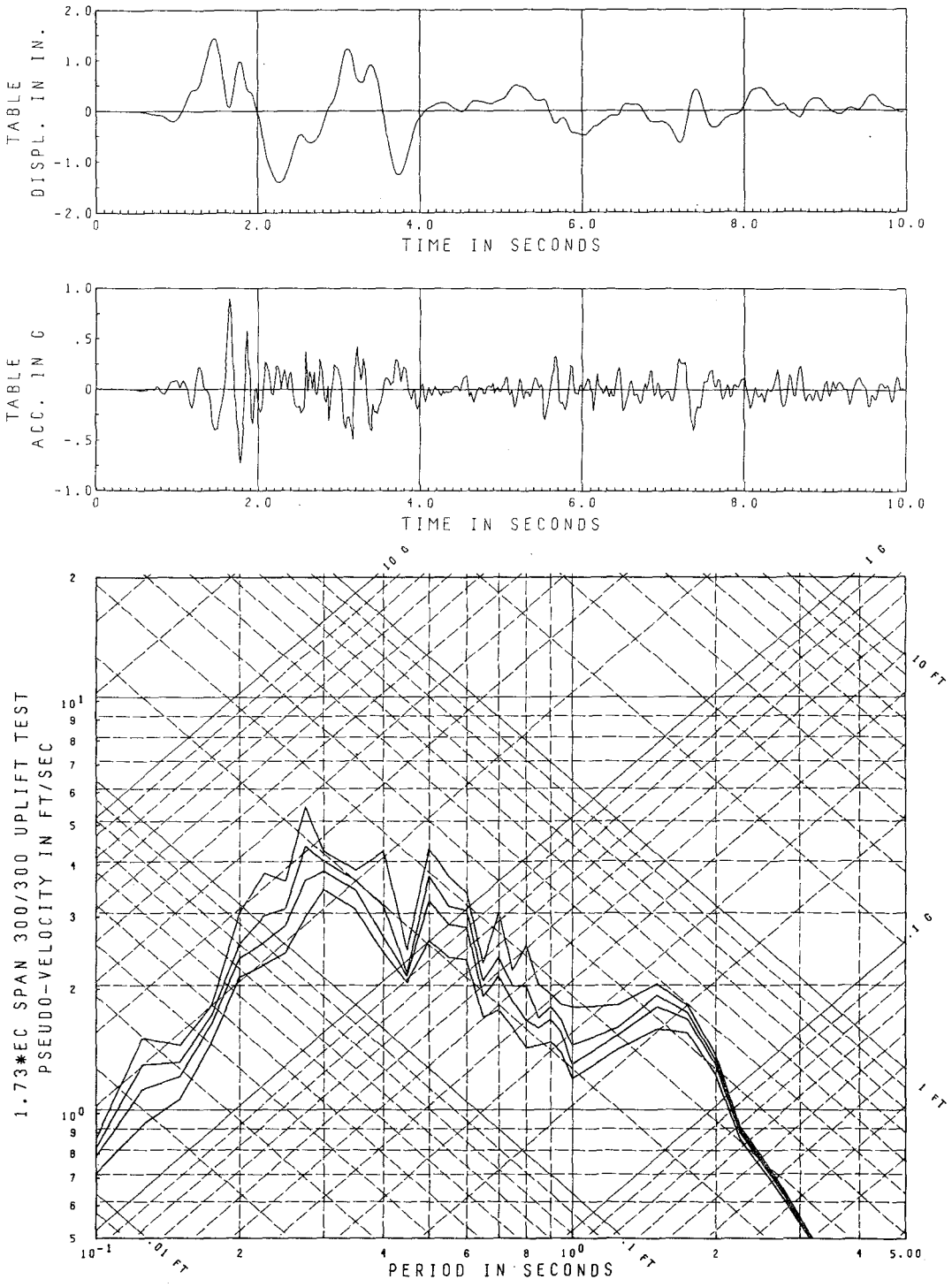

Damping = .01, .02, .03, .05 Critical

Fig. 5.B.3 1.73*EC Span 300/300 Horizontal Table Motion Uplift Test

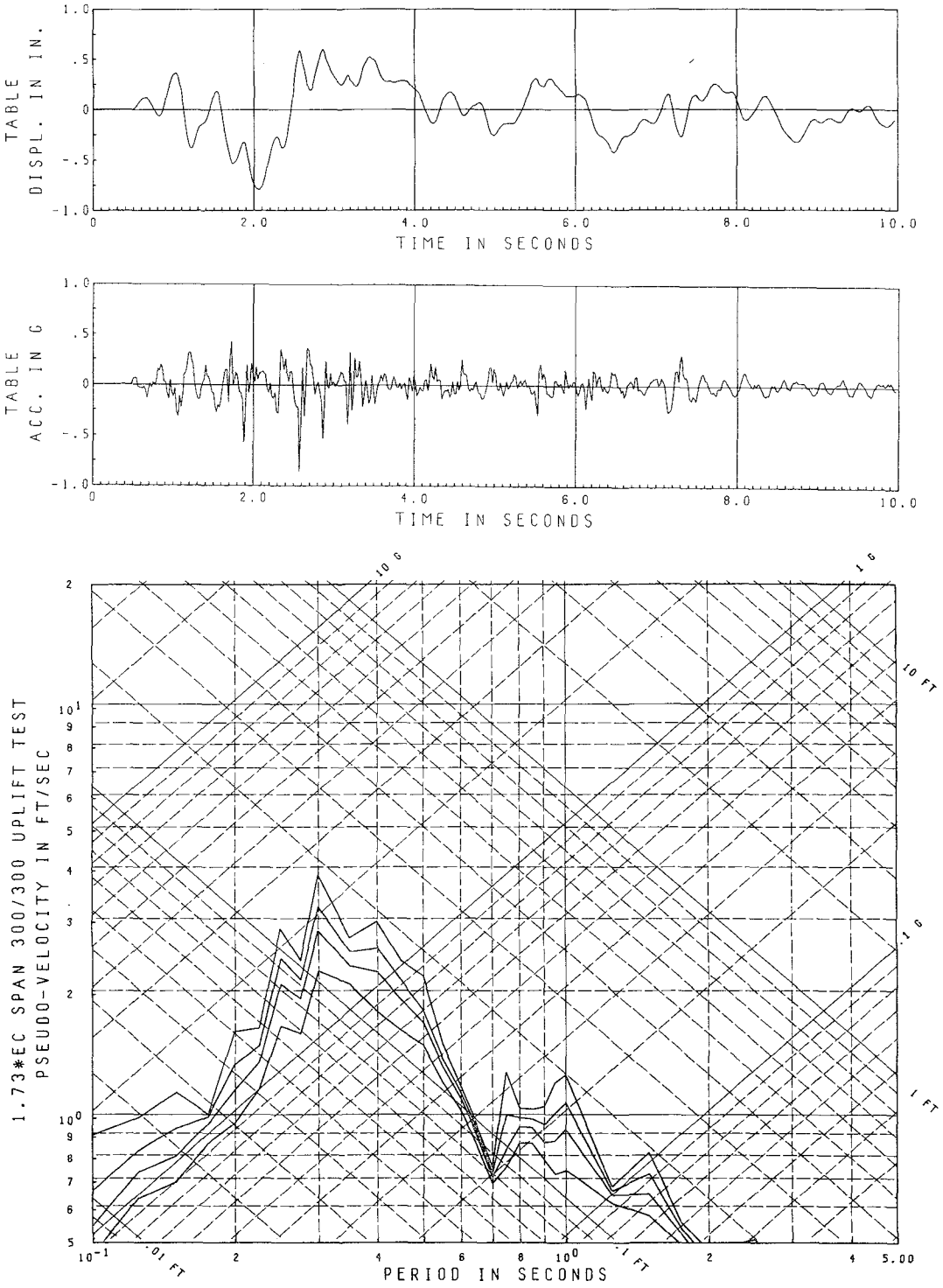

Damping = .01, .02, .03, .05 Critical

Fig. 5.B.4 1.73*EC Span 300/300 Vertical Table Motion Uplift Test

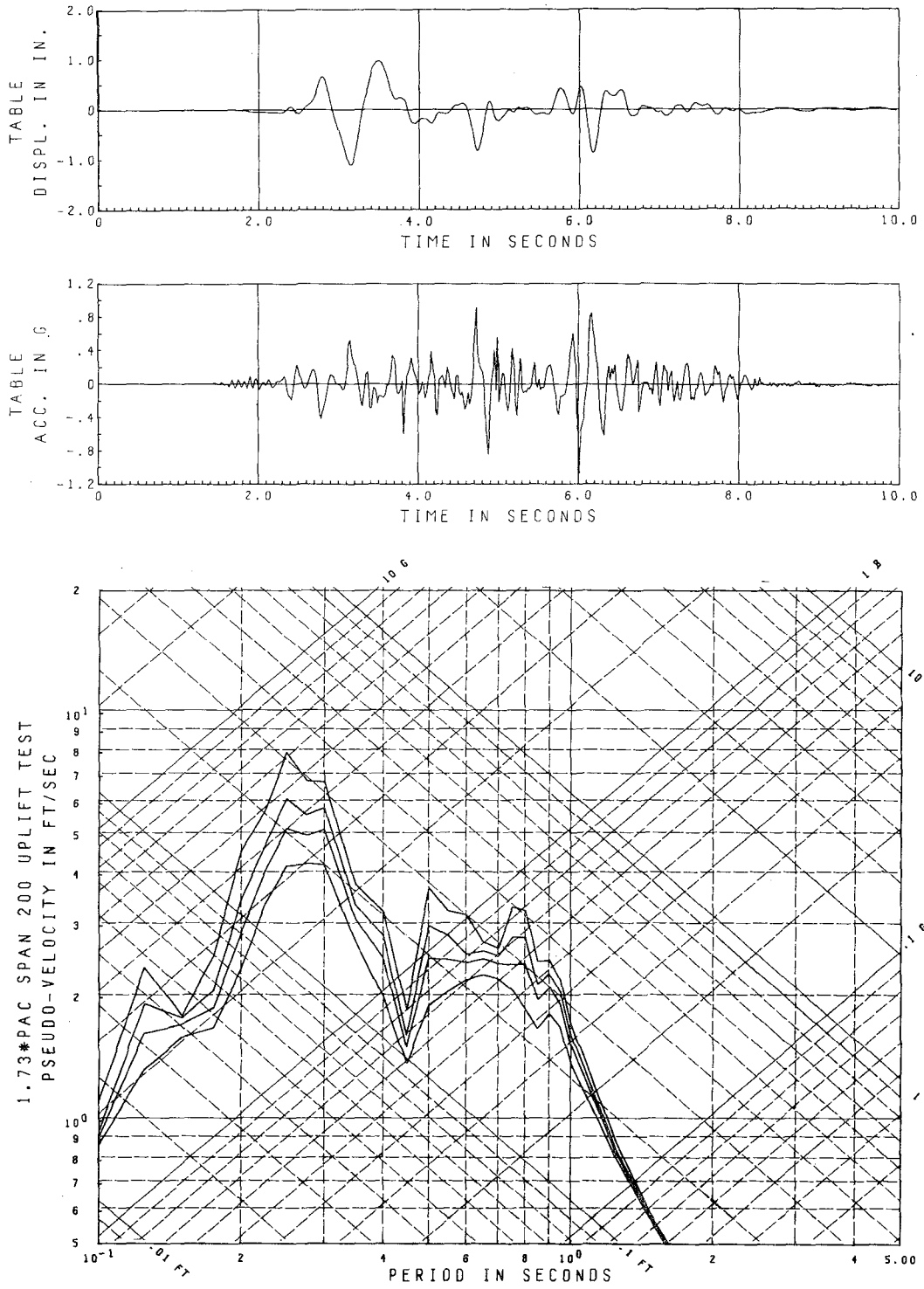

Damping = .01, .02, .03, .05 Critical

Fig. 5.B.5 1.73*PAC Span 200 Horizontal Table Motion Uplift Test

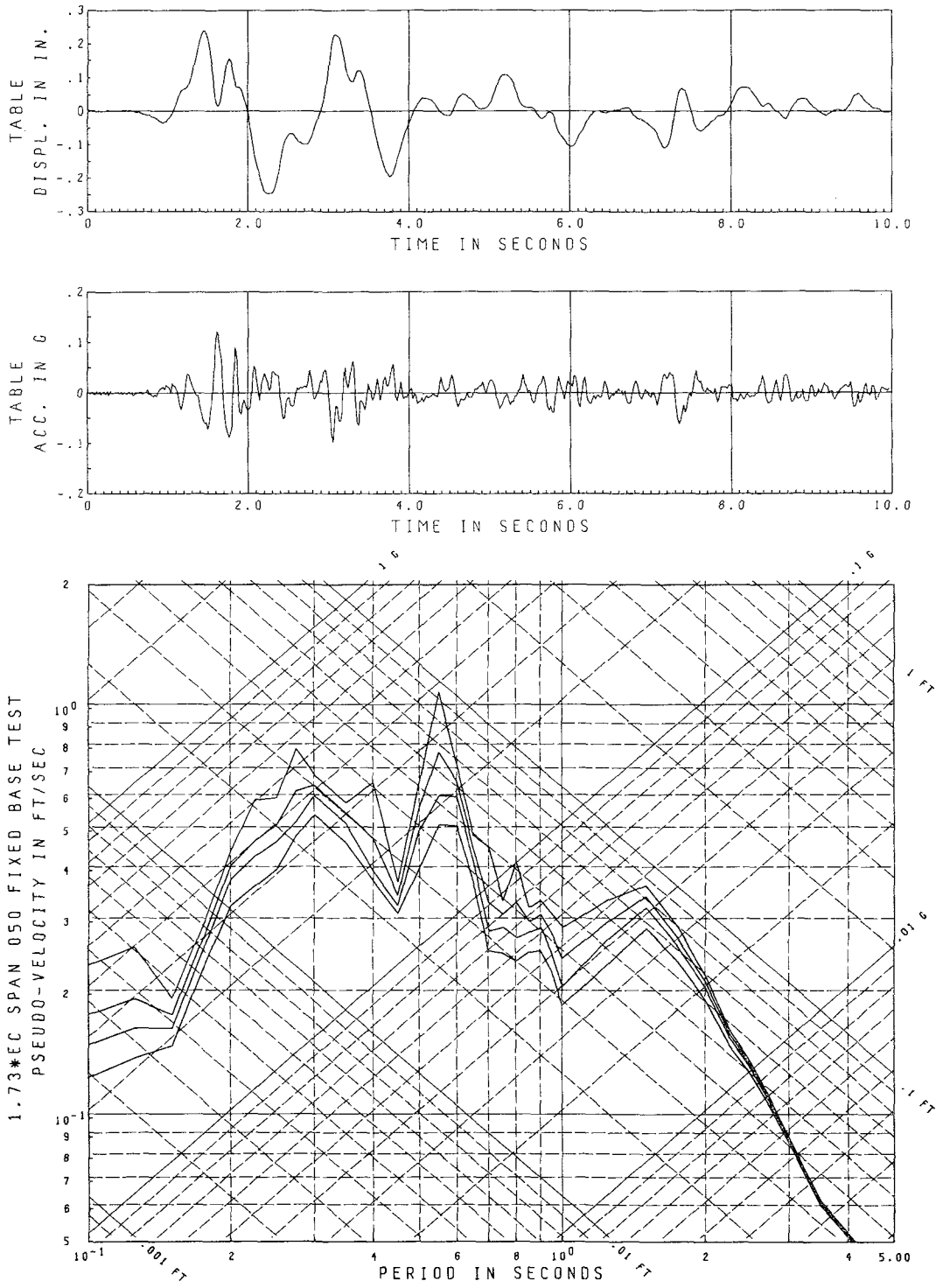

Damping = .01, .02, .03, .05 Critical

Fig. 5.B.6 1.73*EC Span 050 Horizontal Table Motion Fixed Base Test

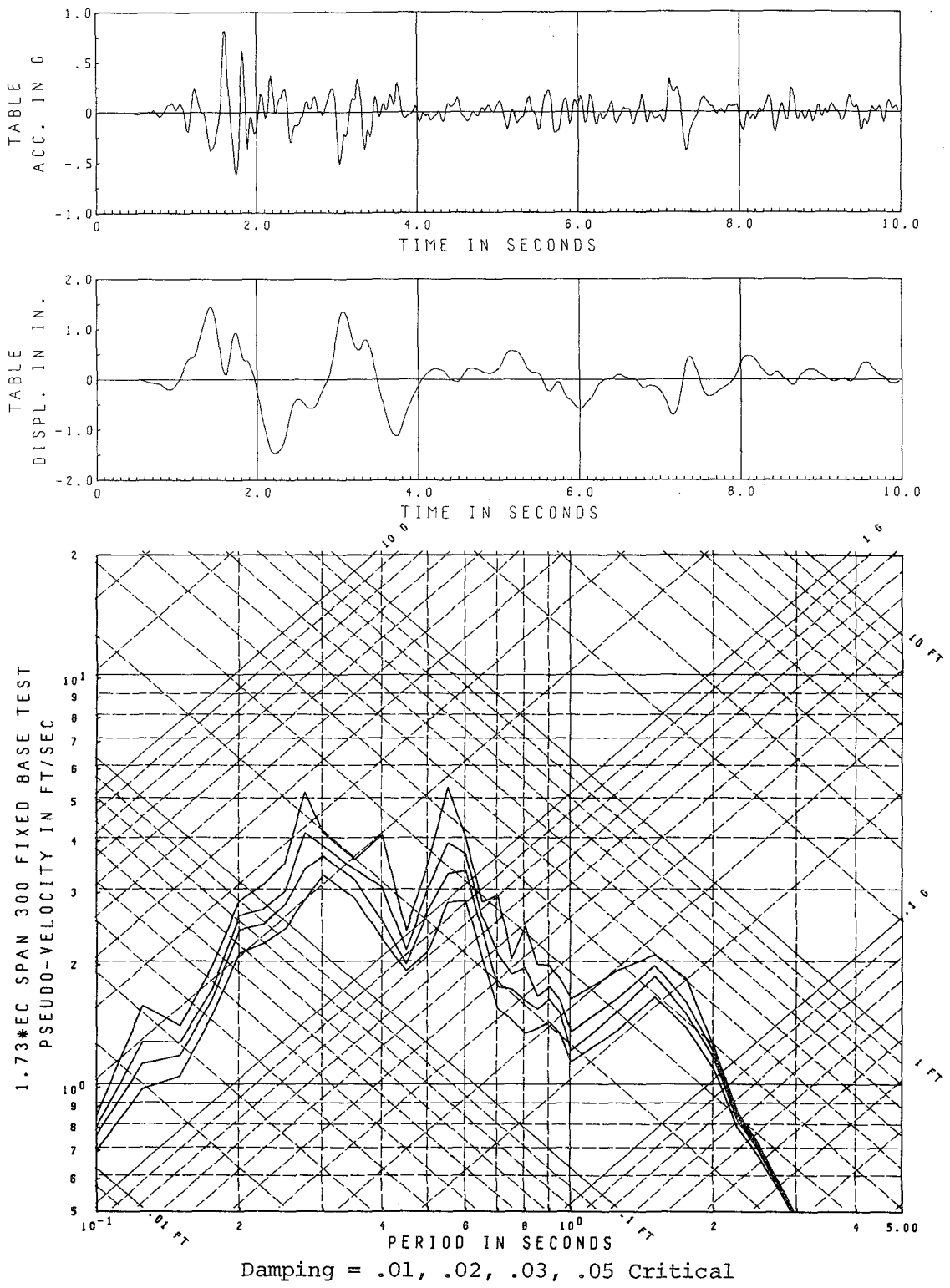

Fig. 5.B.7 1.73*EC Span 300 Horizontal Table Motion Fixed Base Test

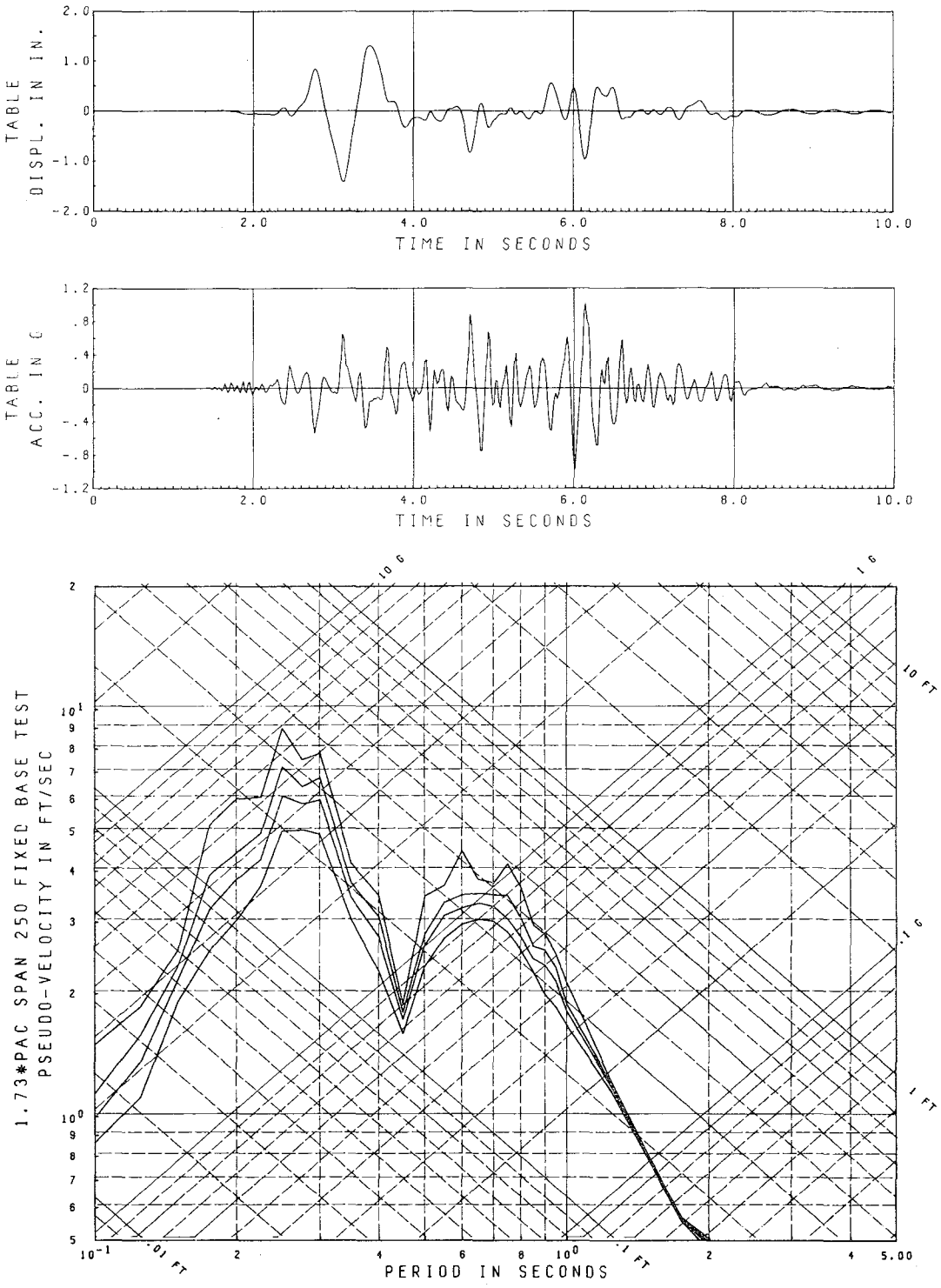

Damping = .01, .02, .03, .05 Critical

Fig. 5.B.8 1.73*PAC Span 250 Horizontal Table Motion Fixed Base Test

6. EXPERIMENTAL RESULTS

Description of Experimental Data

As indicated in Chapter 5, seven tests were selected for detailed data reduction: four tests with column uplift allowed and three tests in the fixed base condition. Of the four uplift tests, three had a significantly nonlinear uplifting response. Of the three fixed base tests, two had significant nonlinear response due to yielding of critical sections.

Data reduction was carried out on two levels: global structural performance and local member behavior. Global response quantities were examined for all tests; the response quantities considered were story accelerations, shears and displacements, uplift displacements, and the base overturning moment. Local member behavior was examined only for the nonlinear cases, and was confined in those cases to members in which significant nonlinear behavior took place. These members were the first floor columns and the first floor interior girder.

In order to have a more compact data presentation, certain representative response quantities are presented rather than the totality of data collected. For example, alternate floor accelerations and displacements are plotted rather than values for all nine floors. Little information of interest is excluded and the selected data can be presented in a more readable manner. The table motion plots of Chapter 5 are presented again, for convenience, with each "package" of test data. The sign convention adopted for data presentation is that all accelerations and displacements are positive to the right (south) and upward. Local force quantities are positive as shown in Fig. 6.1.

Selected maximum (envelope) response quantities are listed in Table 6.1. As can be seen from this table, a wide range of response levels is represented by the seven selected tests.

6.A. 1.73*EC Span 050 Uplift Test

This test, with a peak table acceleration of 0.14 g, produced an essentially linear response. It is of interest to note that the response to this ground motion corresponded very closely to the requirements of the California hospital code for the hypothetical prototype structure.

Fig. 6.A.1 characterizes the table motion. The relative floor displacements shown in Fig. 6.A.2 show a dominant 1st mode response. A more significant 2nd response was evident in the floor accelerations of Fig. 6.A.3. It can be seen here that the reduced 2nd mode response of the 7th floor was generally in phase with the 9th floor but out of phase with the lower floors. This fact is an indication of the correctness of the calculated 2nd mode shape shown in Fig. 3.C.2, which indicates the 2nd mode node point is slightly below the 7th floor. The story shear and base overturning plots of Fig. 6.A.4 again show a dominant 1st mode response.

6.B. 1.73*EC Span 300 Uplift Test

The response observed during this test showed a significant amount of column uplift. The table motion, shown in Fig. 6.B.1, indicates the high intensity of the input. The relative floor displacements, shown in Fig. 6.B.2, indicate an increase of the first mode period from 0.5 sec. to over 0.7 sec. for the highest amplitude cycles. This increase corresponds to a reduction in the effective

first mode stiffness by a factor of about one-half. The actual 1st mode tangent stiffness at the peak displacement was, of course, reduced even more, as was discussed in section 3.B.

The column uplift plots of Fig. 6.B.3 show maximum amplitudes of about 1" for the exterior columns and ½" for the interior columns. In addition, it is apparent that for the highest amplitude cycles, three of the four columns were separated from the foundation.

The floor accelerations of Fig. 6.B.4 show the highly nonlinear effect of column uplift. Intense but very short-lived transient accelerations were generated by the impact of column bases returning to the foundation. This phenomenon also was apparent in the story shears and base overturning moment shown in Fig. 6.B.5. The relatively "flat-topped" peaks of the base overturning moment indicate the action of column uplift as a limiting factor for overturning response.

The 1st floor column forces shown in Fig. 6.B.6 also demonstrate the "fuse" action of column uplift. The "flat-topped" peaks of the axial force plots indicate the levels of static compression; the total axial force in a column separated from the foundation must be zero. The column shear plots again show the influence of impact-induced transients.

The 1st floor column moment plots of Fig. 6.B.7 also demonstrate several points of interest. The unusual nature of the bottom moments, in particular, demonstrates the effect of a sudden transition to a pinned-base condition as the basic plate tilts during uplift motion. The level of dynamic moment at the column bases during uplift was again an indication of the static load levels. The north exterior column moment, for example, shows that the theoretical static moment distribution

shown in Fig. 3.C.3 did not exist, due to fabrication and erection tolerances of the neoprene pads and column bases.

The moments and shear for the 1st floor interior girder are shown in Fig. 6.B.8. The response is seen from these plots to be essentially symmetric in nature for this member. The hysteresis plots of Figs. 6.B.9 and 6.B.10, presenting data for the 1st floor interior column and girder respectively, show that the local member behavior was very nearly linear for this test. The bending strains were higher for these two members than any other members in the frame, therefore, it is evident that no inelastic response was produced.

6.C. 1.73*EC Span 300/300 Uplift Test

This test was, as nearly as possible, a repeat of the preceding test except for the addition of the independent vertical component of table motion. The two components of table motion are shown in Figs. 6.C.1 and 6.C.2.

The relative floor displacements, shown in Fig. 6.C.3, although slightly lower in amplitude, were very similar to those of Fig. 6.B.2. The same observation holds for the uplift plots of fig. 6.C.4, compared to those if Fig. 6.B.3.

The floor accelerations of Fig. 6.C.5 show an even greater similarity to those of the previous test. The story shears and base overturning moment shown in Fig. 6.C.6 also are not appreciably different from those of the test case without a vertical component of table motion.

It would appear from the results observed in this test that the vertical component of excitation did not have a significant effect on the response of the structure. The amplitude of uplift motion was

reduced slightly, but no doubt that is sensitive to the phase of the uplift response compared to the vertical table motion. The same reducing effect was observed for the Pacoima test signals, but probably the opposite effect could be observed for some other specific ground motions. The lateral loading on the structure, however, appears not to be sensitive to the vertical excitation.

It should be pointed out that the static gravity loading on this structure was quite low, and the natural frequencies responding to vertical excitation were quite high. The observations concerning the lack of importance of vertical excitation of this structure should not be generalized to apply to structures not meeting these criteria.

6.D. 1.73*PAC Span 200 Uplift Test

This test, the first discussed utilizing the time-scaled Pacoima Dam input motion, produced the highest amplitude uplift response of any test conducted. As shown in Fig. 6.D.1, the input motion was very intense, with a peak table acceleration of more than 1 g.

The relative floor displacements, shown in Fig. 6.D.2, were of a higher amplitude than the El Centro tests. The reason for this fact is evident from the uplift plots of Fig. 6.D.3; the amount of uplift was more than 1.5", 50% greater than that of the El Centro tests.

The floor accelerations of Fig. 6.D.4 and the story shears and base overturning plots of Fig. 6.D.5 show considerably more intense transients associated with the impact of column bases returning to the foundation. Particularly at about 3.8 seconds in the response, when the north foot impacts following the highest uplift cycle, there was a very sharp spike obvious in the base shear and overturning plots. This extremely short-lived impulse seemed to be resisted primarily by

the inertia of the system; it was not nearly so apparent in the local member forces of the figures to follow. It should be pointed out that the actual peaks of extremely short-lived transients could also have occurred between data samples; the discrete samping intervals for these tests was 0.0192 sec.

The 1st floor column forces of Fig. 6.D.6 demonstrate several interesting points. First, the axial force on the exterior column resulting from the column base impact was not as high as might have been expected. Indeed, it will be seen later that the dynamic compression resulting from the increased overturning moment of the fixed base response was even greater than this impact induced compression. Secondly, the dynamic axial compression on the interior column was very low; it was not even as great as the static load on the column. Apparently the exterior column, slamming down first, cushioned to a large extent the impact of the interior column. Thirdly, as already mentioned, the local member forces did not show the full effect of that very intense loading transient at 3.8 seconds in the response.

The 1st floor column moments of Fig. 6.D.7 again showed the interesting effect of the transition to a pinned base condition during uplift. The exterior column base had been reshimmed prior to this test to produce a static moment closer to the theoretical level.

The 1st floor interior girder moments and shear are shown in Fig. 6.D.8. The left and right moments again appeared to be essentially identical, although an uplifting structure can no longer be treated as a symmetric structure.

The hysteresis plots of Figs. 6.D.9 and 6.D.10 demonstrate the nearly linearly nature of the local member behavior, despite the high

uplift amplitudes and intense transient loading conditions.

6.E. 1.73*EC Span 050 Fixed Base Test

This test, essentially a repeat of the 1.73*EC span 050 uplift test except for the base fixity, again produced an essentially linear response. The input motions of Fig. 6.E.1 are seen to be nearly identical with those of Fig. 6.A.1. This test again produced a loading on the structure about equal to the requirements of the California hospital building code, as mentioned previously.

The relative floor displacements, shown in Fig. 6.E.2, were similar in nature to those of Fig. 6.A.2, at least up to about 7 seconds in the response. The discrepancy beyond that point illustrates dramatically the difficulty of predicting a total earthquake response history accurately; the difference in the 1st mode period due to the effect of the impact pads is very small (about .01 sec.), but over a number of cycles the resulting phase shift can be quite significant in the subsequent response.

There were no other really significant differences between the global response quantities in Figs. 6.E.3 and 6.E.4 and those shown previously for the uplift test in Figs. 6.A.3 and 6.A.4; thus it is evident that the uplifting base connections do not materially affect the behavior of the frame unless uplifting actually occurs.

6.F. 1.73*EC Span 300 Fixed Base Test

This test was intended to be a duplicate of the test described in section 6.B except for the substitution of the fixed base condition. As can be seen from Fig. 6.F.1, the table motion was duplicated very closely.

Fig. 6.F.2 indicates that the relative floor displacements were of similar amplitude to the uplift test; the marked period elongation of the uplift test was not evident, however.

The floor accelerations of Fig. 6.F.3 show a dramatic difference from those of Fig. 6.B.4. Although a significant 2nd mode response was present in the fixed base test, the impact-associated transients were not evident. The 1st mode response, moreover, did not contain the fuse effect of the uplift phenomenon, resulting in considerably higher acceleration levels for the fixed base case.

A similar comparison can be made for the story shears and base overturning moment plots of Fig. 6.F.4 and 6.B.5. The increase in base shear for the fixed base case over the uplifting case was about 50%. The increase in base overturning moment was on the order of 100%.

The 1st floor column forces of Fig. 6.F.5, when compared to those of Fig. 6.B.6, illustrate several differnces in the response for the two base conditions. The maximum dynamic axial compression in the exterior column was increased for the fixed base test, even considering the impact effect present in the uplift test. Axial tension was, of course, increased for the fixed base test, because the total axial force in the uplift case could not exceed zero. The shear demand on the exterior column was slightly higher in the uplift test, but only in one direction; it seems reasonable that if only one column out of four remains in contact with the foundation, its share of the total shear would be increased.

The interior columns displayed somewhat the opposite effect. The dynamic tension was somewhat higher for the uplift test; the total tension still could not exceed zero, however. This increased dynamic tension

merely indicates that the total axial load in the interior columns remained compressive throughout the fixed base test. Compression forces for the interior columns were again somewhat lower for the uplift test. Shear forces for the interior columns were reduced for the uplift test as compared to the fixed base test.

Allowing column uplift is thus seen to have a beneficial redistribution effect on the columns; the interior columns carry a more equitable share of dynamic axial force without being required to develop tension, and the exterior columns carry a more equitable share of the total shear.

This redistribution is also apparent in the column moment plots of Fig. 6.F.6 when compared to those of Fig. 6.B.7. By allowing uplift, more "responsibility" for carrying the required column moments is shifted to the exterior columns. This effect is often desirable, as the exterior columns carry less static axial force normally, and moment capacity can be developed more efficiently.

The 1st floor interior girder forces for the fixed base case of Fig. 6.F.7 are seen to be more than 30% greater than those of Fig. 6.B.8. The only reason the increase was not even greater for the fixed base test was that plastic hinges form at the girder ends, which did not occur in the uplift test.

The hysteresis plots of Figs. 6.F.8 and 6.F.9 indicate that although ductility demands were not great for the fixed base test, some local nonlinear behavior took place which was not present in the uplift test.

6.G. 1.73*PAC Span 250 Fixed Base Test

This test was intended as a comparison to the test described in

section 6.D. The table motions of Fig. 6.G.1 indicate the table displacement was slightly greater for the fixed base test, but that the acceleration peaks were of approximately the same value.

The relative floor displacements of Fig. 6.G.2 were lower in amplitude than those of Fig. 6.D.2. The floor accelerations of Fig. 6.G.3, while having peaks of about the same amplitude as the uplift test, were not characterized by the same type of transient spikes as the uplift test. A considerable 2nd mode response is evident in floor accelerations and the upper floor shears, shown in Fig. 6.G.4. The base overturning moment, however, was again dominated by the 1st mode response. If the 1st mode shapes were exactly triangular in form, modal orthogonality would indicate that only that mode would contribute to base overturning.

The column forces of Figs. 6.G.5 and 6.G.6 were very similar in most respects to those of the 1.73*EC span 300 fixed base test, and the same comments made in discussion of that test applied here also.

The 1st floor interior girder moments and shear, shown in Fig. 6.G.7, were again around 30% greater than for the uplift test, and some nonlinear strains were evident.

The 1st floor interior column hysteresis plots of Fig. 6.G.8 is nearly linear in nature; the 1st floor interior girder moment vs. strain hysteresis plots of Fig. 6.G.9 show slightly more nonlinear response.

Fig. 6.G.10 shows the moment vs. average curvature, over a 6" gage length, for the same section as the moment vs. strain plots of Fig. 6.G.9. The average curvature gage length extended inward from the location of the post-yield strain gage station. Fig. 6.G.11 shows the moment vs. rotation hysteresis plots for this same location.

Two points can be ascertained from this series of hysteresis plots. First, strain ductility was considerably higher than average curvature or rotation ductility. Secondly, at least for this steel wide flange section subjected to reverse curvature bending, nearly all the rotation occurred in a "hinge" length equal to the section depth.

TEST	MAX TABLE ACCL	MAX 9th FLR ACCL	MAX 9th FLR REL DISPL	MAX UPLIFTS	MAX STRAINS	MAX BASE SHEAR	MAX OVERTURNING
1.73*EC 050	.144g	.366g	.783"		$.49 \times 10^{-3}$	19^{k}	350 k-ft
1.73*EC 300	.912g	1.267g	3.39"	1.02"	1.41×10^{-3}	60^{k}	907 k-ft
1.73*EC 300/300	.899g	1.442g	3.17"	.81"	1.42×10^{-3}	61^{k}	964 k-ft
1.73*PAC 200	1.075g	1.92g	4.46"	1.69"	1.76×10^{-3}	111^{k}	1423 k-ft
FIXED BASE TESTS							
1.73*EC 050	.099g	.369g	.834"	-	$.51 \times 10^{-3}$	22^{k}	412 k-ft
1.73*EC 300	.813g	1.639g	3.266"	-	2.13×10^{-3}	79^{k}	1427 k-ft
1.73*PAC 250	1.017g	1.892g	3.625"	-	2.10×10^{-3}	78^{k}	1552 k-ft

Table 6.1

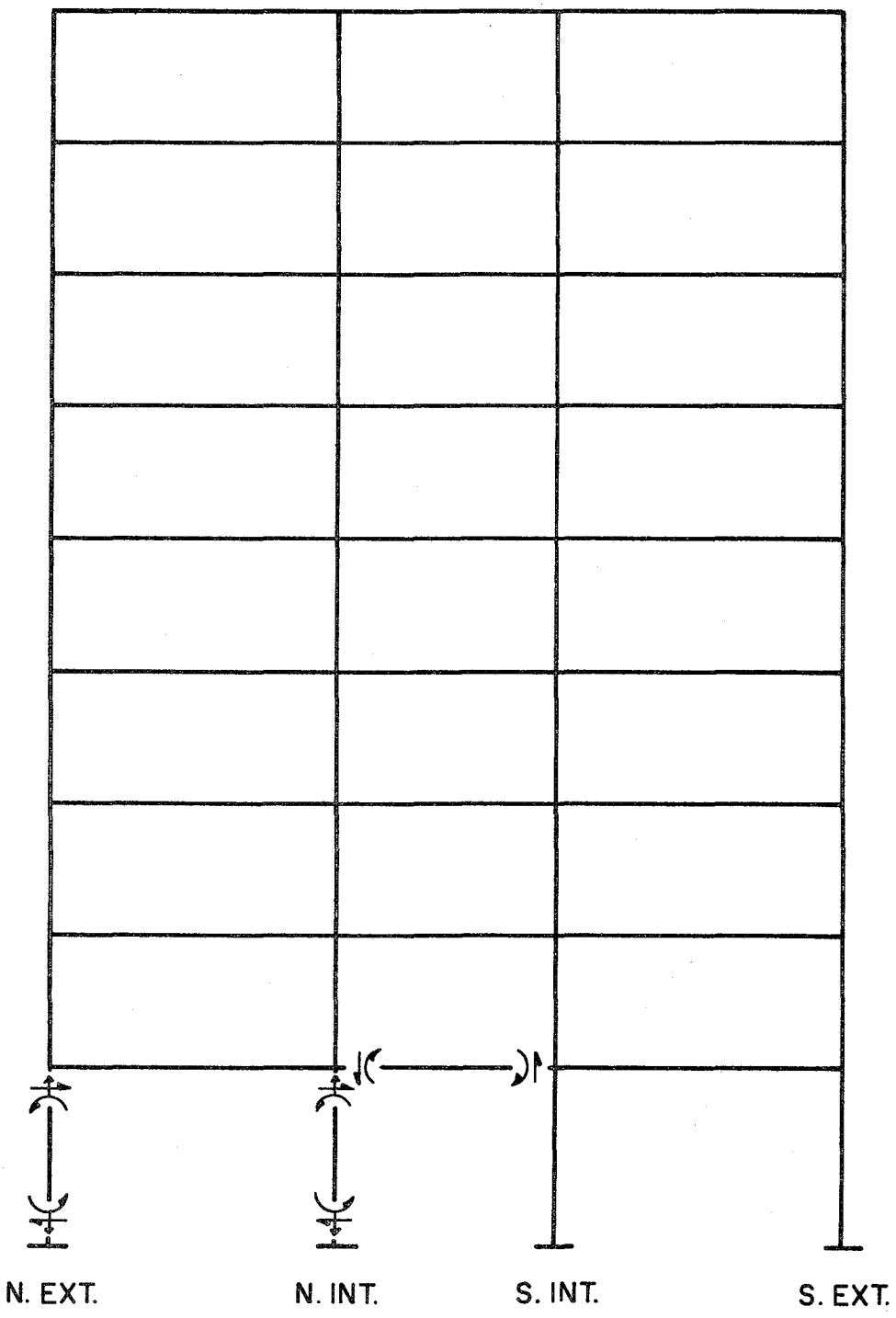

Fig. 6.1 Local Force Sign Convention

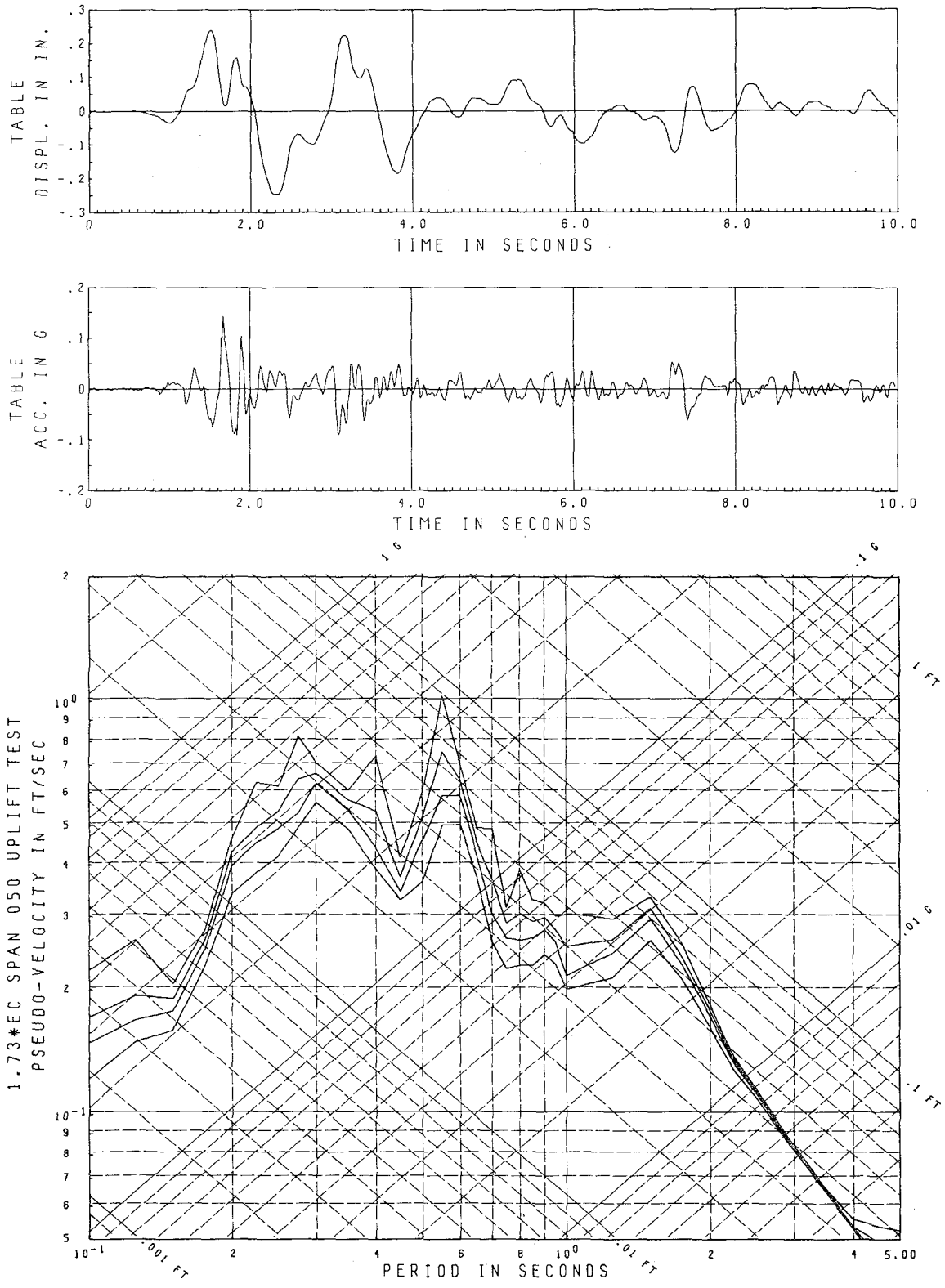

Fig. 6.A.1 El Centro Span 50 Horizontal Table Motion

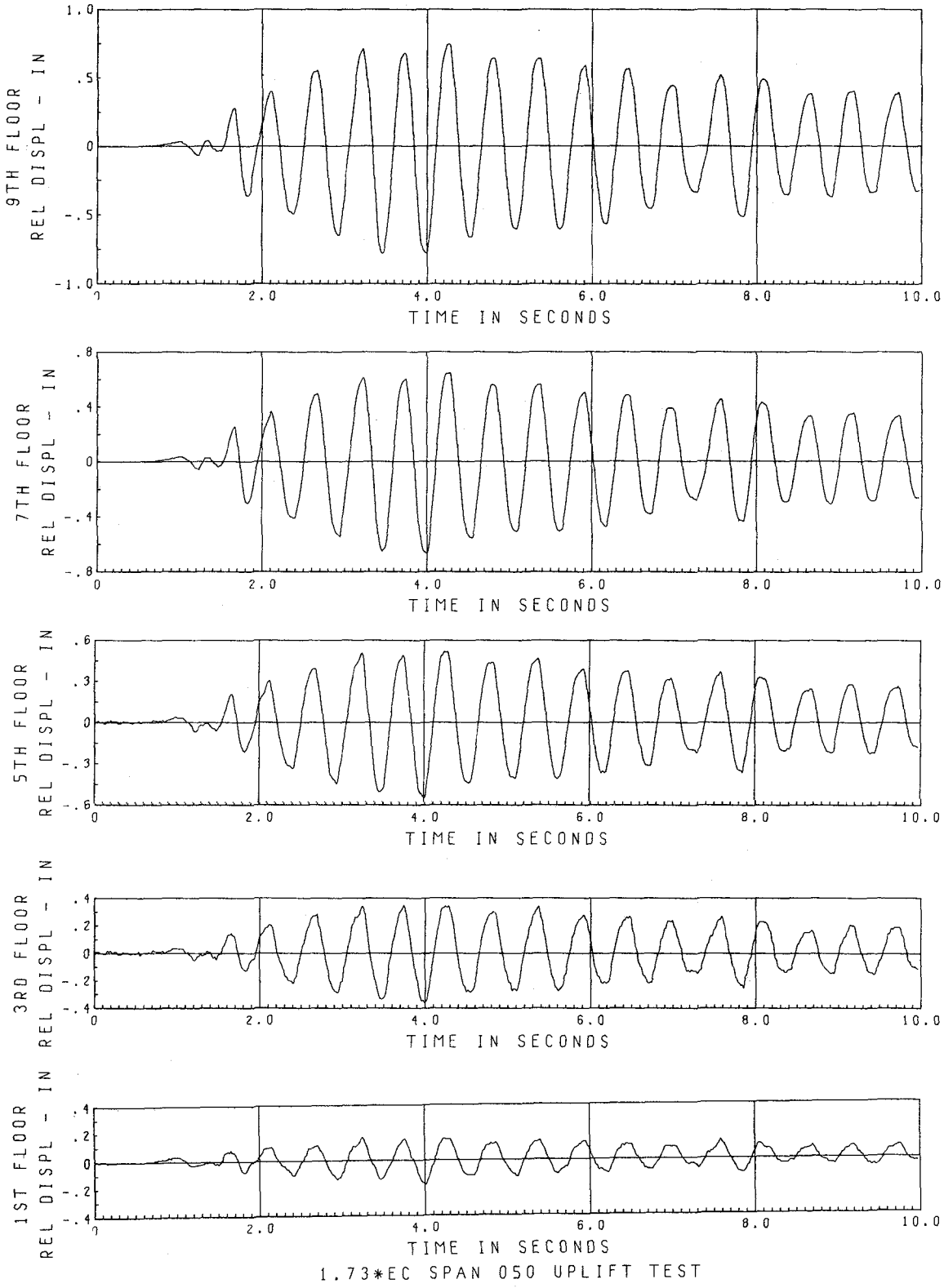

Fig. 6.A.2 Relative Floor Displacements

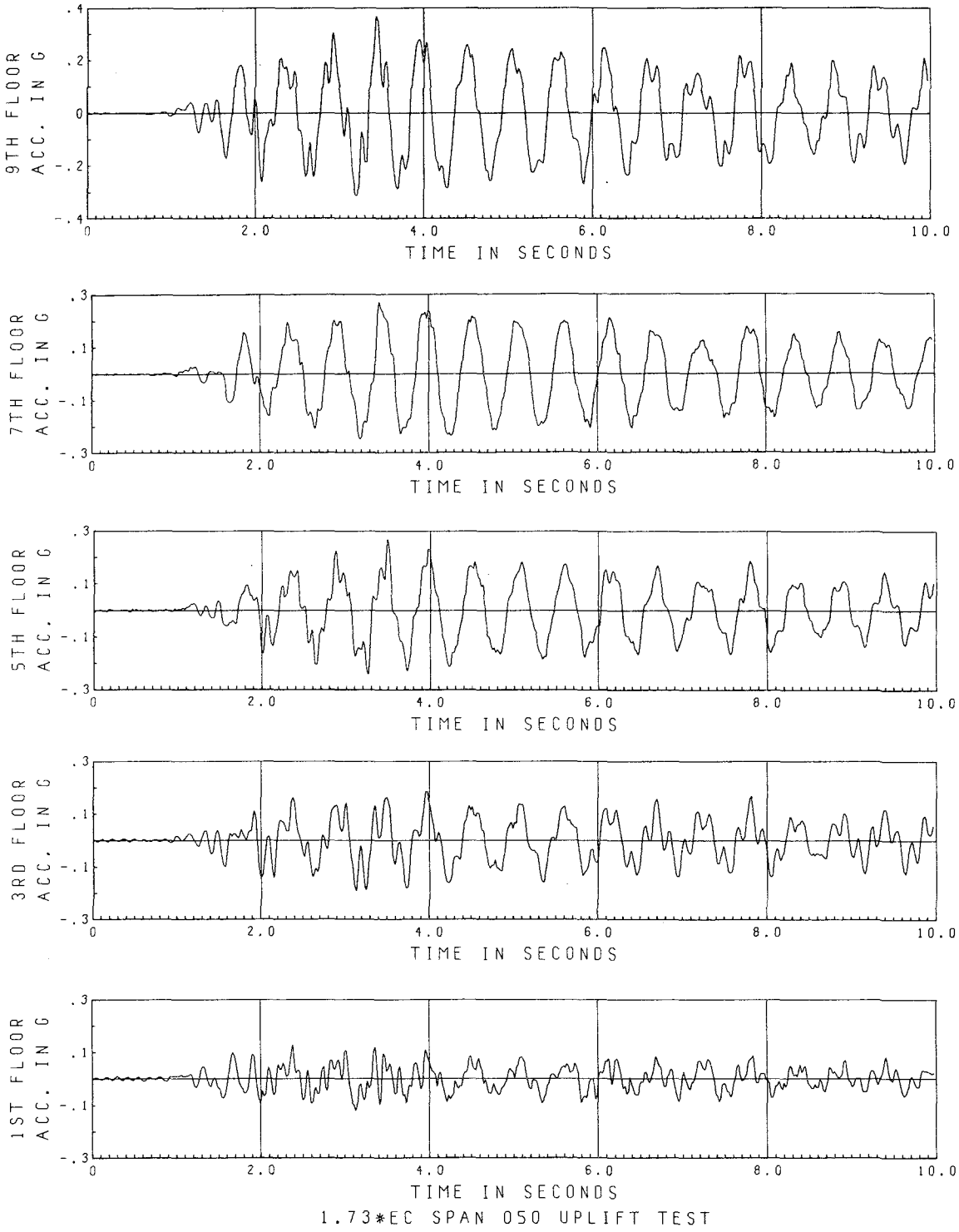

Fig. 6.A.3 Floor Accelerations

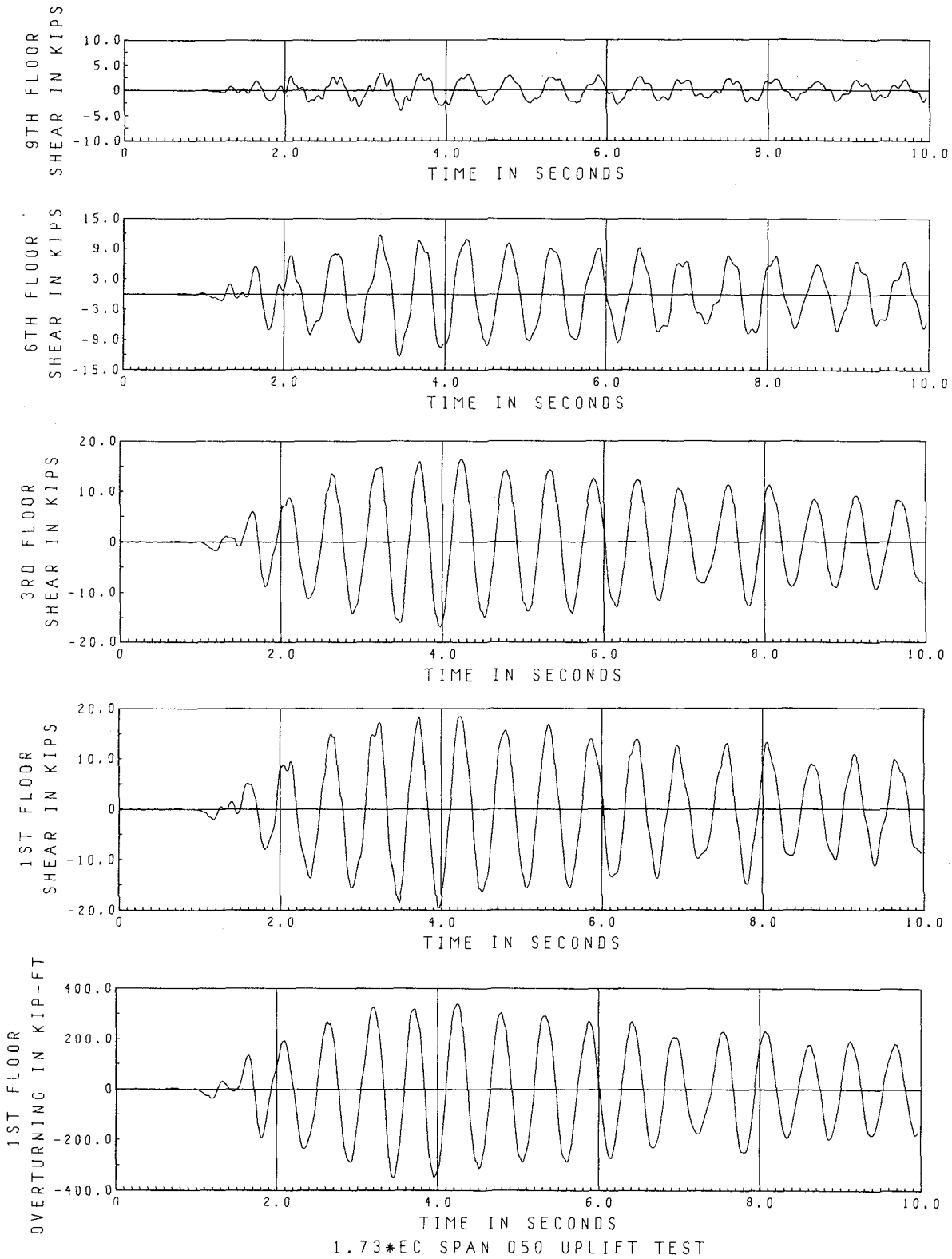

Fig. 6.A.4 Story Shears and Overturning

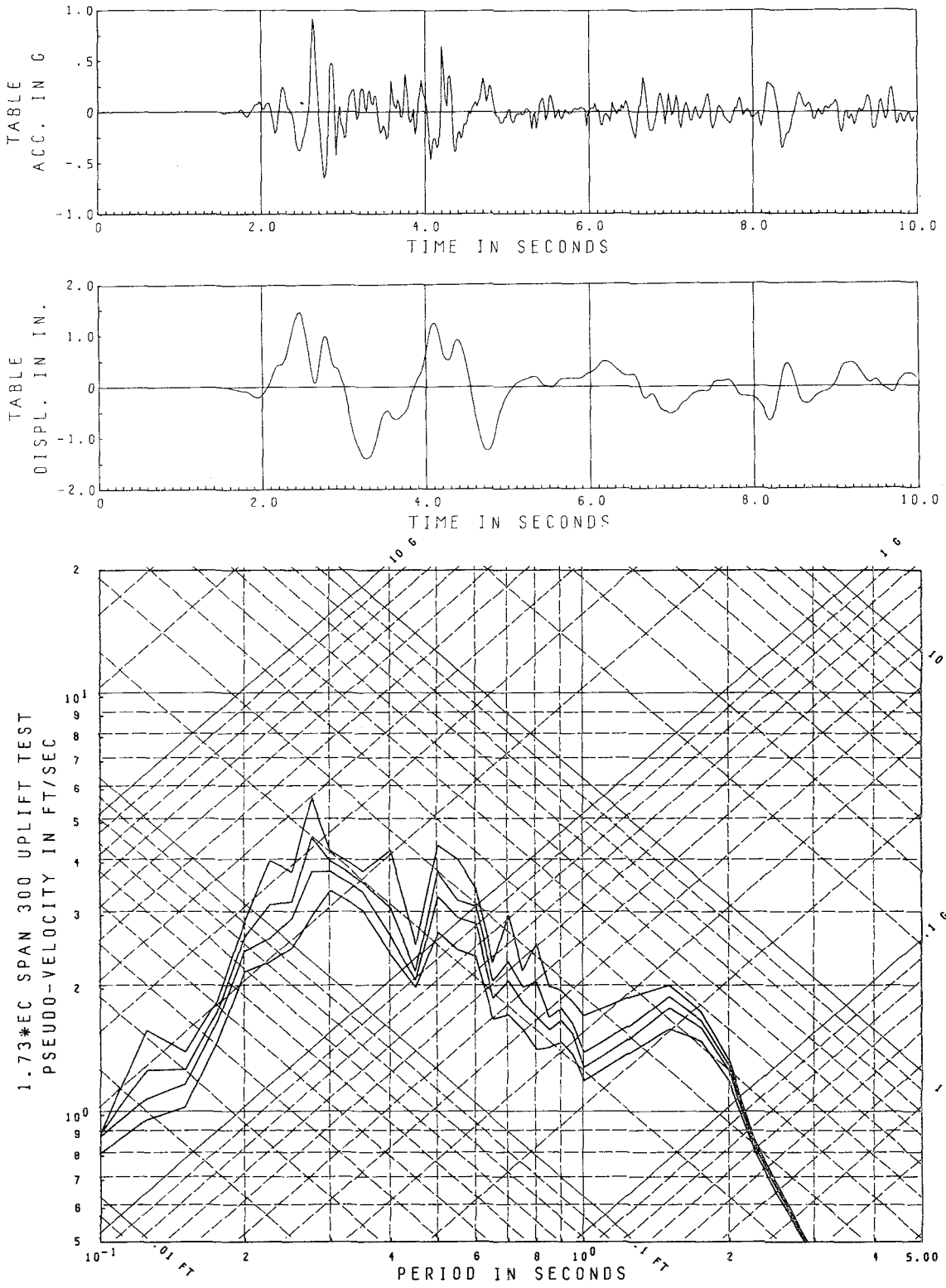

Damping = .01, .02, .03, .05 Critical

Fig. 6.B.1 El Centro Span 300 Horizontal Table Motion

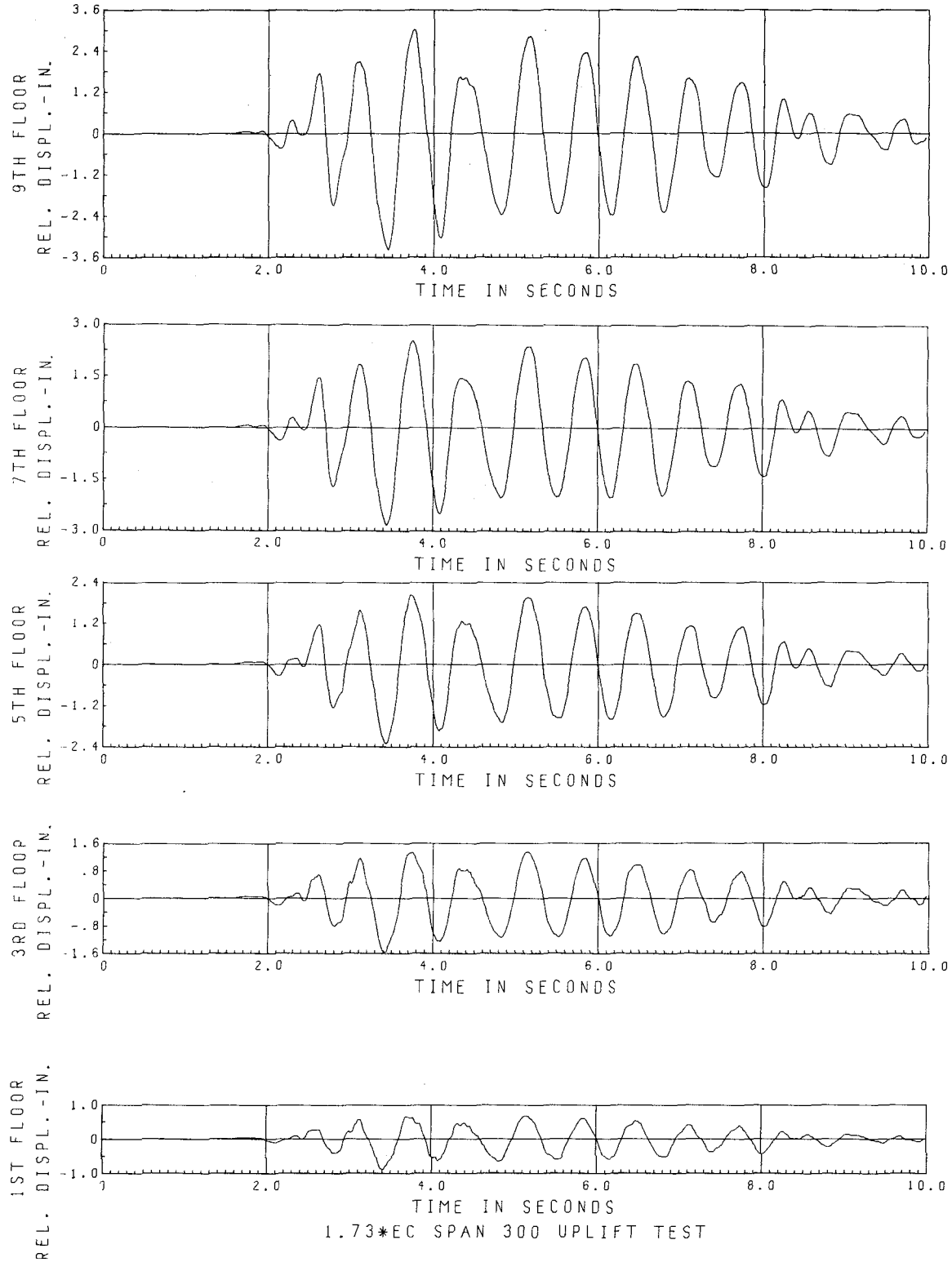

Fig. 6.B.2 Relative Floor Displacements

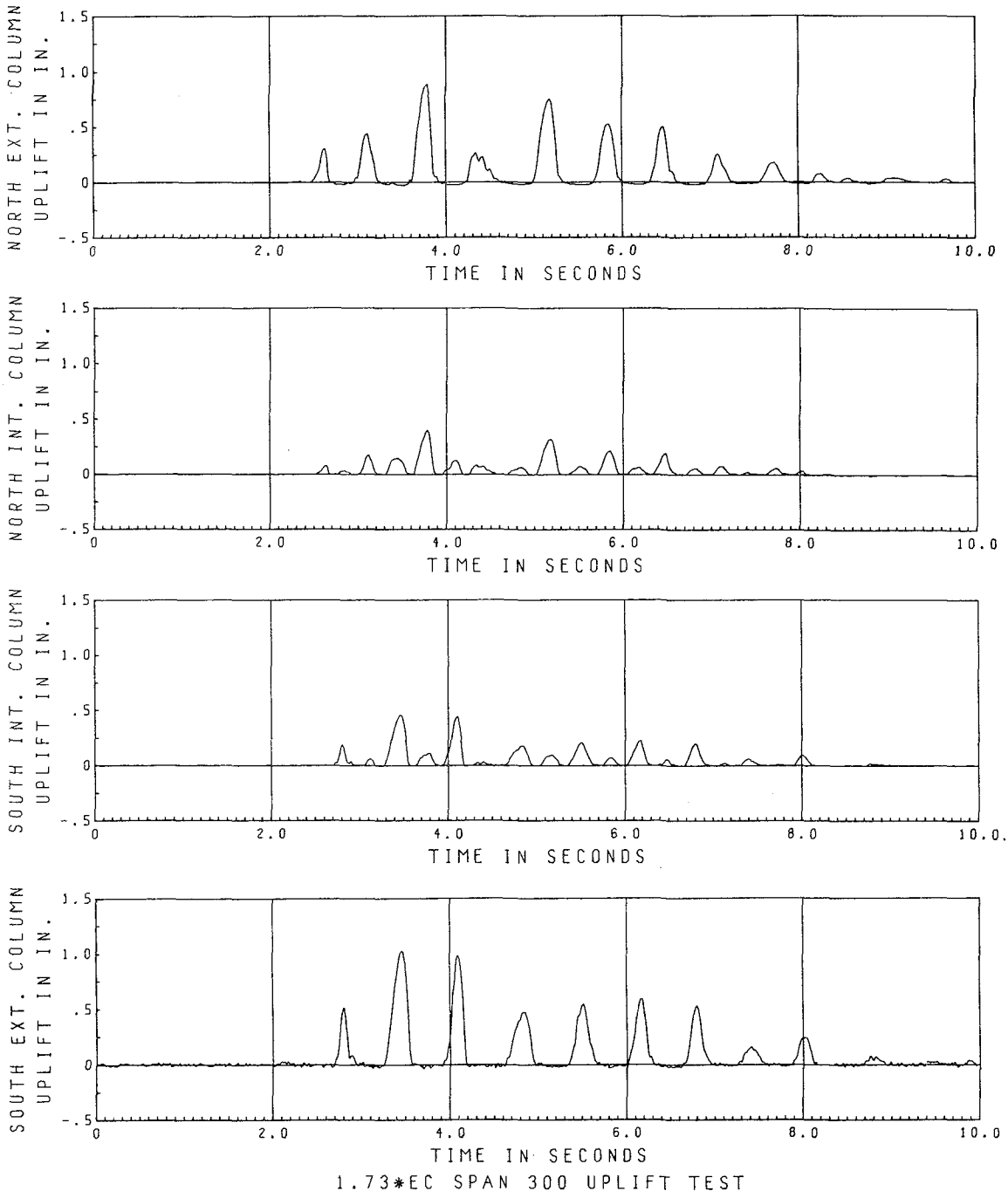

Fig. 6.B.3 Column Uplift Motions

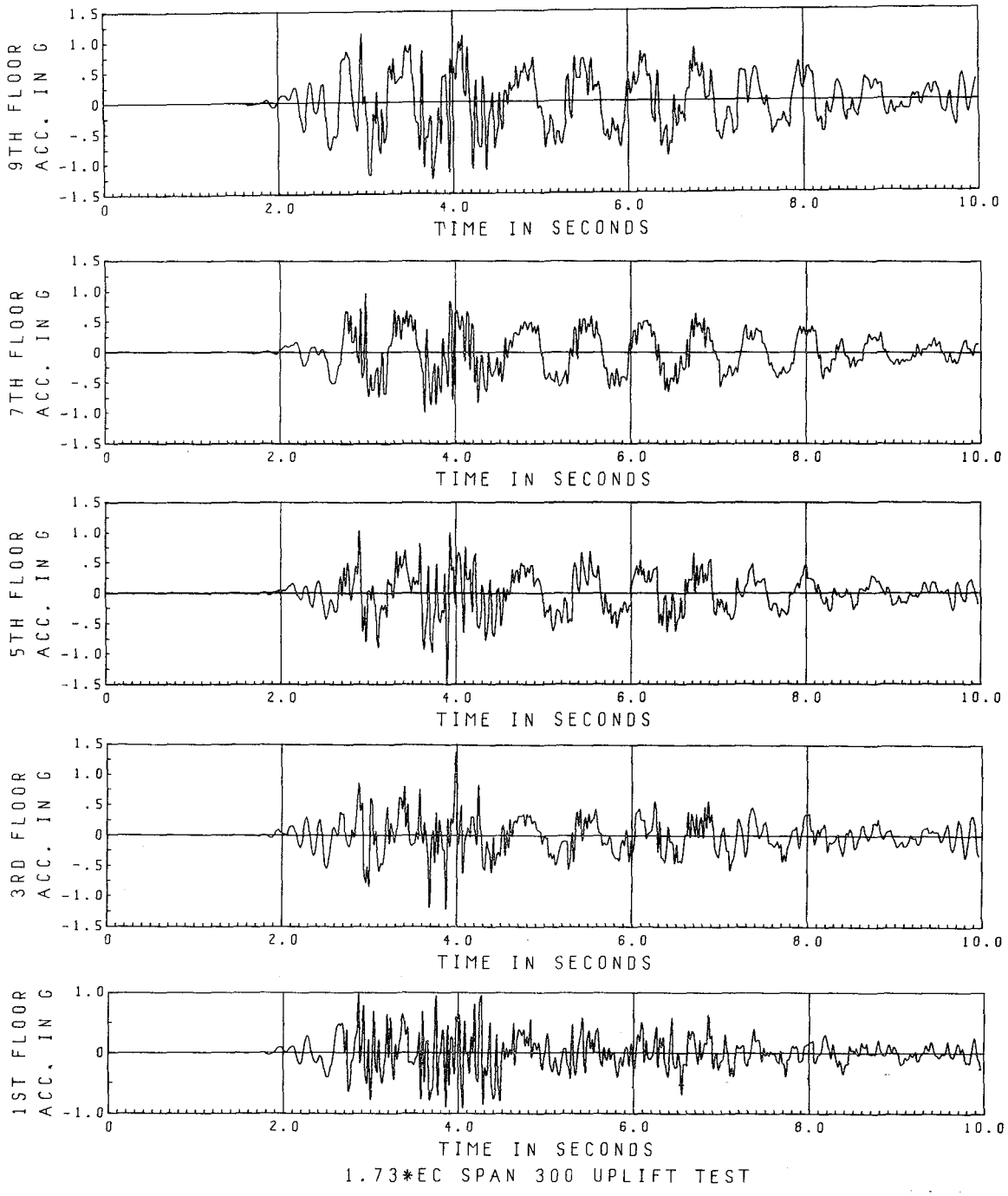

Fig. 6.B.4 Floor Accelerations

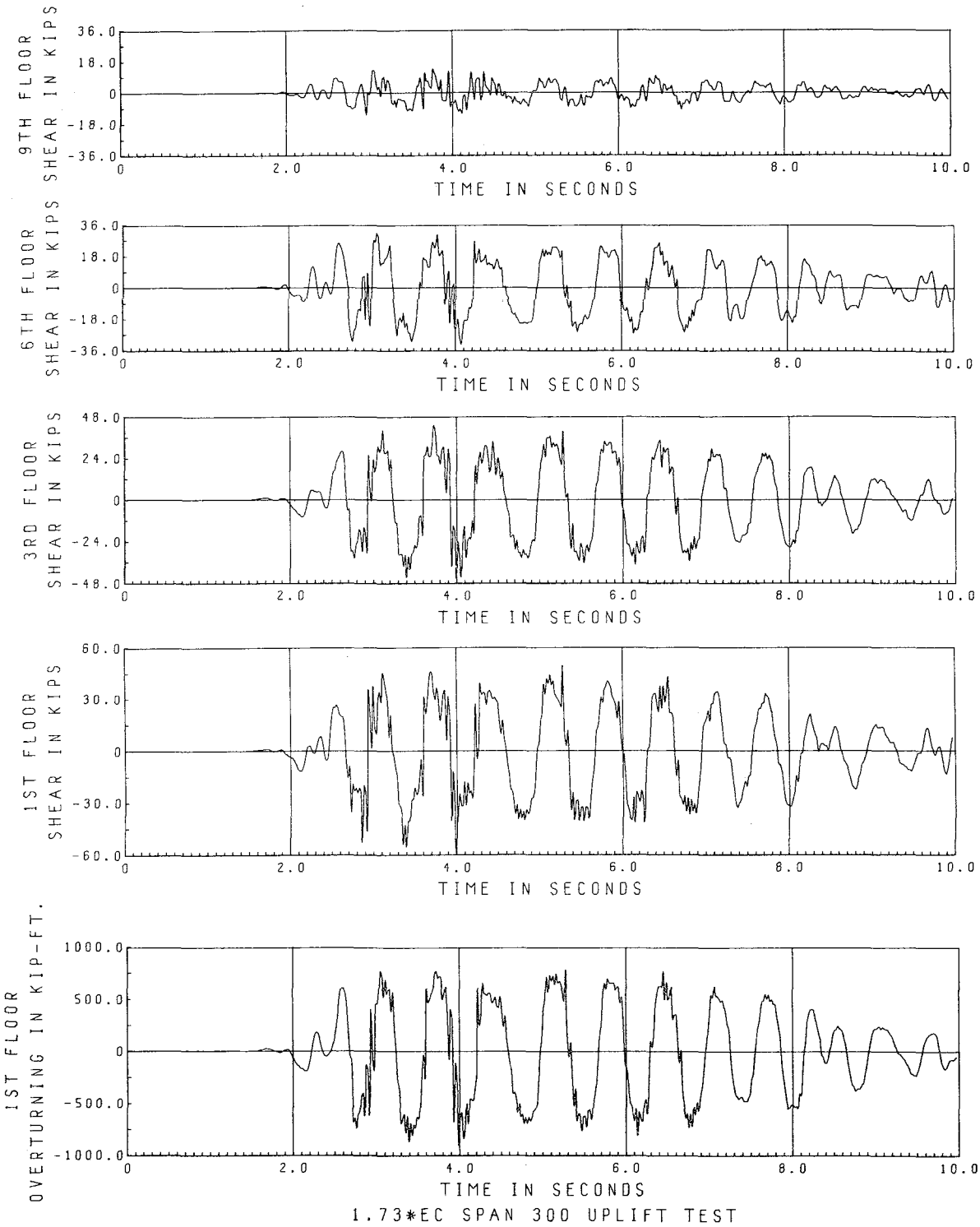

Fig. 6.B.5 Story Shears and Overturning

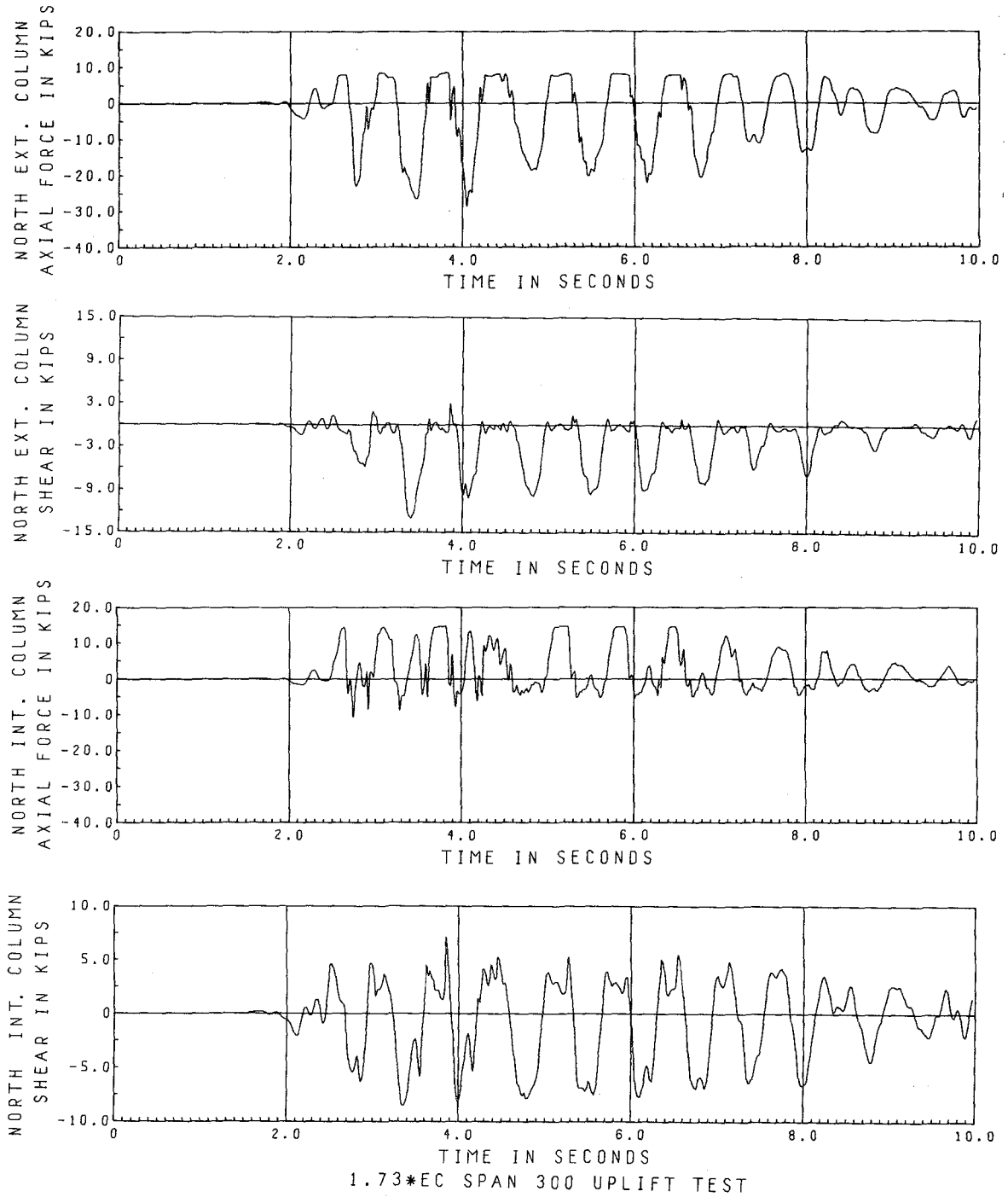

Fig. 6.B.6 1st Floor Column Shears and Axial Forces

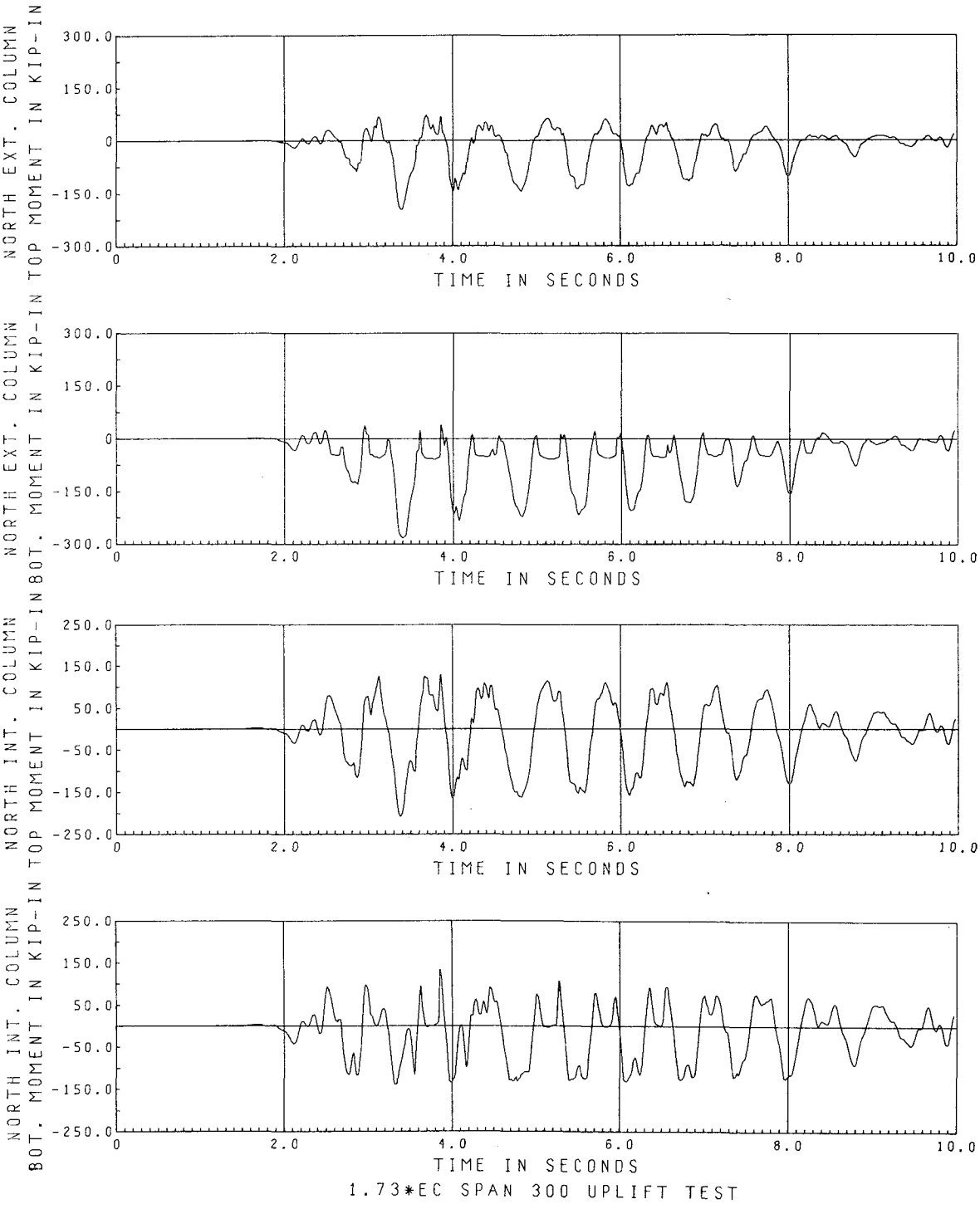

Fig. 6.B.7 1st Floor Column Bending Moments

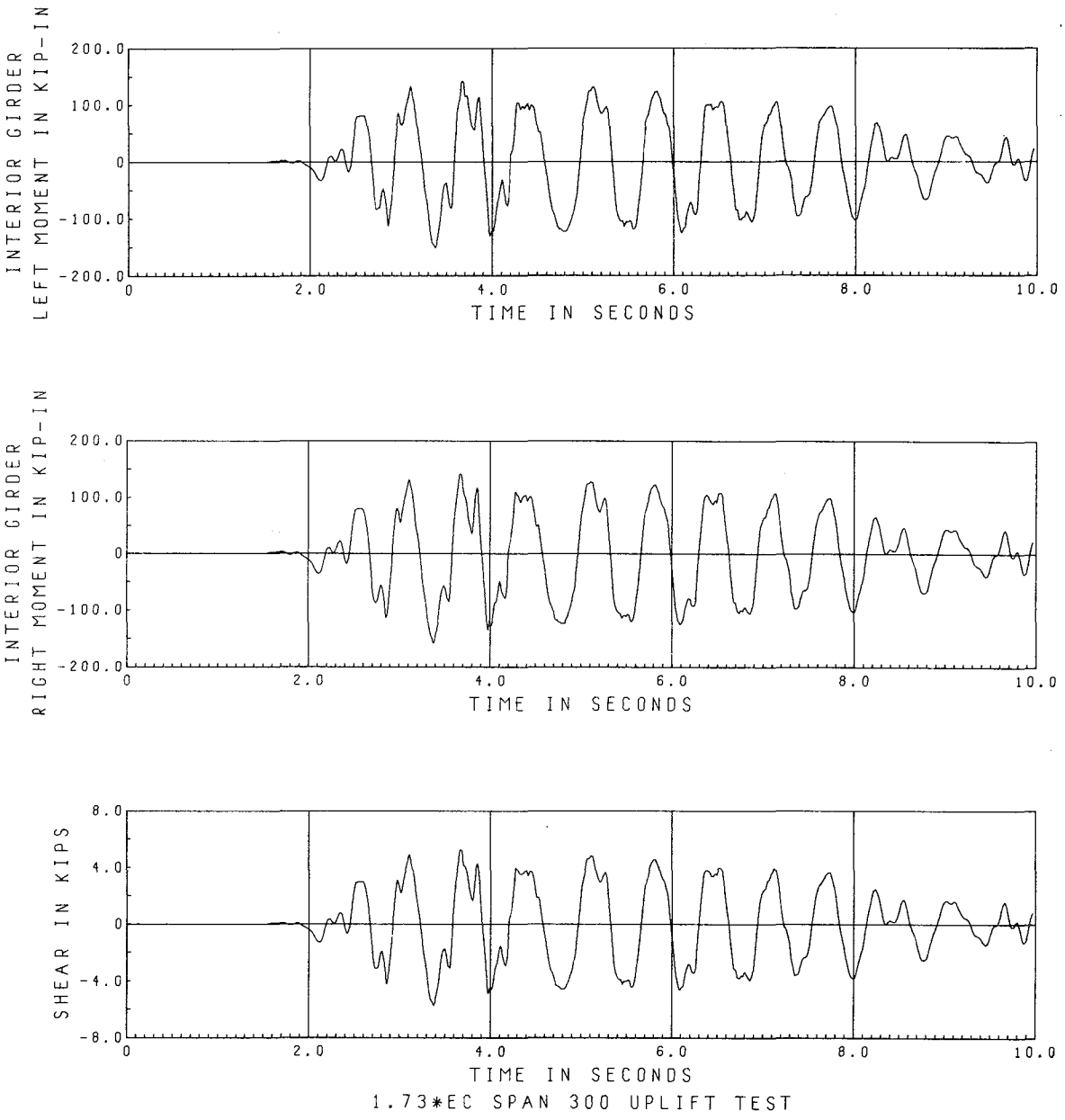

Fig. 6.B.8 1st Floor Girder Shear and Moments

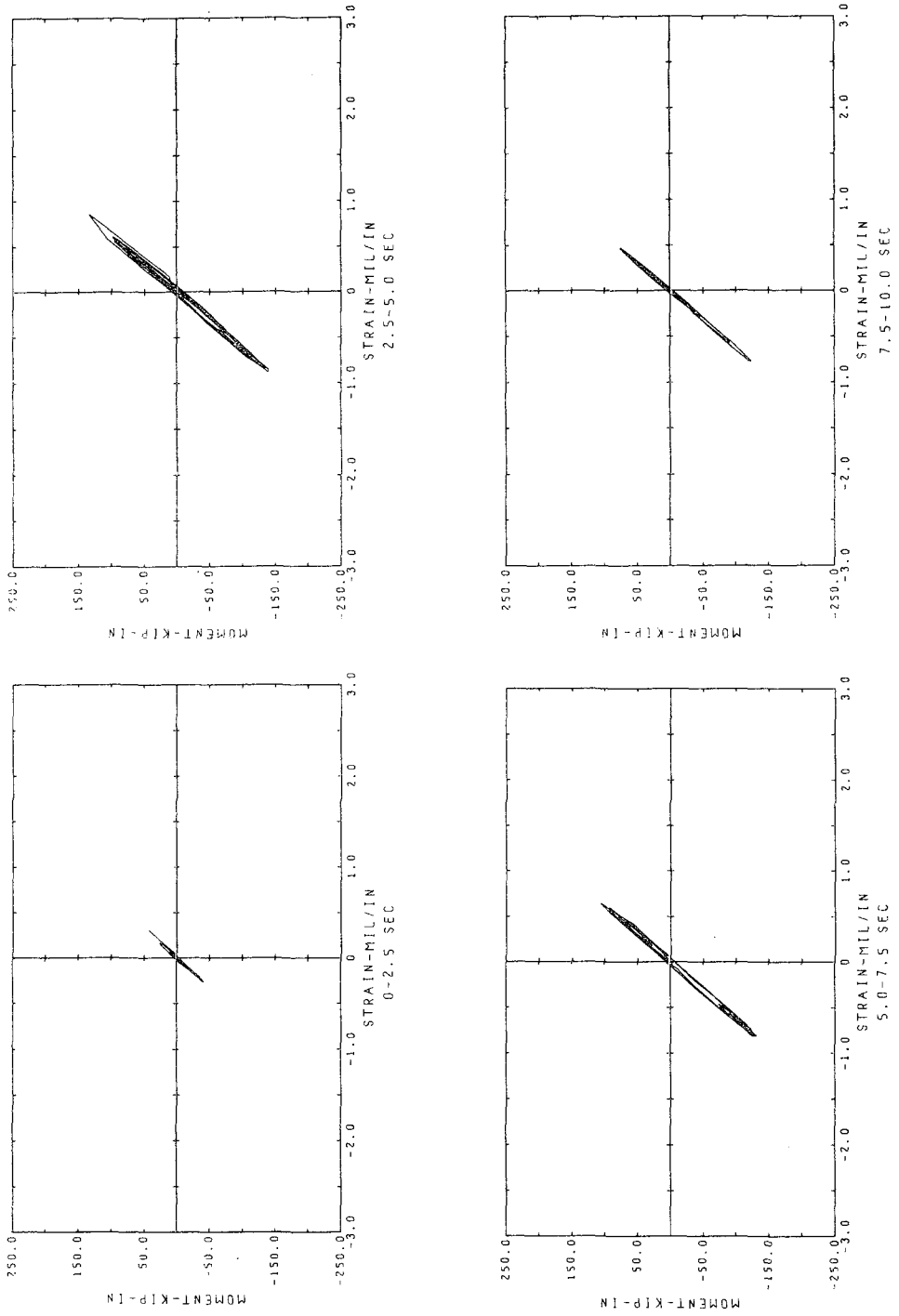

Fig. 6.B.9 1st Floor Column Hysteresis Plots

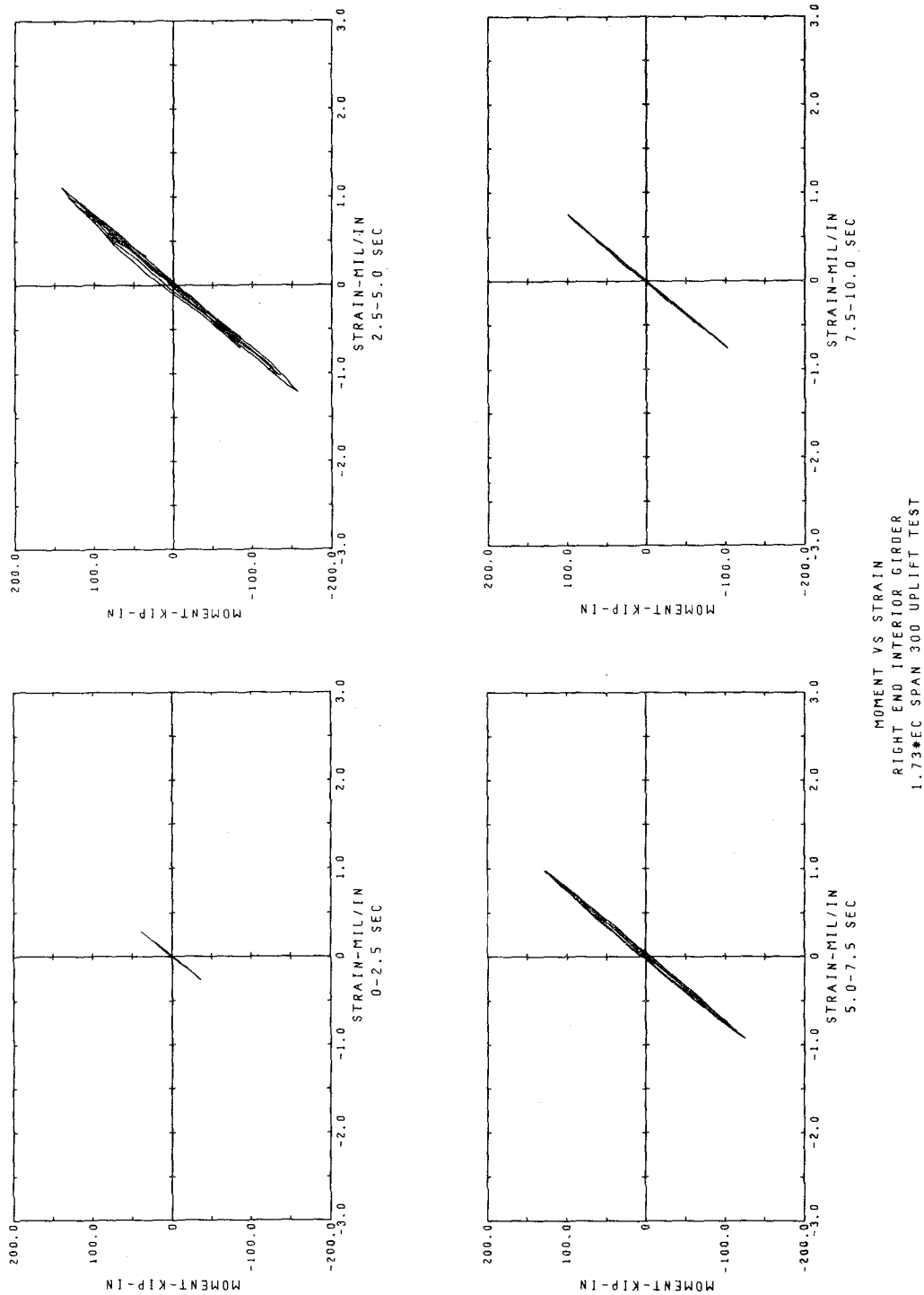

Fig. 6.B.10 1st Floor Interior Girder Hysteresis Plot

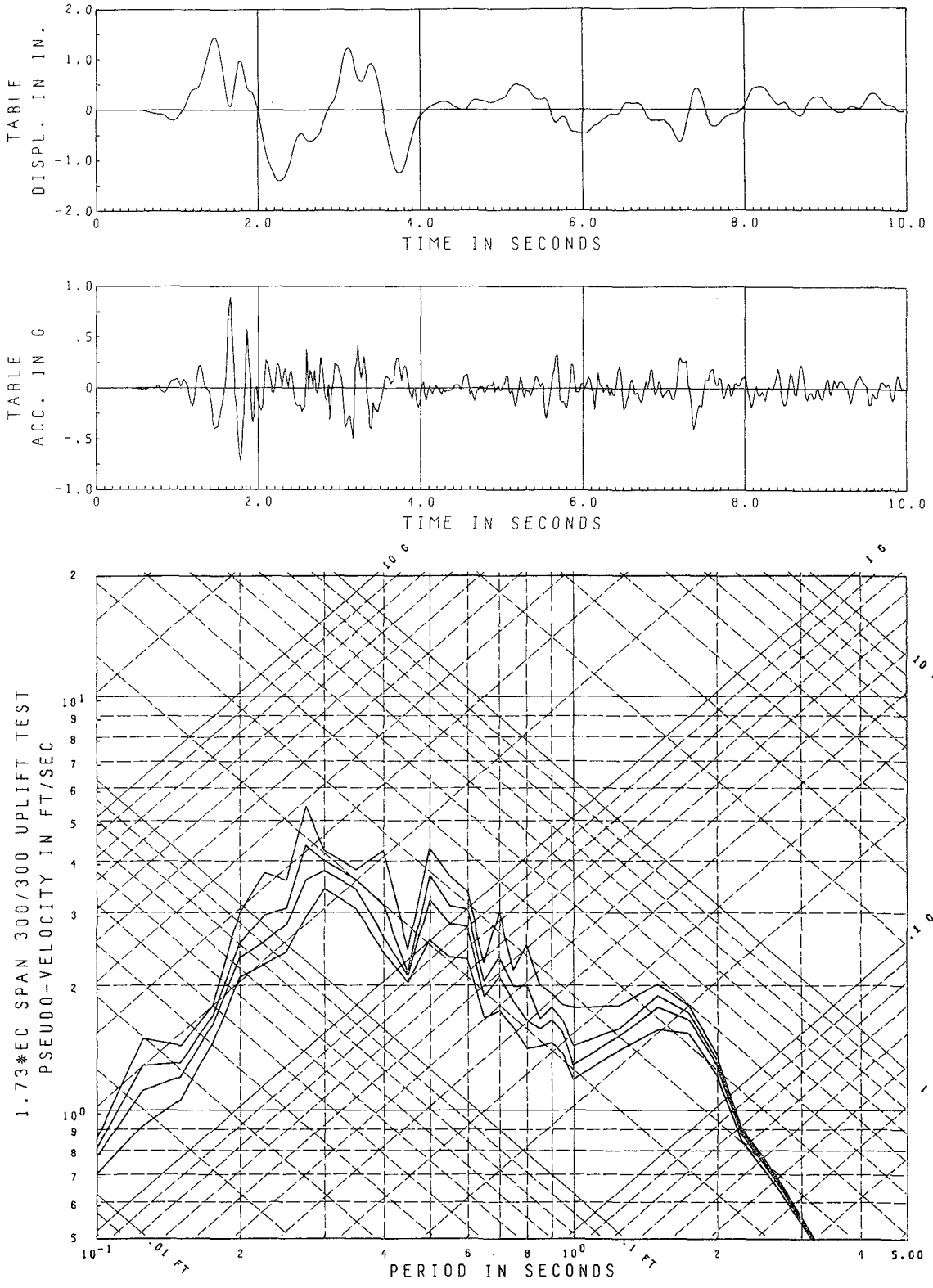

Damping = .01, .02, .03, .05 Critical

Fig. 6.C.1 El Centro Span 300/300 Horizontal Table Motion

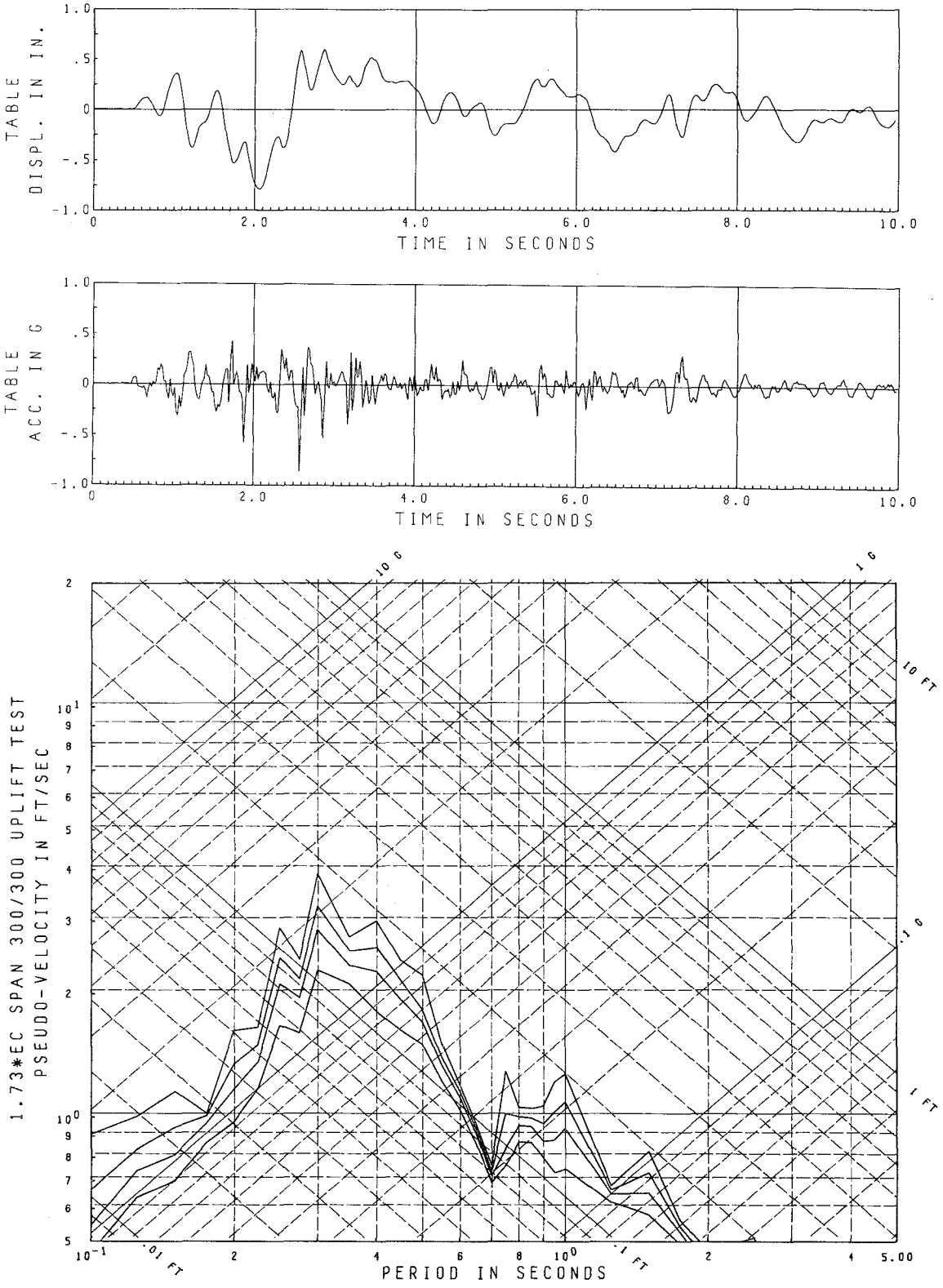

Damping = .01, .02, .03, .05 Critical

Fig. 6.C.2 El Centro Span 300/300 Vertical Table Motion

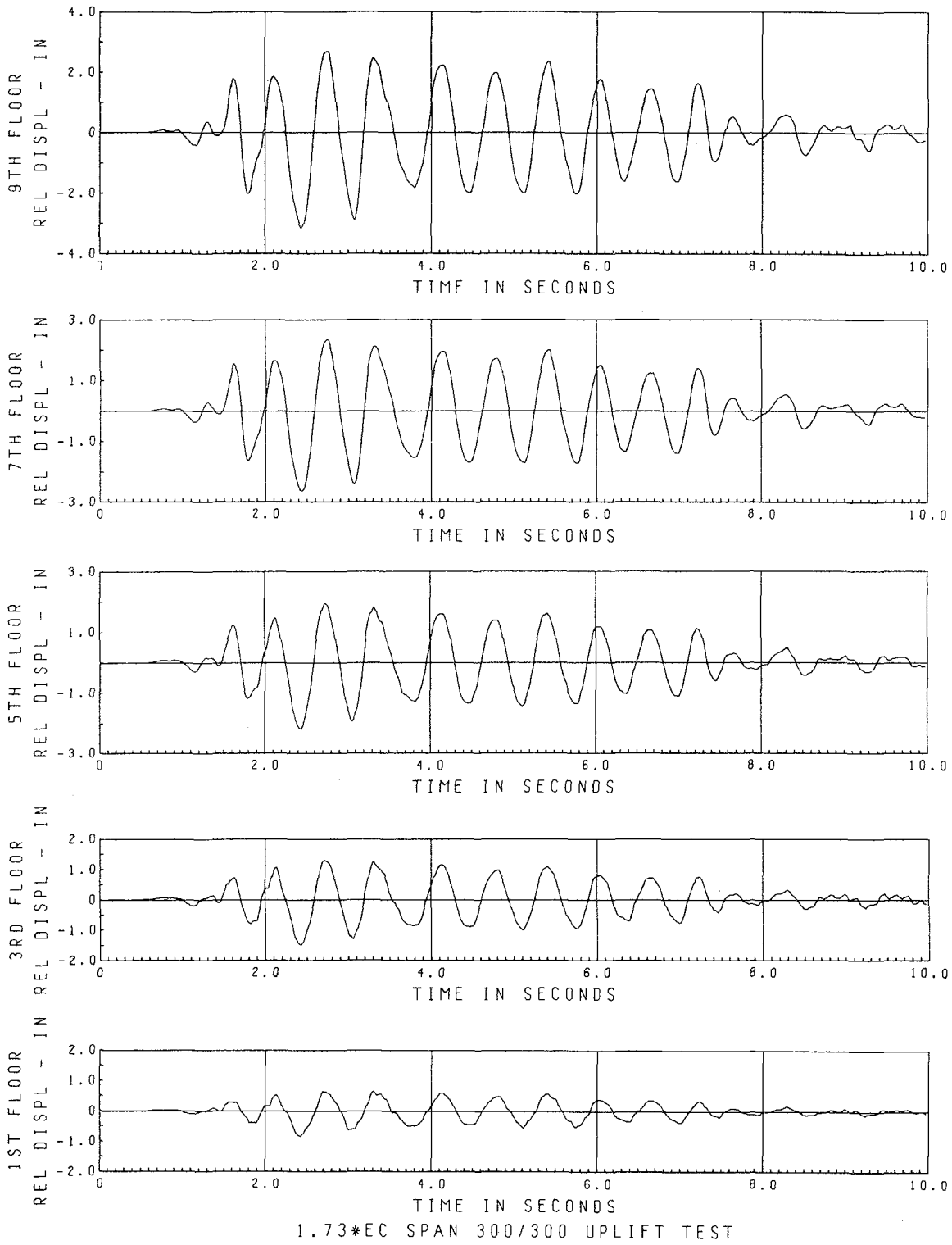

Fig. 6.C.3 Relative Floor Displacements

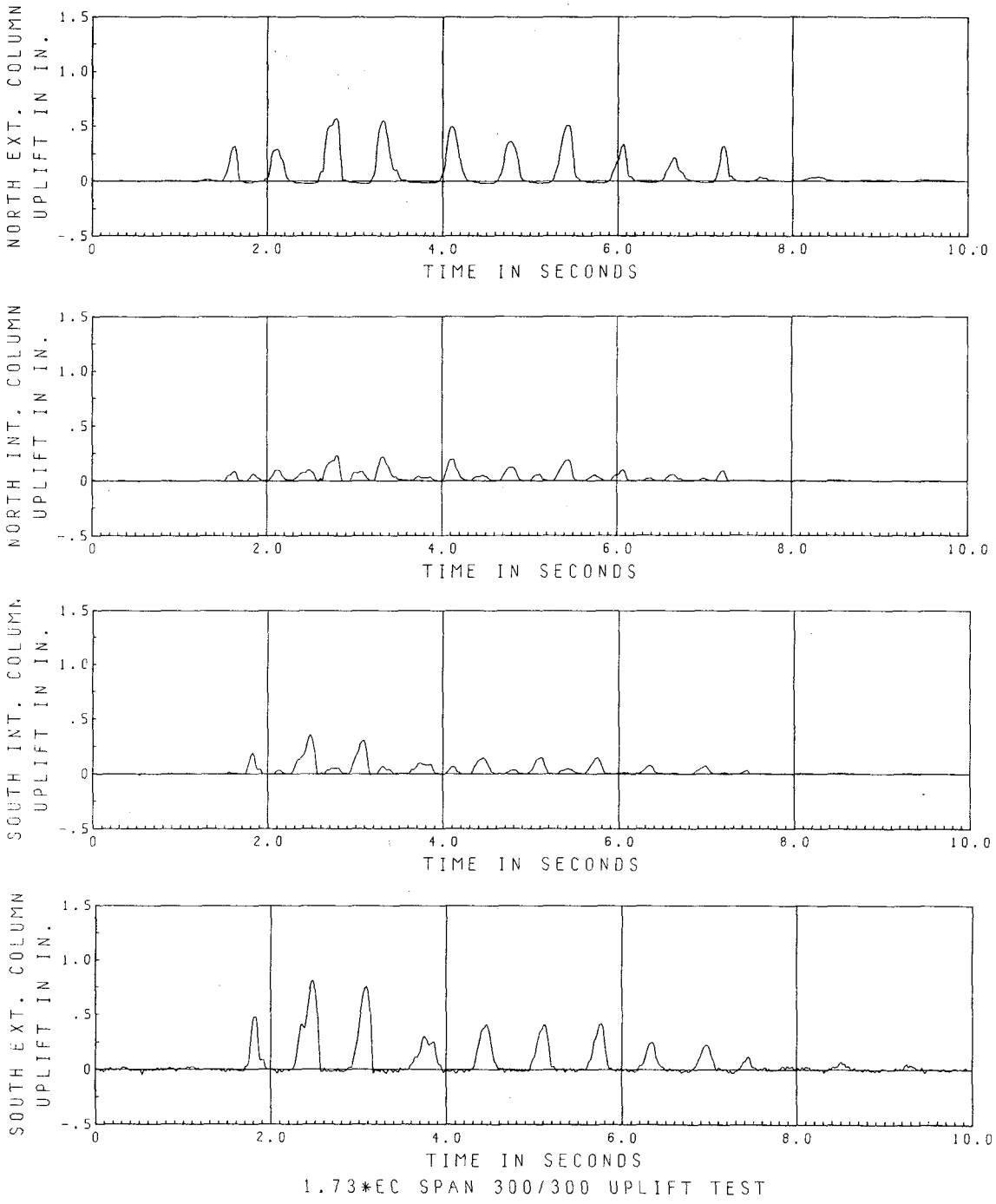

Fig. 6.C.4 Column Uplift Motions

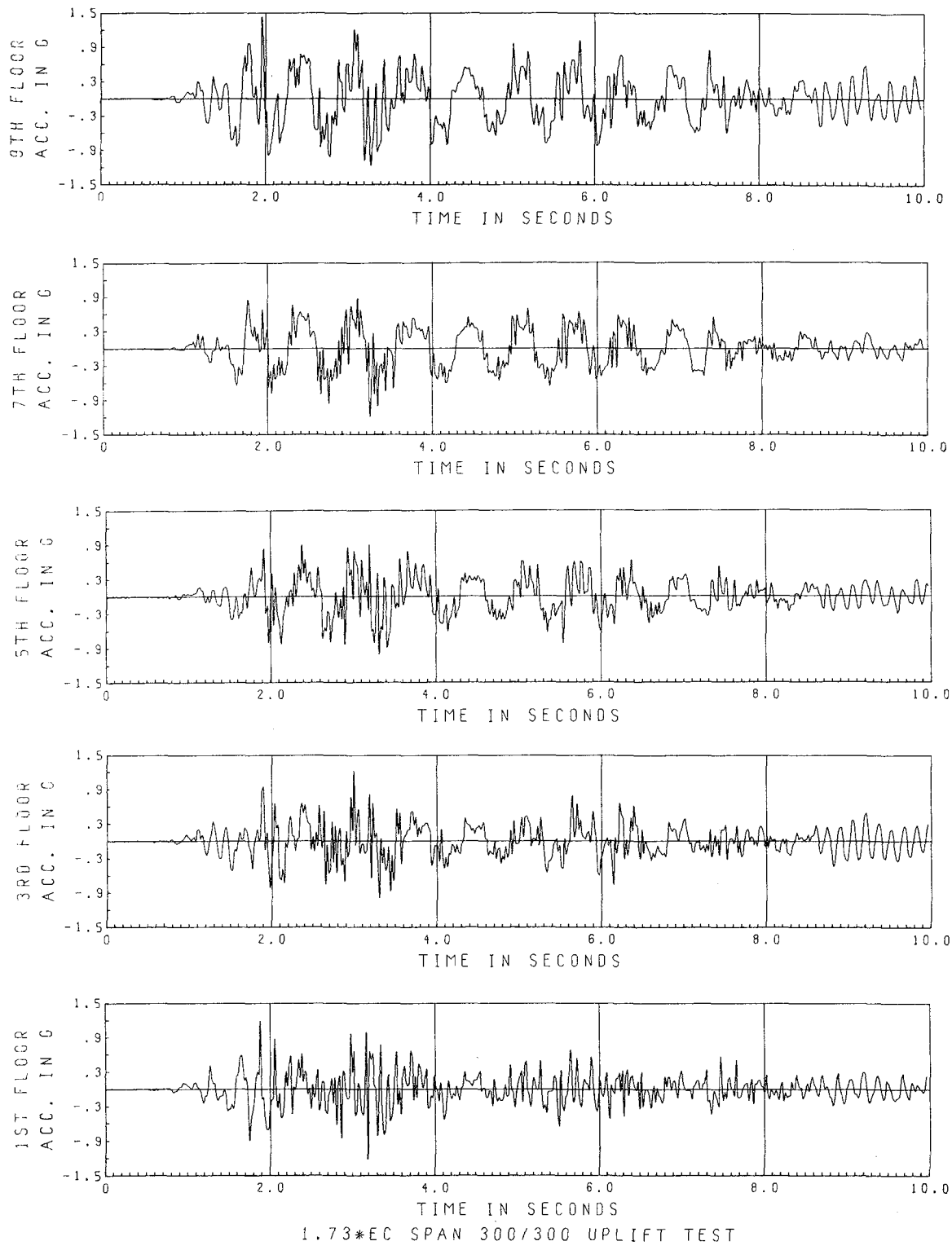

Fig. 6.C.5 Floor Accelerations

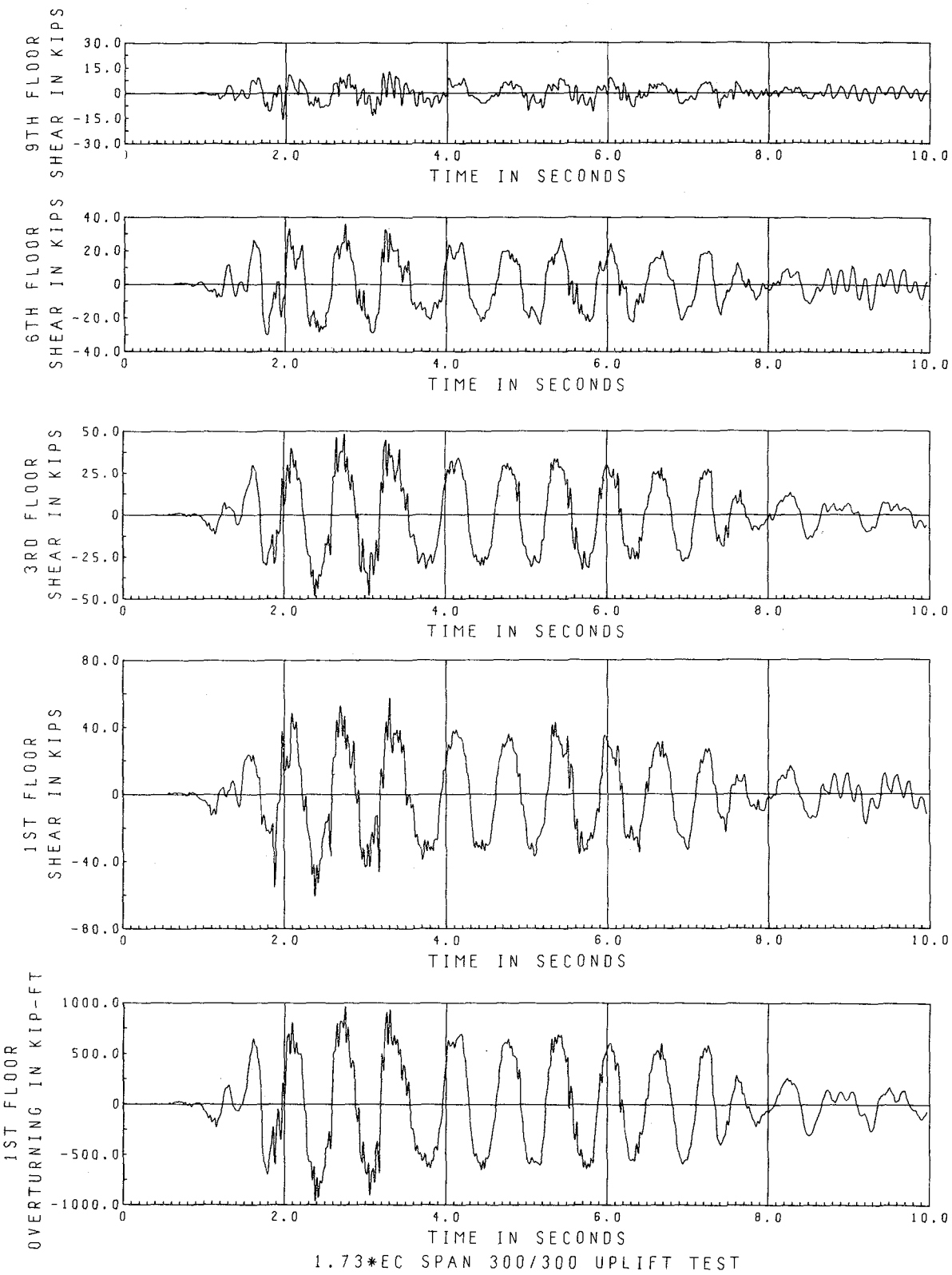

Fig. 6.C.6 Story Shears and Overturning

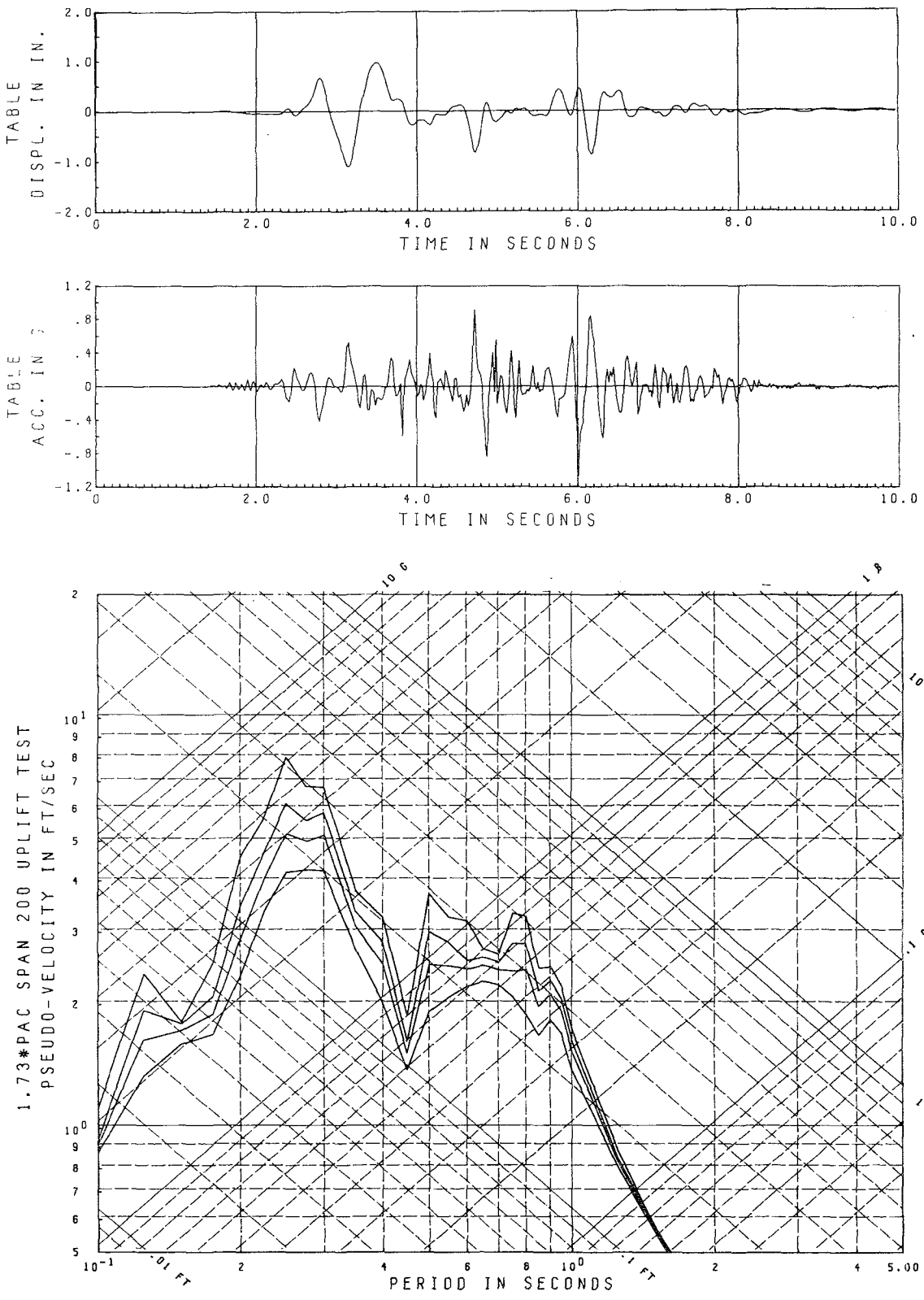

Damping = .01, .02, .03, .05 Critical

Fig. 6.D.1 Pacoima Span 200 Horizontal Table Motion

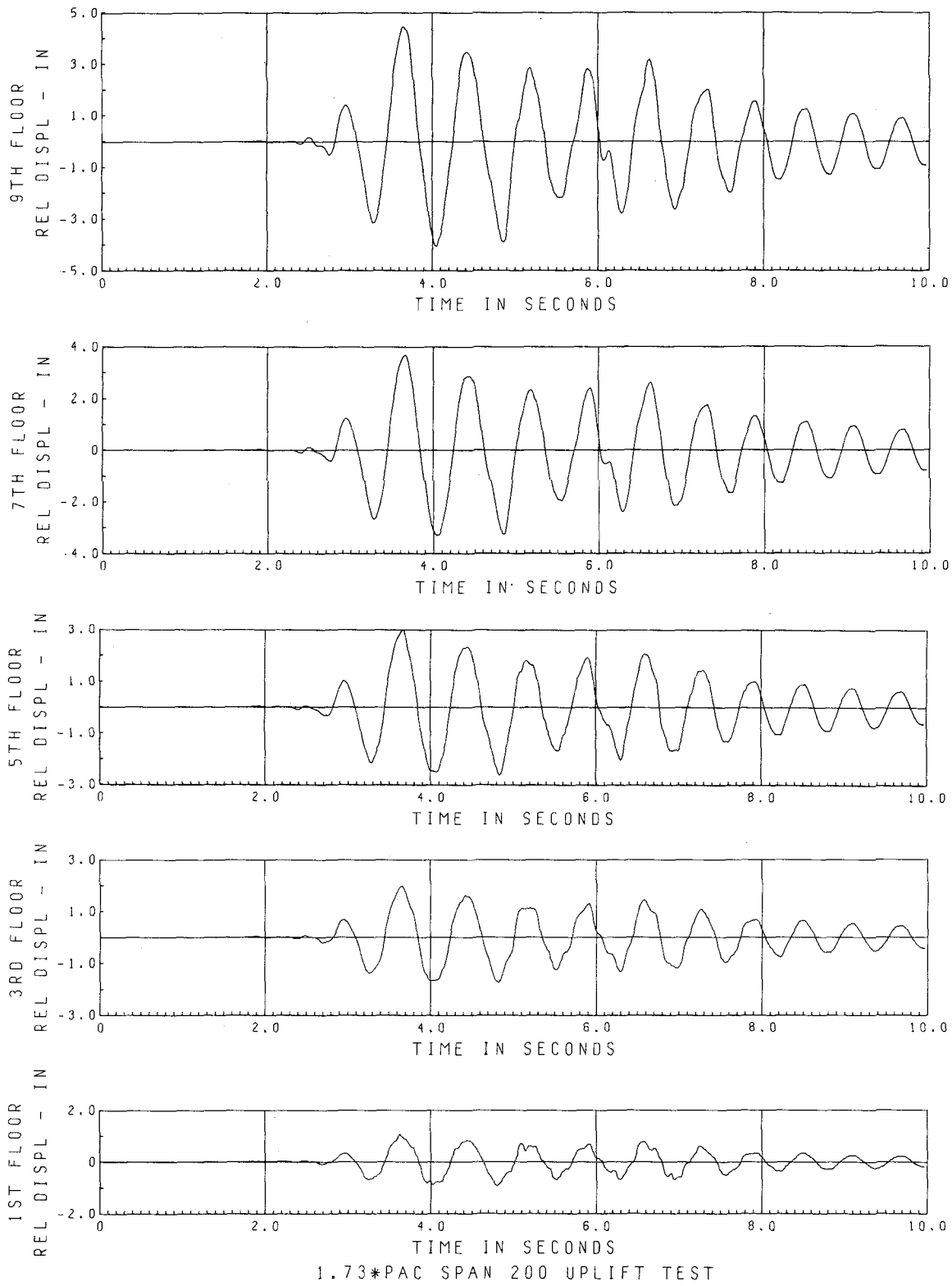

Fig. 6.D.2 Relative Floor Displacements

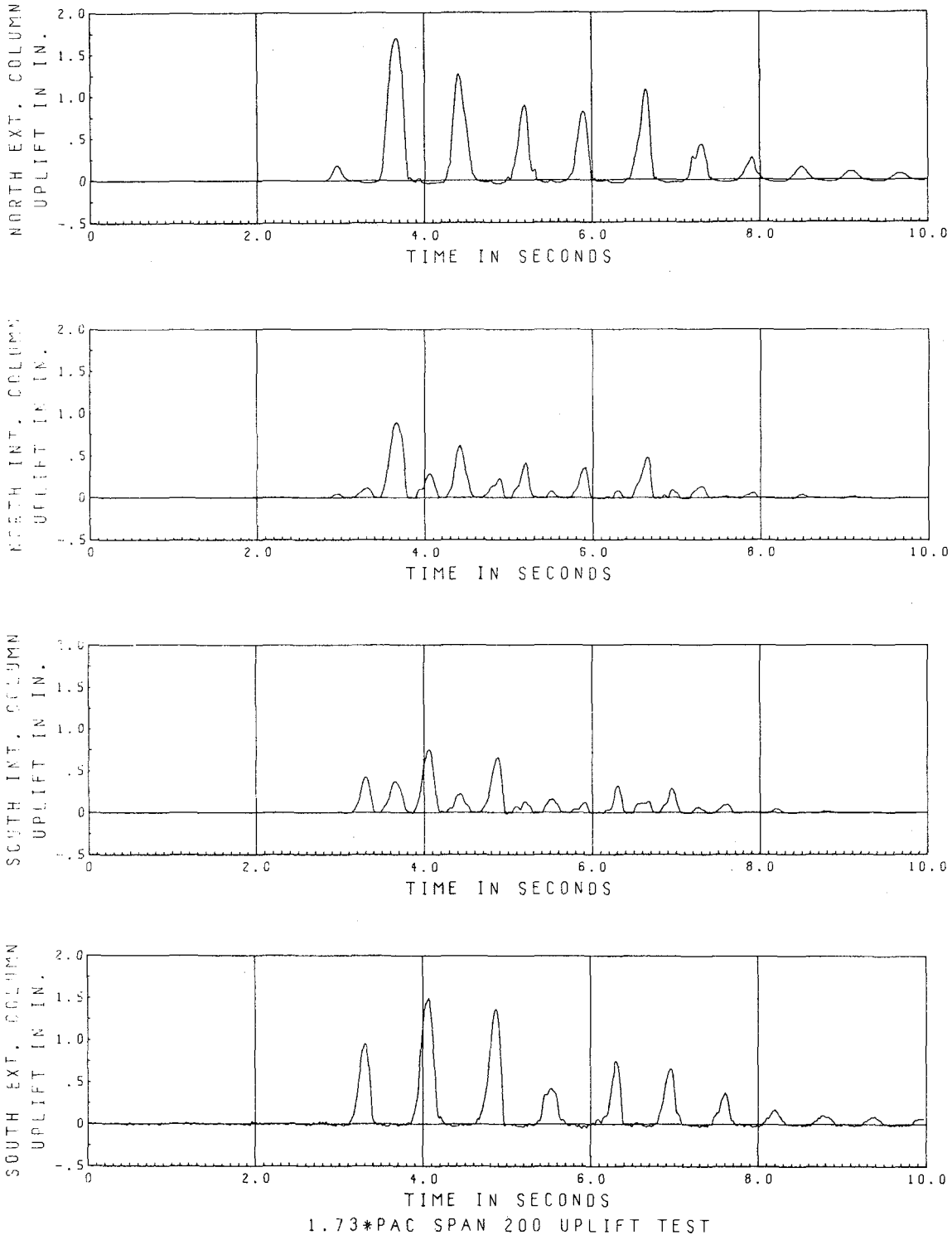

Fig. 6.D.3 Column Uplift Motions

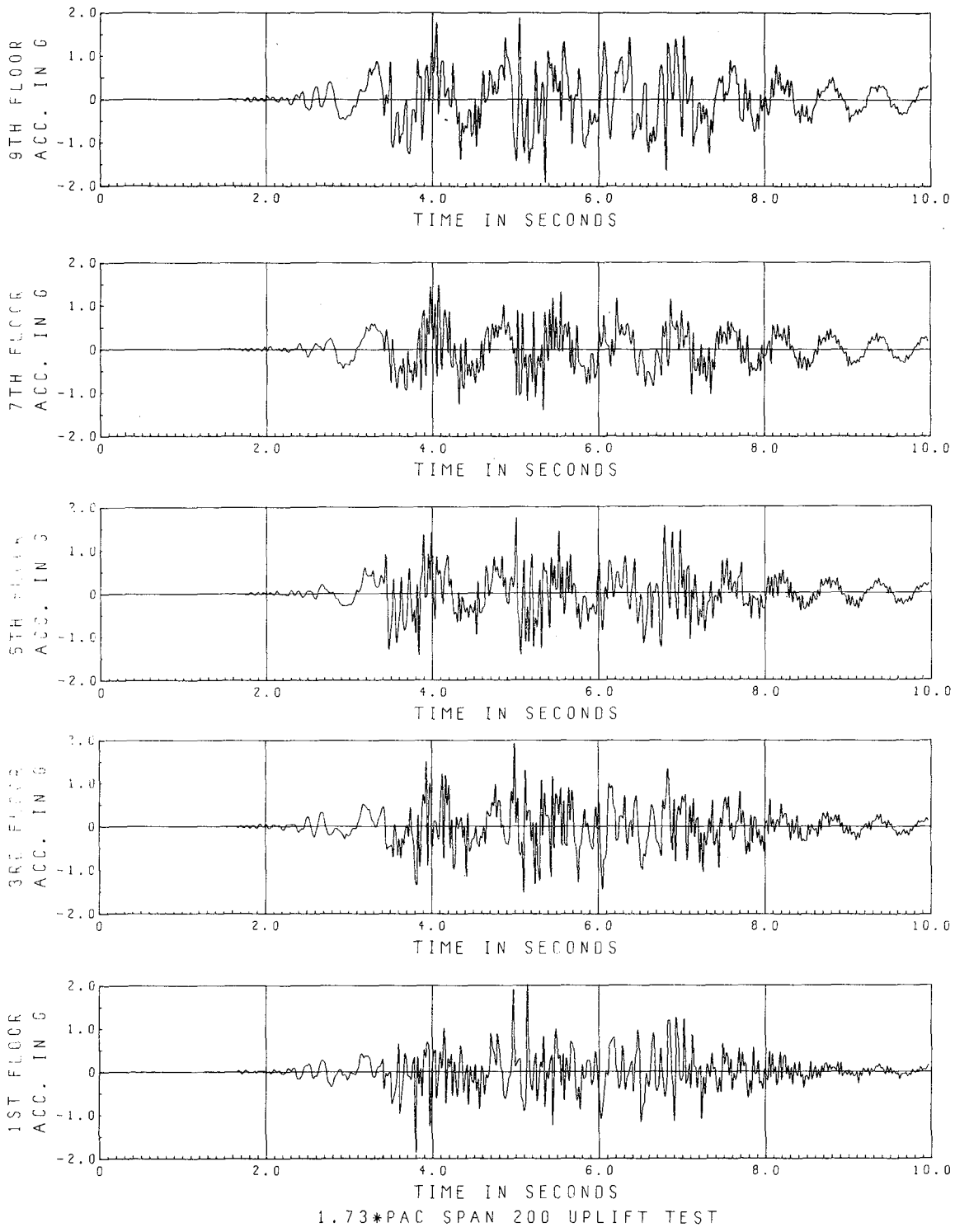

Fig. 6.D.4 Floor Accelerations

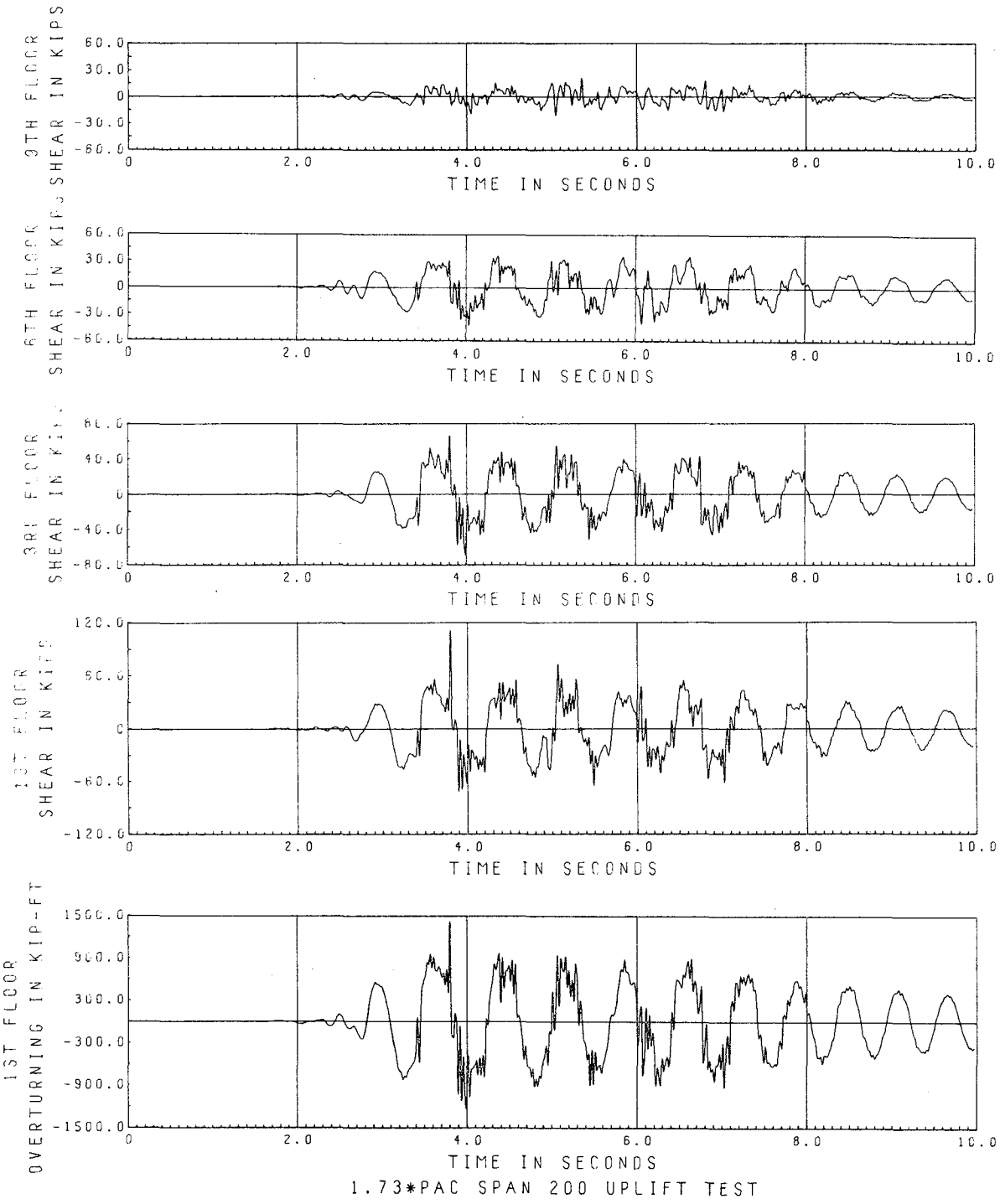

Fig. 6.D.5 Story Shears and Overturning

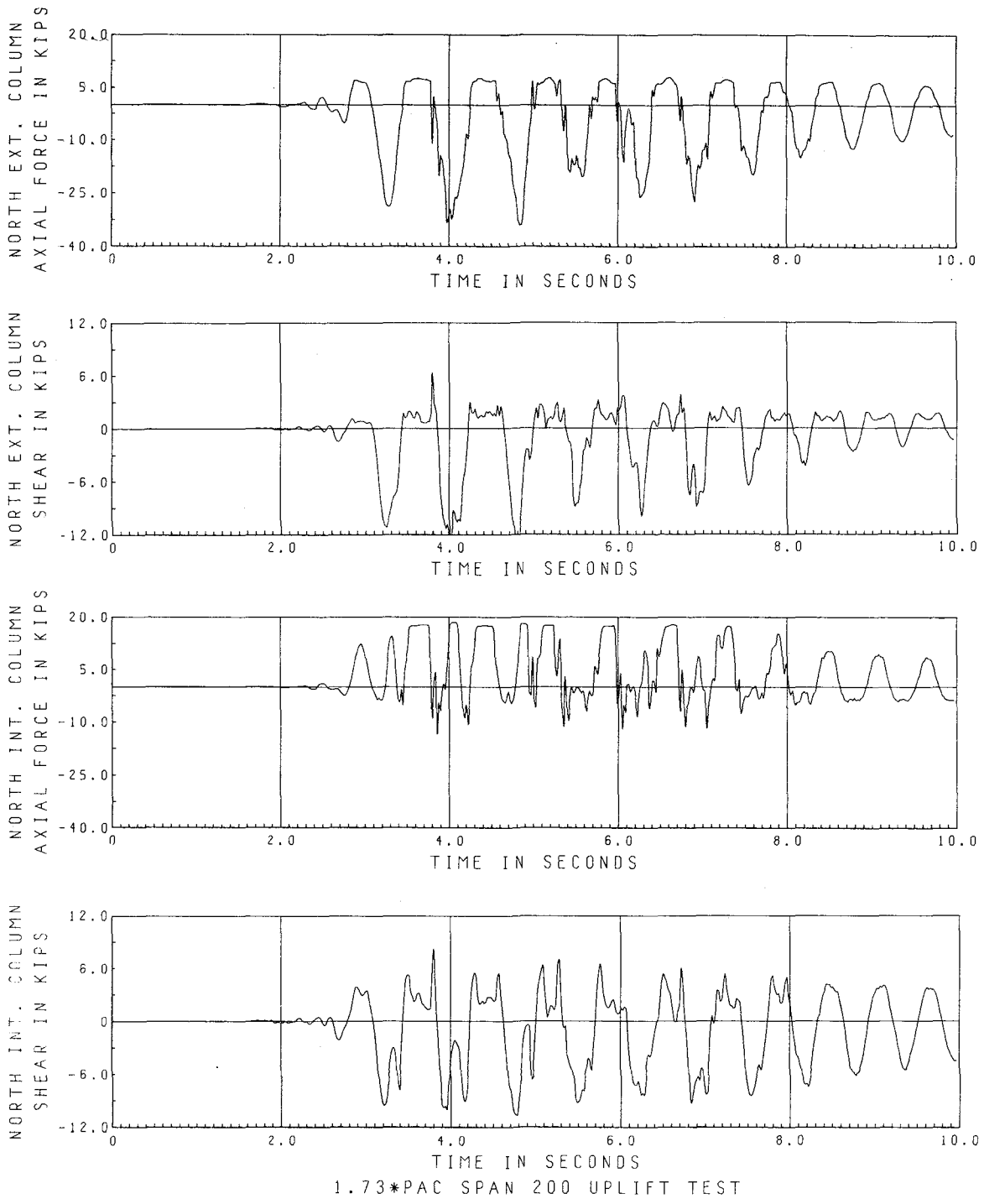

Fig. 6.D.6 1st Floor Column Shears and Axial Forces

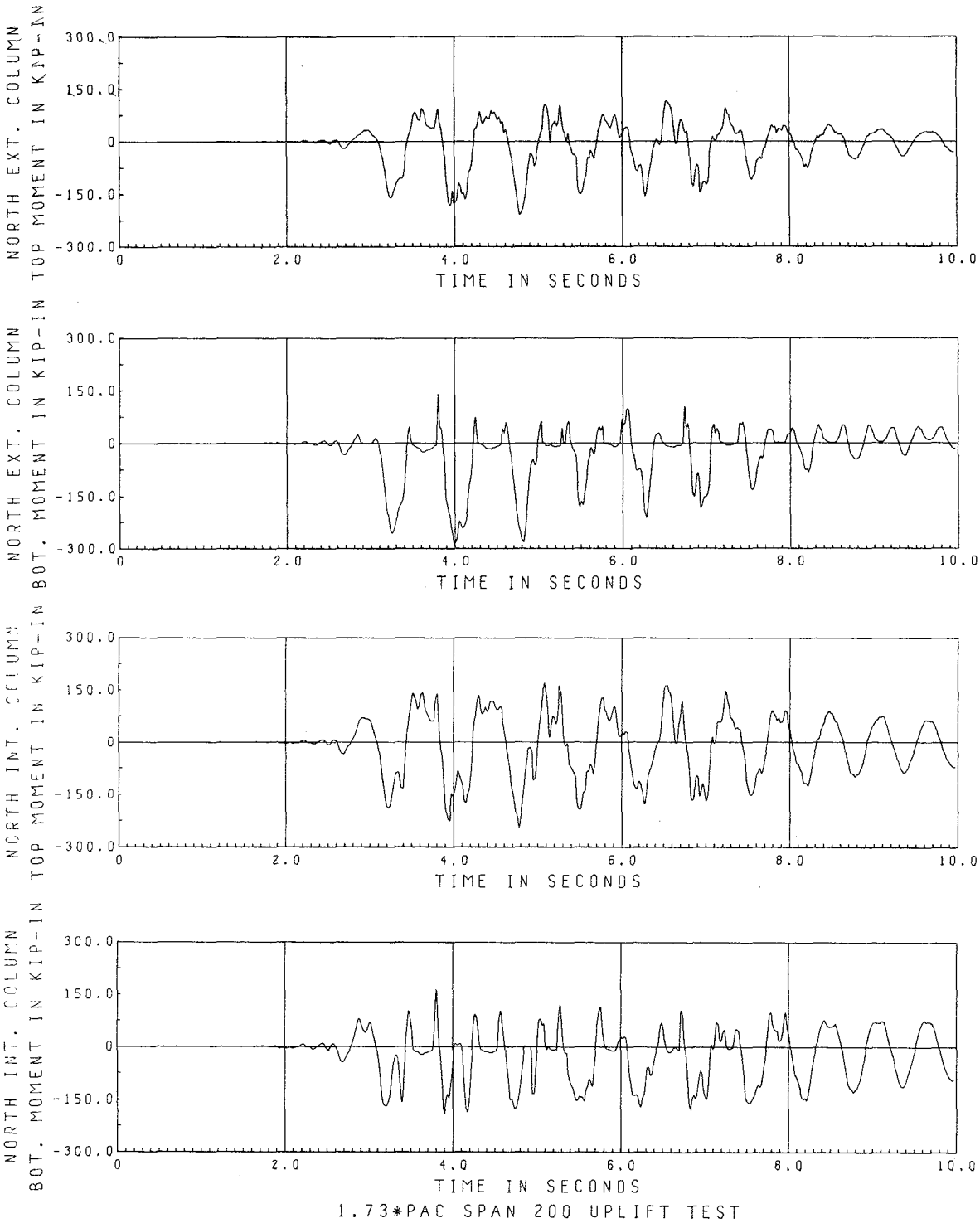

Fig. 6.D.7 1st Floor Column Bending Moments

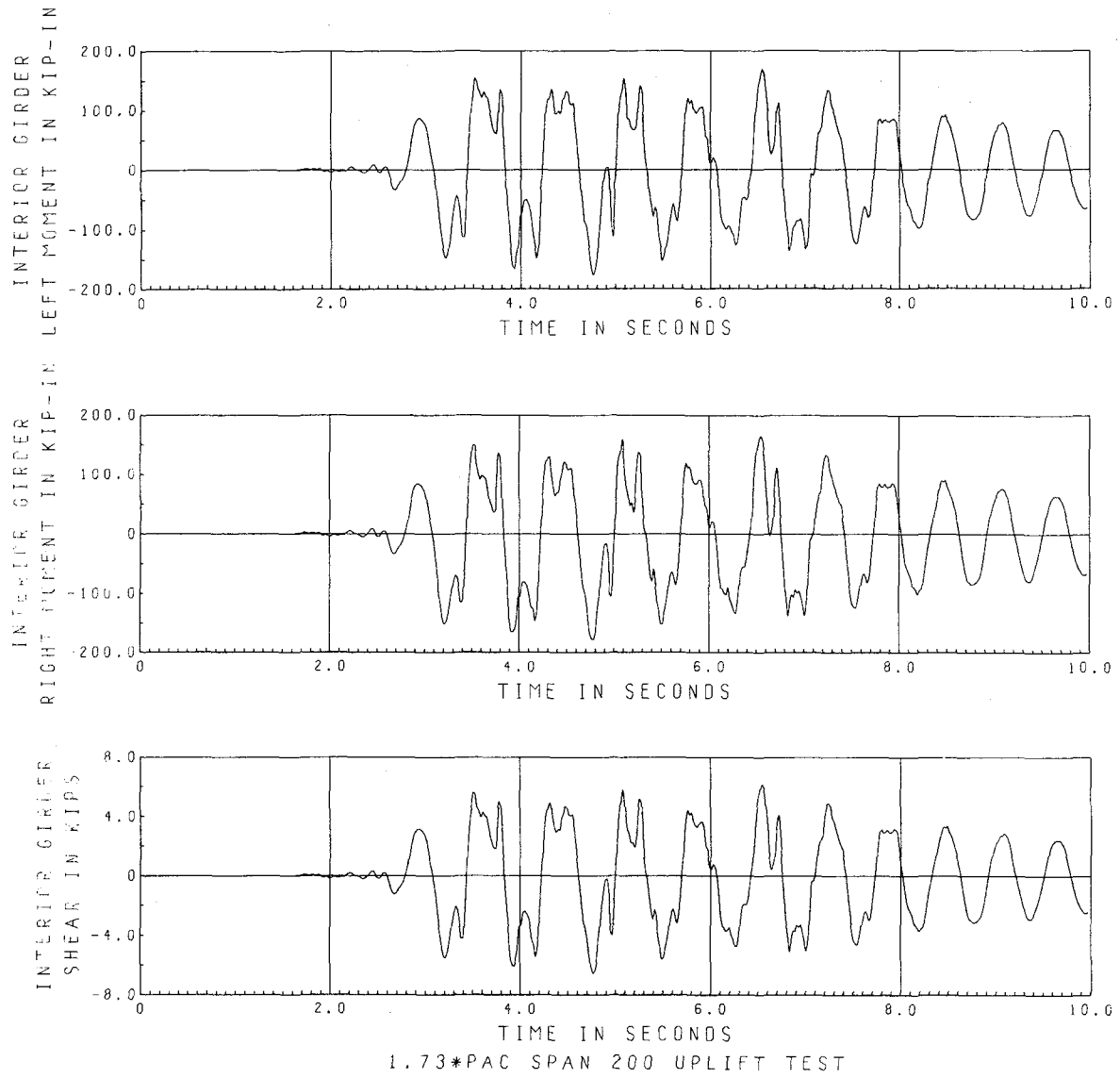

Fig. 6.D.3 1st Floor Girder Shear and Moments

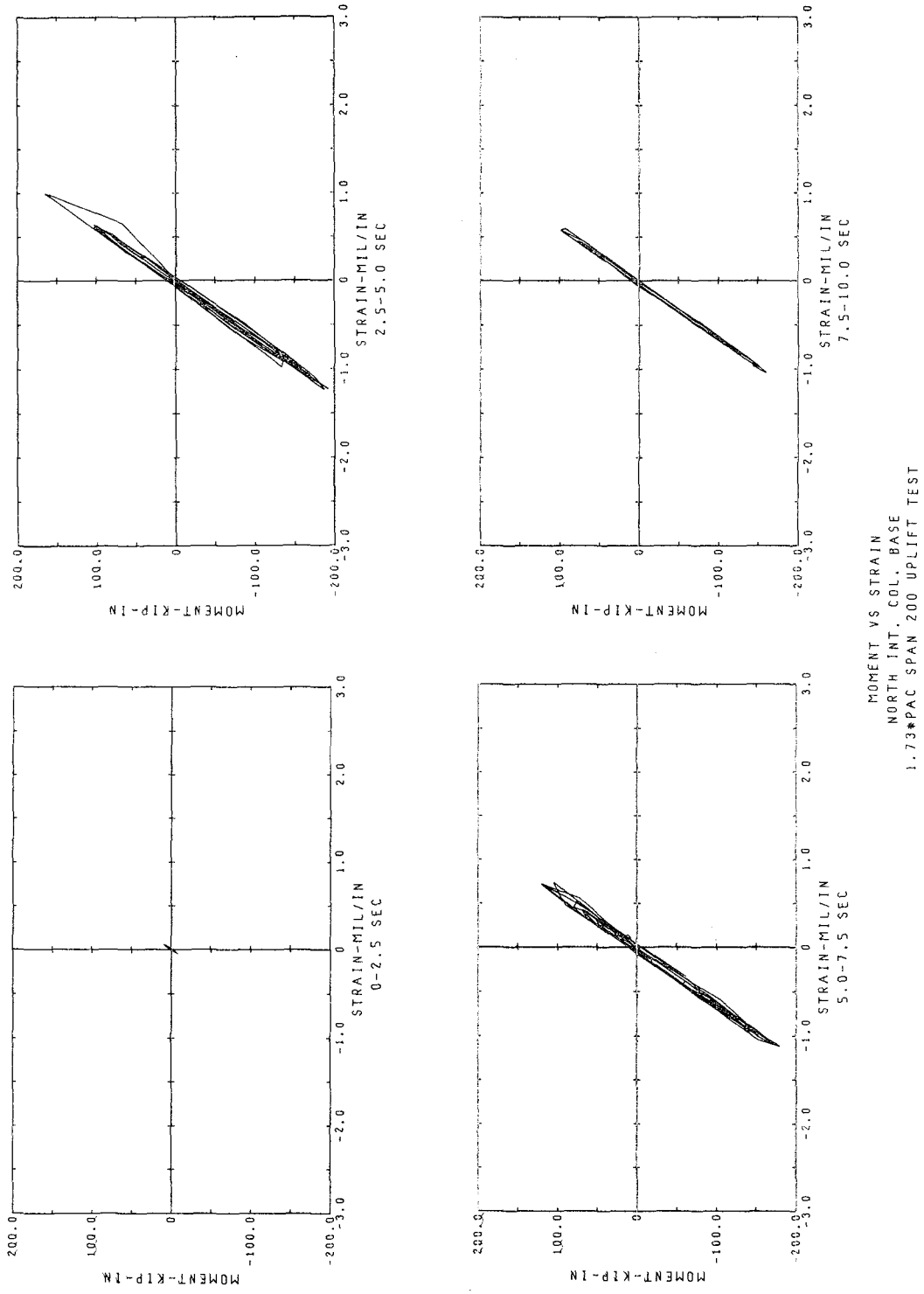

Fig. 6.D.9 1st Floor Column Hysteresis Plots

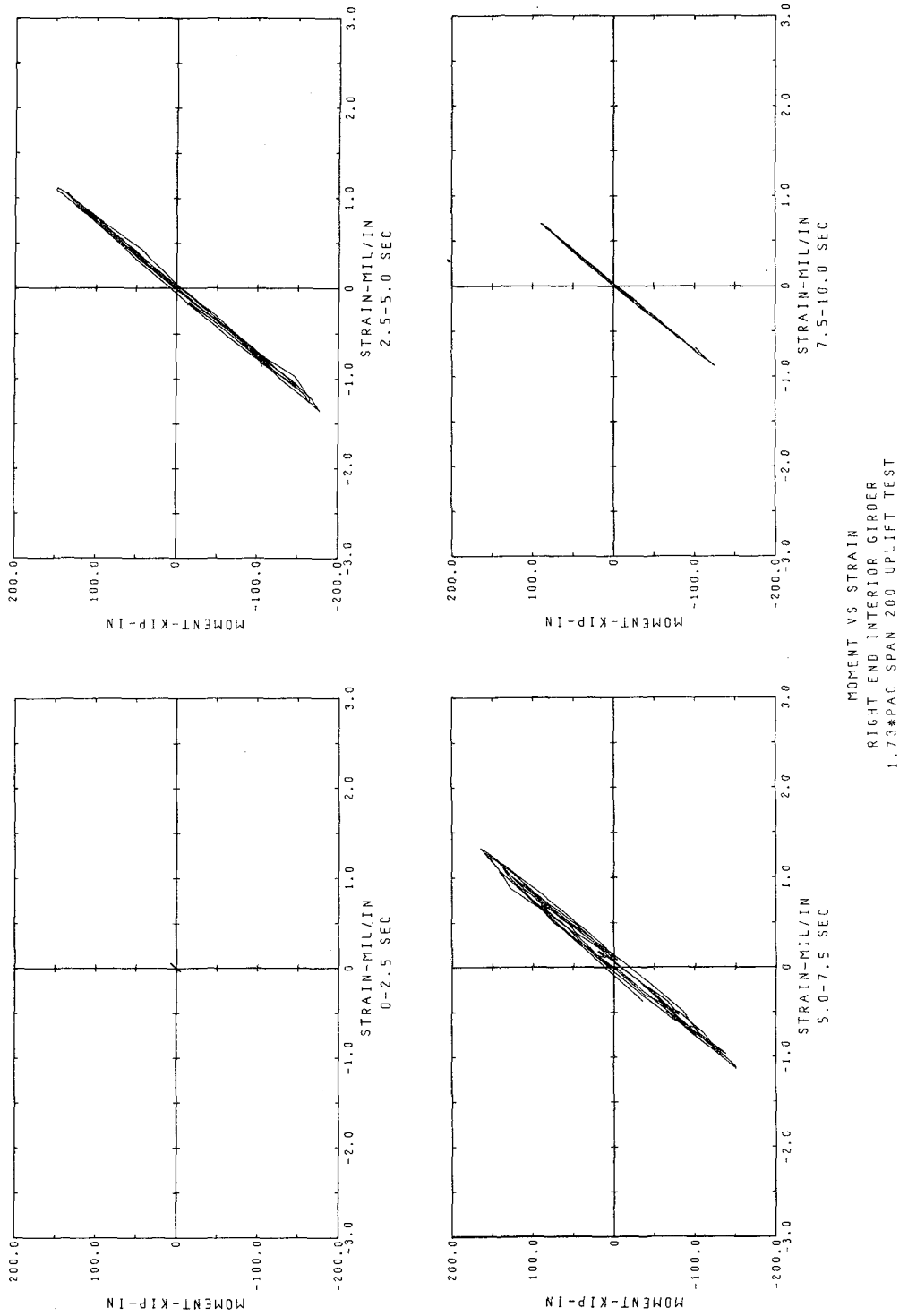

Fig. 6.D.10 1st Floor Girder Hysteresis Plots

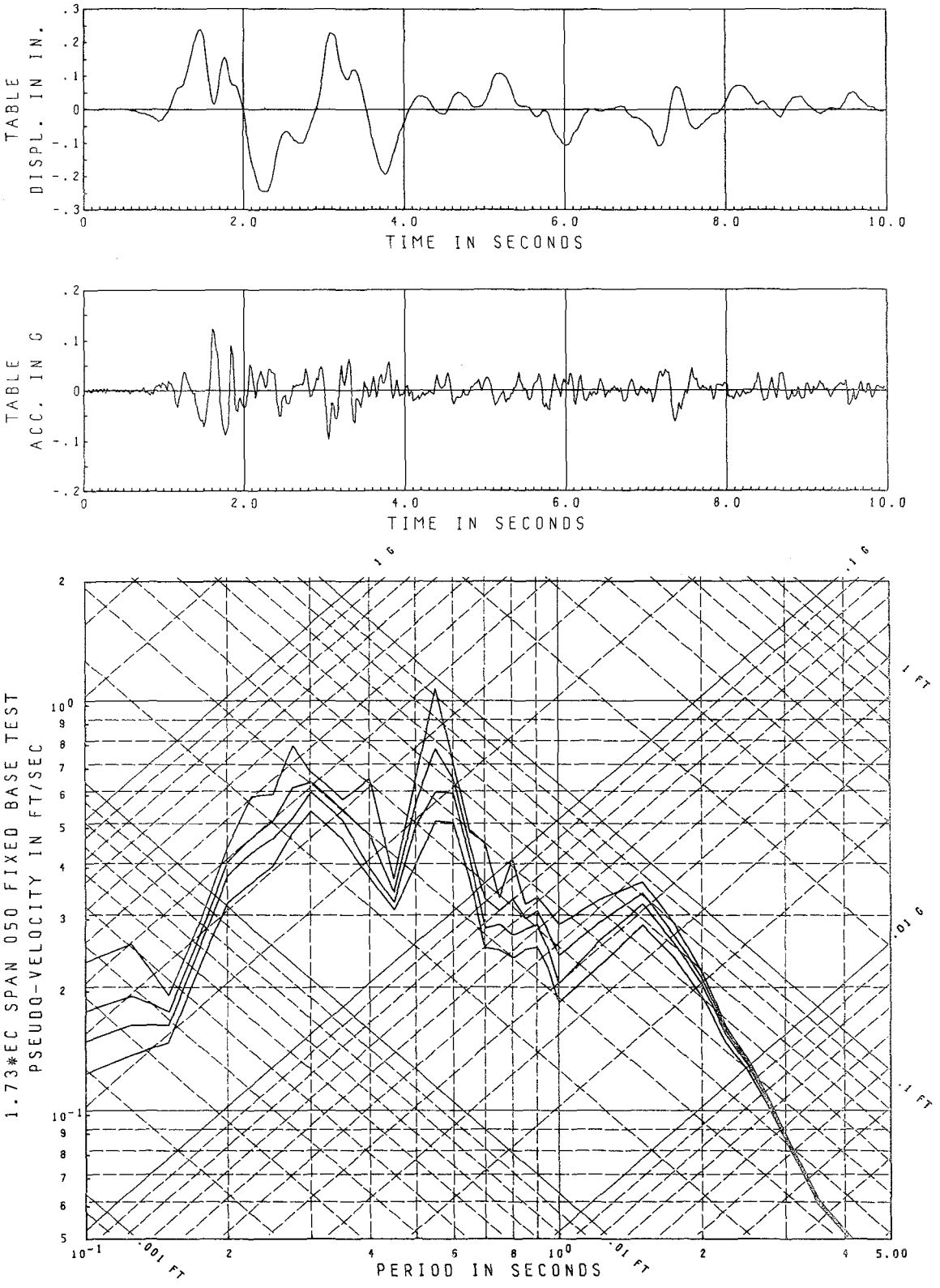

Damping = .01, .02, .03, .05 Critical

Fig. 6.E.1 El Centro Span 50 Horizontal Table Motion

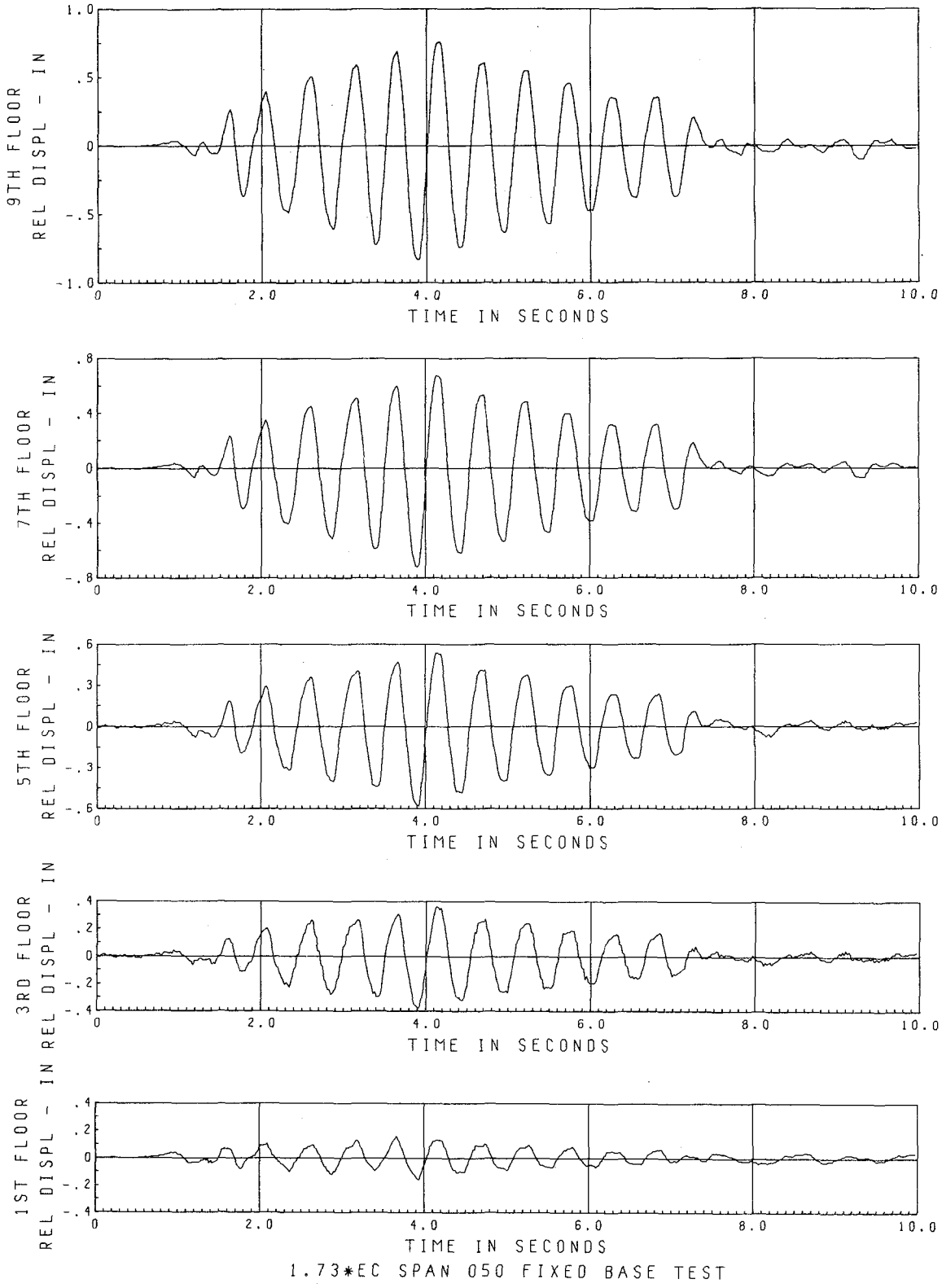

Fig. 6.E.2 Relative Floor Displacements

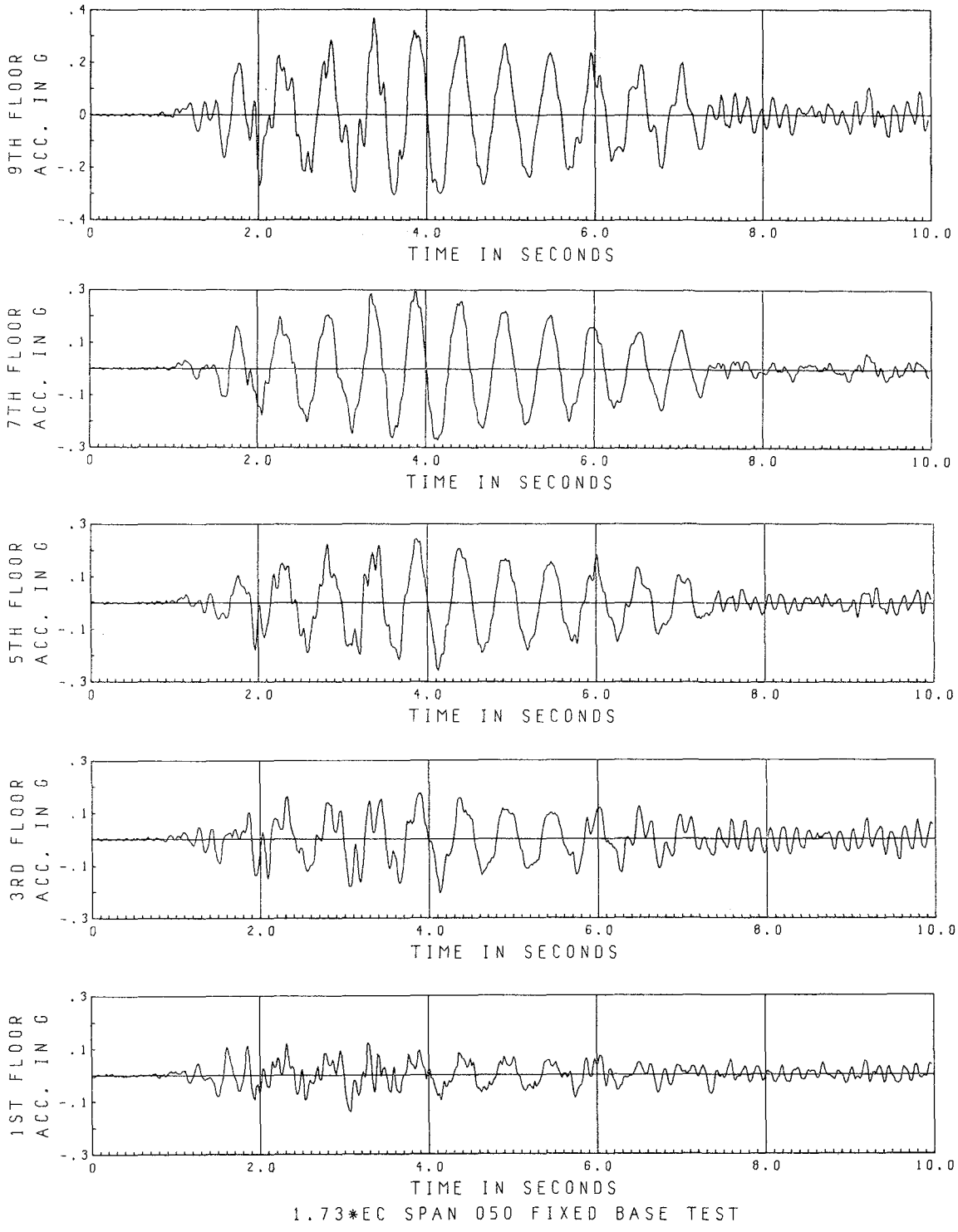

Fig. 6.E.3 Floor Accelerations

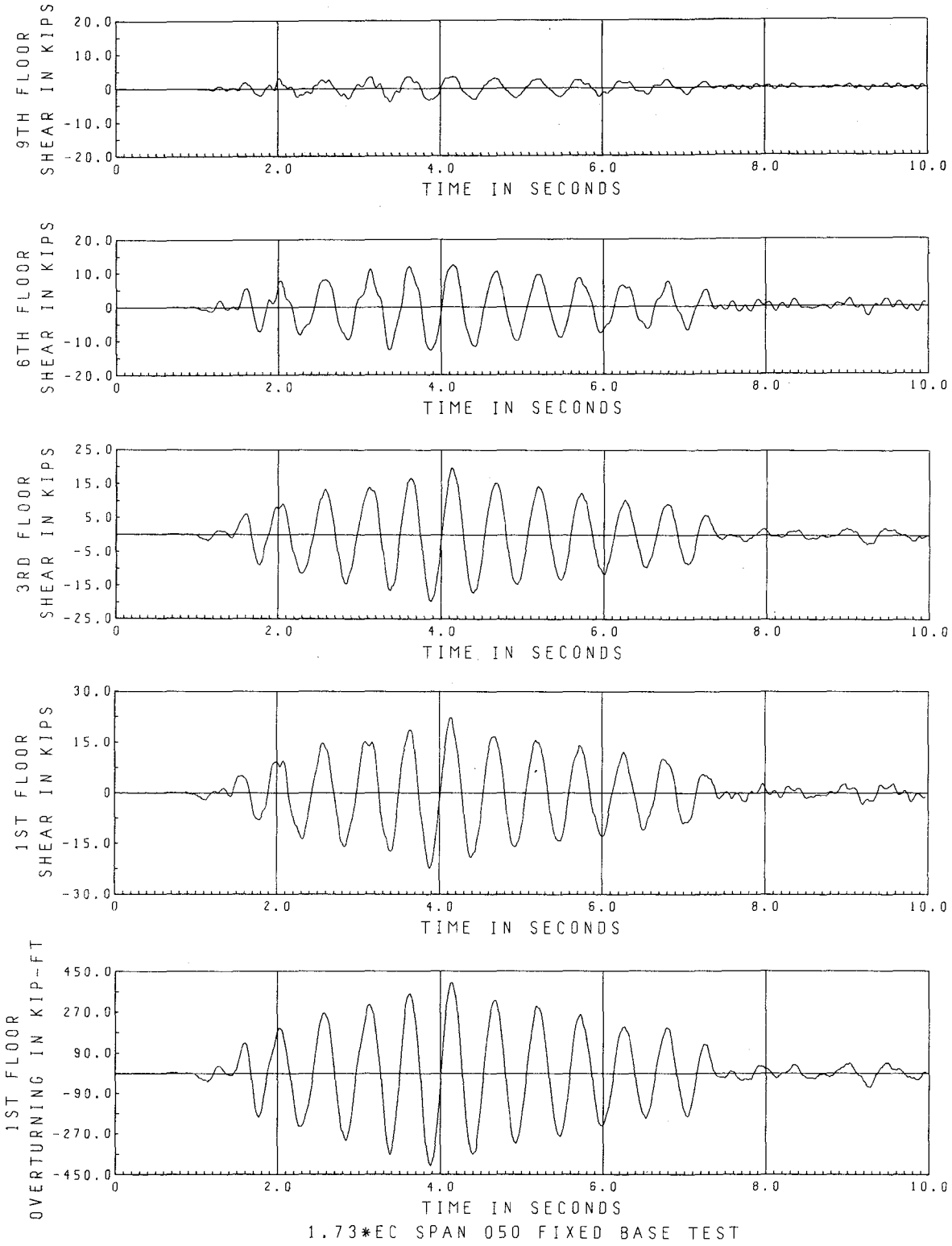

Fig. 6.E.4 Story Shears and Overturning

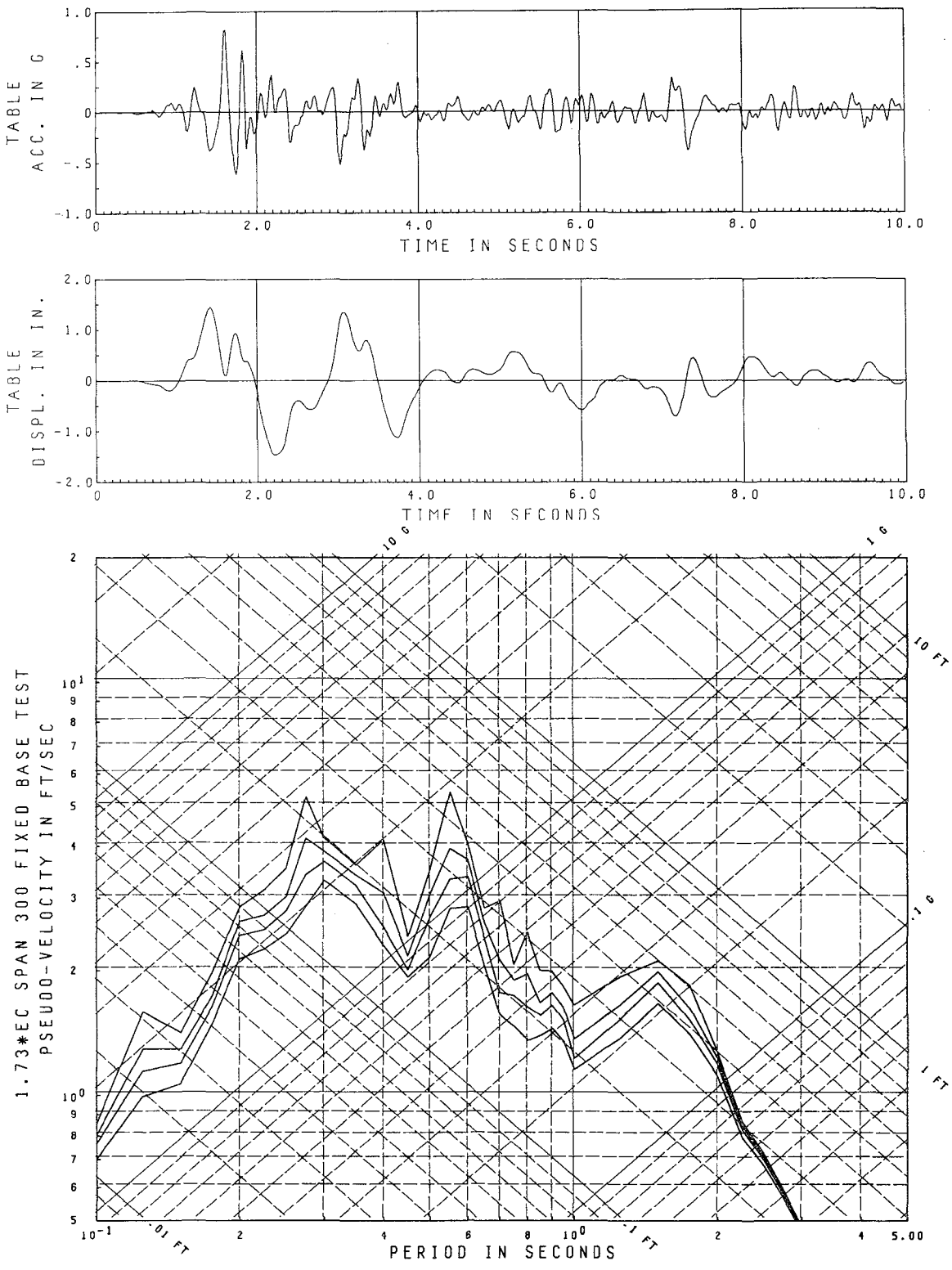

Damping = .01, .02, .03, .05 Critical

Fig. 6.F.1 El Centro Span 300 Horizontal Table Motion

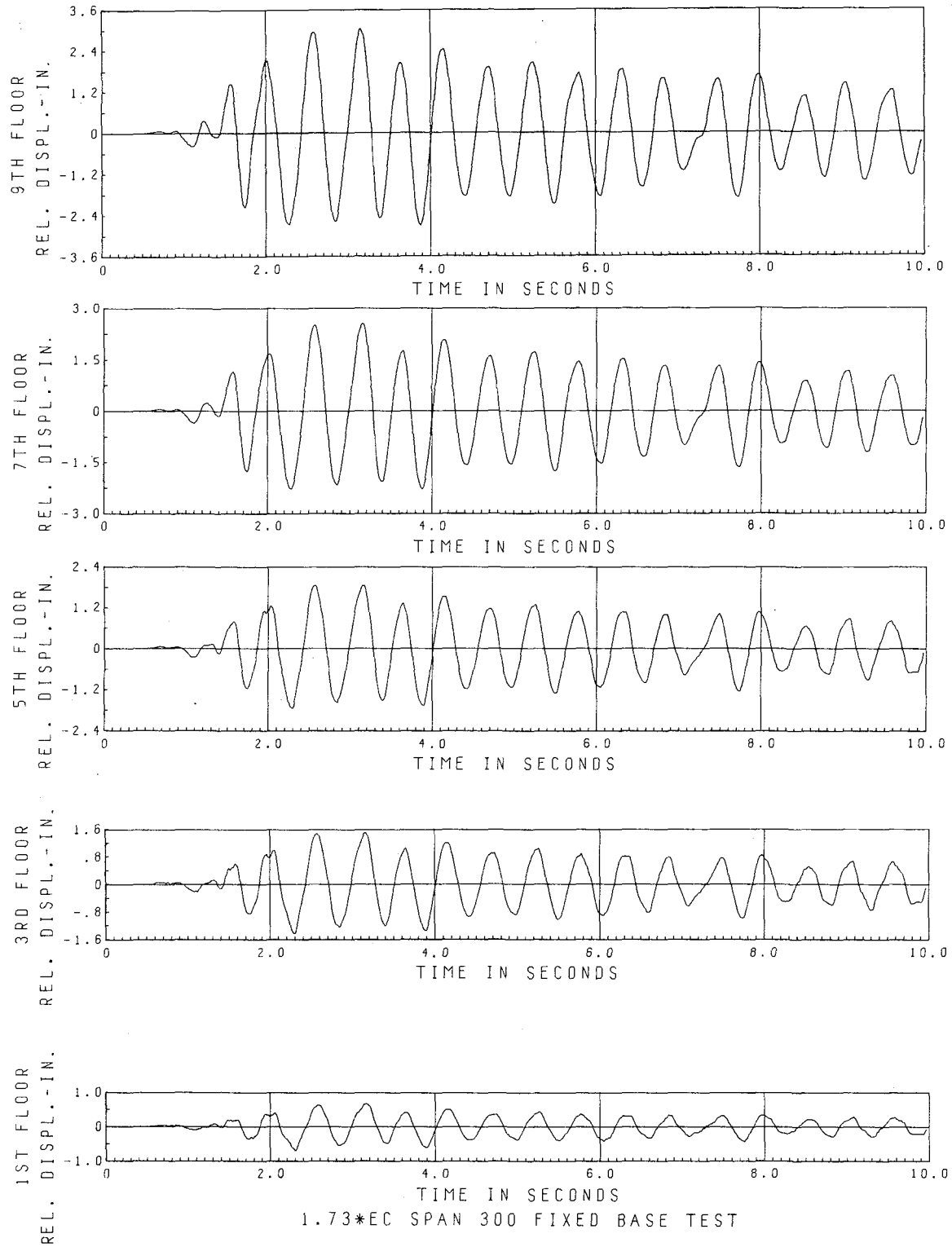

Fig. 6.F.2 Relative Floor Displacements

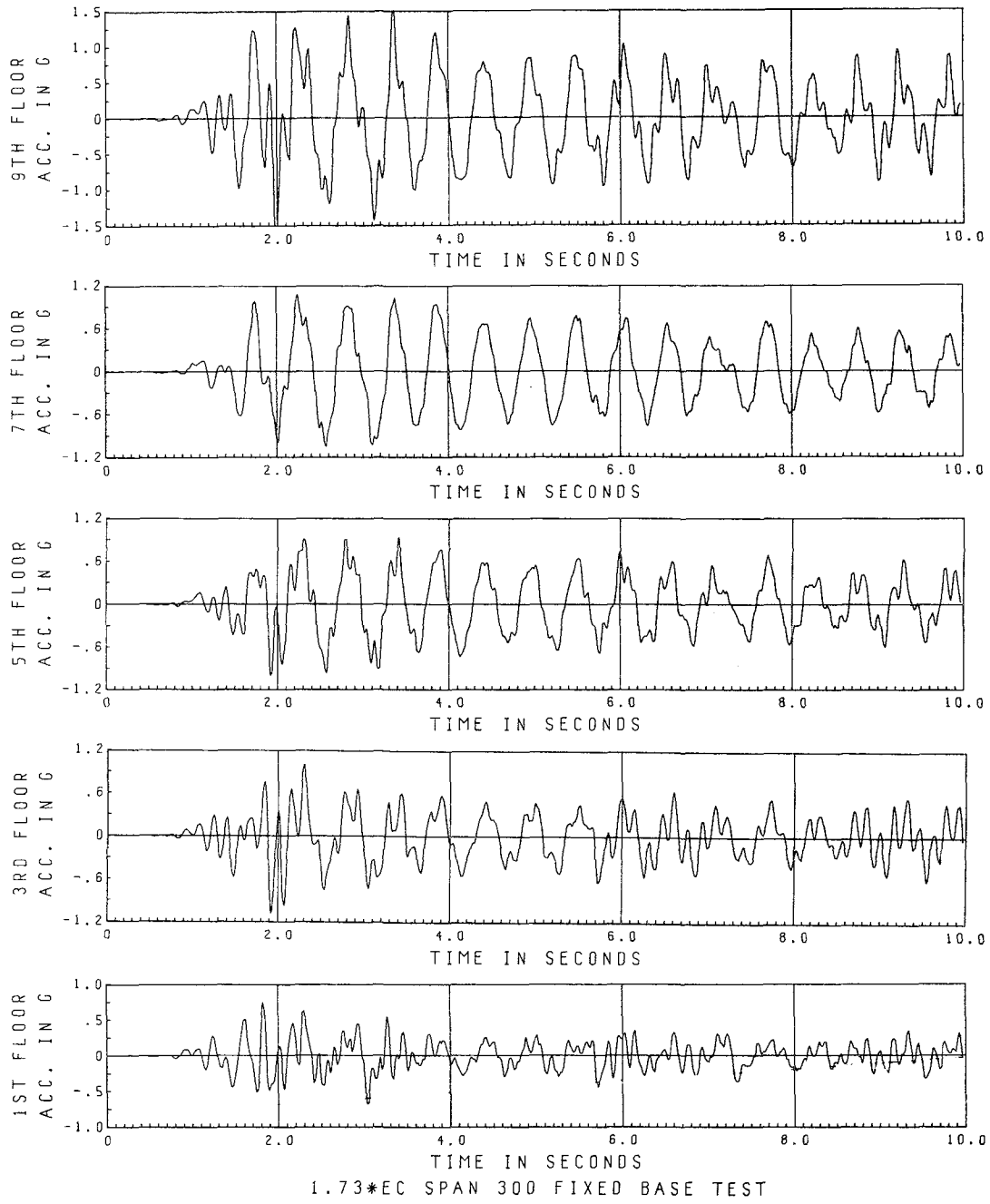

Fig. 6.F.3 Floor Accelerations

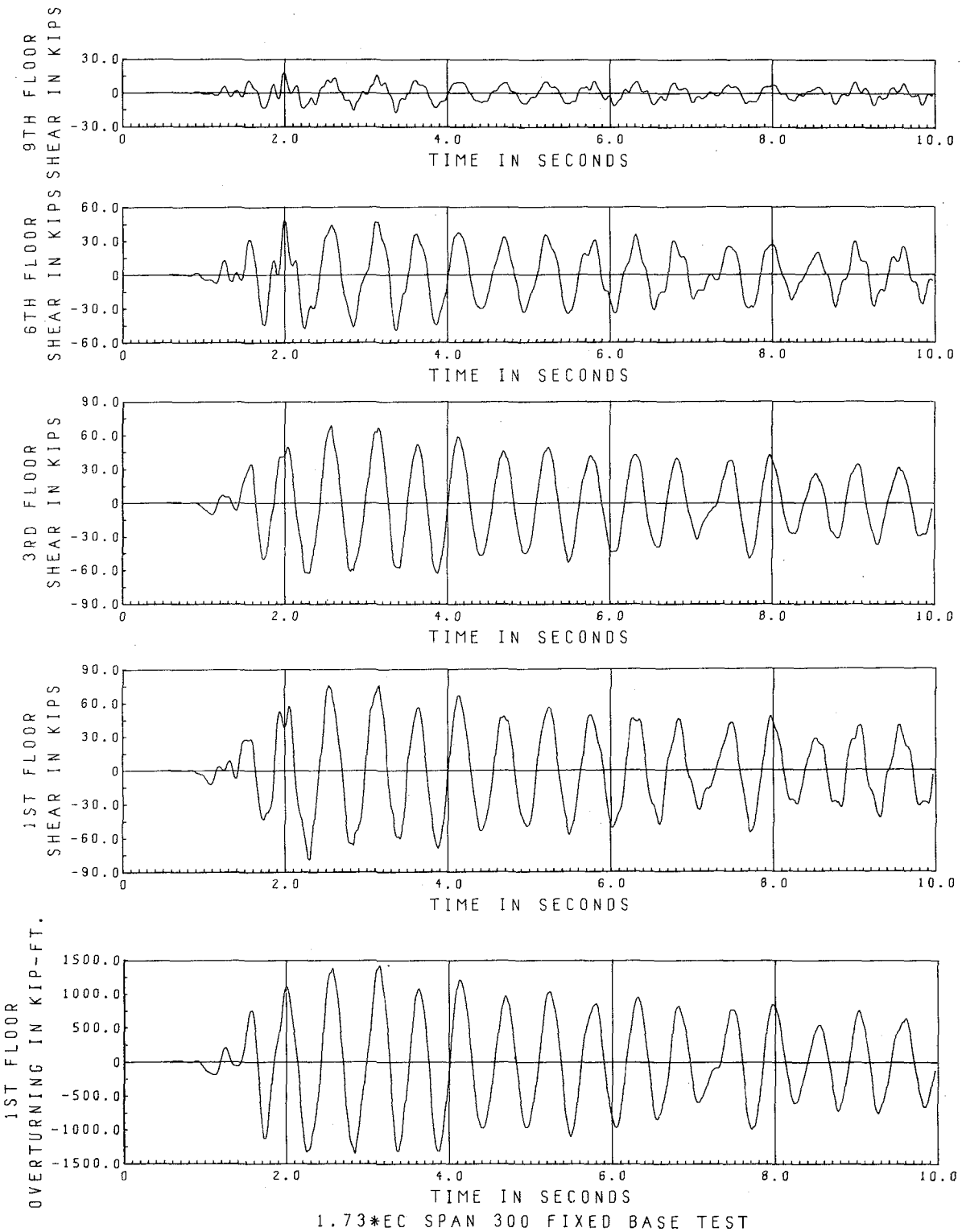

Fig. 6.F.4 Story Shears and Overturning

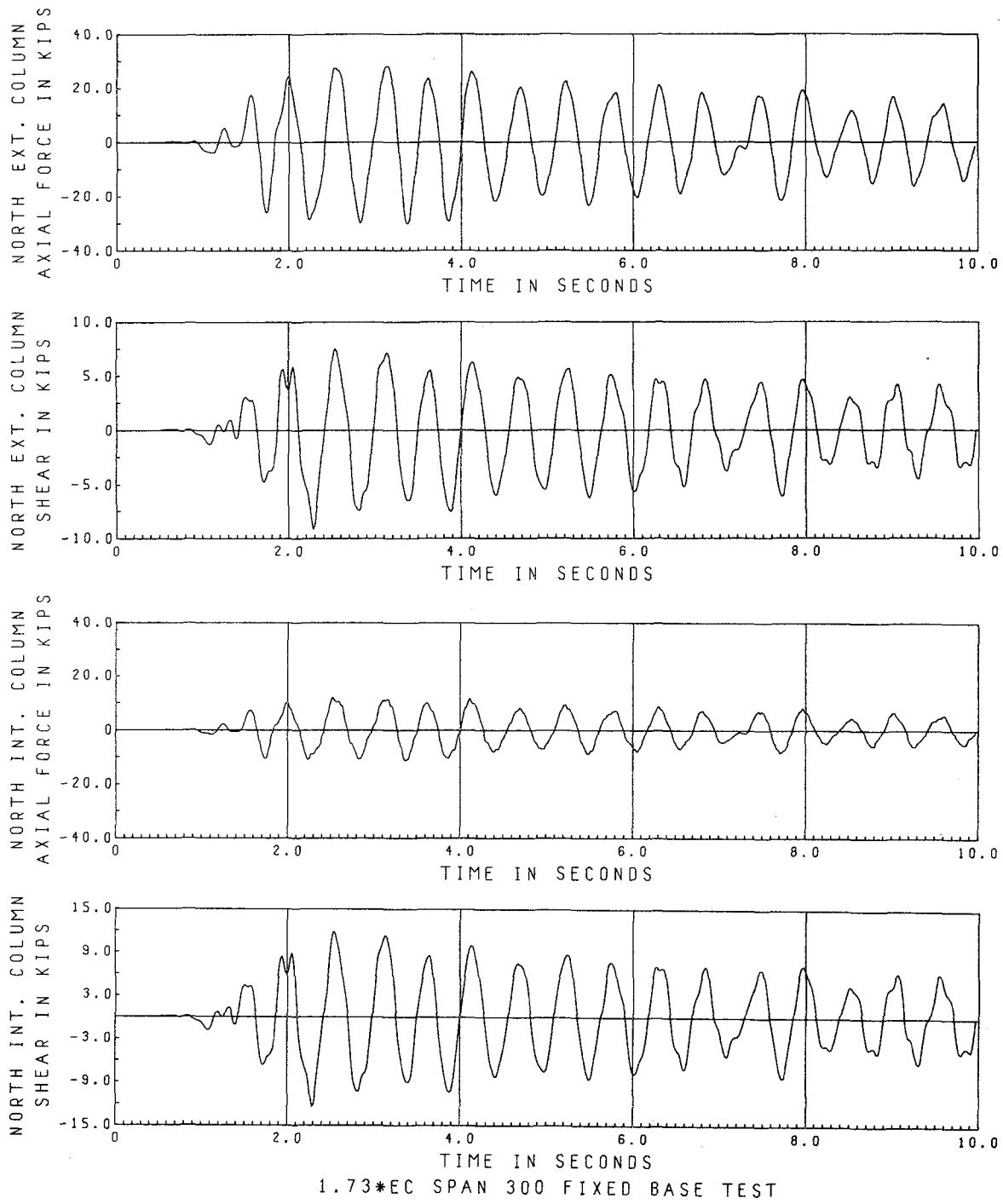

Fig. 6.F.5 1st Floor Column Shears and Axial Forces

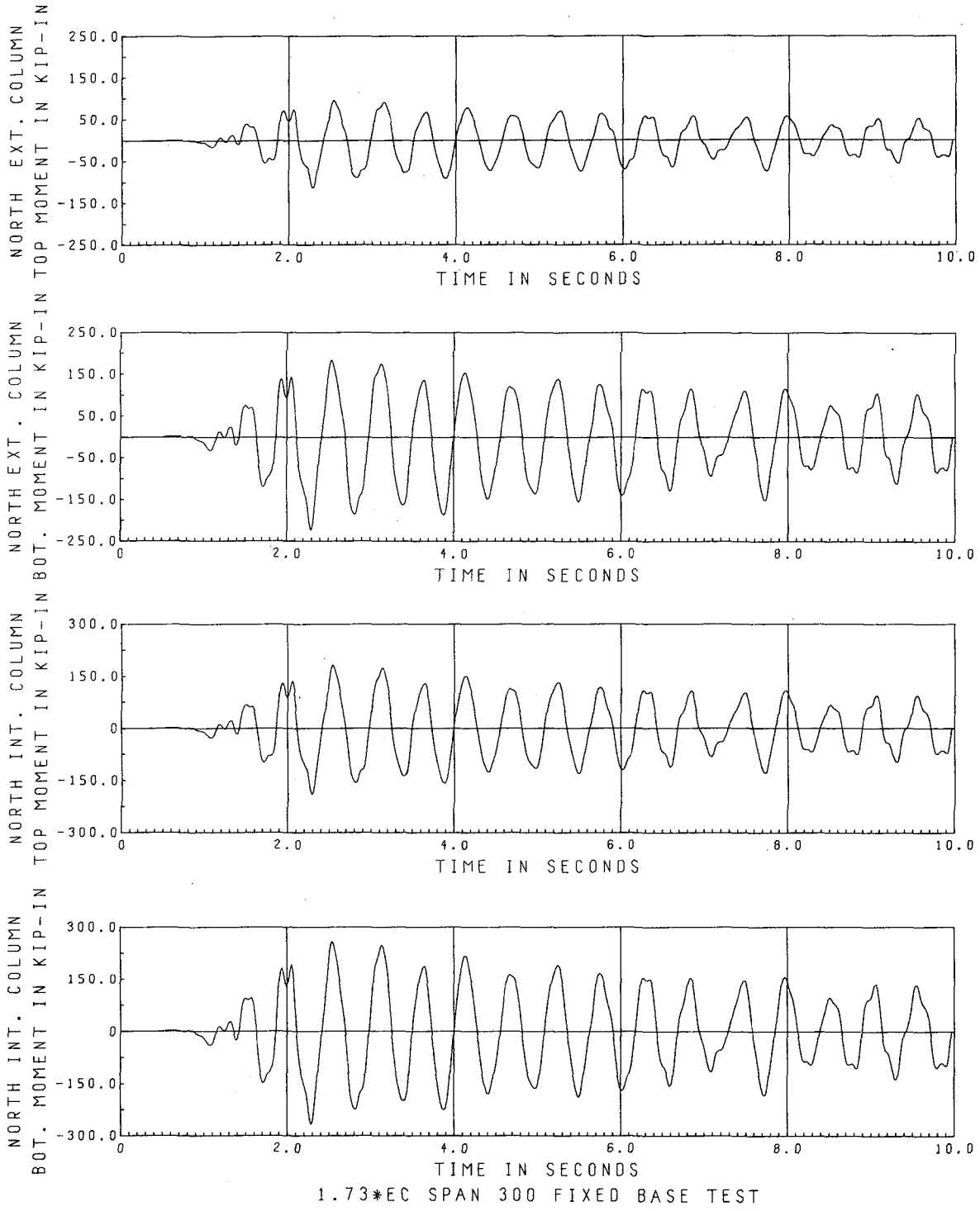

Fig. 6.F.6 1st Floor Column Bending Moments

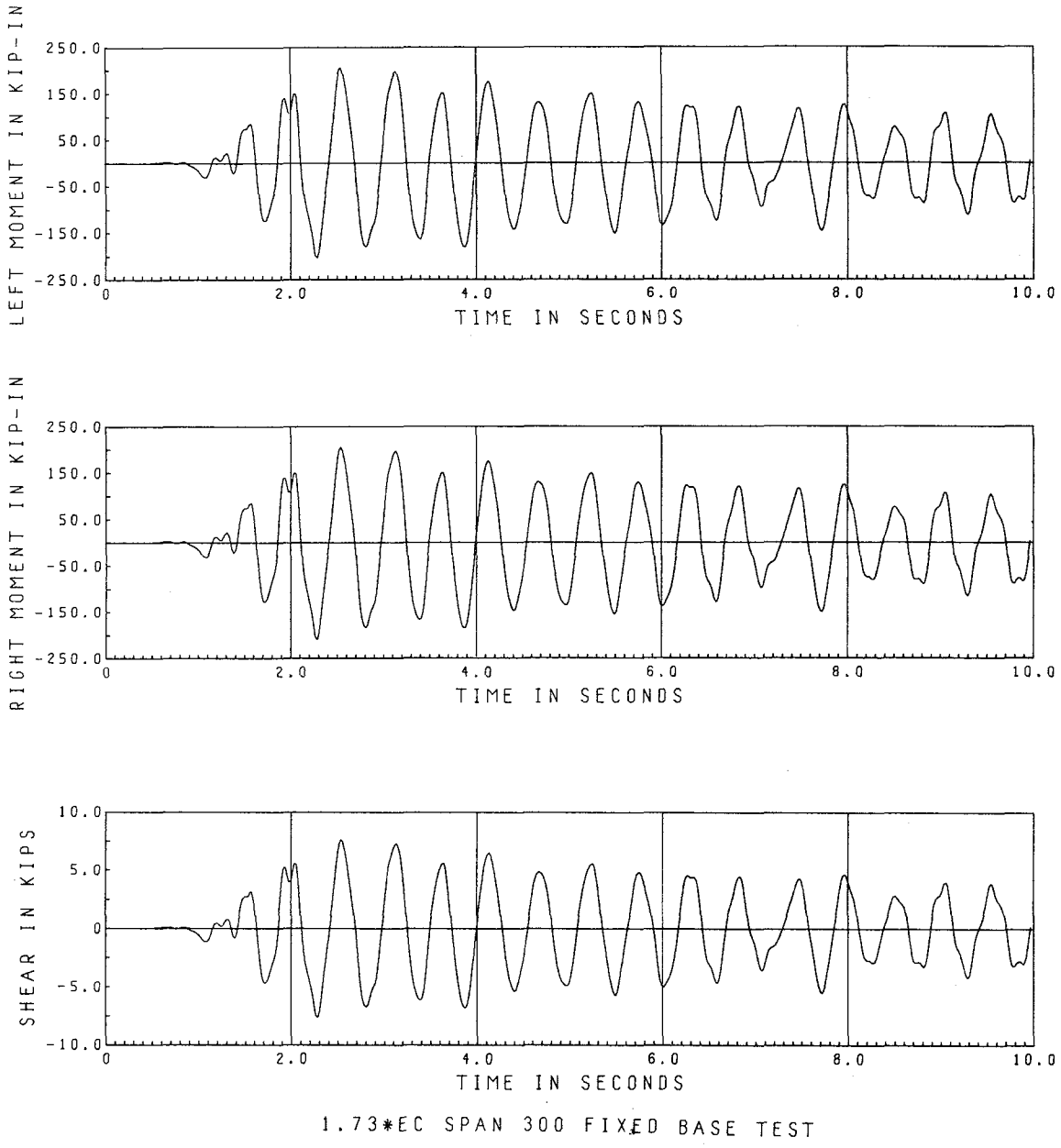

Fig. 6.F.7 1st Floor Girder Shear and Moments

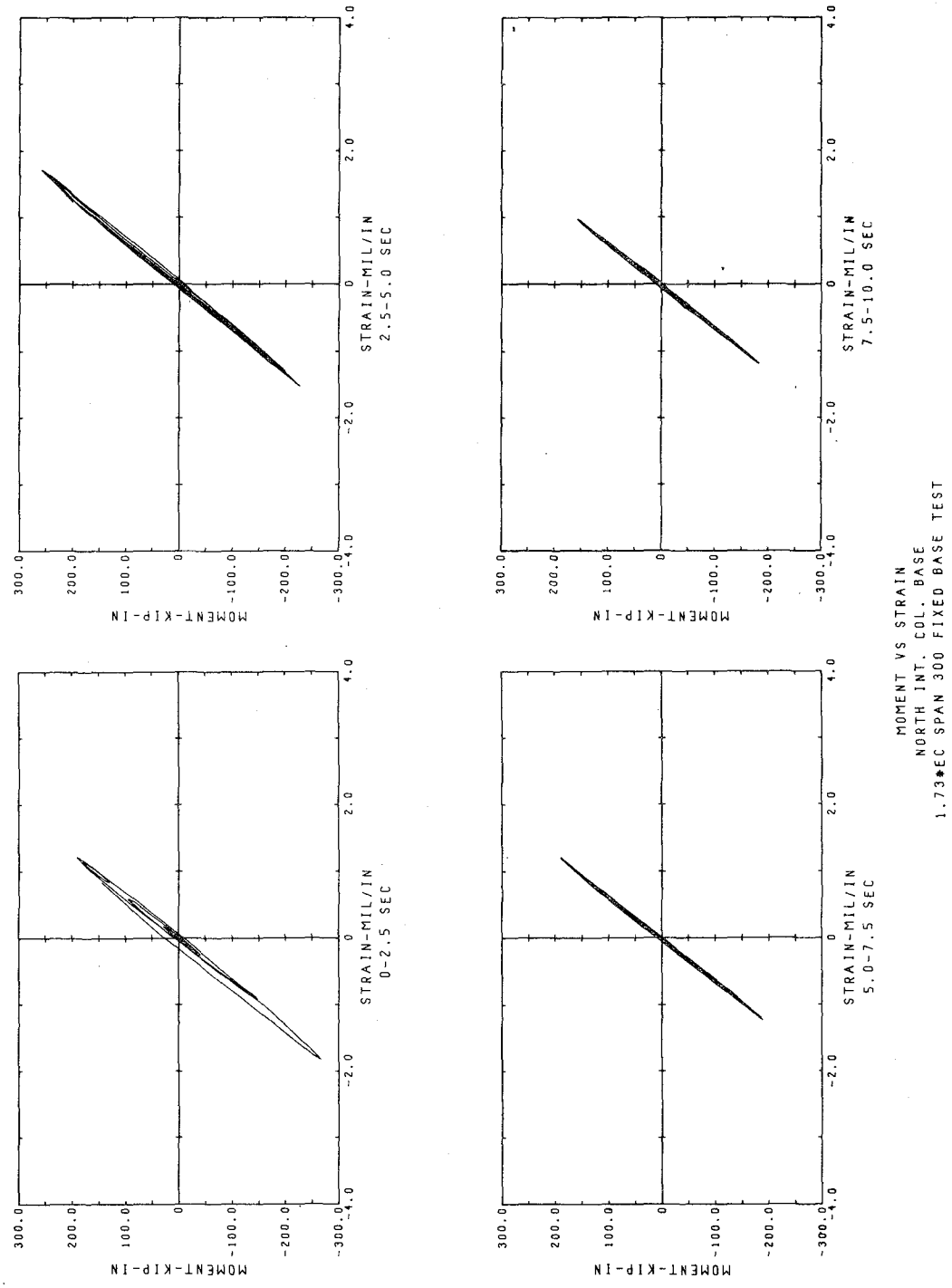

Fig. 6.F.8 1st Floor Column Hysteresis Plots

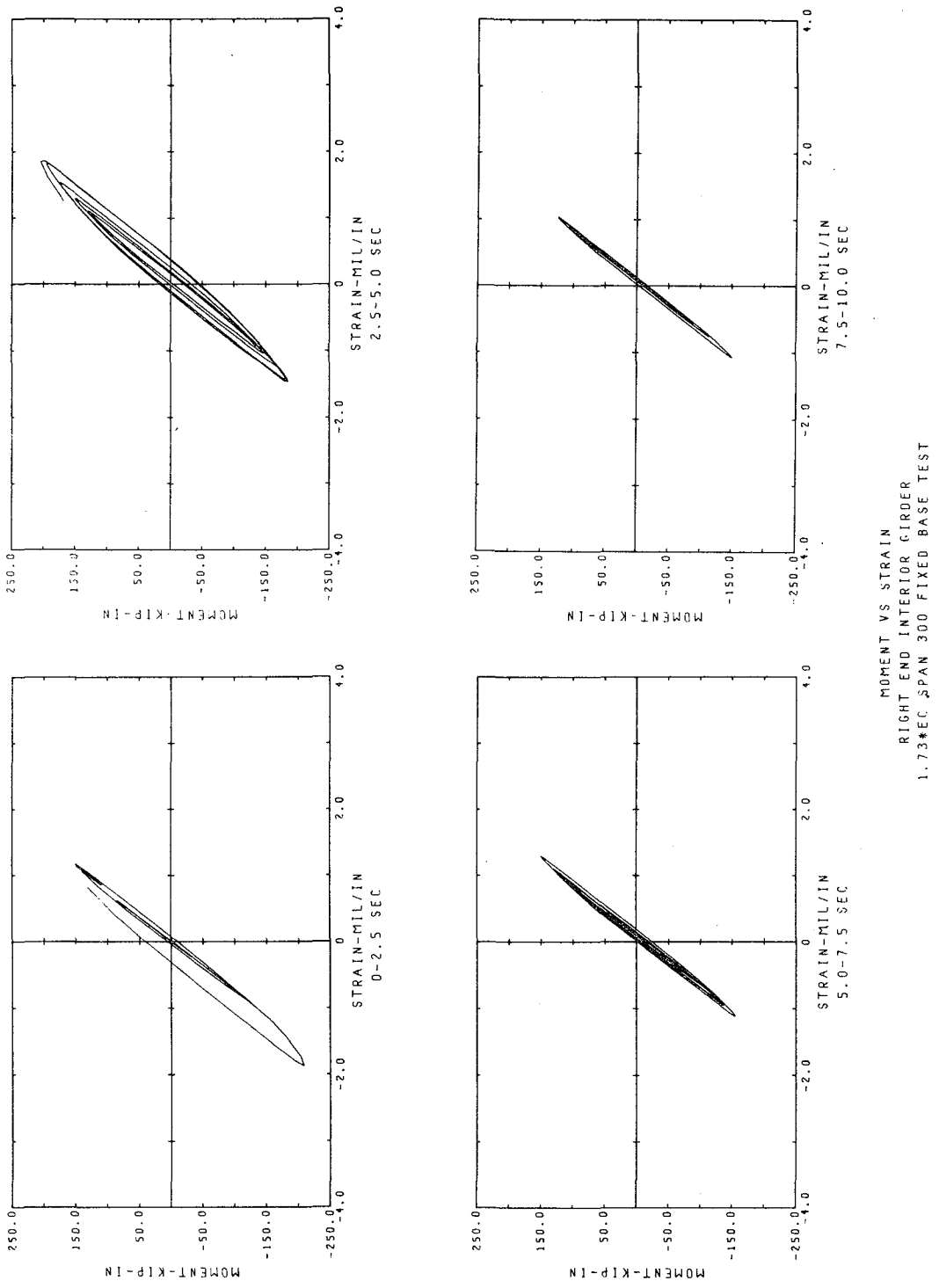

Fig. 6.F.9 1st Floor Girder Hysteresis Plots

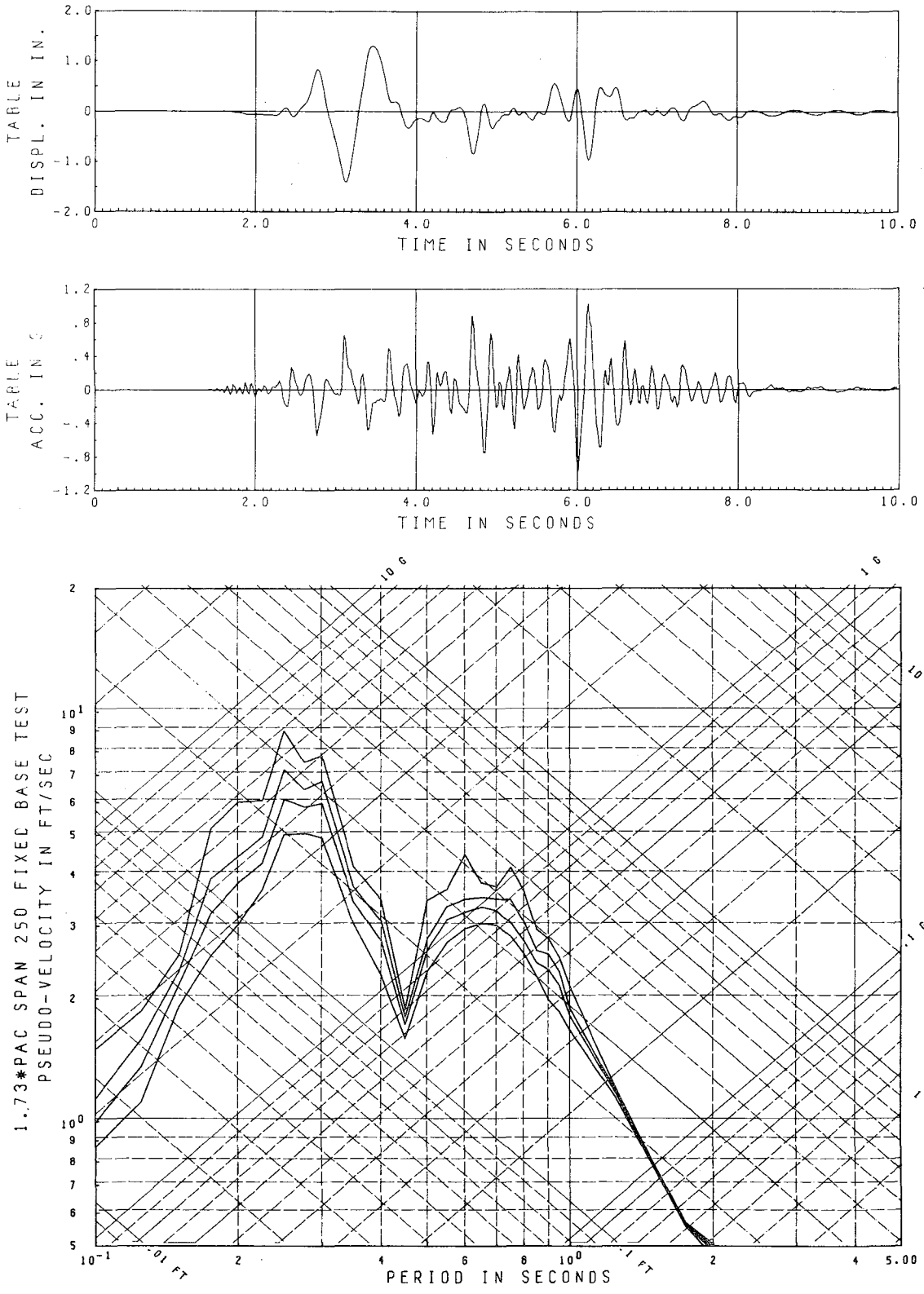

Damping = .01, .02, .03, .05 Critical

Fig. 6.G.1 Pacoima Span 250 Horizontal Table Motion

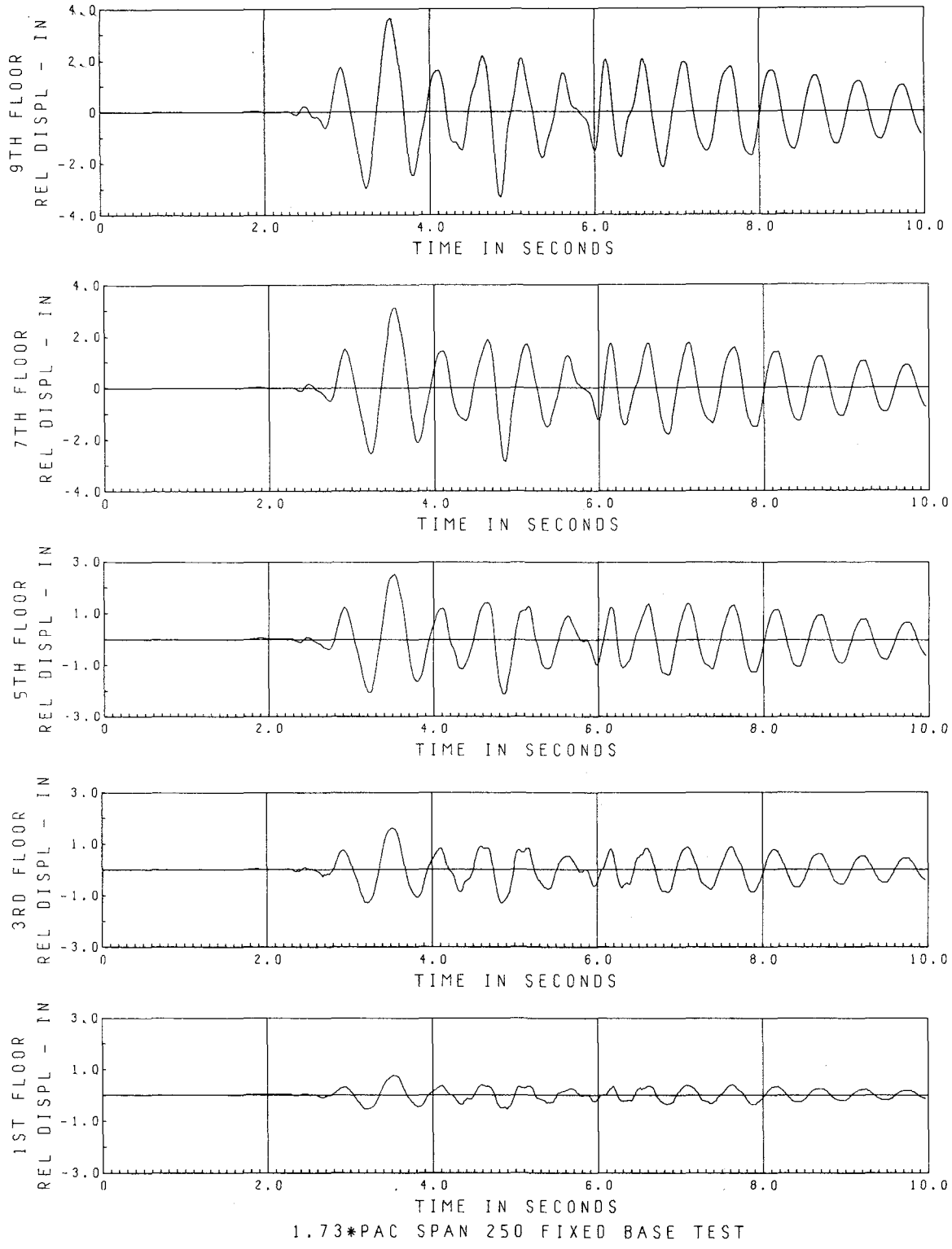

Fig. 6.G.2 Relative Floor Displacements

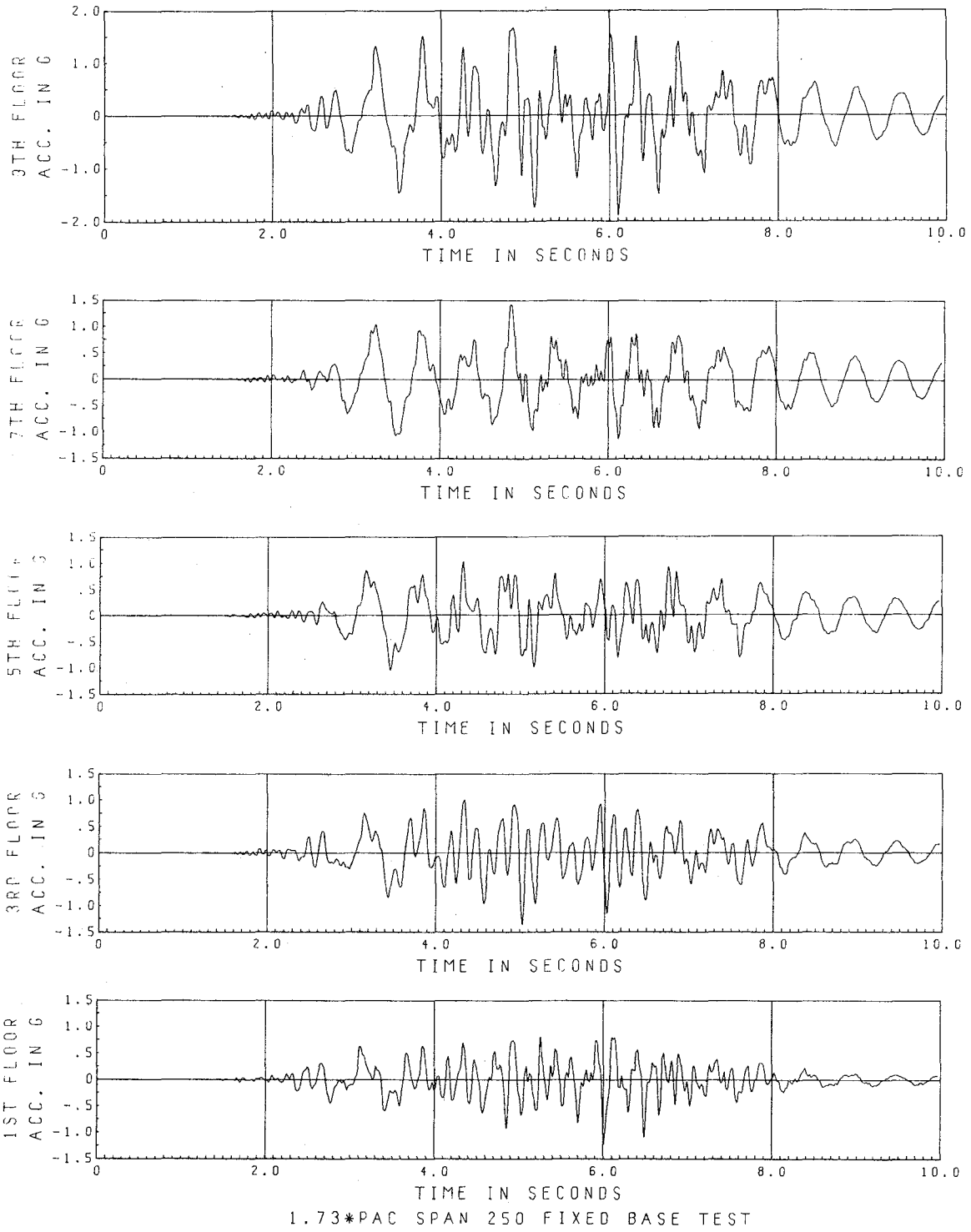

Fig. 6.G.3 Floor Accelerations

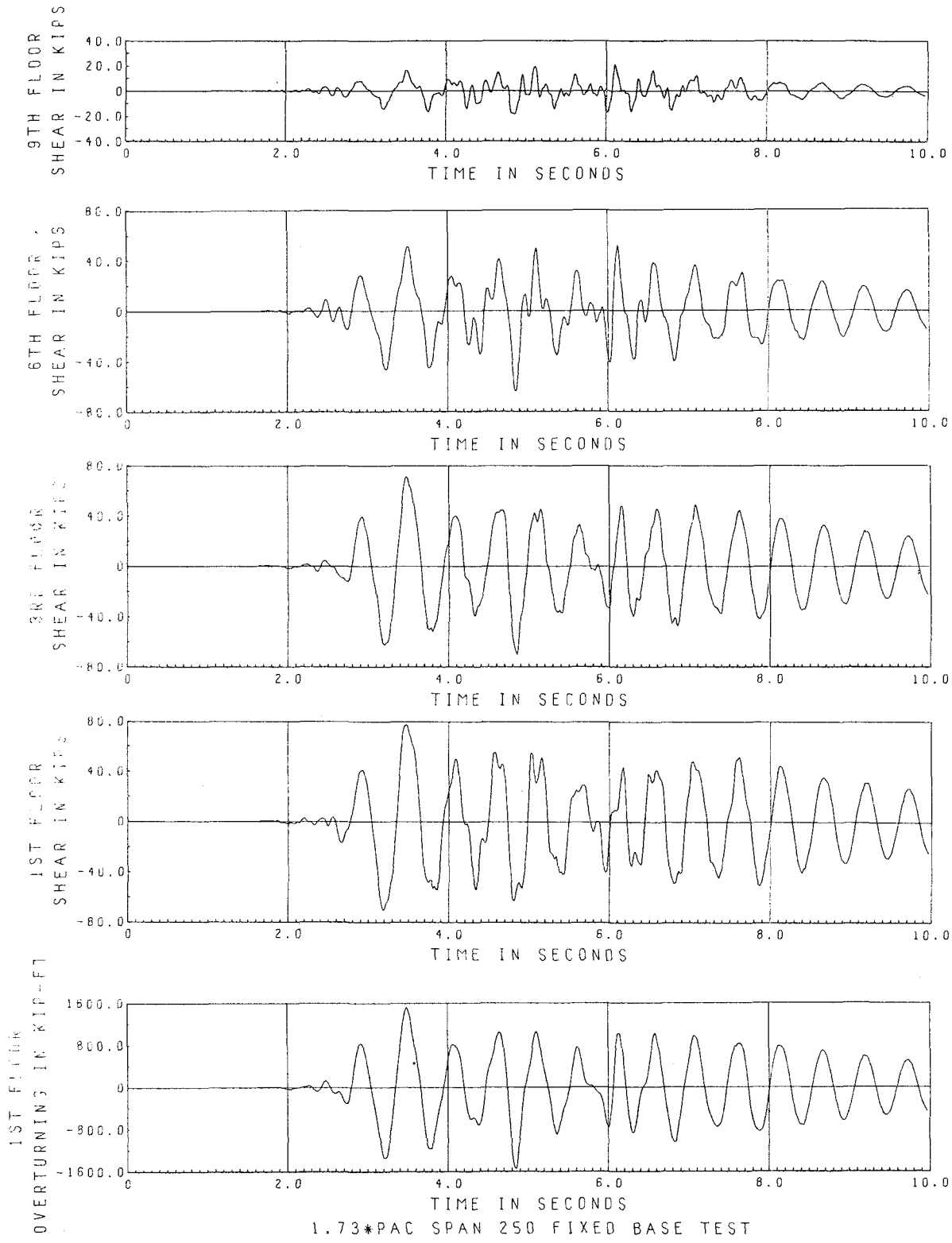

Fig. 6.G.4 Story Shears and Overturning

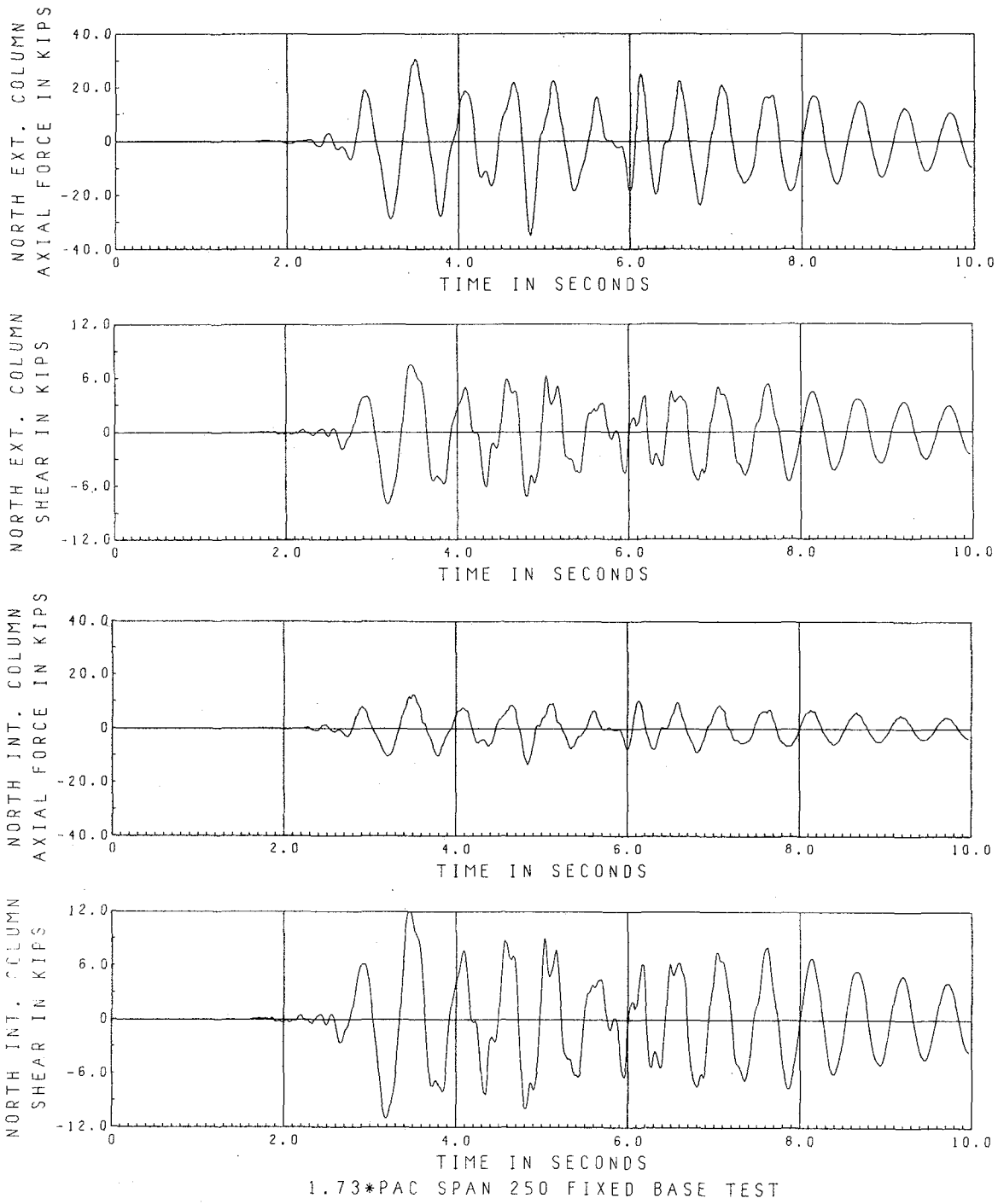

Fig. 6.G.5 1st Floor Column Shears and Axial Forces

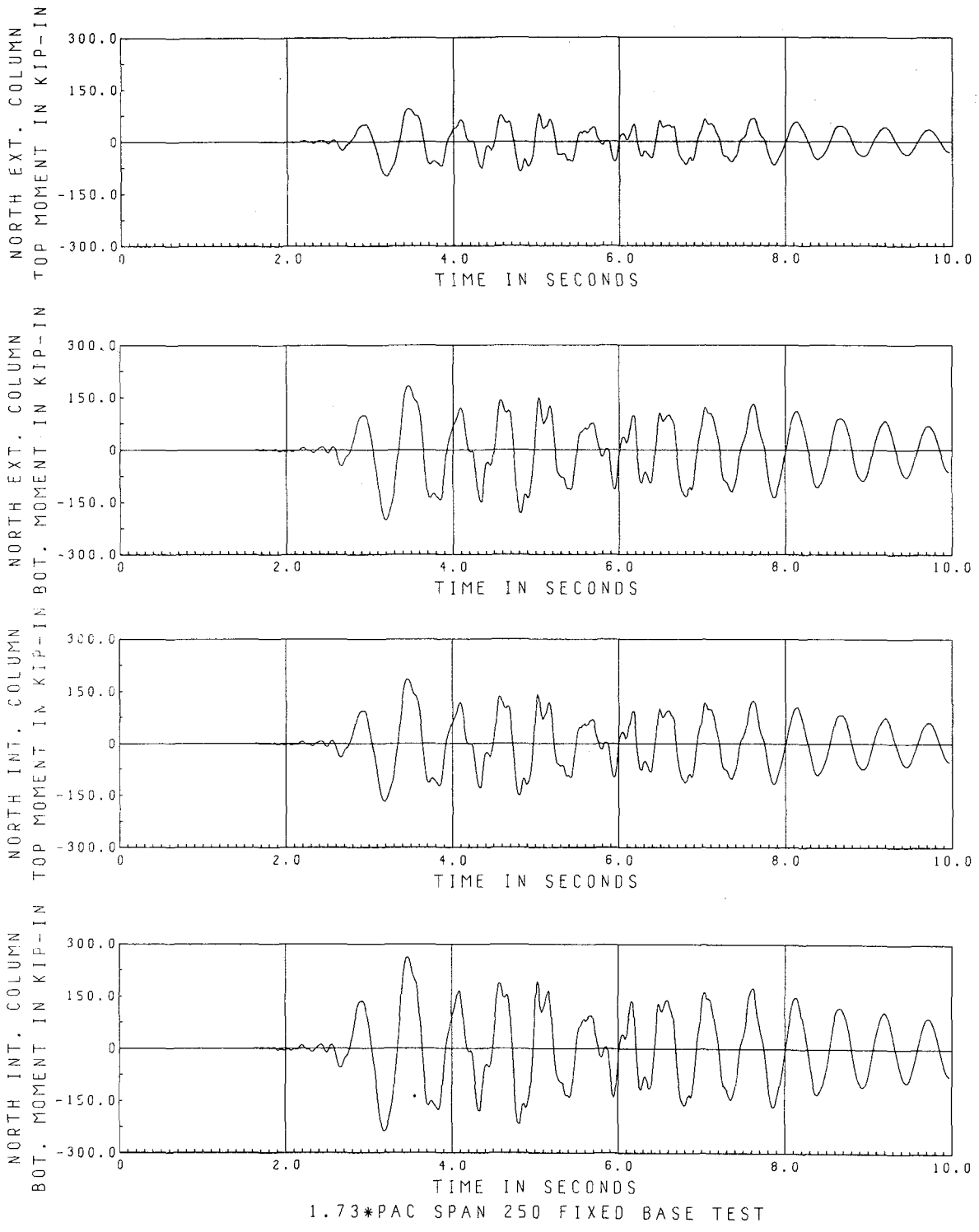

Fig. 6.G.6 1st Floor Column Bending Moments

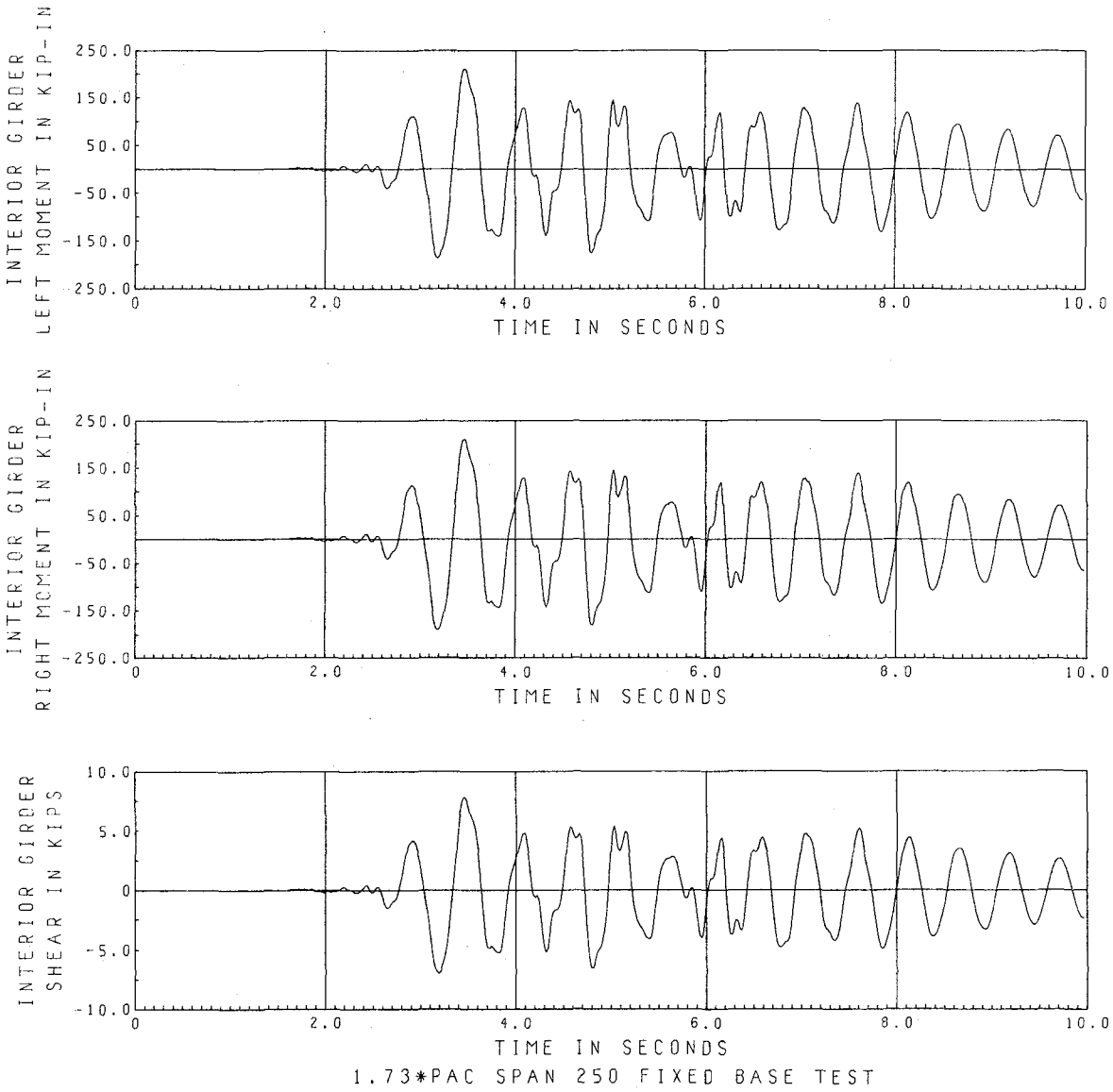

Fig. 6.G.7 1st Floor Girder Shear and Moments

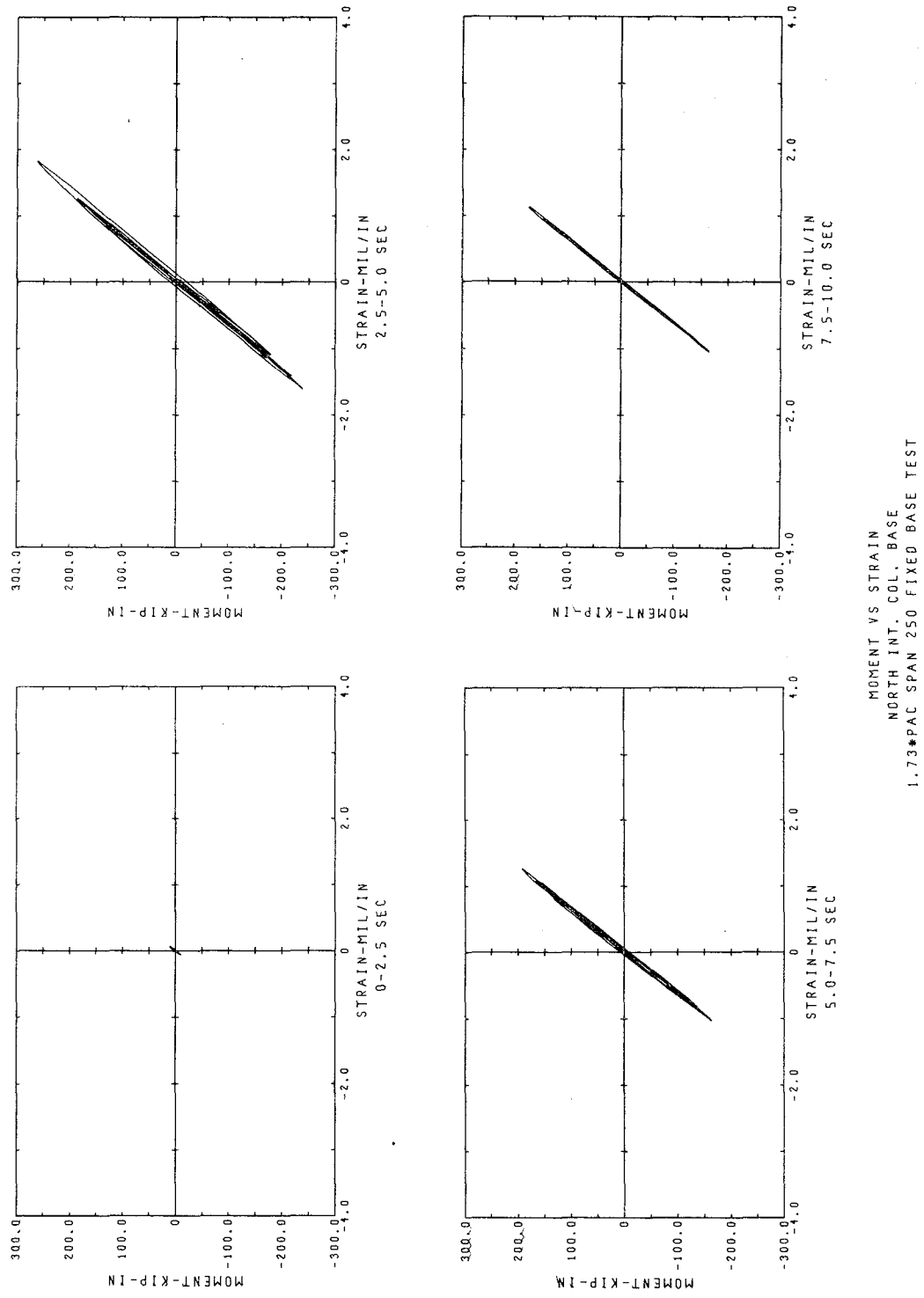

Fig. 6.G.8 1st Floor Column Hysteresis Plots

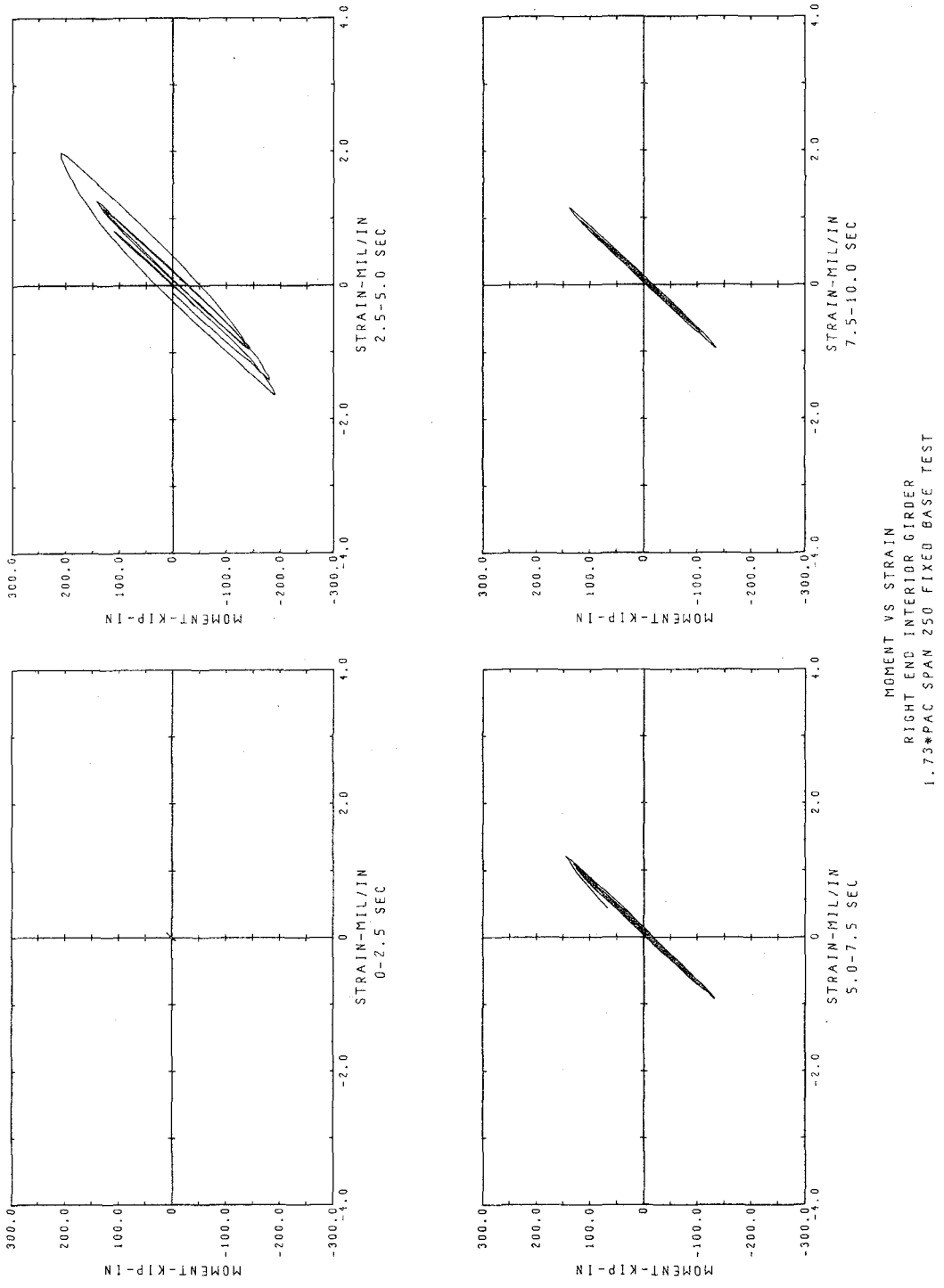

Fig. 6.G.9 1st Floor Girder Hysteresis Plots: Moment vs Strain

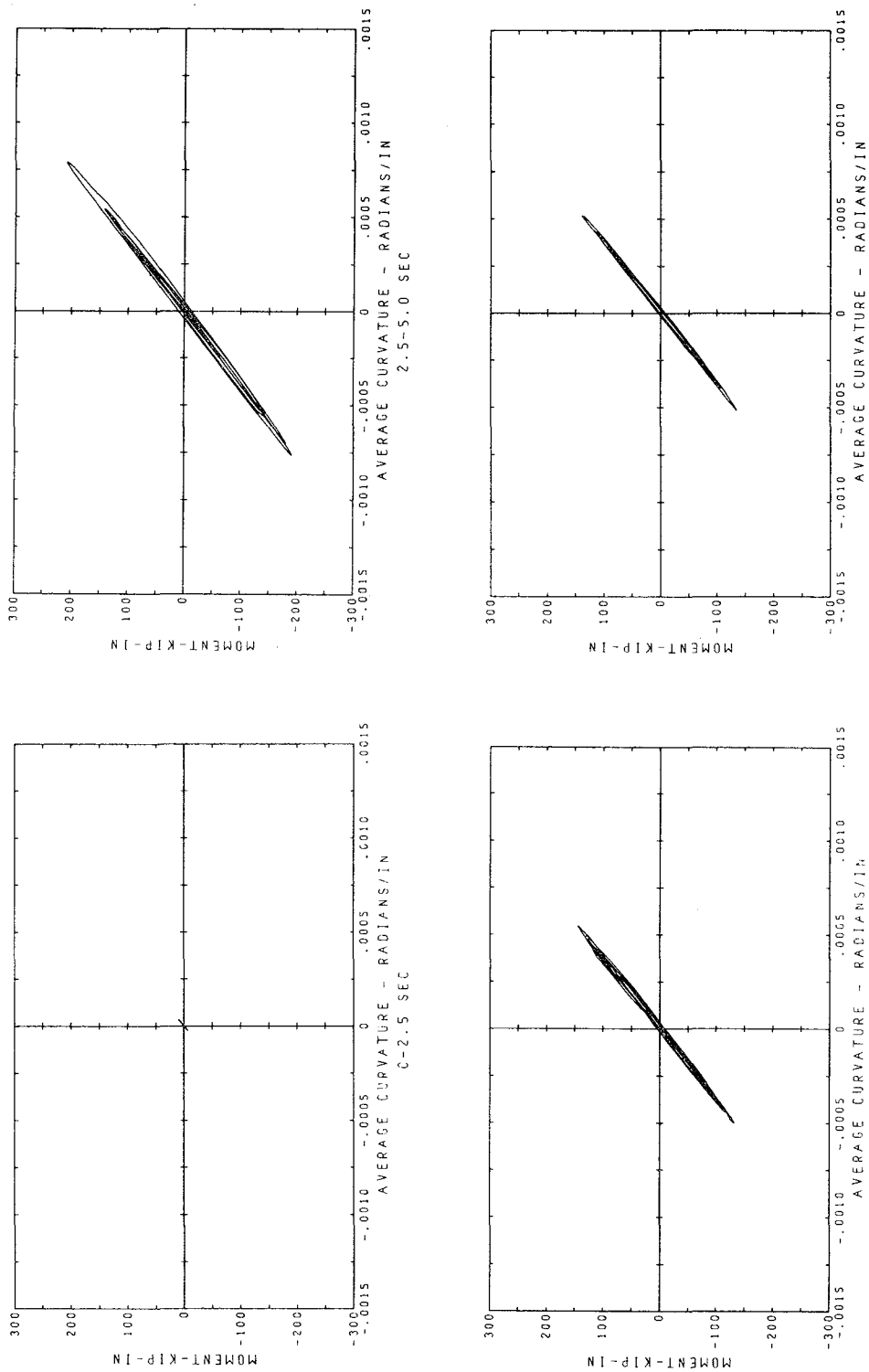

Fig. 6.G.10 1st Floor Girder Hysteresis Plots: Moment vs Average Curvature

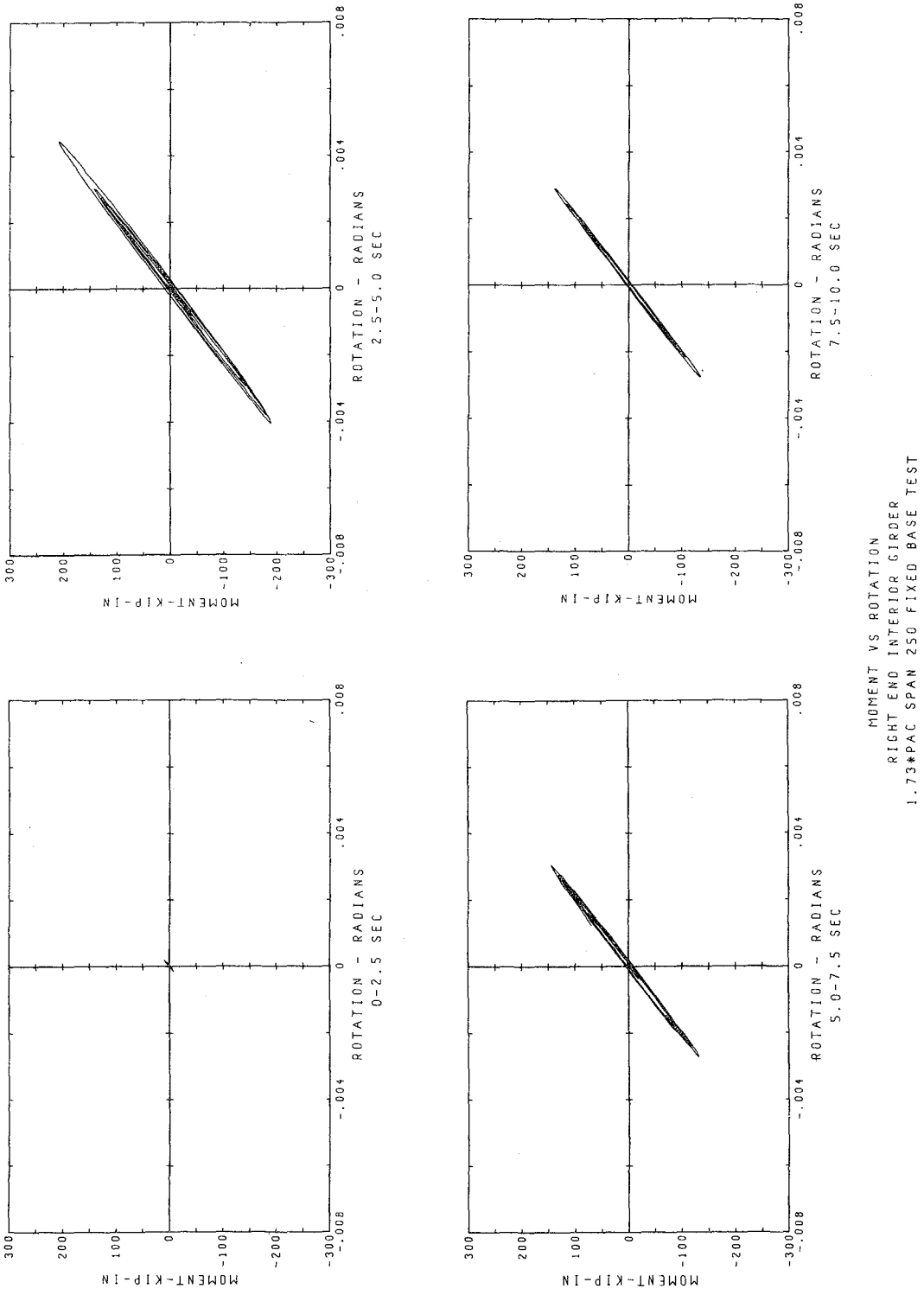

Fig. 6.G.11 1st Floor Girder Hysteresis Plots: Moment vs Rotation

7. ANALYTICAL CORRELATION OF TEST DATA

One of the primary objectives of this test program was the evaluation of currently available nonlinear frame analysis techniques. To accomplish this objective, the experimental input signals were used as the input records for nonlinear analyses, and the resulting analytical responses were compared directly to experimentally observed responses.

The computer program utilized for the nonlinear analytical work was DRAIN-2D, described fully Kanaan and Powell (4). This is a general two-dimensional structural analysis program for computing the nonlinear dynamic response to identical, in-phase motions of all support points. Static loads producing a linear force distribution may be applied prior to the dynamic analysis. The full set of incremental equations of motion are numerically integrated using the assumption of constant average nodal accelerations within each integration time step. Unbalanced loads resulting from stiffness changes are corrected in the following time step, necessitating fairly small time steps to avoid large "overshoots" at instants of significant stiffness changes. Structural elements currently available in the program have a bilinear, softening type of force-deformation behavior. Current damping capabilities include arbitrary combinations of mass proportional, original stiffness proportional, or tangent stiffness proportional viscous damping. Since the coupled equations of motion are integrated, the use of proportional damping is merely a matter of convenience in defining a damping matrix.

The basic analytical model, mentioned briefly in Chapter 3, is shown here again in Fig. 7.1. As mentioned previously, the shaking table compliance is modeled using a passive spring-mass foundation system

with vertical and rotational degrees of freedom.

As the symmetric static loading condition is nearly negligible, the structural symmetry of the model might be utilized to calculate the response to antisymmetric seismic loading in the fixed base analysis. For the uplifting analysis, however, the full model must be included, because uplift eliminates the symmetry of the structure. As a matter of convenience, therefore, the full model was considered for the analyses of both base conditions.

In order to minimize the size of the stiffness matrix for the structure, and thus allow a completely in-core solution for the dynamic analysis, as many degrees of freedom as possible were eliminated from the system. This was accomplished by allowing axial deformations only in the 1st floor columns and foundation spring elements, and assuming the shaking table and column baseplate elements to be completely rigid. The finite dimensions of the joints were considered in the analytical work; the joint panel zones were, however, assumed rigid.

7.A. Uplift Analysis

To analyze the basic model as an uplifting system, the spring elements representing the impact pads between the column baseplates and the shaking table were made bilinear elastic, having no tensile capacity or stiffness in the upward direction. To account for the dead load, these spring elements were prestressed to appropriate force levels. No other static forces were considered in the dynamic analyses, because the static forces were very low, and their distribution in the actual model were difficult to ascertain reliably.

To economize on the analysis, it was felt desirable to include only the minimum local nonlinear behavior necessary to adequately predict

the performance. One analytical assumption used, designated as model 1 in the subsequent discussion, was that only the nonlinear moment-rotation characteristics of the 1st floor columns and the 1st floor interior girder would be considered. A second analytical assumption used, designated model 2, was that the nonlinear behavior of the 1st floor columns, all the 1st floor girders and the 2nd floor interior girder would be considered.

From the experience gained in the analysis of the three-story uplifting steel frame, mentioned in the introduction, it was felt that the damping would be very low during uplift motion. This type of behavior was shown, for the three-story frame, to be modeled well using tangent stiffness proportional viscous damping. The reduced stiffness during uplift motion reduces the damping in a corresponding manner.

The initial analytical work was performed using model 1, as previously described, and the 1.73*PAC span 200 input. The first tangent stiffness damping coefficient, designated β, had a value of .0016; this corresponds to a damping ratio of 1% for the 1st mode response preceding uplift. The north exterior column uplift and the 9th floor relative displacement resulting from this analysis, using an integration time step of .0096 sec. (equal to $\frac{1}{2}$ the experimental data samping interval), are shown in Fig. 7.A.1, along with the corresponding experimental quantities. It should be noted that uplift response represents relative displacement between the column base and the shaking table. The first few cycles of response are seen to be well represented, but the uplift motion was damping too heavily for subsequent cycles.

Another analysis was performed, changing only the value of β to .001425, corresponding to a 1st mode damping ratio of .9%. The results

The results of this analysis are shown in Fig. 7.A.2; the correlation was quite good for the response quantities plotted.

The results of another analysis using this identical model for the 1.73*EC span 300 input are shown in Fig. 7.A.3. Again, the correlation was quite good, for the quantities plotted.

It was noticed, however, that some of the local moments and shears predicted by these analyses were slightly higher than the experimental values. It was decided, therefore, to perform another analysis using model 2 with the Pacoima input. To compensate somewhat for the increased energy dissipation of model 2, the value of β was reduced to .0014. The results of this analysis are shown in Fig. 7.A.4; the damping again seems a little high.

Another analysis was performed, lowering the value of β to .0011 and cutting the integration time step in half. It was felt that this low damping ratio, less than .7%, might lead to numerical stability problems in the analysis. The results of this analysis are shown in Fig. 7.A.5; again the correlation was quite good.

Figs. 7.A.6 through 7.A.10 show additional results from this analysis. The relative floor displacements and column uplifts agreed well. The column axial forces of Fig. 7.A.8 show a little impact-induced numerical stability problem, but not enough to cause major concern. The 1st floor column moments of Fig. 7.A.9 agreed well, as did the 1st floor interior girder moments of Figs. 7.A.10.

It was decided to repeat this analysis, except for doubling the integration time step, back to .0096 sec. The results of this analysis are shown in Figs. 7.A.11 through 7.A.15. The numerical problems associated with the column impact are seen to be more severe for the

coarser time step. If these results are interpreted with a measure of engineering judgment, however, they probably are still entirely usable, at least for design purposes.

Another analysis using model 2 with β = .0011 and the coarser time step of .0096 was performed, using the 1.73*EC span 300 input. The results of this analysis are shown in Figs. 7.A.16 and 7.A.17. As somewhat less impact was involved for the El Centro test, the numerical problems were not as severe. The results of Fig. 7.A.3, using model 1 with β = .001425, however, show a considerably lesser numerical stability problem, and are more satisfactory for this time step.

7.B. Fixed Base Analysis

To analyze the basic model as a fixed base system, the spring elements representing the impact elements for the uplift analysis were converted to essentially rigid elements, with unlimited capacity in both tension and compression. Again analyses were performed with two levels of local nonlinear behavior considered, designated model 1 and model 2, as described previously. An integration time step of .0096 sec. was used throughout the fixed base analysis.

A first analysis was performed using model 1 and the 1.73*EC span 300 input. The damping was specified as tangent stiffness proportional; the value of β selected was .004, corresponding to a 1st mode damping ratio of 2.5%. The resulting 9th floor relative displacement is shown in Fig. 7.B.1; the actual response was overestimated, indicating too little energy dissipation present.

Since the physical model did consist of a bare steel frame, it was felt that the damping ratio should not be very high. For that reason, it was suspected that the shaking table's response was perhaps

more heavily damped than the superstructure system.

In an attempt to provide more damping for the table pitching without increasing the damping for the superstructure, an analysis was performed using mass proportional damping. The shaking table had a very large rotational inertia, which was included in the analysis. The mass proportional damping coefficient, designated α, was selected as 0.628 for this analysis, corresponding to the same 1st mode damping ratio of 2.5%. The results of this analysis are shown in Fig. 7.B.2. The improvement in the correlation was, however, only slight.

Another analysis was performed using model 2 with the same parameters as above. The increased energy dissipation of this model did considerably improve the correlation, as shown in Fig. 7.B.3.

Another analysis was performed, increasing the value of α to 0.800, corresponding to a 1st mode damping ratio of 3.2%. The results of this analysis are shown in Fig. 7.B.4; the correlation was quite good. Results for this same model using the 1.73*PAC span 250 input are shown in Figs. 7.B.5 through 7.B.8. Again, the correlation was generally good.

Mass proportional damping has the characteristics or providing lower damping for the higher response modes. The value of α used, 0.800, thus provided a damping ratio of about 0.7% for the 2nd mode. This fact is apparent in the local force time histories presented in Figs. 7.B.6 through 7.B.8; the 2nd mode response was considerably overestimated in the analysis.

Stiffness proportional damping, on the other hand, has the characteristic of providing progressively higher damping in the higher response modes. For that reason, another analysis was performed for the Pacoima input, using tangent stiffness proportional damping. The

value of β selected was .005127, which gives 1st and 2nd mode damping ratios of 3.2% and 11.5%, respectively. The results of this analysis are shown in Figs. 7.B.9 through 7.B.12.

Comparing the results of the analyses using mass proportional and stiffness proportional damping, it is apparent that both predict quite well the 1st mode response. Mass proportional damping considerably overestimated the 2nd mode response. Stiffness proportional damping predicts approximately the correct amplitude of 2nd mode response. The natural frequency of the 2nd mode response was overestimated by the analytical model, however, leading to discrepancies in the time history prediction for even stiffness proportional damping. By using combined mass and stiffness proportional damping, it would be theoretically possible to obtain any desired damping ratios in two response modes. The frequency discrepancy, however, would still exist for the higher mode.

Relative floor displacements using the same model as the previous analysis but with the El Centro input are shown in Fig. 7.B.13. Again, the correlation was quite good.

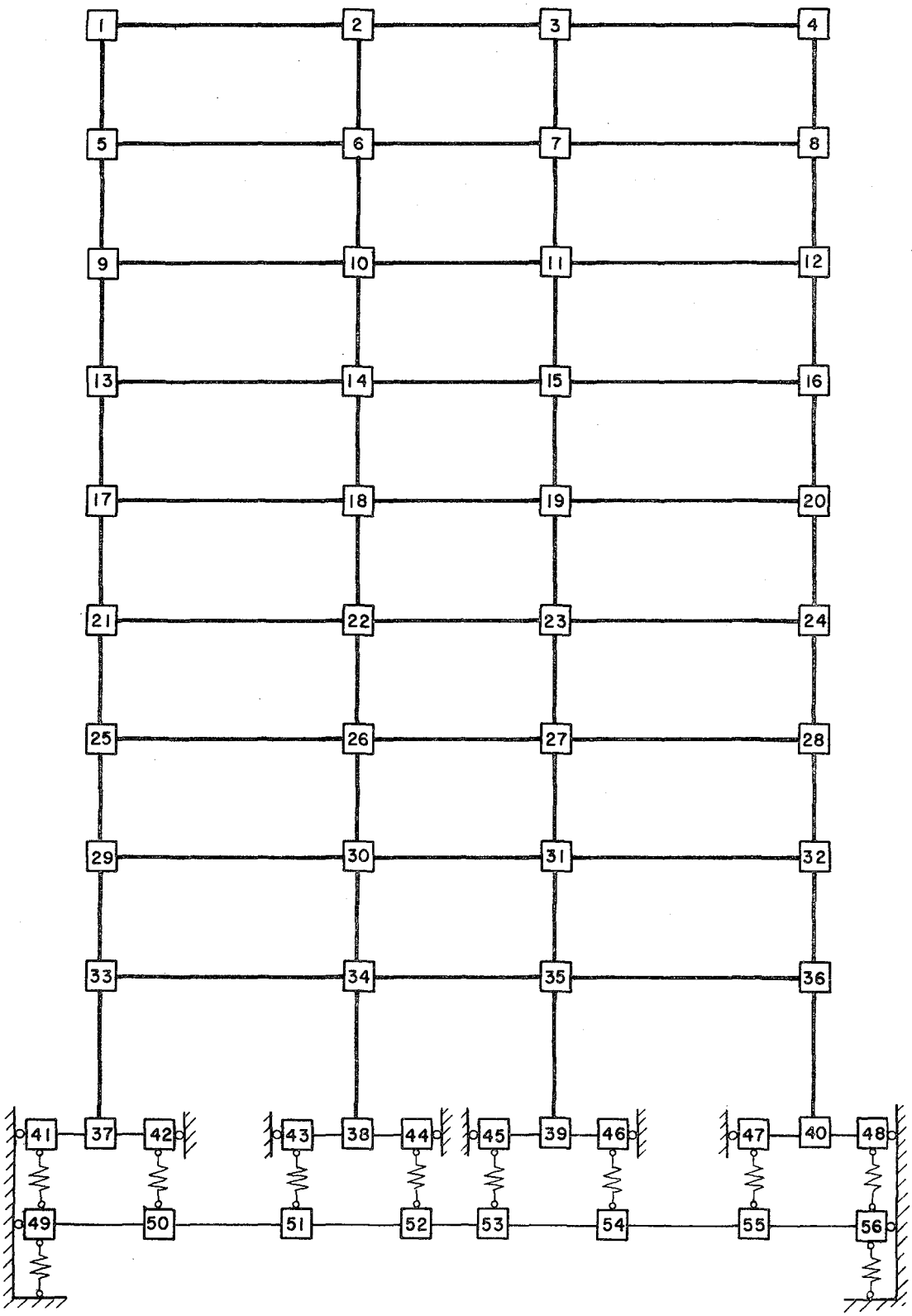

Fig. 7.1 Analytical Model

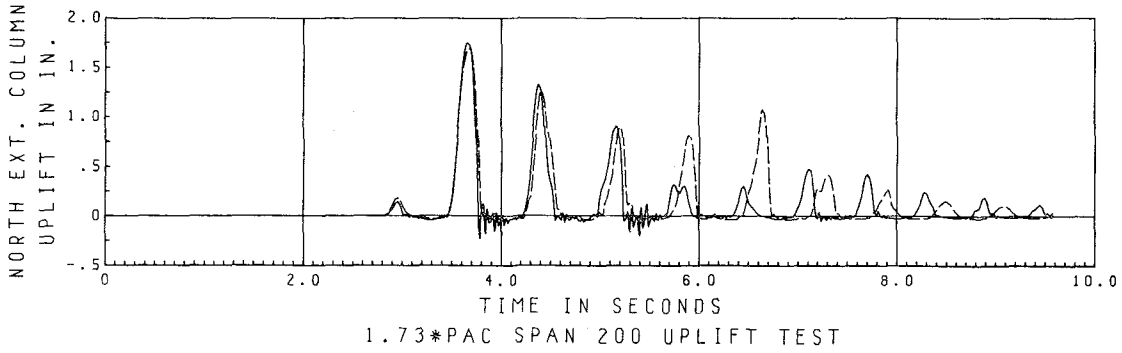

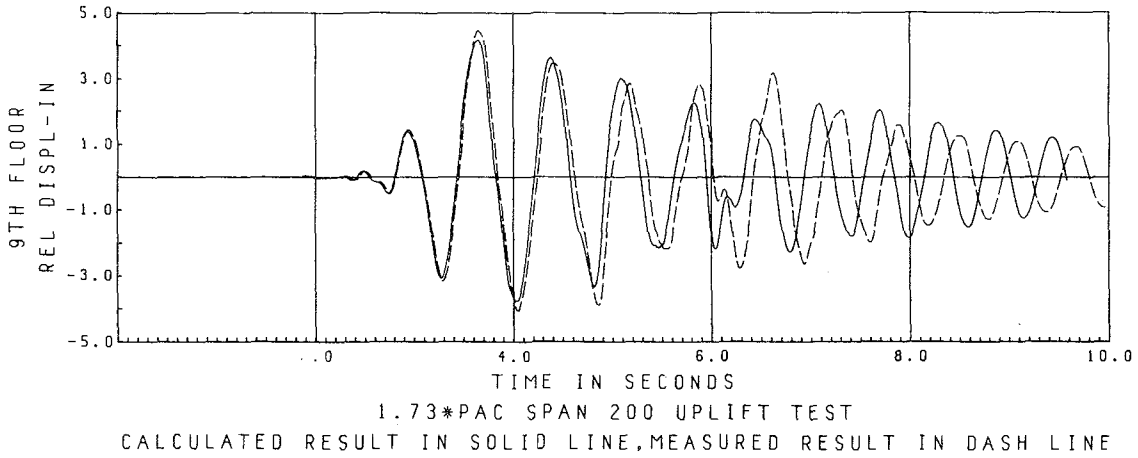

Fig. 7.A.1 Model 1, β = .0016, Δt = .0096

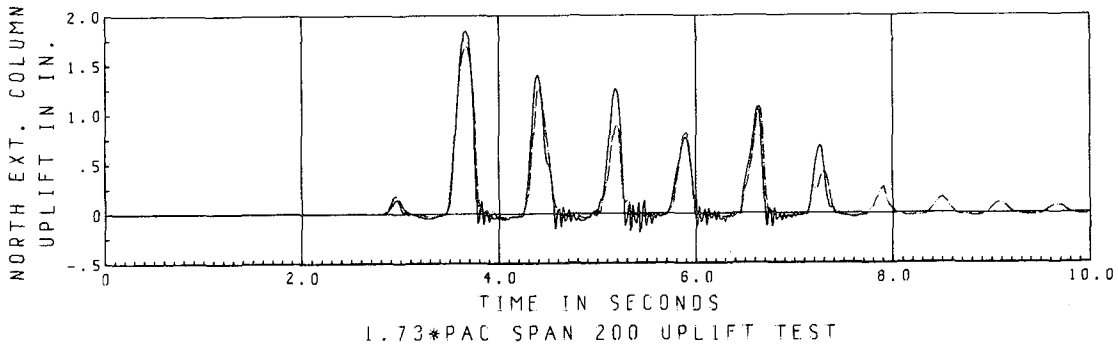

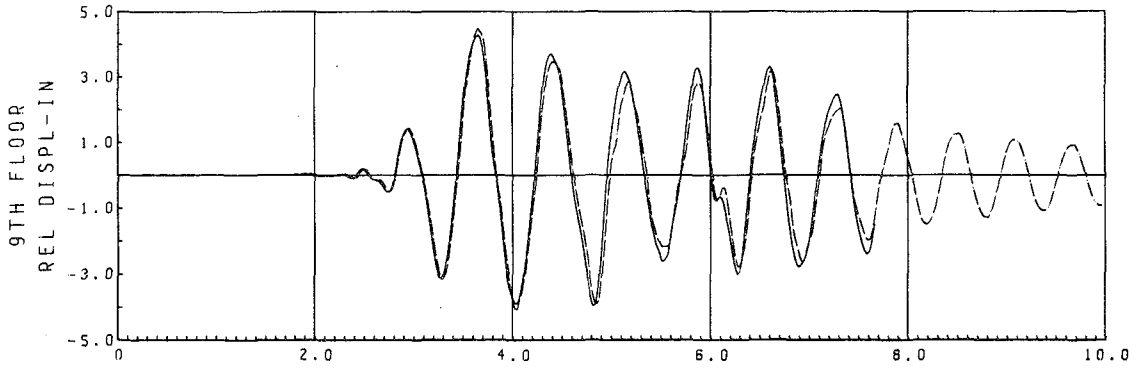

Fig. 7.A.2 Model 1, β = .001425, Δt = .0096

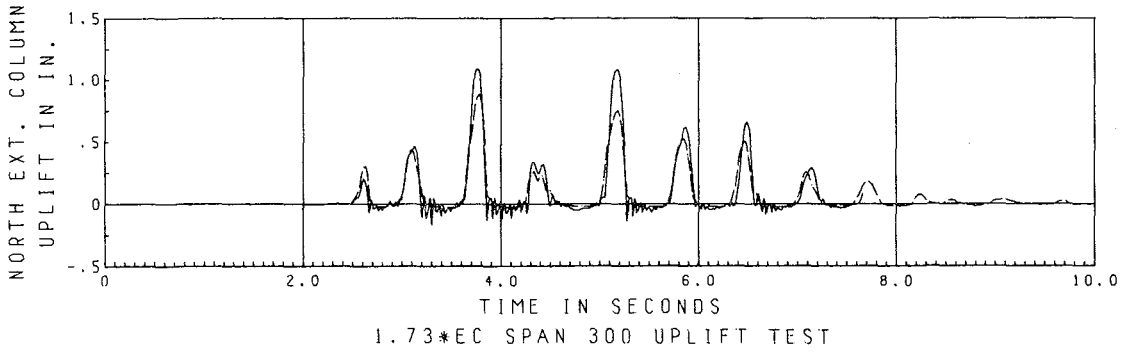

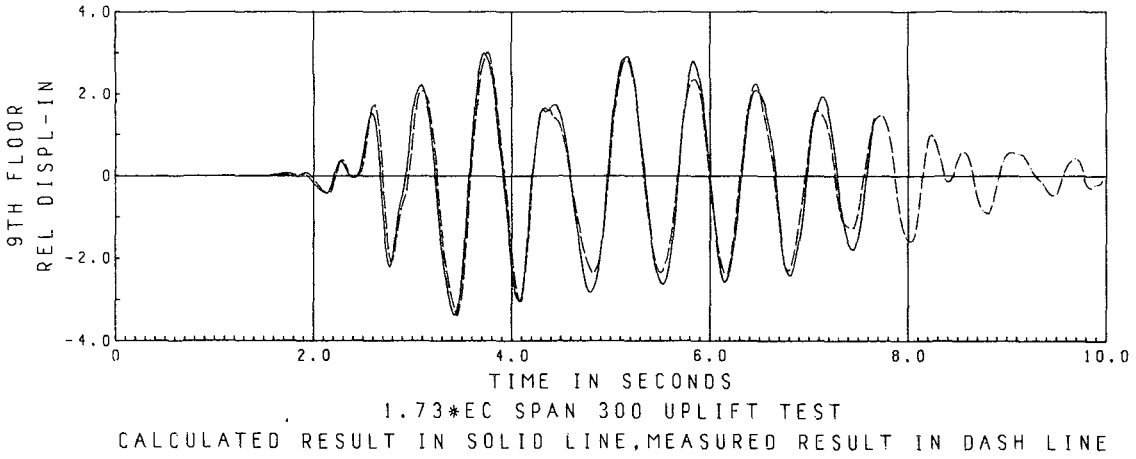

Fig. 7.A.3 Model 1, β = .001425, Δt = .0096

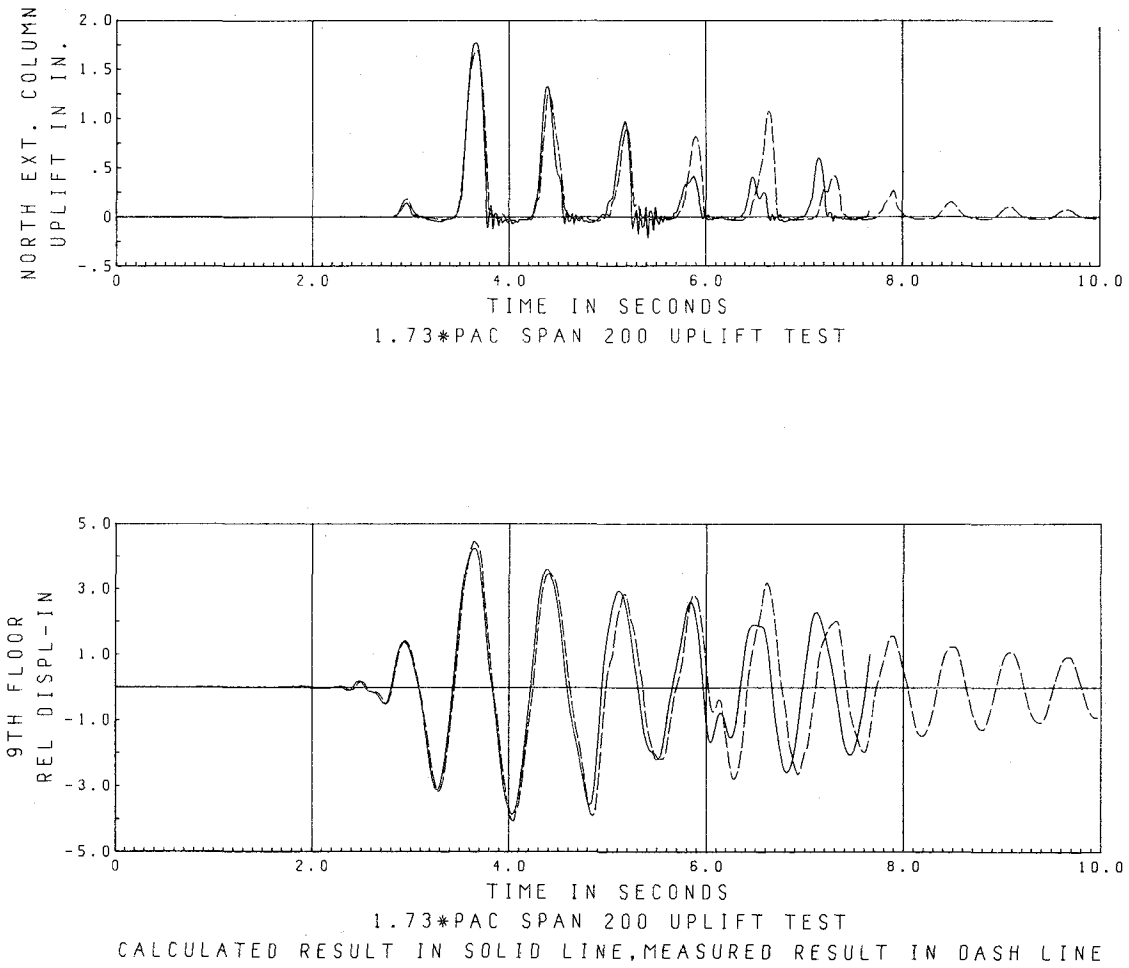

Fig. 7.A.4 Model 2, $\beta = .0014$, $\Delta t = .0096$

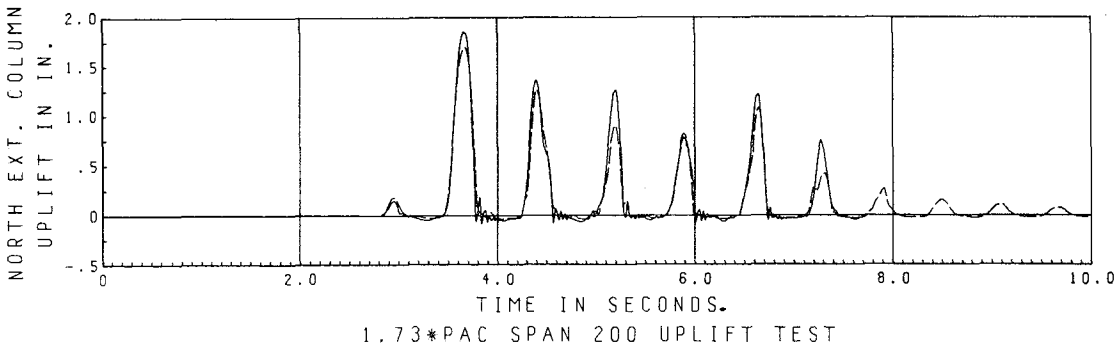

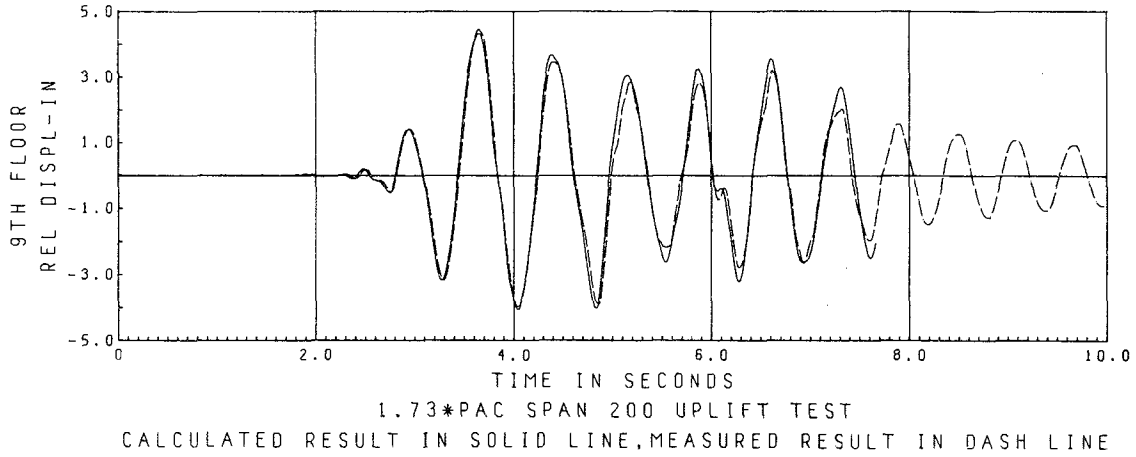

Fig. 7.A.5 Model 2, β = .0011, Δt = .0048

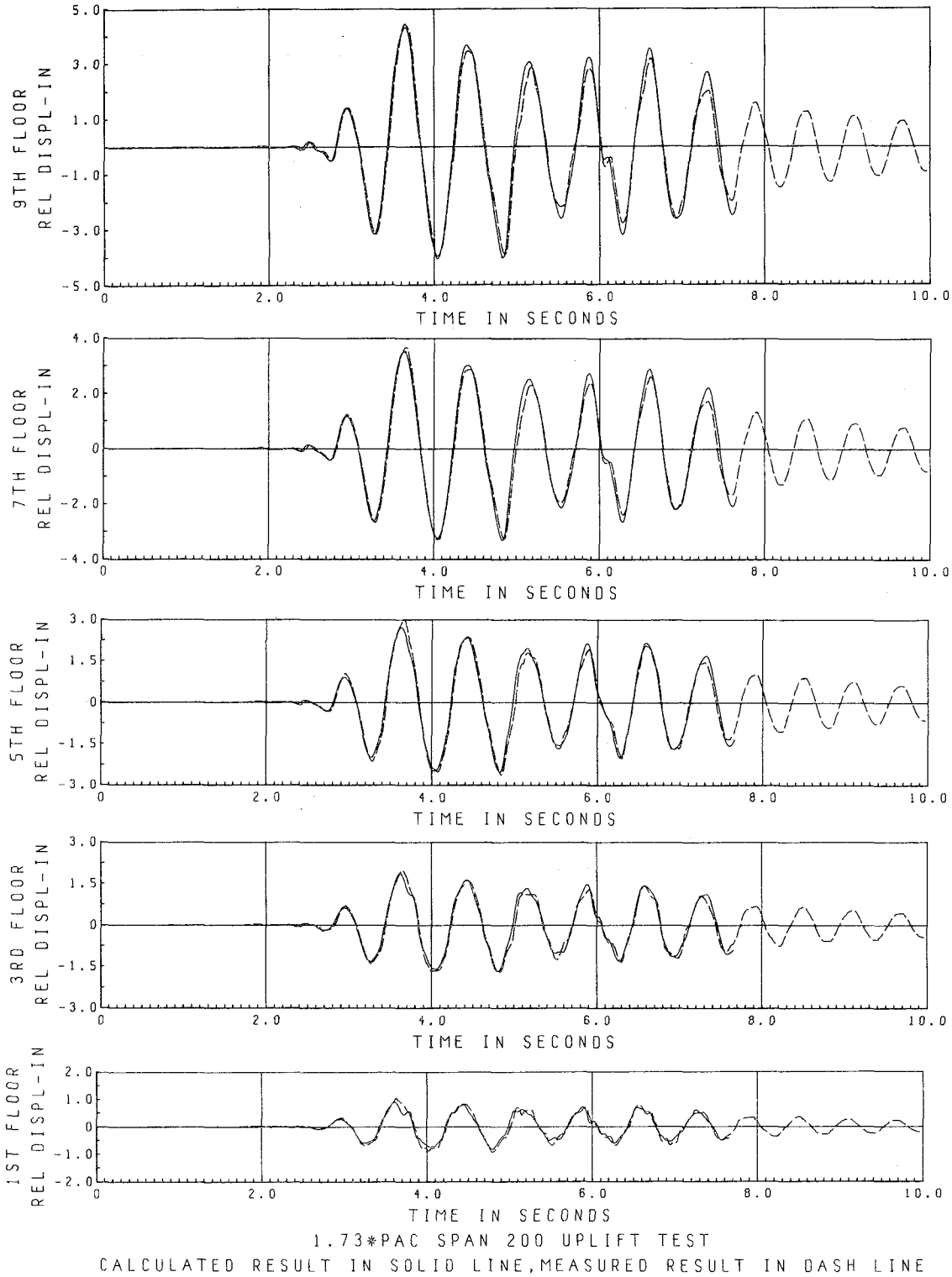

Fig. 7.A.6 Model 2, β = .0011, Δt = .0048

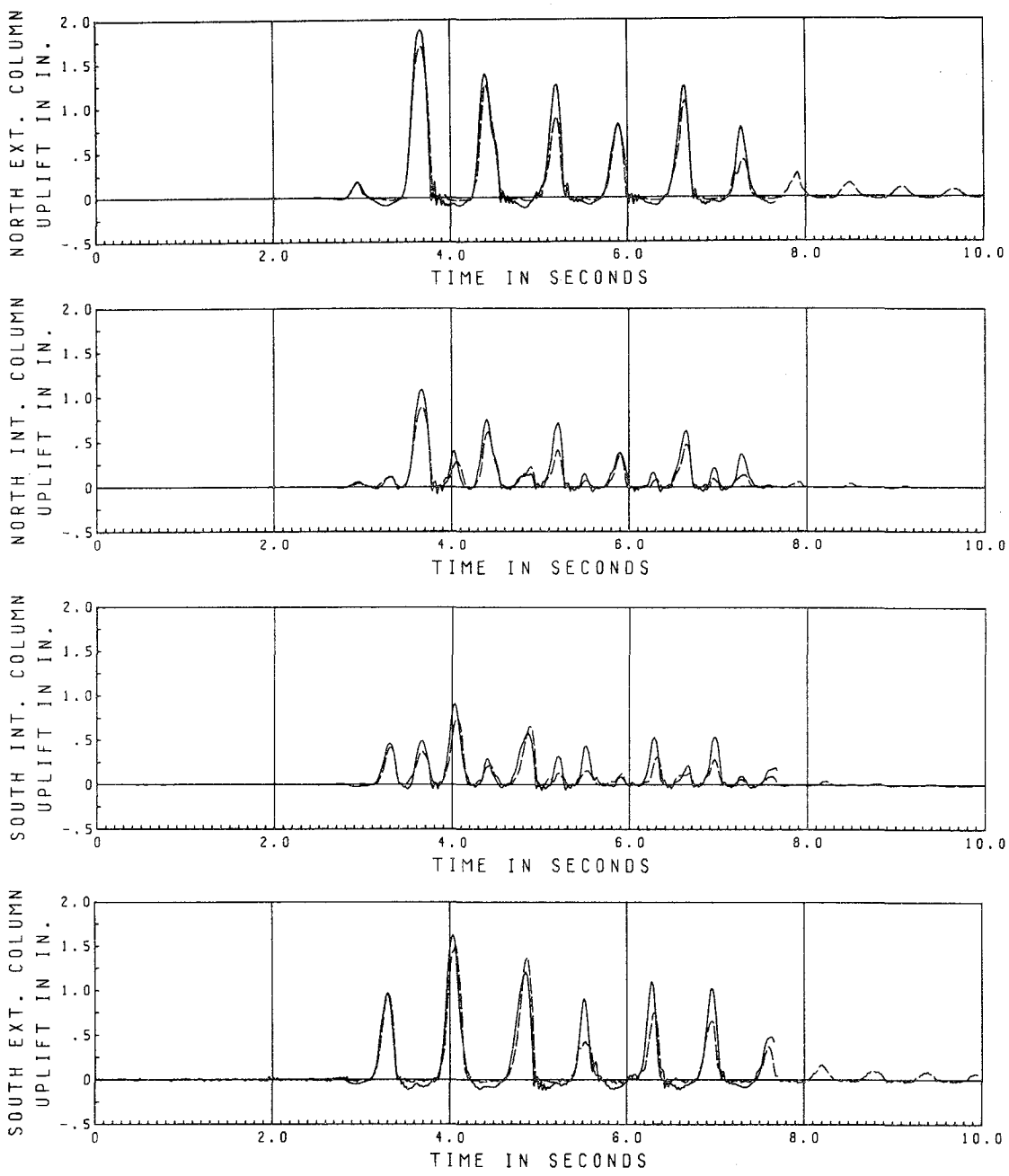

Fig. 7.A.7 Model 2, β = .0011, Δt = .0048

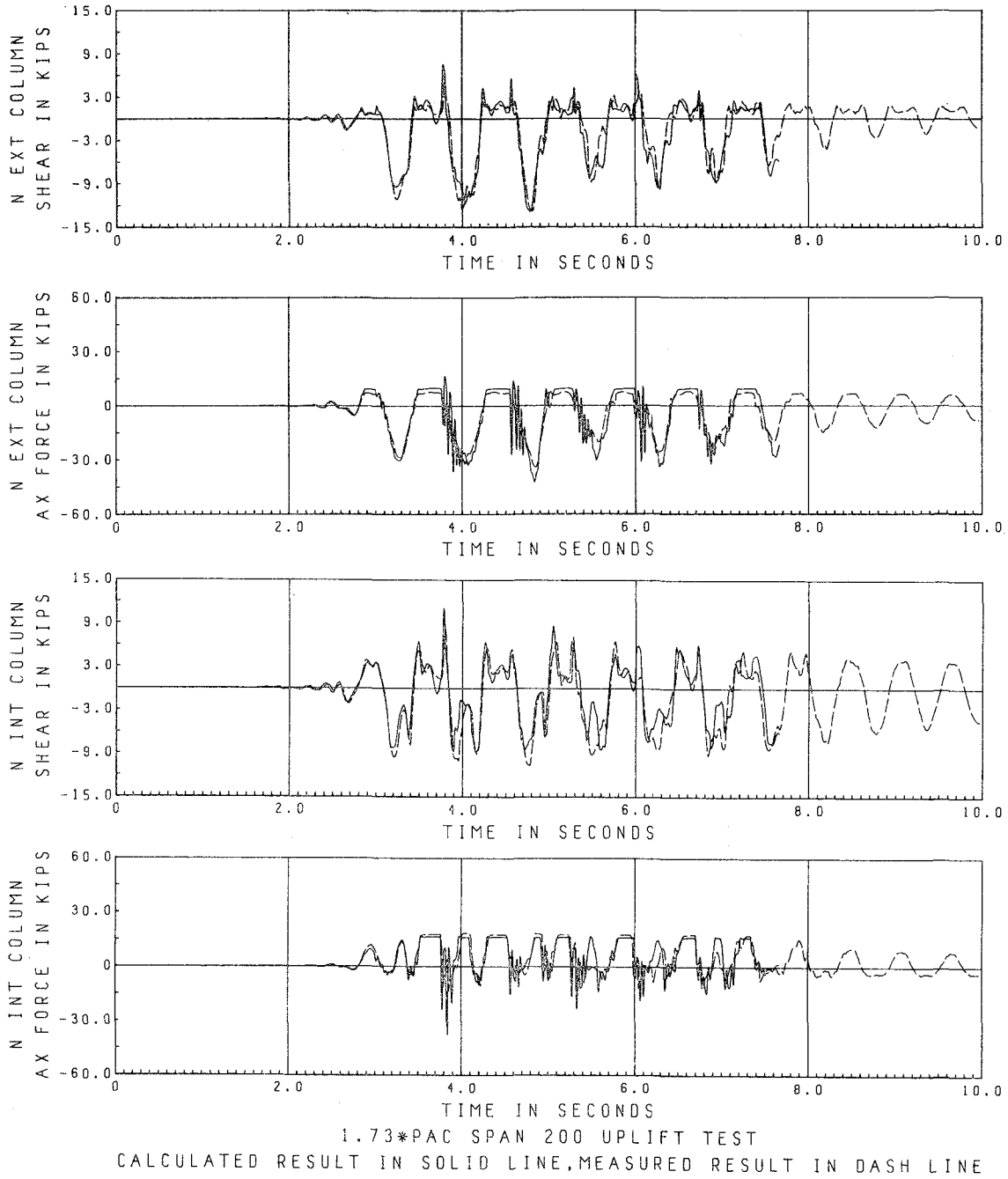

Fig. 7.A.8 Model 2, β = .0011, Δt = .0048 1st Floor Column Forces

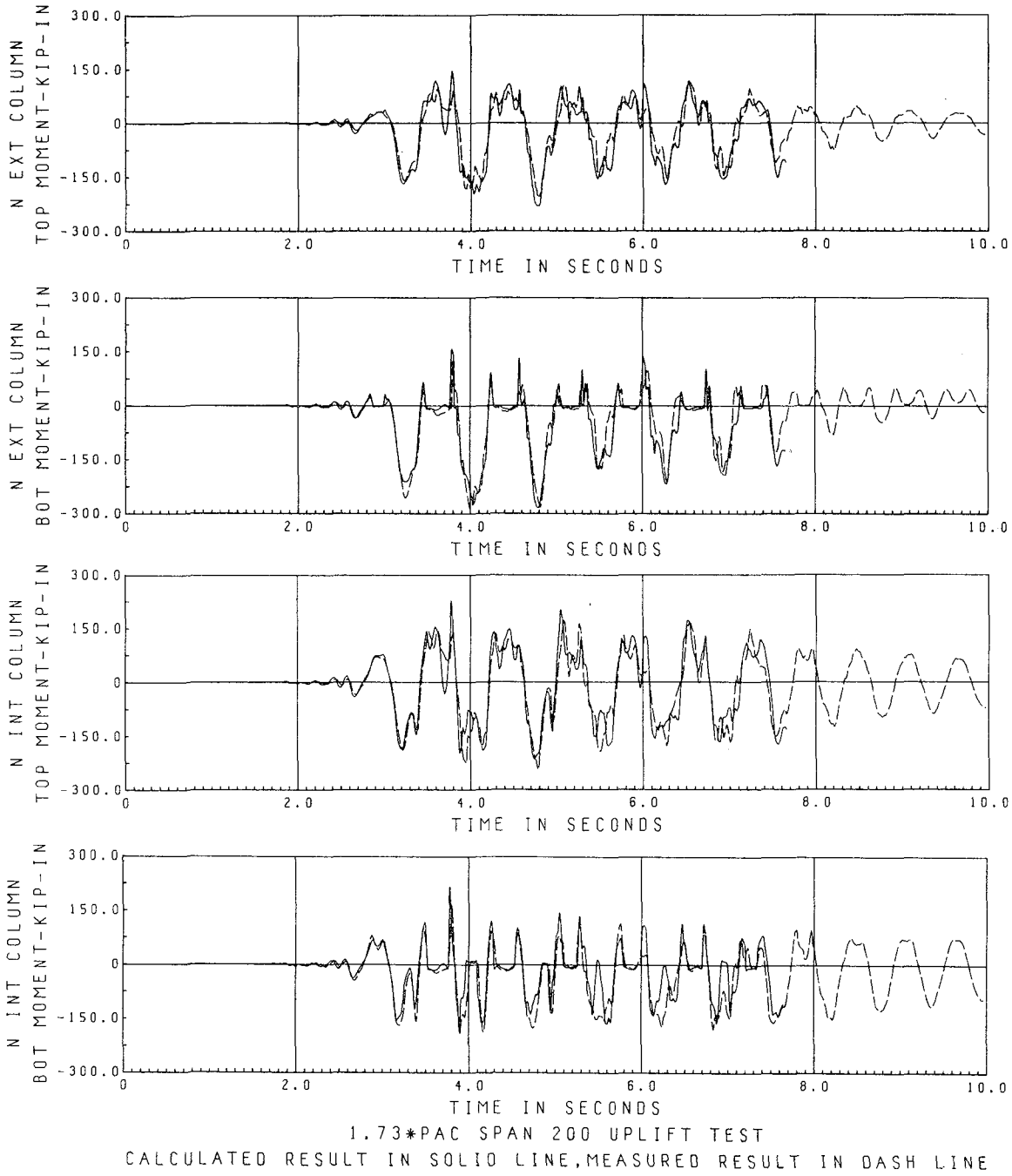

Fig. 7.A.9 Model 2, β = .0011, Δt = .0048 1st Floor Column Moments

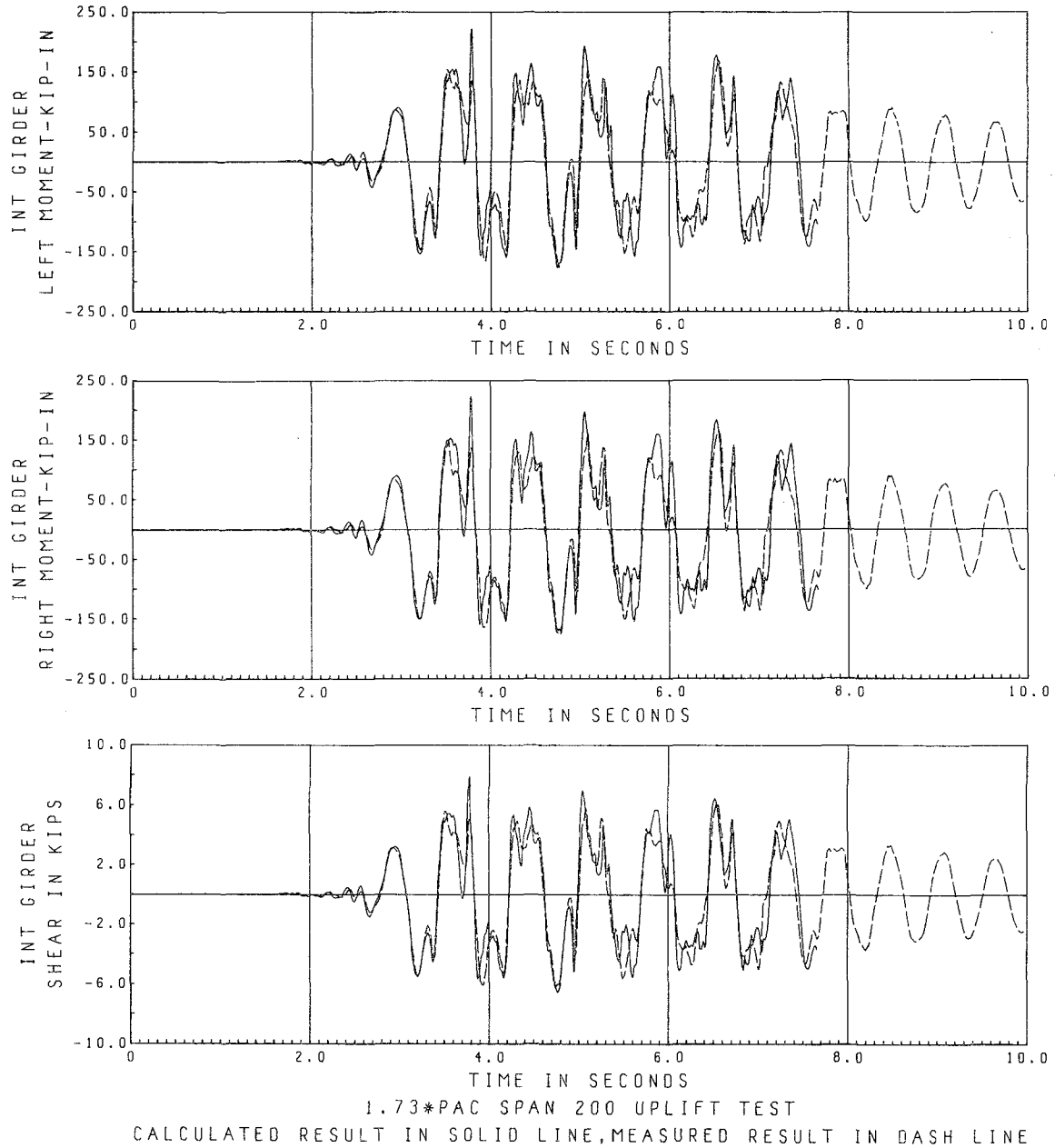

Fig. 7.A.10 Model 2, β = .0011, Δt = .0048 1st Floor Girder Forces

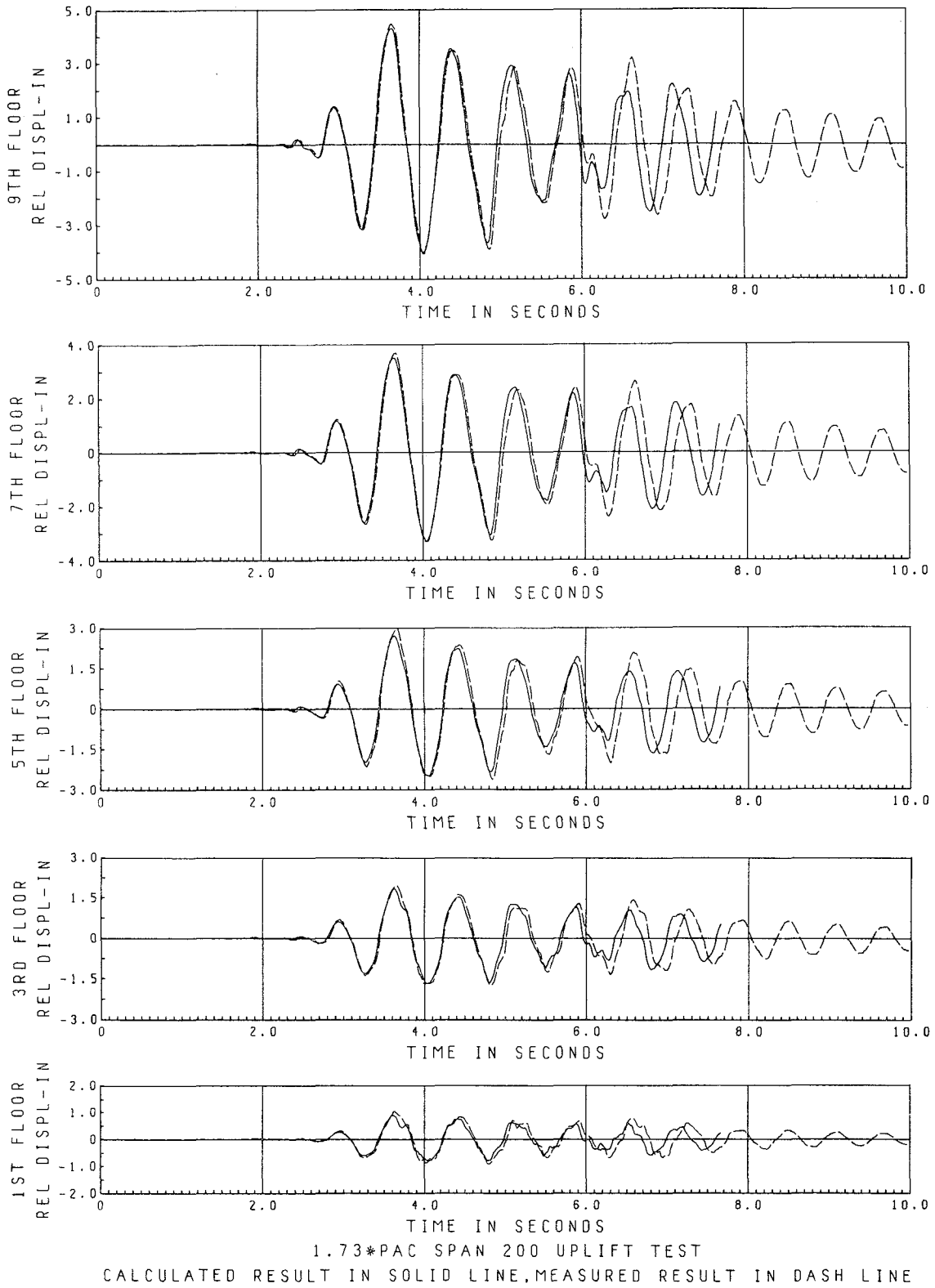

Fig. 7.A.11 Model 2, β = .0011, Δt = .0096

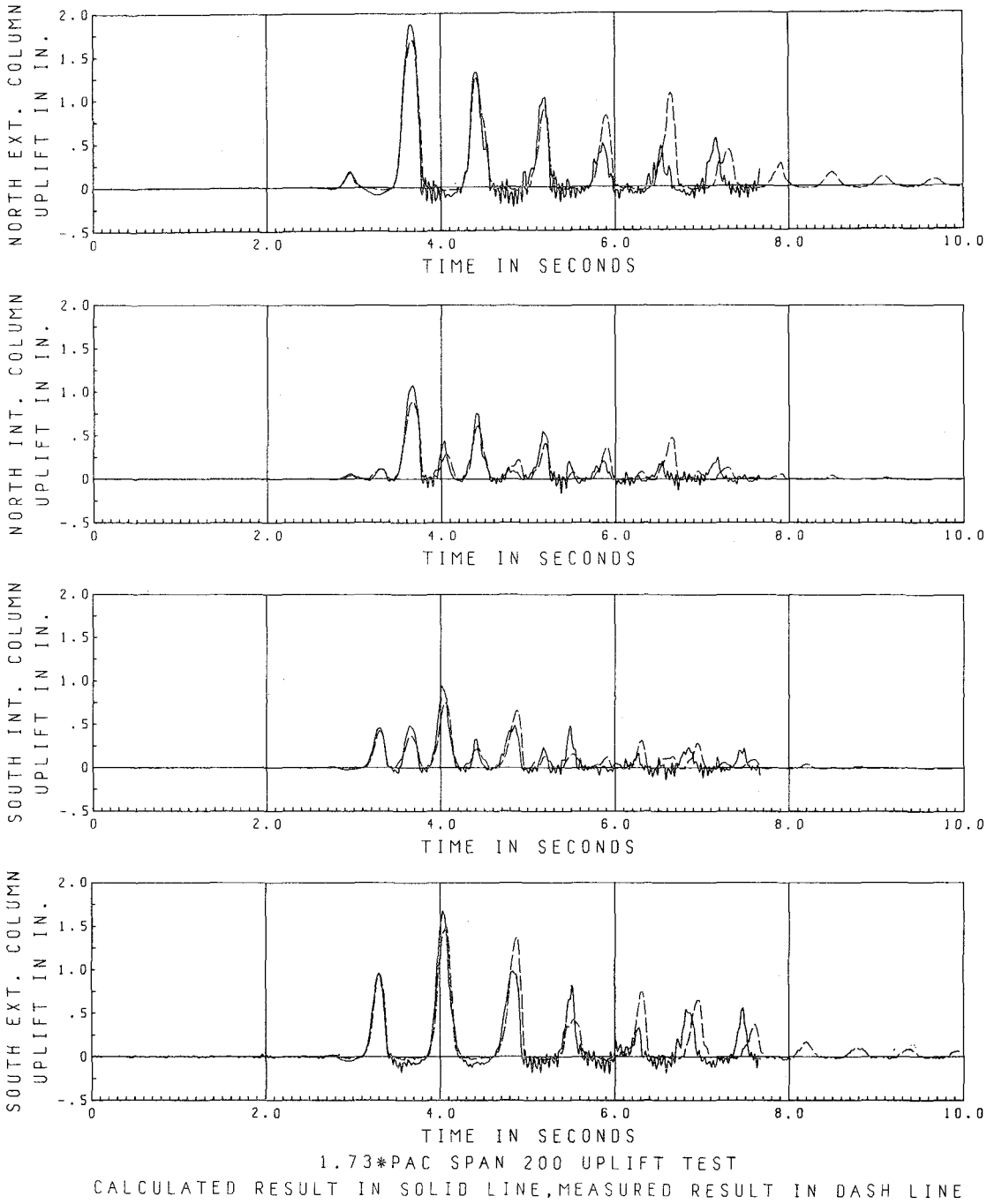

Fig. 7.A.12 Model 2, β = .0011, Δt = .0096

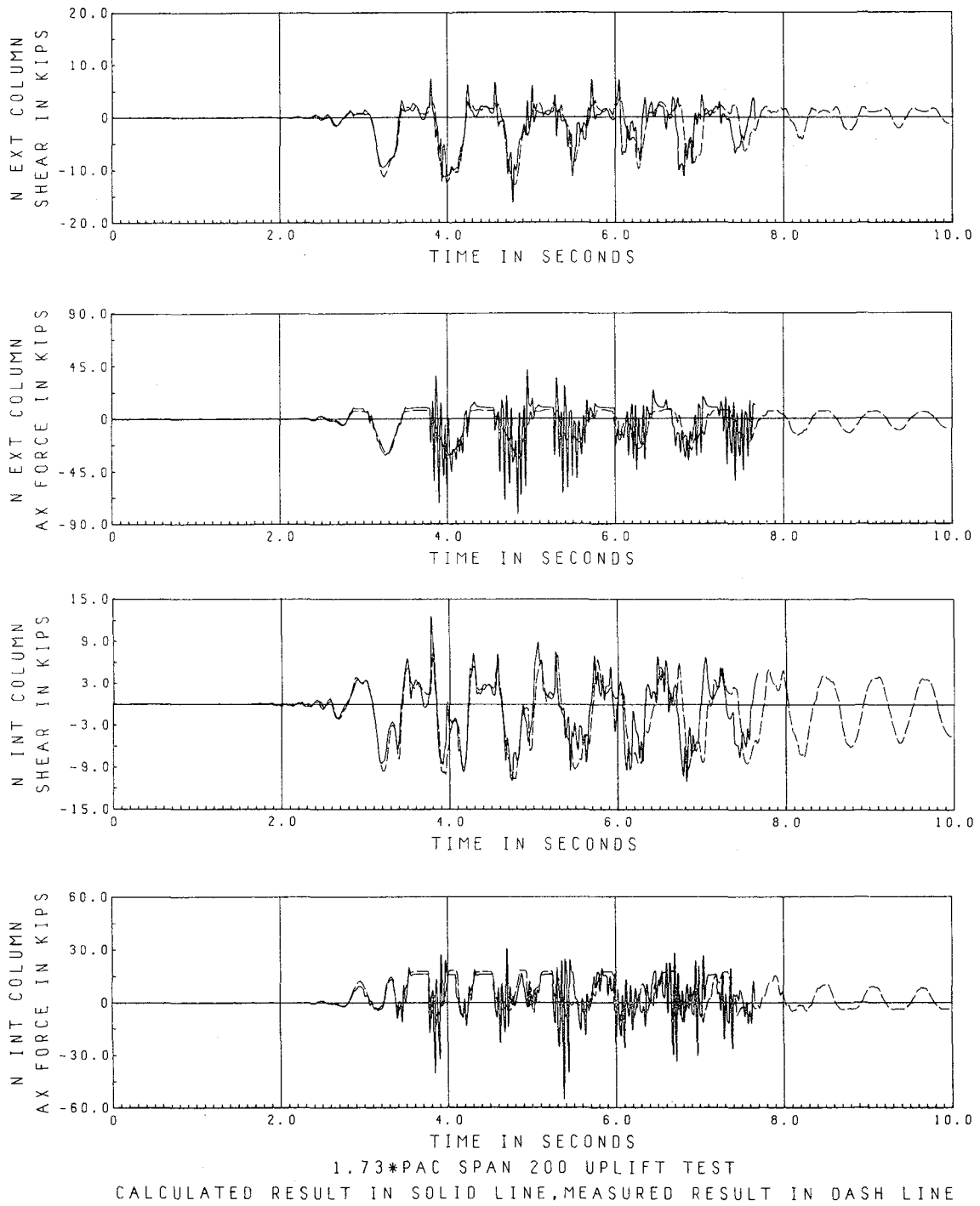

Fig. 7.A.13 Model 2, β = .0011, Δt = .0096 1st Floor Column Forces

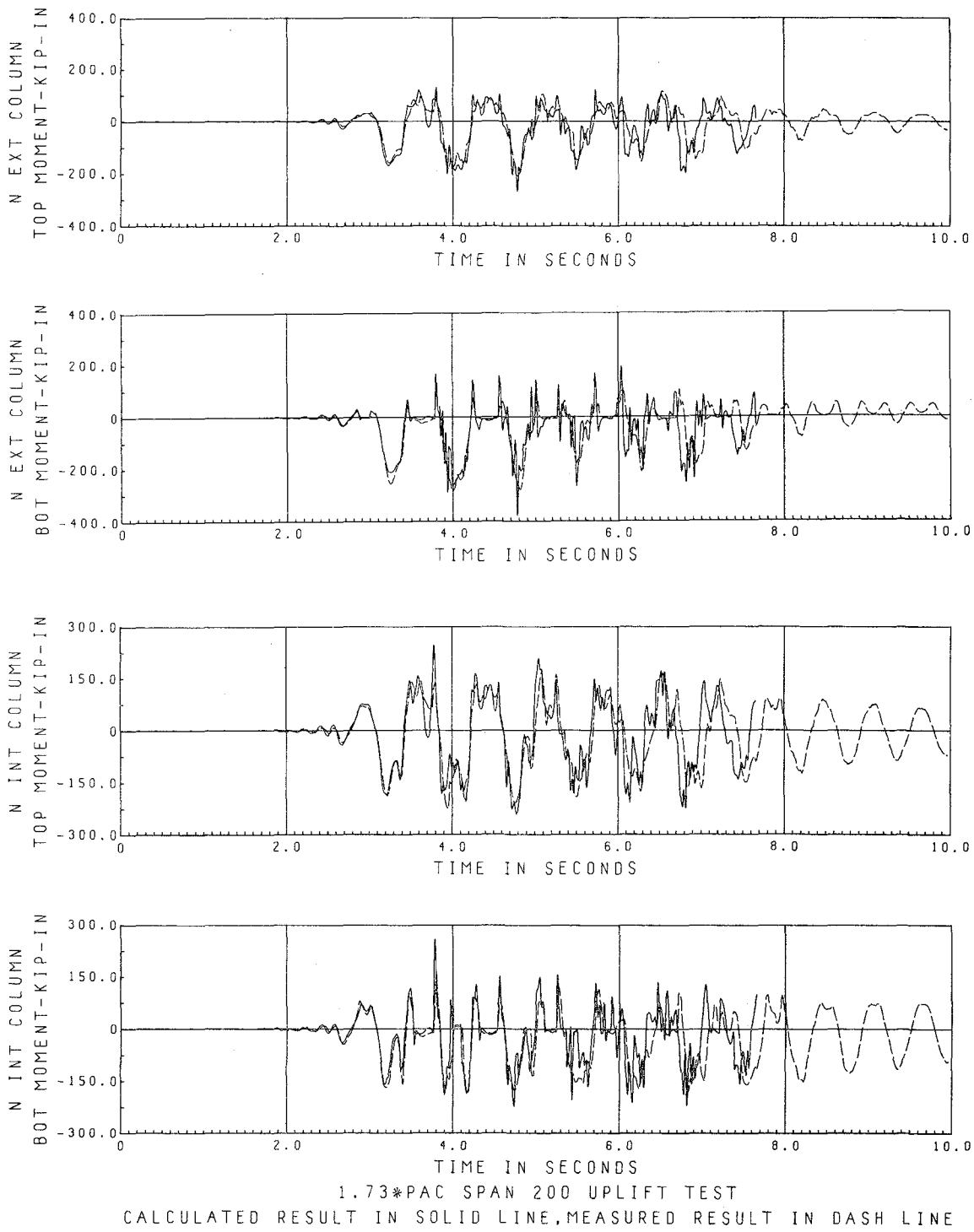

Fig. 7.A.14 Model 2, β = .0011, Δt = .0096 1st Floor Column Moments

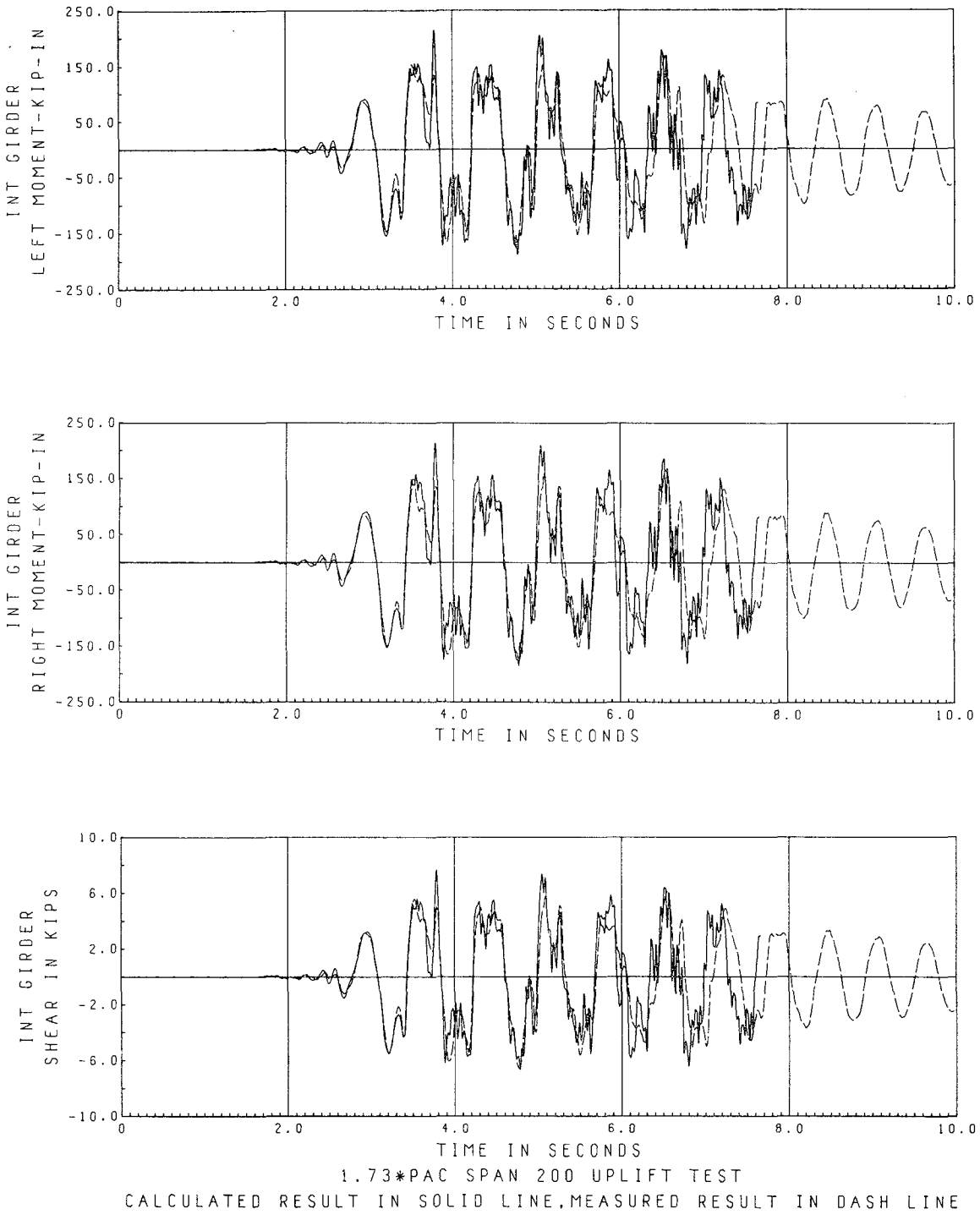

Fig. 7.A.15 Model 2, β = .0011, Δt = .0096 1st Floor Girder Forces

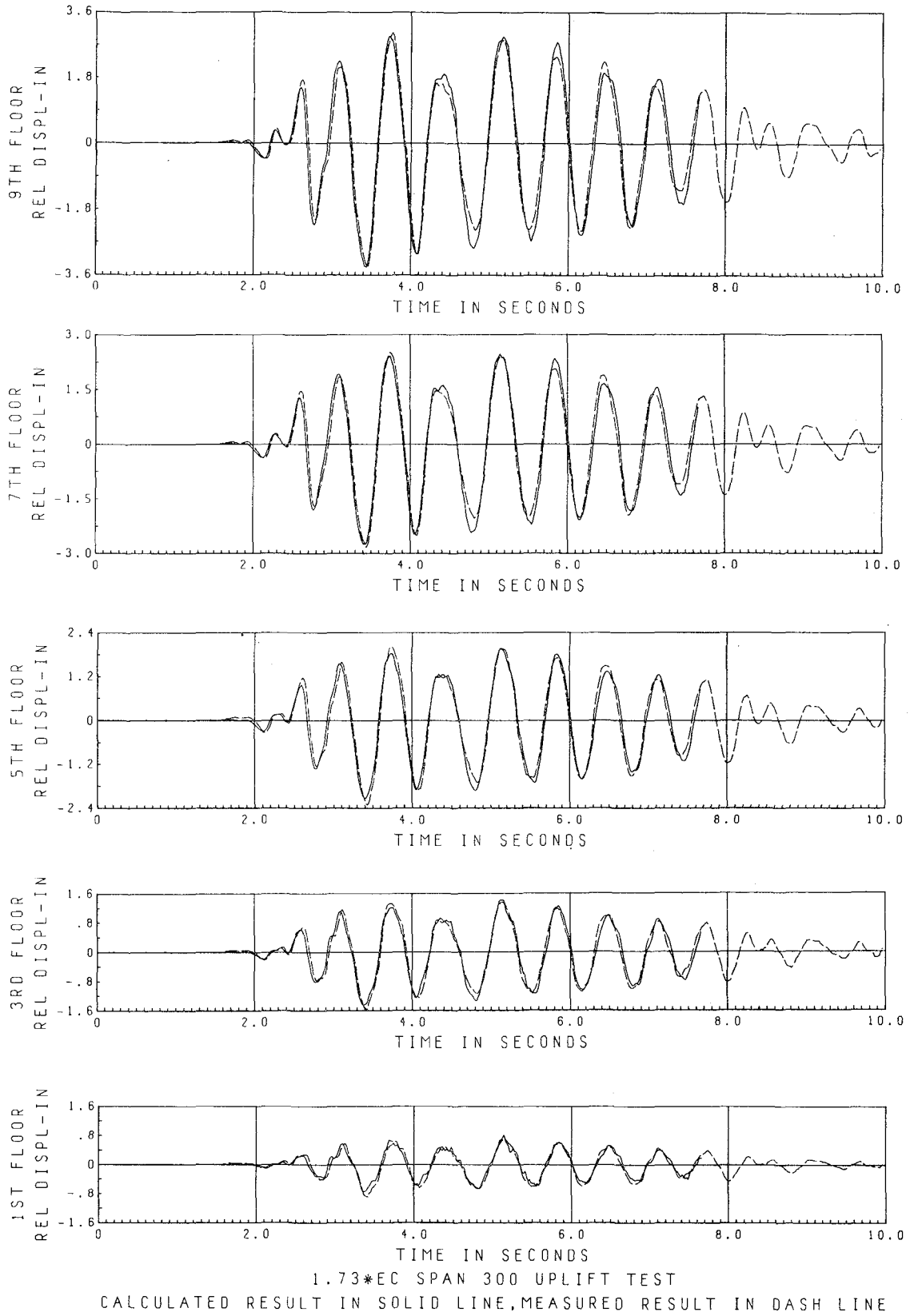

Fig. 7.A.16 Model 2, β = .0011, Δt = .0096

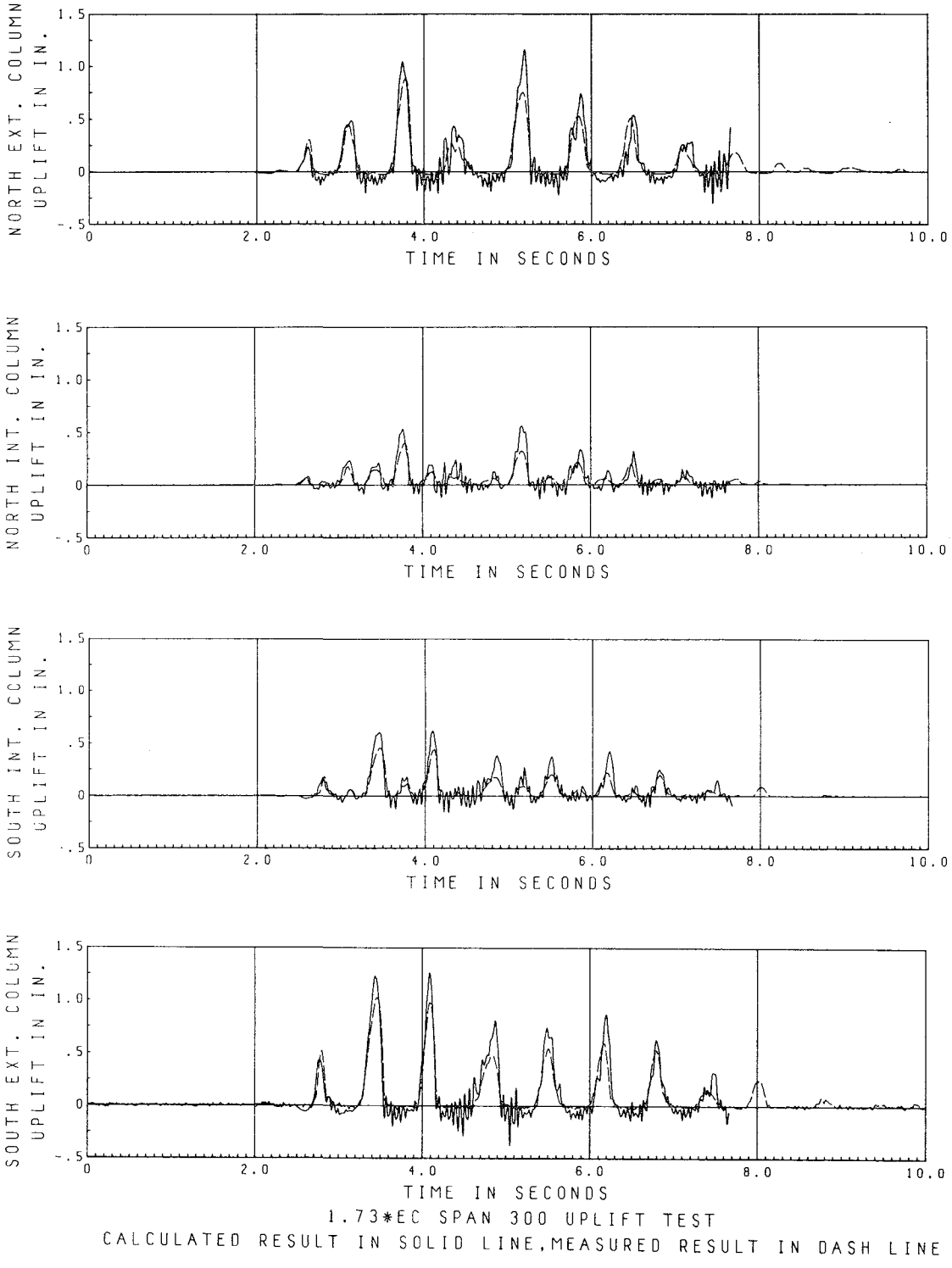

Fig. 7.A.17 Model 2, β = .0011, Δt = .0096

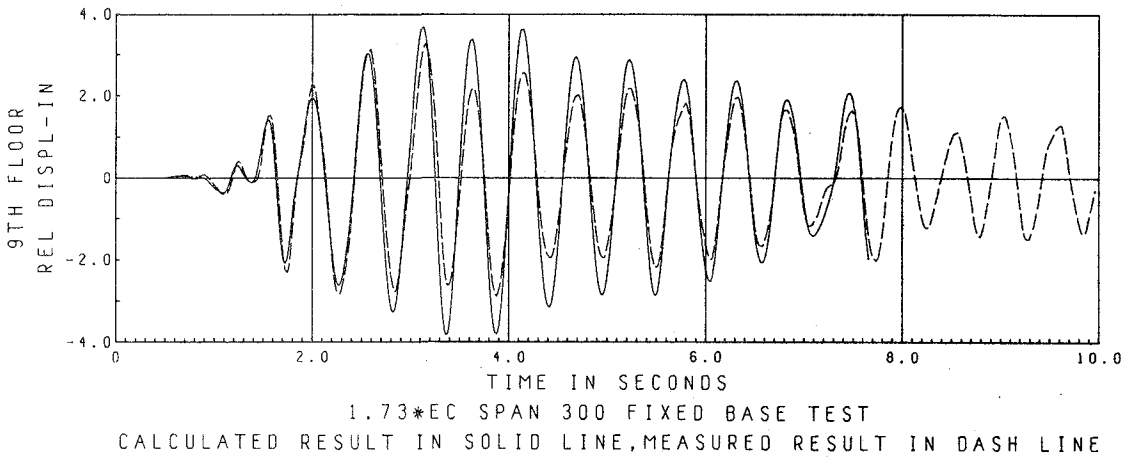

Fig. 7.B.1 Model 1, β = .004, Δt = .0096

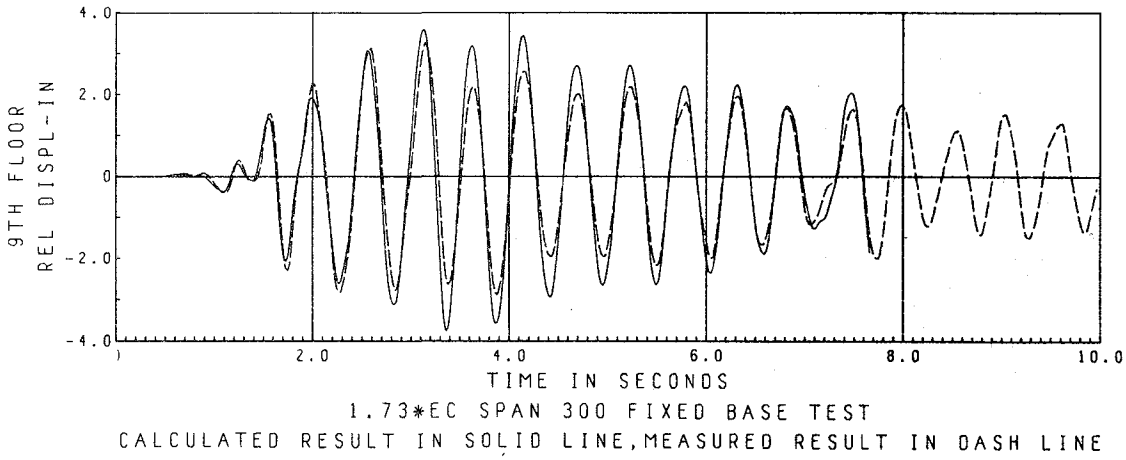

Fig. 7.B.2 Model 1, α = .628, Δt = .0096

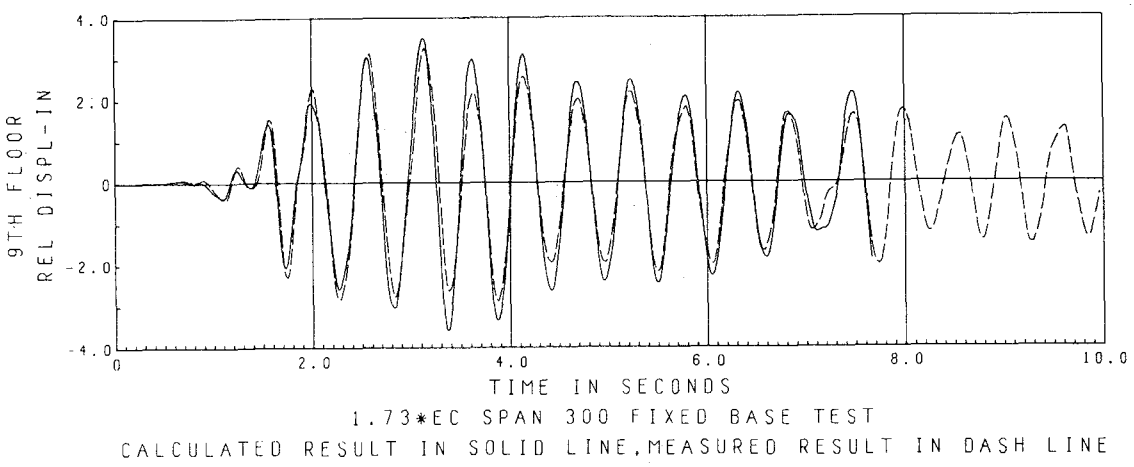

Fig. 7.B.3 Model 2, α = .628, Δt = .0096

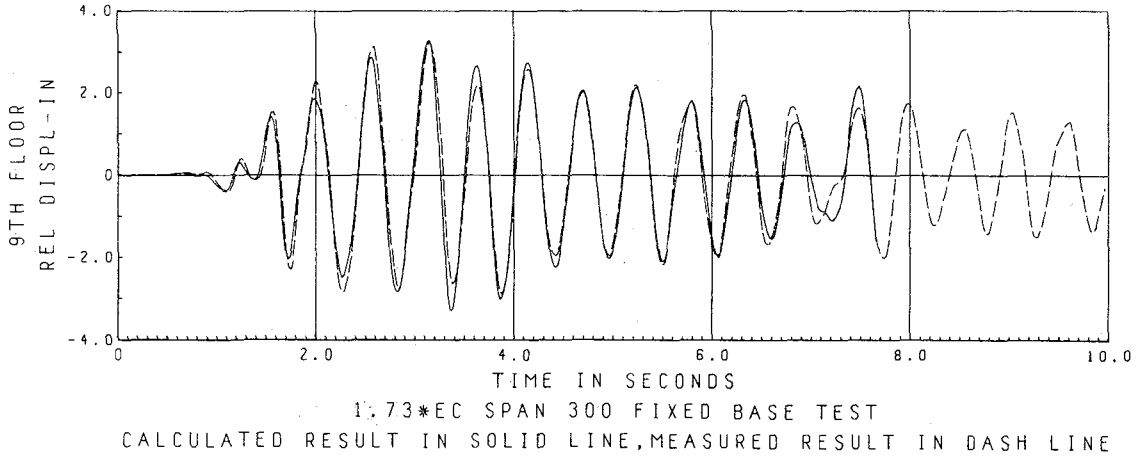

Fig. 7.B.4 Model 2, α = .800, Δt = .0096

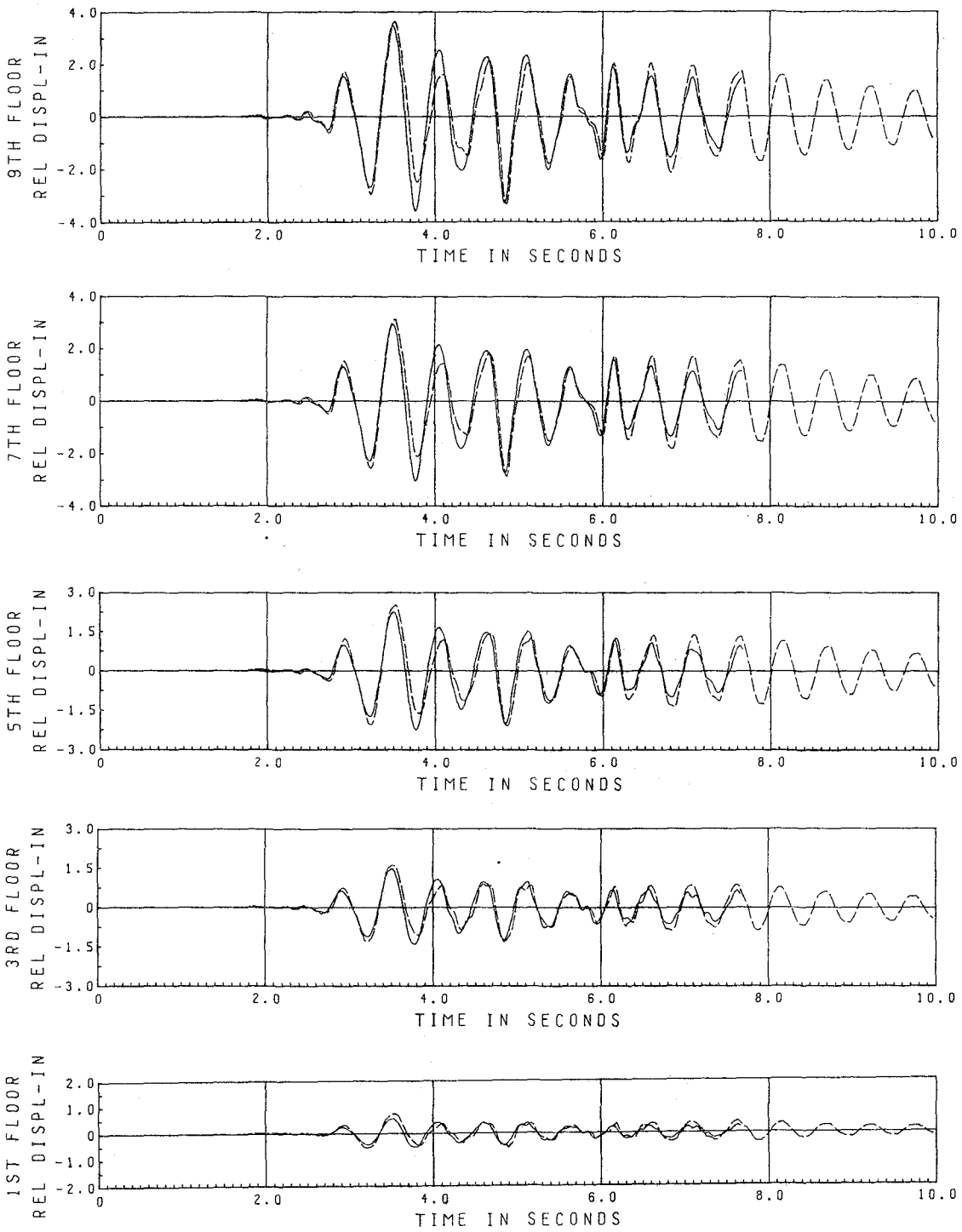

Fig. 7.B.5 Model 2, α = .800, Δt = .0096

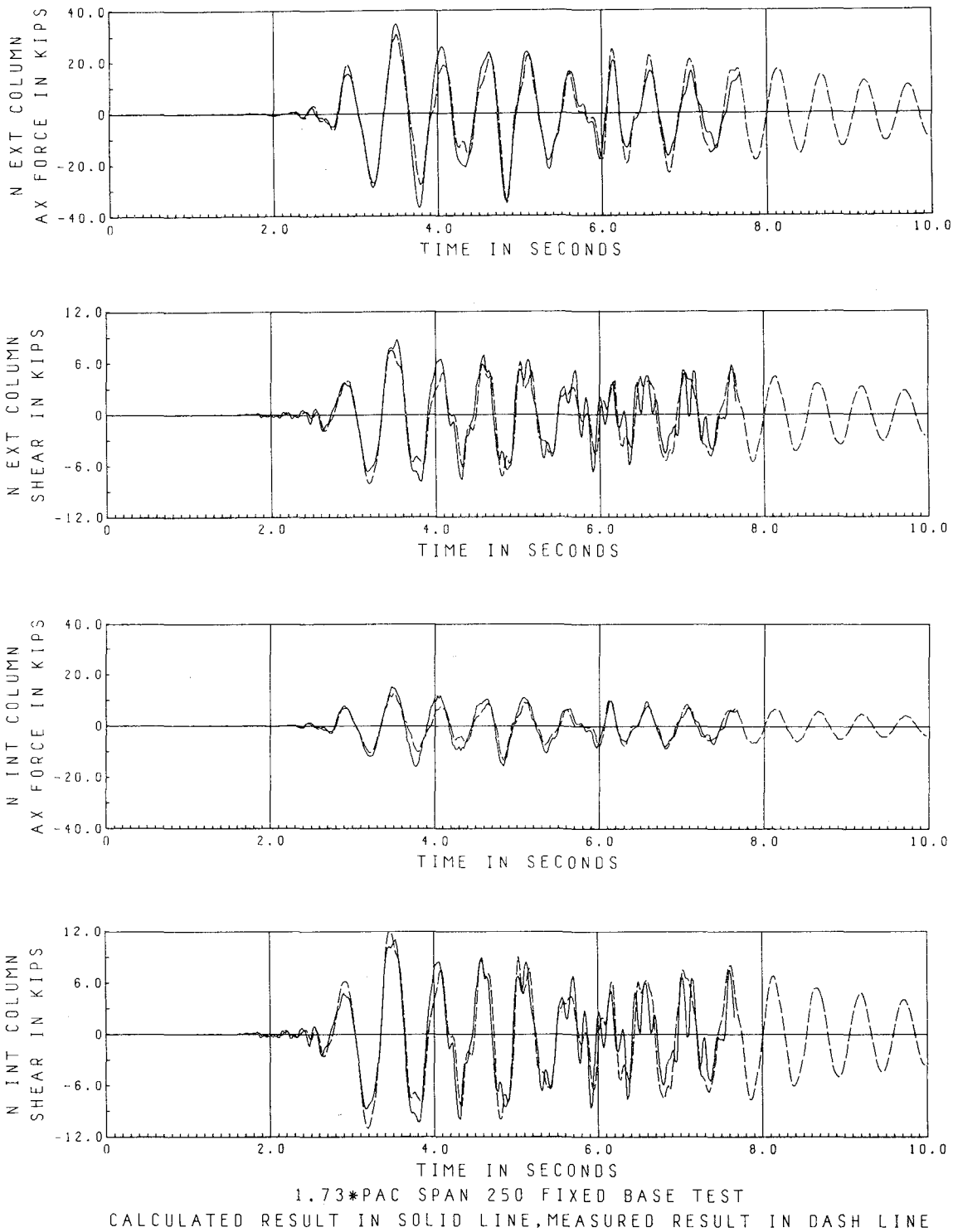

Fig. 7.B.6 Model 2, $\alpha = 0.800$, $\Delta t = .0096$ 1st Floor Column Forces

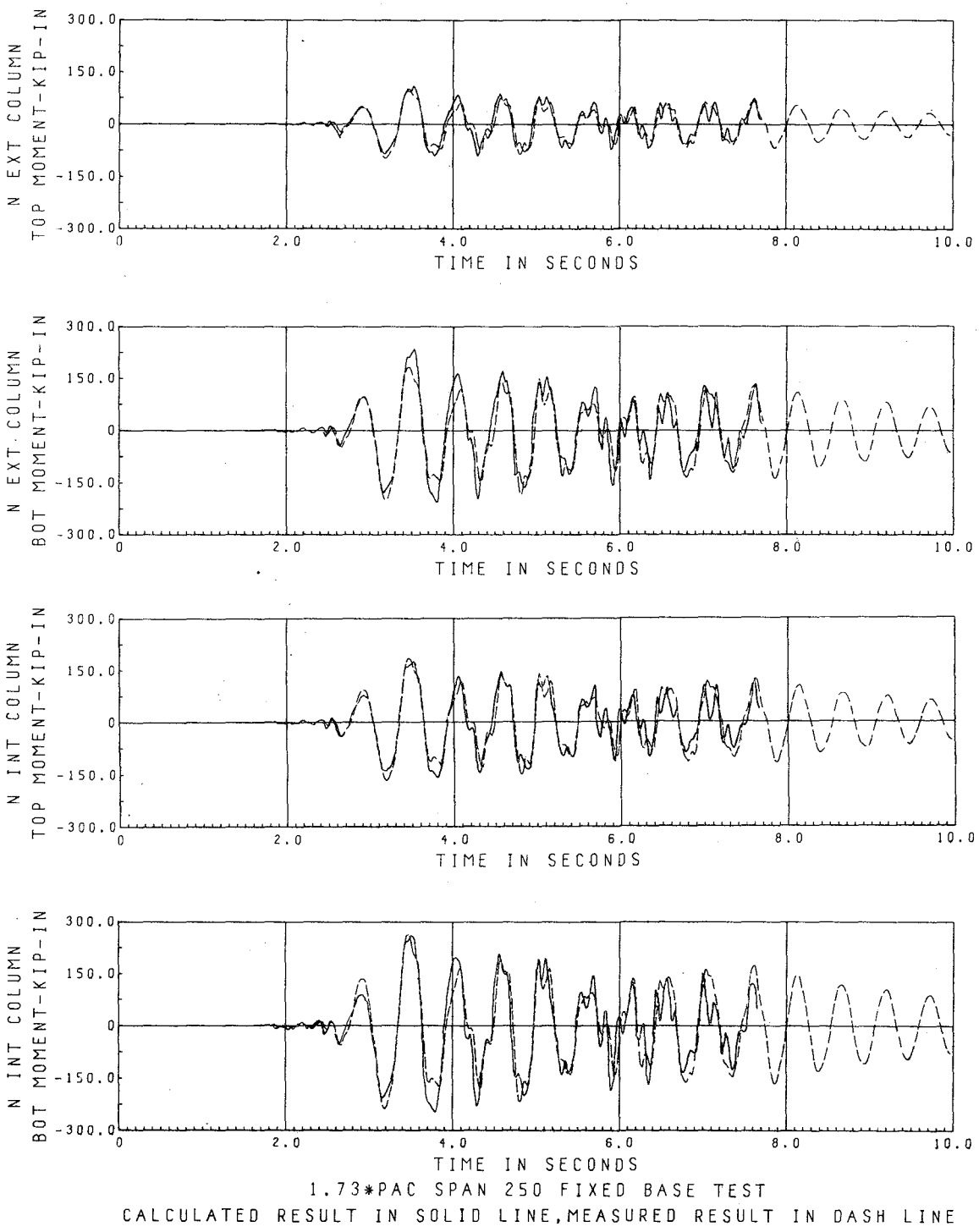

Fig. 7.B.7 Model 2, α = 0.800, Δt = .0096 1st Floor Column Moments

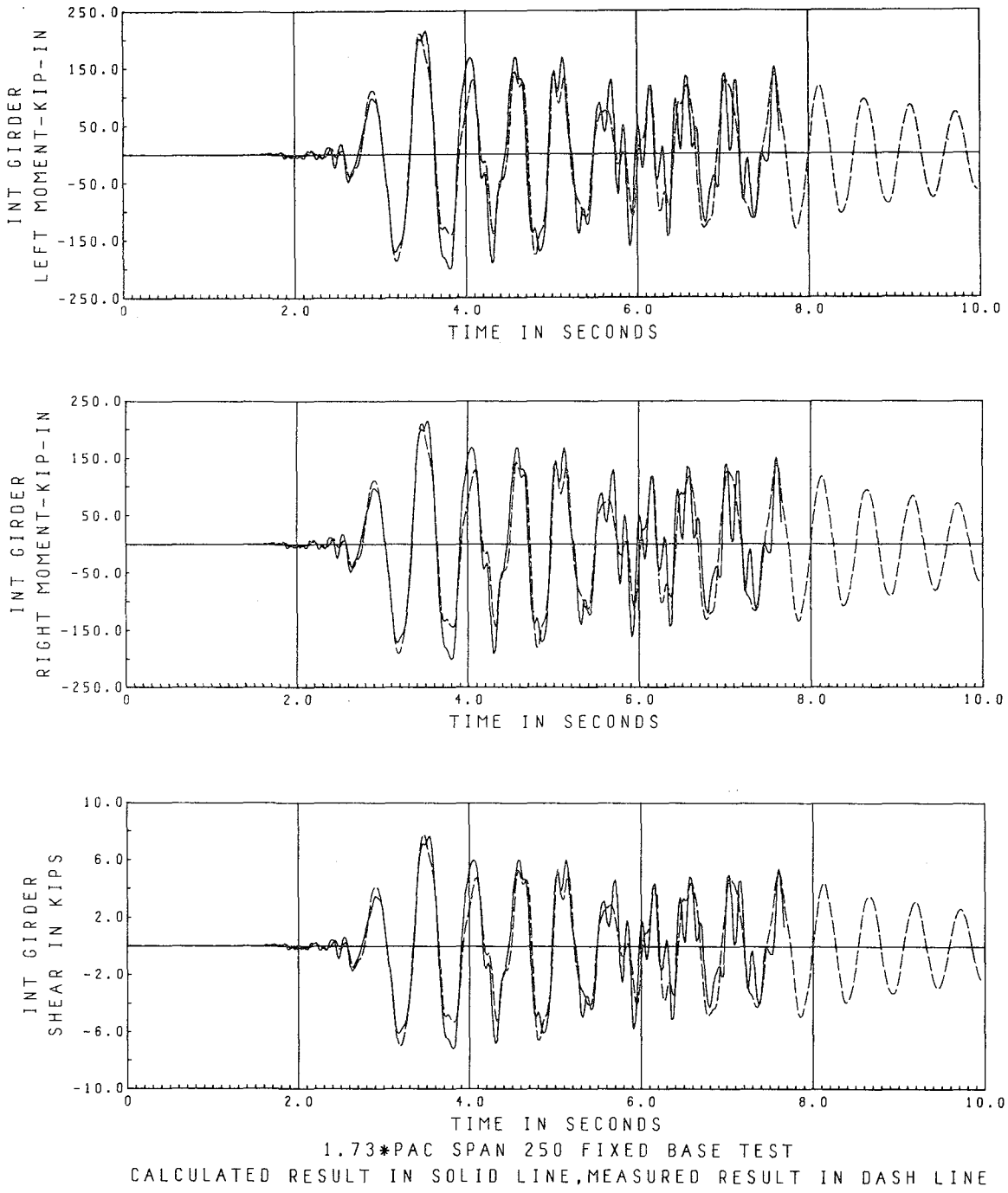

Fig. 7.B.8 Model 2, $\alpha = 0.800$, $\Delta t = .0096$ 1st Floor Girder Forces

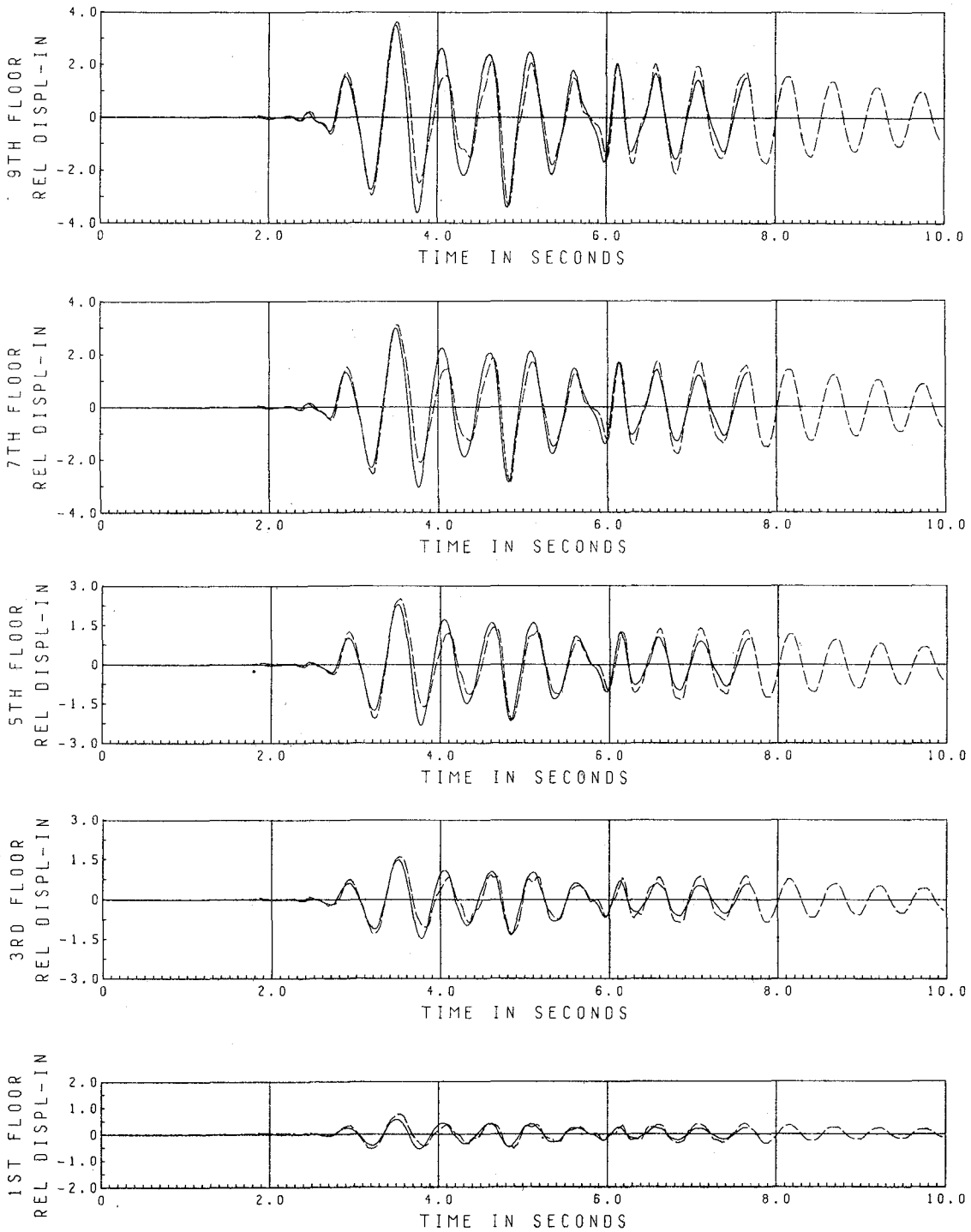

Fig. 7.B.9 Model 2, β = .005127, Δt = .0096

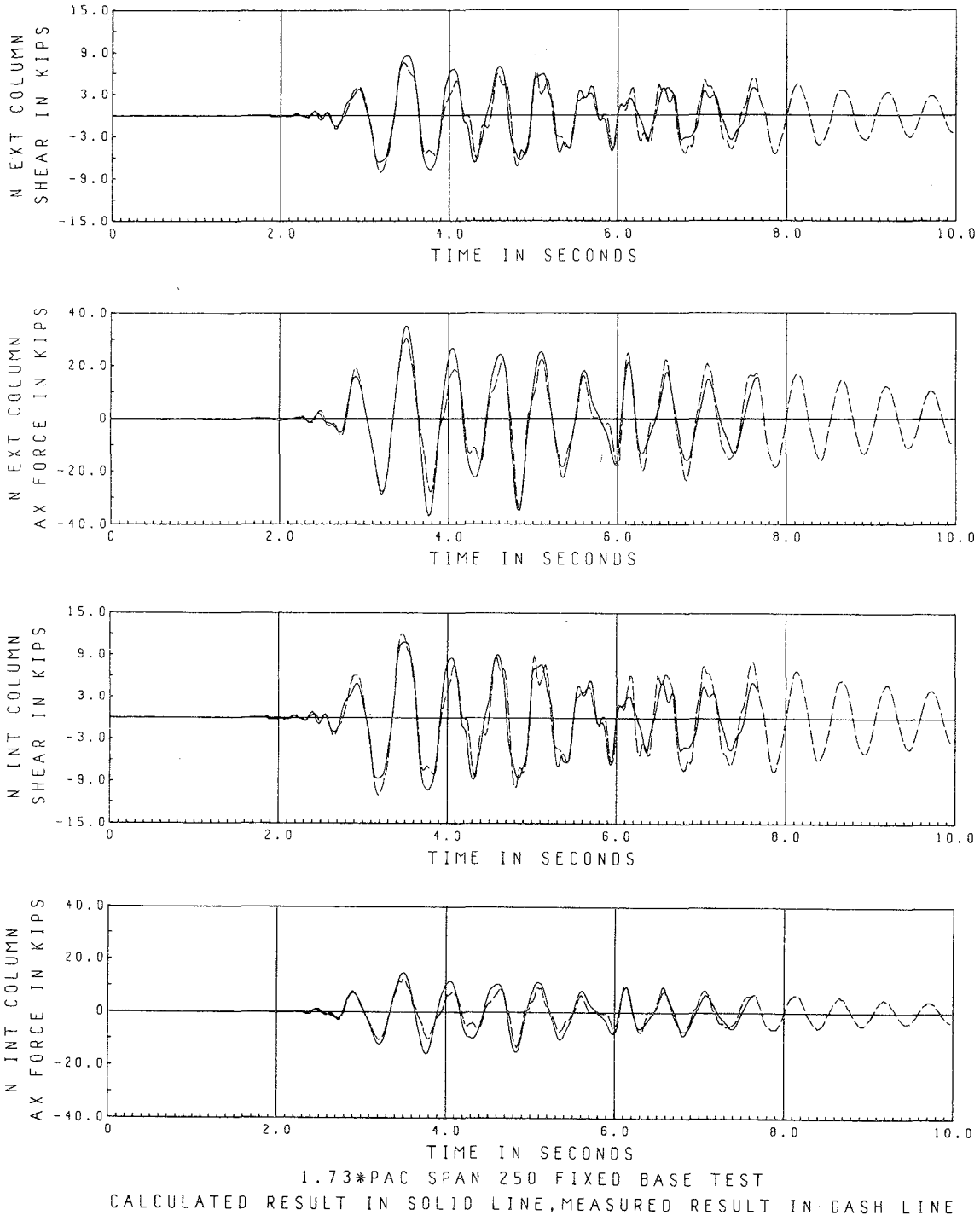

Fig. 7.B.10 Model 2, β = .005127, Δt = .0096 1st Floor Column Forces

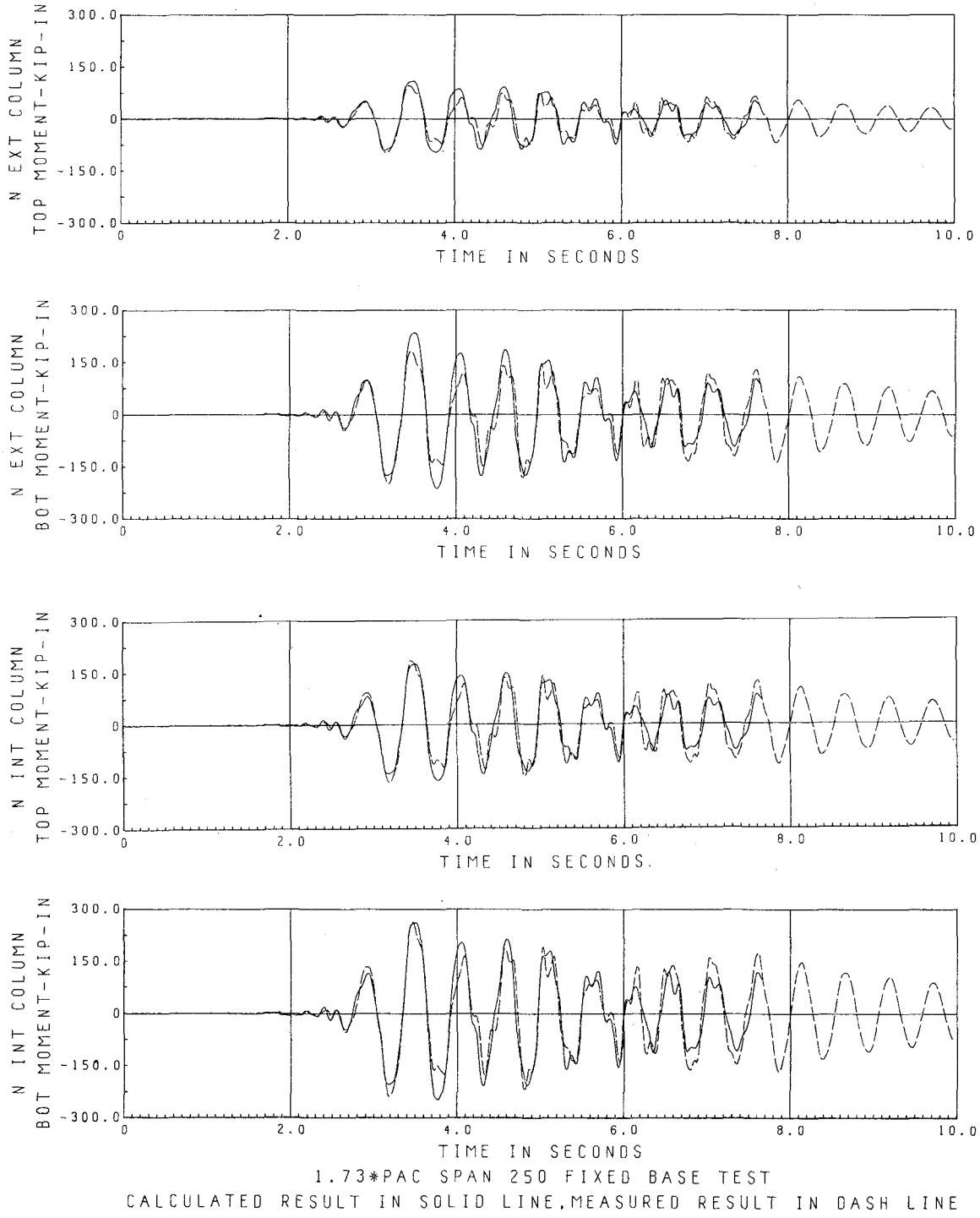

Fig. 7.B.11 Model 2, β = .005127, Δt = .0096 1st Floor Column Moments

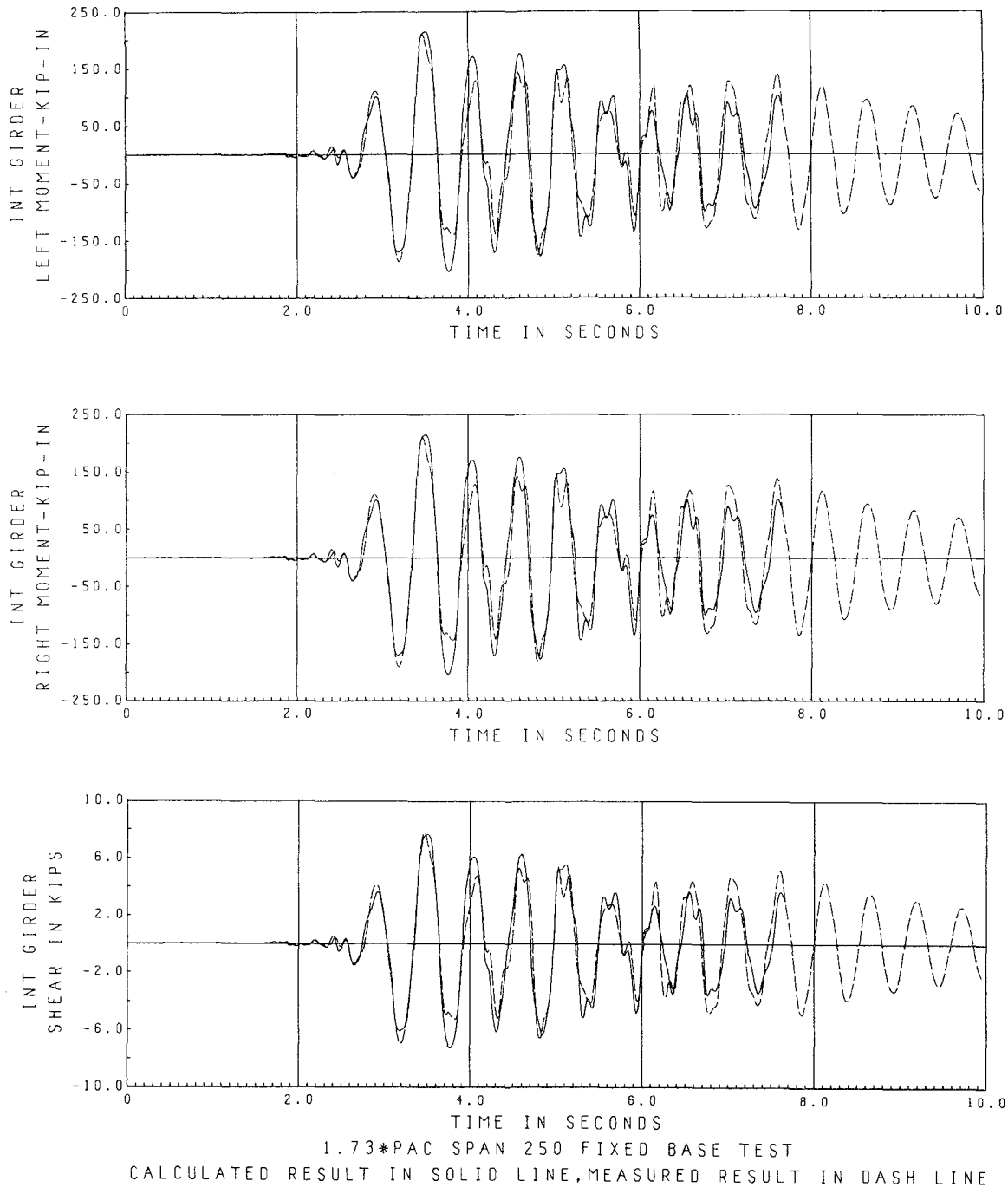

Fig. 7.B.12 Model 2, β = .005127, Δt = .0096 1st Floor Girder Forces

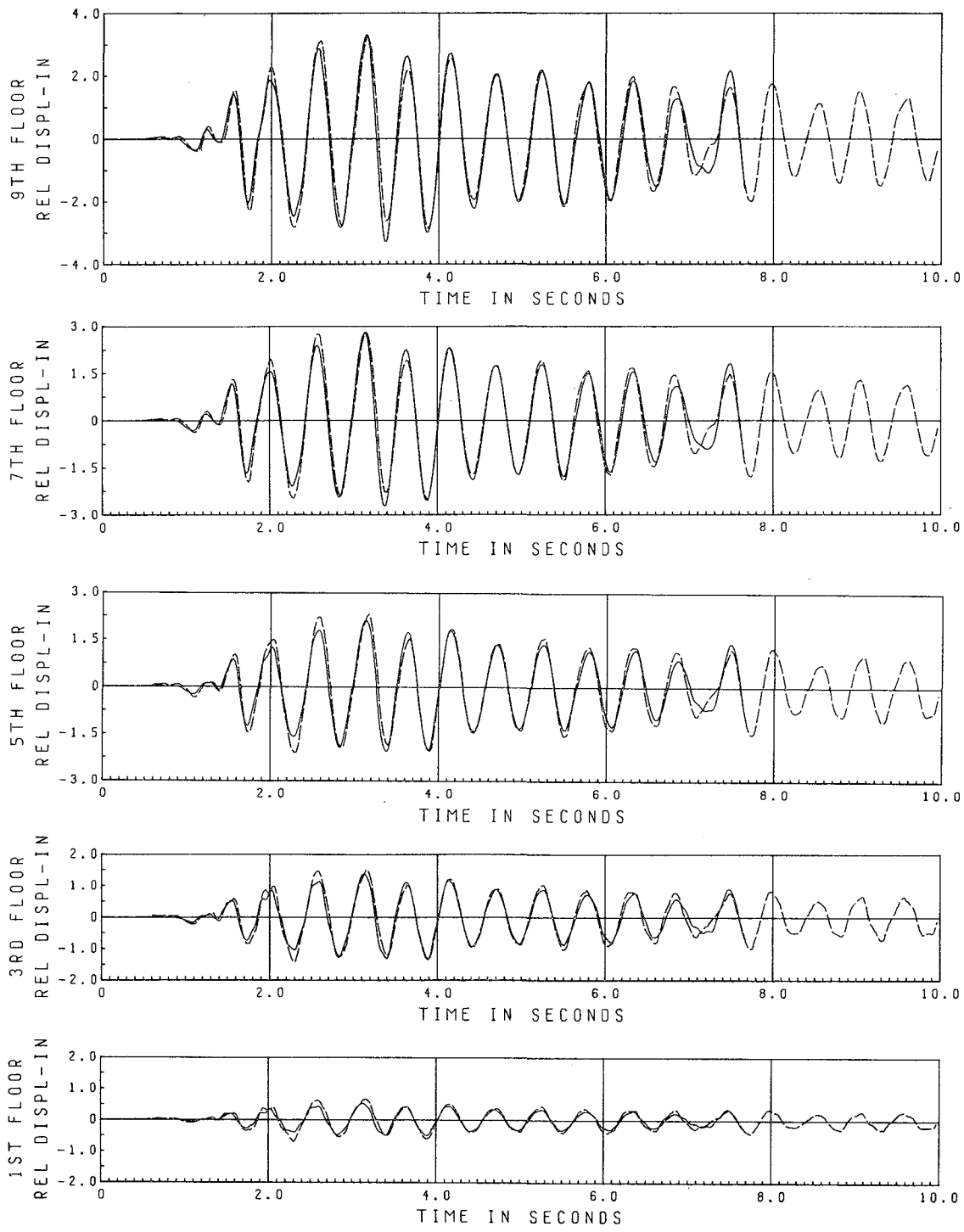

Fig. 7.B.13 β = .005127, Δt = .0096

8. CONCLUSIONS

8.A. Implications of Test Results for Prototype Structures

From the results observed during this test program, it would appear that a prototype system would be able to very successfully undergo an uplifting type of response to severe seismic excitation. Indeed, the tests indicate that many systems designed for relatively low code lateral loadings would exhibit this behavior whether intended or not, under credible ground shaking, if no supplementary anchorage was provided.

To ensure that successful uplift response would be achieved, however, it should be considered in the design and not ignored, as is usually now the case. Consideration of uplift response to severe seismic excitation is compatible with the concept of two design levels; a service loading involving no damage and a maximum credible loading, for which nonstructural damage and even noncatastrophic structural damage would be tolerated. For most designs meeting current code provisions, uplift response would fall in the latter design category, and would help greatly in reducing damage and preventing catastrophic failures. For a code such as the California hospital code, allowing column uplift could even lead to more economical designs, particularly when the foundation costs are considered. Performance under severe shaking would still be enhanced, even for these structures, because the hospital code loadings are still considerably below maximum credible loadings for regions of high seismicity.

8.B. Comparison of Uplift and Fixed Base Behavior

As was pointed out during the discussion of the experimental results,

the response of an uplifting system is drastically different from one in which supplementary anchorage is provided. Allowing uplift, in effect, establishes a ceiling for the lateral loading which may be applied. Transient loadings exceeding the ceiling produce increased motion, but do not produce significant increases in the internal forces of the structural system. An uplifting system has a large energy absorption capacity in the form of potential energy stored by the mass in increasing its relative elevation. This energy "reservoir" can be more economically exploited than that of systems whose total energy absorption capacity is in the form of internal strain energy.

The internal forces of a system with unlimited overturning resistance, on the other hand, will continue to increase in response to increased dynamic loading until some internal "failure" mechanism establishes a ceiling. Designers have long relied on ductile plastic hinges, for example, as a safe "failure" mechanism which allows more economical moment-frame designs. Providing large amounts of ductility, however, which has the desirable characteristics of high energy absorption and dissipation, can be expensive. Particularly in reinforced concrete structures, ductility requires a lot of confinement reinforcement, with increased material and labor costs, for the extra steel placement. Even in steel structures, extra precaution against buckling must be taken in the presence of large plastic hinge rotations.

As a direct consequence of providing extra overturning capacity in the superstructure, the designer then faces the task of providing the same overturning capacity in the substructure. Providing a tensile anchorage to the foundation can be a very expensive operation, requiring deep piles or caissons. The only alternative, providing some type of

outrigger, may be impractical due to space limitations. The problems encountered, thus, can be severe and self-inflicted in origin.

8.C. Evaluation of Current Uplift Analysis Capability

From the analytical results presented in section 7.A., it is apparent that the tools currently exist to very accurately predict the response of an uplifting system, provided the superstructure behavior is understood. It is essential to realize that uplift behavior is inherently very lightly damped; if the motion approaches rigid body rotation it is essentially undamped. The only exceptions would be systems with mechanical damping devices added, or systems where significant nonstructural damage could occur, such as a core-stiffened system with flexible periphery columns.

The other major consideration in the analysis of an uplifting system is the selection of an appropriate integration time step. A time step which is too large can lead to numerical problems in the analysis; a time step which is too small leads to unnecessary computational expense. This matter will continue to require judgment on the part of the analyst, considering such factors as the relative stiffness of the impact elements, the size and complexity of the superstructure, and even the intended occupancy of the superstructure. A critical emergency or communication facility, for example, might merit a greater effort and investment in the design and analysis phase than an unoccupied mattress warehouse. An alternative solution to this problem could be an iteration scheme at each time step to eliminate load unbalances, or to subdivide time steps during significant stiffness changes.

8.D. Evaluation of the Fixed Base Analysis

Although the analytical results for the fixed base tests were in good agreement with the experimental results, the behavior was not highly nonlinear in nature. Several conclusions concerning the analysis of this frame can, however, be drawn from the results of this program.

In only moderately nonlinear response, such as that observed in this test series, the amounts of energy dissipated through viscous and nonlinear hysteretic behavior can be somewhat ambiguous. Displacements can often be accurately predicted without even including the nonlinear behavior, provided the viscous energy dissipation is increased properly. It is necessary, however, to include the nonlinear hysteretic behavior in order to accurately predict the local force distribution.

For responses which extend further into the nonlinear range than those of this test series, the accurate modeling of the nonlinear hysteretic behavior becomes essential to predict even the displacement response. The accurate modeling of the nonlinear behavior will very often necessitate the consideration of some type of stiffness degradation with repeated cycling. Even structural steel exhibits a considerable Bauschinger effect under repeated loading. The reason why the uplift response was relatively easily predicted was the complete lack of any degradation effect in the uplift phenomenon; this form of nonlinearity is mathematically simple.

Also apparent in the fixed base analyses was the difficulty in predicting higher mode response. It seems that damping is higher for these response modes, but the analytical model did not predict accurately enough their natural response frequencies for a really good correlation. Any constraints placed on the analytical model by the assumptions involved

in its construction will tend to increase the computed frequencies of the modes of vibration. To overcome this difficulty requires an ever more sophisticated analytical model, usually beyond justifiable computational effort.

8.E. Feasibility of Prototype Application

The test results seem to indicate that allowing column uplift could be very beneficial to many structures subjected to severe seismic excitation. Structures which are designed with a considerable reserve capacity would have the imposed loads substantially reduced. Structures which are designed with little reserve capacity would have their ductility demands reduced substantially. Either effect would be considered desirable. To achieve this result, however, a rational design including provisions for column uplift would have to be carried out.

Such a design should include at least the following consideration:

1. Relatively little restraint to vertical separation of the column bases from the foundation. (This does not imply that the installation of some relatively flexible energy dissipation mechanism could not be included.) Sufficient resistance to prevent uplift under wind loading must, of course, be provided.

2. A reliable "shear key" to prevent columns from walking off the foundation. The flexure plate concept used in the test program seems worthy of serious consideration. In practice, it would have to be extended to allow for a biaxial type of response.

3. An impact element which would tolerate transient impact and protect potentially more brittle components, if necessary.

4. Required flexibility in service connections to the structure. A centrally located service core, where little or no separation should occur, would be a logical system.

5. A reasonable dynamic analysis considering the uplift response, to ensure a tolerable amplitude of uplift would occur, even under the most severe "credible" seismic conditions.

While this study was only concerned with a steel moment frame, there would seem to be no reason to limit uplift designs to this category of structural system. Indeed, there are other systems whose economy or seismic behavior could be enhanced to an even greater degree. The expense of providing ductility in reinforced concrete frame structure has already been mentioned. Application of the concept to shear wall or core-stiffened systems also seems promising.

When the potential benefits to the superstructure are combined with the potential economy of the substructure, the case for rationally designing uplift capability into structures located in seismic regions seems quite impressive. Somewhat greater effort in the design and analysis phases could pay off exceedingly well, to both the owners and the users of the structures we build.

REFERENCES

1. Beck, J. L. and Skinner, R. I., "The Seismic Response of a Reinforced Concrete Bridge Pier Designed to Step," Earthquake Engineering and Structural Dynamics, v. 2, no. 4, 1974, pp 343 - 358.

2. Clough, R. W. and Huckelbridge, A. A., "Preliminary Experimental Study of Seismic Uplift of a Steel Frame," U. C. Berkeley EERC Report 77/22, 1977.

3. Clough, R. W. and Li, L. Y., "The Dynamic Behavior of a First Story Girder of a Three-Story Steel Frame Subjected to Earthquake Loading," U. C. Berkeley EERC Report 75-35, 1975.

4. Kanaan, A. and Powell, G. H., "General Purpose Computer Program for Inelastic Response of Plane Structures," U. C. Berkeley EERC Report 73-5, 1973.

5. Meek, J. L., "Effects of Foundation Tipping on Dynamic Response," ASCE Journal of the Structural Division, v. 101, no. ST7, July, 1975.

6. Nigam, N. C. and Jennings, P. C., "Digital Calculation of Response Spectra from Strong-Motion Earthquake Records," EERL, Cal. Institute of Technology, Pasadena, 1968.

7. Rea, D. and Penzien, J., "Dynamic Response of a 20' x 20' Shaking Table," Proceedings of the 5th World Conference on Earthquake Engineering, Rome, 1973.

Appendix A

Coupon Test Results

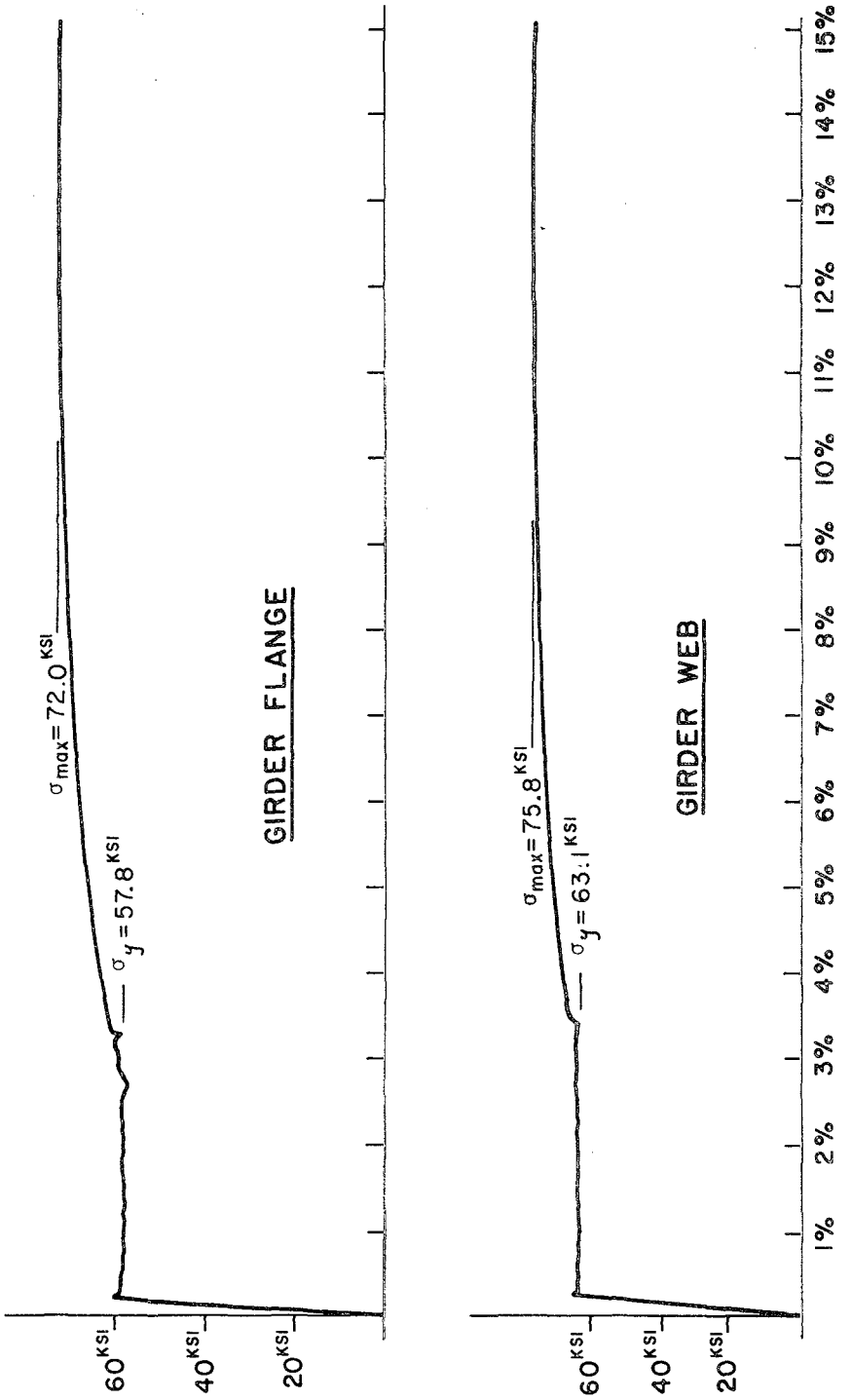

Fig. A.1 Girder Coupon Results

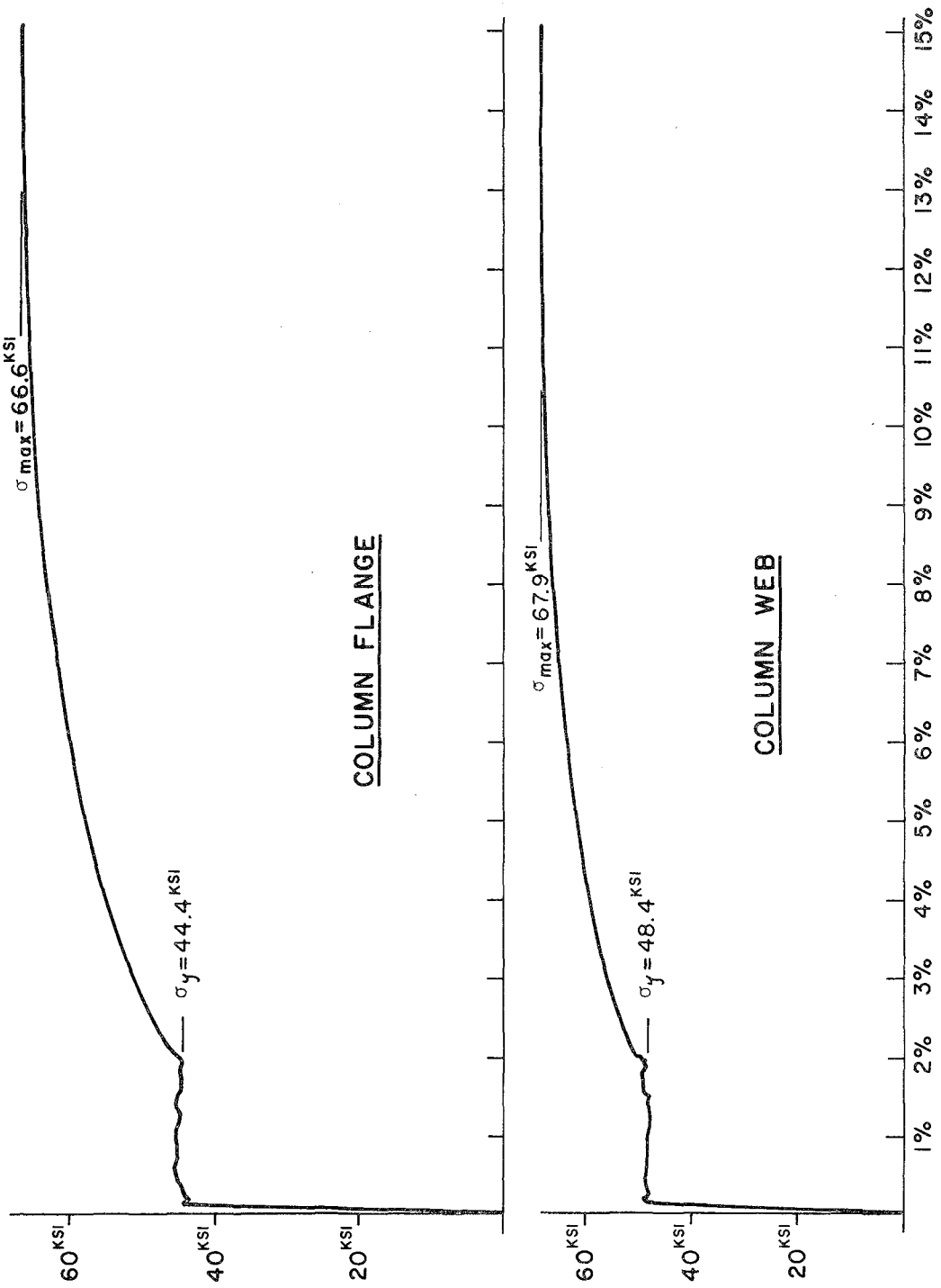

Fig. A.2 Column Coupon Results

Appendix B

List of Data Channels

Channel	Name	Description
0	ybmflxnai4	4th flr int beam north end post-yield flx strain
1	ybmflxsai4	4th flr int beam south end post-yield flx strain
2	ybmflxnai5	5th flr int beam north end post-yield flx strain
3	ybmflxsai5	5th flr int beam south end post-yield flx strain
4	av h t disp	average horizontal table displacement
5	av v t disp	average vertical table displacement
6	av h t acc	average horizontal table acceleration
7	av v t acc	average vertical table acceleration
8	pitch	rotational acc in pitching mode
9	roll	rotational acc in rolling mode
10	twist	rotational acc in twisting mode
11	force h1	horizontal actuator force
12	force h2	horizontal actuator force
13	force h3	horizontal actuator force
14	acc h1	individual horizontal table accelerometer
15	acc h2	individual horizontal table accelerometer
16	ybmflxnai6	6th flr int beam north end post-yield flx strain
17	ybmflxsai6	6th flr int beam south end post-yield flx strain
18	ybmflxnai7	7th flr int beam north end post-yield flx strain
19	ybmflxnai8	8th flr int beam north end post-yield flx strain
20	force v1	vertical actuator force
21	force v2	vertical actuator force
22	force v3	vertical actuator force
23	force v4	vertical actuator force
24	disp v1	individual vertical table displacement
25	disp v2	individual vertical table displacement
26	disp v3	individual vertical table displacement
27	disp v4	individual vertical table displacement
28	disp h1	individual horizontal table displacement
29	disp h2	individual horizontal table displacement
30	disp h3	individual horizontal table displacement
31	blank	
32	ps force 1	vertical stabilizer force
33	ps force 2	vertical stabilizer force
34	ps force 3	vertical stabilizer force
35	ps force 4	vertical stabilizer force
36	flr acc 9	9th floor absolute acceleration
37	flr acc 7	7th floor absolute acceleration
38	flr acc 5	5th floor absolute acceleration
39	flr acc 3	3rd floor absolute acceleration
40	flr acc 8	8th floor absolute acceleration
41	flr acc 6	6th floor absolute acceleration
42	flr acc 4	4th floor absolute acceleration
43	flr acc 2	2nd floor absolute acceleration
44	flr acc 1	1st floor absolute acceleration
45	lflr acc 9n	9th floor lateral acceleration north end
46	lflr acc 9s	9th floor lateral acceleration south end
47	ybmflxnai9	9th floor int beam north end post-yield flx strain
48	flr disp 9	9th floor absolute displacement
49	flr disp 8	8th floor absolute displacement
50	flr disp 7	7th floor absolute displacement

51	flr disp 6	6th floor absolute displacement
52	flr disp 5	5th floor absolute displacement
53	flr disp 4	4th floor absolute displacement
54	flr disp 3	3rd floor absolute displacement
55	flr disp 2	2nd floor absolute displacement
56	flr disp 1	1st floor absolute displacement
57	na out up	north exterior column uplift, west frame
58	na in up	north interior column uplift, west frame
59	sa in up	south interior column uplift, west frame
60	sa out up	south exterior column uplift, west frame
61	nb out up	north exterior column uplift, east frame
62	sb out up	south exterior column uplift, east frame
63	blank	
64	clflxnaotl	1st flr north ext col flx strain, top, west frame
65	clflxnaobl	1st flr north ext col flx strain, bot, west frame
66	clflxnaitl	1st flr north int col flx strain, top, west frame
67	clflxnaibl	1st flr north int col flx strain, bot, west frame
68	clflxsaitl	1st flr south int col flx strain, top, west frame
69	clflxsaibl	1st flr south int col flx strain, bot, west frame
70	clflxsaotl	1st flr south ext col flx strain, top, west frame
71	clflxsaobl	1st flr south ext col flx strain, bot, west frame
72	clflxnbotl	1st flr north ext col flx strain, top, east frame
73	clflxnbobl	1st flr north ext col flx strain, bot, east frame
74	clflxnbitl	1st flr north int col flx strain, top, east frame
75	clflxnbibl	1st flr north int col flx strain, bot, east frame
76	clflxsbitl	1st flr south int col flx strain, top, east frame
77	clflxsbibl	1st flr south int col flx strain, bot, east frame
78	clflxsbotl	1st flr south ext col flx strain, top, east frame
79	clflxsbobl	1st flr south ext col flx strain, bot, east frame
80	claxnaol	1st flr north ext col ax strain, west frame
81	claxnail	1st flr north int col ax strain, west frame
82	claxsail	1st flr south int col ax strain, west frame
83	claxsaol	1st flr south ext col ax strain, west frame
84	yclflxnaitl	1st flr north int col post-yield flx strain, top
85	yclflxnaibl	1st flr north int col post-yield flx strain, bot
86	yclflxsaitl	1st flr south int col post-yield flx strain, top
87	yclflxsaibl	1st flr south int col post-yield flx strain, bot
88	cldcdtnaool	col dcdt, north face north ext col, 1st flr
89	cldcdtnaoil	col dcdt, south face north ext col, 1st flr
90	cldcdtnaiol	col dcdt, north face north int col, 1st flr
91	cldcdtnaiil	col dcdt, south face north int col, 1st flr
92	cldcdtsaiil	col dcdt, north face south int col, 1st flr
93	cldcdtsaiol	col dcdt, south face south int col, 1st flr
94	cldcdtsaiol	col dcdt, north face south ext col, 1st flr
95	cldcdtsaool	col dcdt, south face south ext col, 1st flr
96	ybmflxnail	1st flr int beam post-yield flx strain, north end
97	ybmflxsail	1st flr int beam post-yield flx strain, south end
98	ybmflxnaol	1st flr n ext beam post-yield flx strain, south end
99	ybmflxsaol	1st flr s ext beam post-yield flx strain north end
100	jtdcdtnat	joint rotation dcdt, north end, top position

101	jtdcdtnab	joint rotation dcdt, north end, bot position
102	jtdcdtsat	joint rotation dcdt, south end, top position
103	jtdcdtsab	joint rotation dcdt, south end, bot position
104	bmflxnail	1st flr int beam flx strain, north end
105	bmflxsail	1st flr int beam flx strain, south end
106	yclflxnaib2	2nd flr north int col post-yield flx strain, bot
107	yclflxsaib2	2nd flr south int col post-yield flx strain, bot
108	bmdcdtnaotl	1st flr n ext beam dcdt, top position, south end
109	bmdcdtnaobl	1st flr n ext beam dcdt, bot position, south end
110	bmdcdtnaitl	1st flr int beam dcdt, top position north end
111	bmdcdtnaibl	1st flr int beam dcdt, bot position north end
112	bmdcdtsaitl	1st flr int beam dcdt, top position south end
113	bmdcdtsaibl	1st flr int beam dcdt, bot position south end
114	bmdcdtsaotl	1st flr s ext beam dcdt, top position, north end
115	bmdcdtsaobl	1st flr s ext beam dcdt, bot position, north end
116	clflxnait2	2nd flr n int col flx strain, top
117	clflxnaib2	2nd flr n int col flx strain, bottom
118	clflxsait2	2nd flr s int col flx strain, top
119	clflxsaib2	2nd flr s int col flx strain, bottom
120	bmdcdtnbitl	1st flr int beam dcdt, east frame, n end top
121	bmdcdtnbibl	1st flr int beam dcdt, east frame, n end bottom
122	bmdcdtsbitl	1st flr int beam dcdt, east frame, s end top
123	bmdcdtsbibl	1st flr int beam dcdt, east frame, s end bottom
124	ybmflxnai2	2nd flr int beam post-yield flx strain, north end
125	ybmflxsai2	2nd flr int beam post-yield flx strain, south end
126	ybmflxnai3	3rd flr int beam post-yield flx strain, north end
127	ybmflxsai3	3rd flr int beam post-yield flx strain, south end

Appendix C

Data Noise Readings

*Data Acquisition time = 3.68 sec. = 140 data/channel

Channel	Max Value	Min Value	Channel	Max Value	Min Value
0	.001 mil/"	-.002 mil/"	51	.006"	-.010"
1	.002 mil/"	-.002 mil/"	52	.018"	-.012"
2	.002 mil/"	-.002 mil/"	53	.009"	-.004"
3	.001 mil/"	-.002 mil/"	54	.023"	-.014"
4	.004"	-.003"	55	.007"	-.006"
5	.001"	-.000	56	.007"	-.007"
6	.005g	-.004g	57	.005"	-.008"
7	.005g	-.004g	58	.005"	-.007"
8	.028r/s/s	-.017r/s/s	59	.006"	-.010"
9	.026r/s/s	-.022r/s/s	60	.025"	-.041"
10	.020r/s/s	-.019r/s/s	61	.009"	-.017"
11	.261 kip	-.281 kip	62	.006"	-.008"
12	.424 kip	-.462 kip	63		
13	.150 kip	-.202g	64	.000 mil/"	-.000 mil/"
14	.006g	-.007g	65	.000 mil/"	-.000 mil/"
15	.006g	-.007g	66	.000 mil/"	-.000 mil/"
16	.001 mil/"	-.002 mil/"	67	.000 mil/"	-.000 mil/"
17	.002 mil/"	-.004 mil/"	68	.000 mil/"	-.000 mil/"
18	.001 mil/"	-.003 mil/"	69	.000 mil/"	-.000 mil/"
19	.002 mil/"	-.003 mil/"	70	.000 mil/"	-.000 mil/"
20	.246 kip	-.221 kip	71	.000 mil/"	-.000 mil/"
21	.293 kip	-.254 kip	72	.000 mil/"	-.000 mil/"
22	.273 kip	-.225 kip	73	.000 mil/"	-.000 mil/"
23	.347 kip	-.316 kip	74	.000 mil/"	-.000 mil/"
24	.000"	-.000"	75	.000 mil/"	-.000 mil/"
25	.000"	-.000"	76	.000 mil/"	-.000 mil/"
26	.000"	-.000"	77	.000 mil/"	-.000 mil/"
27	.000"	-.000"	78	.000 mil/"	-.000 mil/"
28	.003"	-.002"	79	.000 mil/"	-.000 mil/"
29	.003"	-.002"	80	.000 mil/"	-.000 mil/"
30	.002"	-.002"	81	.000 mil/"	-.000 mil/"
31			82	.000 mil/"	-.000 mil/"
32	.050 kip	-.067 kip	83	.000 mil/"	-.000 mil/"
33	.049 kip	-.051 kip	84	.009 mil/"	-.007 mil/"
34	.046 kip	-.057 kip	85	.004 mil/"	-.006 mil/"
35	.054 kip	-.046 kip	86	.004 mil/"	-.003 mil/"
36	.003g	-.004g	87	.006 mil/"	-.005 mil/"
37	.005g	-.005g	88	.000"	-.000"
38	.007g	-.006g	89	.000"	-.000"
39	.006g	-.007g	90	.000"	-.000"
40	.004g	-.004g	91	.000"	-.000"
41	.004g	-.003g	92	.000"	-.000"
42	.004g	-.004g	93	.000"	-.000"
43	.004g	-.004g	94	.000"	-.000"
44	.006g	-.005g	95	.000"	-.000"
45	.003g	-.003g	96	.007 mil/"	-.006 mil/"
46	.003g	-.004g	97	.004 mil/"	-.006 mil/"
47	.001 mil/"	-.002 mil/"	98	.003 mil/"	-.004 mil/"
48	.005"	-.004"	99	.009 mil/"	-.004 mil/"
49	.005"	-.005"	100	.000"	-.000"
50	.003"	-.002"	101	.000"	-.000"

102	.000"	-.000"
103	.000"	-.000"
104	.000 mil/"	-.000 mil/"
105	.000 mil/"	-.000 mil/"
106	.002 mil/"	-.003 mil/"
107	.002 mil/"	-.004 mil/"
108	.000 mil/"	-.000 mil/"
109	.000"	-.000"
110	.000"	-.000"
111	.000"	-.000"
112	.000"	-.000"
113	.000"	-.000"
114	.000"	-.000"
115	.000"	-.000"
116	.000 mil/"	-.000 mil/"
117	.000 mil/"	-.000 mil/"
118	.000 mil/"	-.000 mil/"
119	.000 mil/"	-.000 mil/"
120	.000"	-.000"
121	.000"	-.000"
122	.000"	-.000"
123	.000"	-.000"
124	.002 mil/"	-.003 mil/"
125	.002 mil/"	-.002 mil/"
126	.002 mil/"	-.002 mil/"
127	.003 mil/"	-.003 mil/"

Appendix D

Sequential List of Dynamic Tests Performed on Shaking Table

Sequence #	Data File Name	Source Signal	Span Settings	Uplift Allowed	Comments
1	200477.1	PAC	050/000	yes	excessive torsion noted
2	200477.2	PAC	075/000	yes	" " "
3	200477.3	PAC	100/000	yes	" " "
4	200477.4	EC	050/000	yes	" " "
5	200477.5	EC	100/000	yes	" " "
6	200477.6	EC	200/000	yes	" " "
7	200477.7	EC	300/000	yes	" " "
8	220477.1	PAC	075/000	yes	table twist corrected,
9	220477.2	PAC	100/000	yes	torsion now reduced
10	220477.3	PAC	125/000	yes	
11	250477.1	PAC	050/000	yes	16 mm film (overall)
12	250477.2	PAC	150/000	yes	16 mm film (overall)
13	250477.3	PAC	175/000	yes	16 mm film (overall)
14		PAC	150/000	yes	16 mm film (column base)
15	250477.4	EC	100/000	yes	16 mm film (overall)
16	250477.5	EC	200/000	yes	16 mm film (overall)
17	250477.6	EC	300/000	yes	data lost
18	250477.7	EC	300/000	yes	16 mm film (column base)
19	250477.8	EC	200/000	yes	axial strain gages required
20	250477.9	EC	050/000	yes	
21	250477.10	EC	300/000	yes	16 mm film (column base)
22	250477.11	EC	400/000	yes	
23	250477.12	EC	450/000	yes	
24	250477.13	PAC	050/000	yes	
25	250477.14	PAC	175/000	yes	9th floor weight moved
26	260477.1	PAC	175/000	yes	
27	260477.2	PAC	050/050	yes	
28	260477.3	PAC	075/075	yes	
29	260477.4	PAC	100/100	yes	
30	260477.5	PAC	125/125	yes	
31	260477.6	PAC	150/150	yes	
32	260477.7	PAC	175/175	yes	
33	260477.8	EC	100/100	yes	newly integrated signal
34	260477.9	EC	200/200	yes	
35	260477.10	EC	300/300	yes	1.73*EC 300/300 Uplift
36	260477.11	EC	300/300	yes	1.73*EC 300 Uplift
37	270477.1	EC	050/050	yes	data file erased
38	270477.2	EC	050/000	yes	data file erased
39	280477.1	PAC	050/000	no	
40	280477.2	PAC	100/000	no	
41	280477.3	PAC	125/000	no	16 mm film (overall
42	280477.4	PAC	150/000	no	16 mm film (overall)
43	290477.1	EC	050/000	no	
44	290477.2	EC	100/000	no	
45	290477.3	EC	150/000	no	foundation beam moved
46	290477.4	EC	050/000	no	1.73*EC 050 Fixed Base
47	290477.5	EC	165/000	no	
48	290477.6	EC	180/000	no	
49	290477.7	EC	200/000	no	
50	290477.8	EC	220/000	no	

51	290477.9	EC	240/000	no	
52	290477.10	EC	265/000	no	
53	290477.11	EC	300/000	no	1.73*EC 300 Fixed Base
54	020577.1	PAC	050/000	no	
55	020577.2	PAC	050/050	no	
56	020577.3	EC	050/050	no	
57	020577.4	PAC	165/000	no	
58	020577.5	PAC	180/000	no	
59	020577.6	PAC	210/000	no	
60	020577.7	PAC	230/000	no	
61	020577.8	PAC	250/000	no	1.73*PAC 250 Fixed Base
62	040577.1	EC	050/000	yes	1.73*EC 050 Uplift
63	040577.2	EC	050/050	yes	
64	040577.3	PAC	200/000	yes	1.73*PAC 200 Uplift
65	040577.4	PAC	200/000	yes	videotape made
66		EC	020/000	yes	SEAOC demonstration
67		EC	200/000	yes	SEAOC demonstration

EARTHQUAKE ENGINEERING RESEARCH CENTER REPORTS

EARTHQUAKE ENGINEERING RESEARCH CENTER REPORTS

NOTE: Numbers in parentheses are Accession Numbers assigned by the National Technical Information Service; these are followed by a price code. Copies of the reports may be ordered from the National Technical Information Service, 5285 Port Royal Road, Springfield, Virginia, 22161. Accession Numbers should be quoted on orders for reports (PB--- ---) and remittance must accompany each order. Reports without this information were not available at time of printing. Upon request, EERC will mail inquirers this information when it becomes available.

EERC 67-1 "Feasibility Study of Large-Scale Earthquake Simulator Facility," by J. Penzien, J. G. Bouwkamp, R. W. Clough, and D. Rea - 1967 (PB 187 905)A07

EERC 68-1 Unassigned

EERC 68-2 "Inelastic Behavior of Beam-to-Column Subassemblages under Repeated Loading," by V. V. Bertero - 1968 (PB 184 888)A05

EERC 68-3 "A Graphical Method for Solving the Wave Reflection-Refraction Problem," by H. D. McNiven and Y. Mengi - 1968 (PB 187 943)A03

EERC 68-4 "Dynamic Properties of McKinley School Buildings," by D. Rea, J. G. Bouwkamp, and R. W. Clough - 1968 (PB 187 902)A07

EERC 68-5 "Characteristics of Rock Motions during Earthquakes," by H. B. Seed, I. M. Idriss, and F. W. Kiefer - 1968 (PB 188 338)A03

EERC 69-1 "Earthquake Engineering Research at Berkeley," - 1969 (PB 187 906)A11

EERC 69-2 "Nonlinear Seismic Response of Earth Structures," by M. Dibaj and J. Penzien - 1969 (PB 187 904)A08

EERC 69-3 "Probabilistic Study of the Behavior of Structures during Earthquakes," by R. Ruiz and J. Penzien - 1969 (PB 187 886)A06

EERC 69-4 "Numerical Solution of Boundary Value Problems in Structural Mechanics by Reduction to an Initial Value Formulation," by N. Distefano and J. Schujman - 1969 (PB 187 942)A02

EERC 69-5 "Dynamic Programming and the Solution of the Biharmonic Equation," by N. Distefano - 1969 (PB 187 941)A03

EERC 69-6 "Stochastic Analysis of Offshore Tower Structures," by A. K. Malhotra and J. Penzien - 1969 (PB 187 903)A09

EERC 69-7 "Rock Motion Accelerograms for High Magnitude Earthquakes," by H. B. Seed and I. M. Idriss - 1969 (PB 187 940)A02

EERC 69-8 "Structural Dynamics Testing Facilities at the University of California, Berkeley," by R. M. Stephen, J. G. Bouwkamp, R. W. Clough and J. Penzien - 1969 (PB 189 111)A04

EERC 69-9 "Seismic Response of Soil Deposits Underlain by Sloping Rock Boundaries," by H. Dezfulian and H. B. Seed - 1969 (PB 189 114)A03

EERC 69-10 "Dynamic Stress Analysis of Axisymmetric Structures under Arbitrary Loading," by S. Ghosh and E. L. Wilson - 1969 (PB 189 026)A10

EERC 69-11 "Seismic Behavior of Multistory Frames Designed by Different Philosophies," by J. C. Anderson and V. V. Bertero - 1969 (PB 190 662)A10

EERC 69-12 "Stiffness Degradation of Reinforcing Concrete Members Subjected to Cyclic Flexural Moments," by V. V. Bertero, B. Bresler, and H. Ming Liao - 1969 (PB 202 942)A07

EERC 69-13 "Response of Non-Uniform Soil Deposits to Travelling Seismic Waves," by H. Dezfulian and H. B. Seed - 1969 (PB 191 023)A03

EERC 69-14 "Damping Capacity of a Model Steel Structure," by D. Rea, R. W. Clough, and J. G. Bouwkamp - 1969 (PB 190 663)A06

EERC 69-15 "Influence of Local Soil Conditions on Building Damage Potential during Earthquakes," by H. B. Seed and I. M. Idriss - 1969 (PB 191 036)A03

EERC 69-16 "The Behavior of Sands under Seismic Loading Conditions," by M. L. Silver and H. B. Seed - 1969 (AD 714 982)A07

EERC 70-1 "Earthquake Response of Gravity Dams," by A. K. Chopra - 1970 (AD 709 640)A03

EERC 70-2 "Relationships between Soil Conditions and Building Damage in the Caracas Earthquake of July 29, 1967," by H. B. Seed, I. M. Idriss, and H. Dezfulian - 1970 (PB 195 762)A05

EERC 70-3 "Cyclic Loading of Full Size Steel Connections," by E. P. Popov and R. M. Stephen - 1970 (PB 213 545)A04

EERC 70-4 "Seismic Analysis of the Charaima Building, Caraballeda, Venezuela," by Subcommittee of the SEAONC Research Committee: V. V. Bertero, P. F. Fratessa, S. A. Mahin, J. H. Sexton, A. C. Scordelis, E. L. Wilson, L. A. Wyllie, H. B. Seed, and J. Penzien, Chairman - 1970 (PB 201 455)A06

EERC 70-5 "A Computer Program for Earthquake Analysis of Dams," by A. K. Chopra and P. Chakrabarti - 1970 (AD 723 994)A05

EERC 70-6 "The Propagation of Love Waves Across Non-Horizontally Layered Structures," by J. Lysmer and L. A. Drake - 1970 (PB 197 896)A03

EERC 70-7 "Influence of Base Rock Characteristics on Ground Response," by J. Lysmer, H. B. Seed, and P. B. Schnabel - 1970 (PB 197 897)A03

EERC 70-8 "Applicability of Laboratory Test Procedures for Measuring Soil Liquefaction Characteristics under Cyclic Loading," by H. B. Seed and W. H. Peacock - 1970 (PB 198 016)A03

EERC 70-9 "A Simplified Procedure for Evaluating Soil Liquefaction Potential," by H. B. Seed and I. M. Idriss - 1970 (PB 198 009)A03

EERC 70-10 "Soil Moduli and Damping Factors for Dynamic Response Analysis," by H. B. Seed and I. M. Idriss - 1970 (PB 197 869)A03

EERC 71-1 "Koyna Earthquake of December 11, 1967 and the Performance of Koyna Dam," by A. K. Chopra and P. Chakrabarti - 1971 (AD 731 496)A06

EERC 71-2 "Preliminary In-Situ Measurements of Anelastic Absorption in Soils using a Prototype Earthquake Simulator," by R. D. Borcherdt and P. W. Rodgers - 1971 (PB 201 454)A03

EERC 71-3 "Static and Dynamic Analysis of Inelastic Frame Structures," by F. L. Porter and G. H. Powell - 1971 (PB 210 135)A06

EERC 71-4 "Research Needs in Limit Design of Reinforced Concrete Structures," by V. V. Bertero - 1971 (PB 202 943)A04

EERC 71-5 "Dynamic Behavior of a High-Rise Diagonally Braced Steel Building," by D. Rea, A. A. Shah, and J. G. Bouwkamp - 1971 (PB 203 584)A06

EERC 71-6 "Dynamic Stress Analysis of Porous Elastic Solids Saturated with Compressible Fluids," by J. Ghaboussi and E. L. Wilson - 1971 (PB 211 396)A06

EERC 71-7 "Inelastic Behavior of Steel Beam-to-Column Subassemblages," by H. Krawinkler, V. V. Bertero, and E. P. Popov - 1971 (PB 211 355)A14

EERC 71-8 "Modification of Seismograph Records for Effects of Local Soil Conditions," by P. Schnabel, H. B. Seed, and J. Lysmer - 1971 (PB 214 450)A03

EERC 72-1 "Static and Earthquake Analysis of Three Dimensional Frame and Shear Wall Buildings," by E. L. Wilson and H. H. Dovey - 1972 (PB 212 904)A05

EERC 72-2 "Accelerations in Rock for Earthquakes in the Western United States," by P. B. Schnabel and H. B. Seed - 1972 (PB 213 100)A03

EERC 72-3 "Elastic-Plastic Earthquake Response of Soil-Building Systems," by T. Minami - 1972 (PB 214 868)A08

EERC 72-4 " Stochastic Inelastic Response of Offshore Towers to Strong Motion Earthquakes," by M. K. Kaul - 1972 (PB 215 713)A05

EERC 72-5 "Cyclic Behavior of Three Reinforced Concrete Flexural Members with High Shear," by E. P. Popov, V. V. Bertero, and H. Krawinkler - 1972 (PB 214 555)A05

EERC 72-6 "Earthquake Response of Gravity Dams Including Reservoir Interaction Effects," by P. Chakrabarti and A. K. Chopra - 1972 (AD 762 330)A08

EERC 72-7 "Dynamic Properties of Pine Flat Dam," by D. Rea, C. Y. Liaw, and A. K. Chopra - 1972 (AD 763 928)A05

EERC 72-8 "Three Dimensional Analysis of Building Systems," by E. L. Wilson and H. H. Dovey - 1972 (PB 222 438)A06

EERC 72-9 "Rate of Loading Effects on Uncracked and Repaired Reinforced Concrete Members," by S. Mahin, V. V. Bertero, D. Rea and M. Atalay - 1972 (PB 224 520)A08

EERC 72-10 "Computer Program for Static and Dynamic Analysis of Linear Structural Systems," by E. L. Wilson, K.-J. Bathe, J. E. Peterson and H. H. Dovey - 1972 (PB 220 437)A04

EERC 72-11 "Literature Survey - Seismic Effects on Highway Bridges," by T. Iwasaki, J. Penzien, and R. W. Clough - 1972 (PB 215 613)A19

EERC 72-12 "SHAKE - A Computer Program for Earthquake Response Analysis of Horizontally Layered Sites," by P. B. Schnabel and J. Lysmer - 1972 (PB 220 207)A06

EERC 73-1 "Optimal Seismic Design of Multistory Frames," by V. V. Bertero and H. Kamil - 1973

EERC 73-2 "Analysis of the Slides in the San Fernando Dams during the Earthquake of February 9, 1971," by H. B. Seed, K. L. Lee, I. M. Idriss, and F. Makdisi - 1973 (PB 223 402)A14

EERC 73-3 "Computer Aided Ultimate Load Design of Unbraced Multistory Steel Frames," by M. B. El-Hafez and G. H. Powell - 1973 (PB 248 315)A09

EERC 73-4 "Experimental Investigation into the Seismic Behavior of Critical Regions of Reinforced Concrete Components as Influenced by Moment and Shear," by M. Celebi and J. Penzien - 1973 (PB 215 884)A09

EERC 73-5 "Hysteretic Behavior of Epoxy-Repaired Reinforced Concrete Beams," by M. Celebi and J. Penzien - 1973 (PB 239 568)A03

EERC 73-6 "General Purpose Computer Program for Inelastic Dynamic Response of Plane Structures," by A. Kanaan and G. H. Powell - 1973 (PB 221 260)A08

EERC 73-7 "A Computer Program for Earthquake Analysis of Gravity Dams Including Reservoir Interaction," by P. Chakrabarti and A. K. Chopra - 1973 (AD 766 271)A04

EERC 73-8 "Behavior of Reinforced Concrete Deep Beam-Column Subassemblages under Cyclic Loads," by O. Küstü and J. G. Bouwkamp - 1973 (PB 246 117)A12

EERC 73-9 "Earthquake Analysis of Structure-Founation Systems," by A. K. Vaish and A. K. Chopra - 1973 (AD 766 272)A07

EERC 73-10 "Deconvolution of Seismic Response for Linear Systems," by R. B. Reimer - 1973 (PB 227 179)A08

EERC 73-11 "SAP IV: A Structural Analysis Program for Static and Dynamic Response of Linear Systems," by K.-J. Bathe, E. L. Wilson, and F. E. Peterson - 1973 (PB 221 967)A09

EERC 73-12 "Analytical Investigations of the Seismic Response of Long, Multiple Span Highway Bridges," by W. S. Tseng and J. Penzien - 1973 (PB 227 816)A10

EERC 73-13 "Earthquake Analysis of Multi-Story Buildings Including Foundation Interaction," by A. K. Chopra and J. A. Gutierrez - 1973 (PB 222 970)A03

EERC 73-14 "ADAP: A Computer Program for Static and Dynamic Analysis of Arch Dams," by R. W. Clough, J. M. Raphael, and S. Mojtahedi - 1973 (PB 223 763)A09

EERC 73-15 "Cyclic Plastic Analysis of Structural Steel Joints," by R. B. Pinkney and R. W. Clough - 1973 (PB 226 843)A08

EERC 73-16 "QUAD-4: A Computer Program for Evaluating the Seismic Response of Soil Structures by Variable Damping Finite Element Procedures," by I. M. Idriss, J. Lysmer, R. Hwang, and H. B. Seed - 1973 (PB 229 424)A05

EERC 73-17 "Dynamic Behavior of a Multi-Story Pyramid Shaped Building," by R. M. Stephen, J. P. Hollings, and J. G. Bouwkamp - 1973 (PB 240 718)A06

EERC 73-18 "Effect of Different Types of Reinforcing on Seismic Behavior of Short Concrete Columns," by V. V. Bertero, J. Hollings, O. Küstü, R. M. Stephen, and J. G. Bouwkamp - 1973

EERC 73-19 "Olive View Medical Center Materials Studies, Phase I," by B. Bresler and V. V. Bertero - 1973 (PB 235 986)A06

EERC 73-20 "Linear and Nonlinear Sesismic Analysis Computer Programs for Long Multiple-Span Highway Bridges," by W. S. Tseng and J. Penzien - 1973

EERC 73-21 "Constitutive Models for Cyclic Plastic Deformation of Engineering Materials," by J. M. Kelly and P. P. Gillis - 1973 (PB 226 024)A03

EERC 73-22 "DRAIN-2D User's Guide," by G. H. Powell - 1973 (PB 227 016)A05

EERC 73-23 "Earthquake Engineering at Berkeley - 1973 " 1973 (PB 226 033)A11

EERC 73-24 Unassigned

EERC 73-25 "Earthquake Response of Axisymmetric Tower Structures Surrounded by Water," by C. Y. Liaw and A. K. Chopra - 1973 (AD 773 052)A09

EERC 73-26 "Investigation of the Failures of the Olive View Stairtowers during the San Fernando Earthquake and Their Implications on Seismic Design," by V. V. Bertero and R. G. Collins - 1973 (PB 235 106)A13

EERC 73-27 "Further Studies on Seismis Behavior of Steel Beam-Column Subassemblages," by V. V. Bertero, H. Krawinkler, and E. P. Popov - 1973 (PB 234 172)A06

EERC 74-1 "Seismic Risk Analysis," by C. S. Oliveira - 1974 (PB 235 920)A06

EERC 74-2 "Settlement and Liquefaction of Sands under Multi-Directional Shaking," by R. Pyke, C. K. Chan, and H. B. Seed - 1974

EERC 74-3 "Optimum Design of Earthquake Resistant Shear Buildings," by D. Ray, K. S. Pister, and A. K. Chopra - 1974 (PB 231 172)A06

EERC 74-4 "LUSH - A Computer Program for Complex Response Analysis of Soil-Structure Systems," by J. Lysmer, T. Udaka, H. B. Seed, and R. Hwang - 1974 (PB 236 796)A05

EERC 74-5 "Sensitivity Analysis for Hysteretic Dynamic Systems: Applications to Earthquake Engineering," by D. Ray - 1974 (PB 233 213)A06

EERC 74-6 "Soil Structure Interaction Analyses for Evaluating Seismic Response," by H. B. Seed, J. Lysmer, and R. Hwang - 1974 (PB 236 519)A04

EERC 74-7 Unassigned

EERC 74-8 "Shaking Table Tests of a Steel Frame - A Progress Report," by R. W. Clough and D. Tang - 1974 (PB 240 869)A03

EERC 74-9 "Hysteretic Behavior of Reinforced Concrete Flexural Members with Special Web Reinforcement," by V. V. Bertero, E. P. Popov, and T. Y. Wang - 1974 (PB 236 797)A07

EERC 74-10 "Applications of Realiability-Based, Global Cost Optimization to Design of Earthquake Resistant Structures," by E. Vitiello and K. S. Pister - 1974 (PB 237 231)A06

EERC 74-11 "Liquefaction of Gravelly Soils under Cyclic Loading Conditions," by R. T. Wong, H. B. Seed, and C. K. Chan - 1974 (PB 242 042)A03

EERC 74-12 "Site-Dependent Spectra for Earthquake-Resistant Design," by H. B. Seed, C. Ugas, and J. Lysmer - 1974 (PB 240 953)A03

EERC 74-13 "Earthquake Simulator Study of a Reinforced Concrete Frame," by P. Hidalgo and R. W. Clough - 1974 (PB 241 944)A13

EERC 74-14 "Nonlinear Earthquake Response of Concrete Gravity Dams," by N. Pal - 1974 (AD/A 006 583)A06

EERC 74-15 "Modeling and Identification in Nonlinear Structural Dynamics - I. One Degree of Freedom Models," by N. Distefano and A. Rath - 1974 (PB 241 548)A06

EERC 75-1 "Determination of Seismic Design Criteria for the Dumbarton Bridge Replacement Structure, Vol. I: Description, Theory and Analytical Modeling of Bridge and Parameters," by F. Baron and S.-H. Pang - 1975 (PB 259 407)A15

EERC 75-2 "Determination of Seismic Design Criteria for the Dumbarton Bridge Replacement Structure, Vol. II: Numerical Studies and Establishment of Seismic Design Criteria," by F. Baron and S.-H. Pang - 1975 (PB 259 408)A11 [For set of EERC 75-1 and 75-2 (PB 241 454)A09]

EERC 75-3 "Seismic Risk Analysis for a Site and a Metropolitan Area," by C. S. Oliveira - 1975 (PB 248 134)A09

EERC 75-4 "Analytical Investigations of Seismic Response of Short, Single or Multiple-Span Highway Bridges," by M.-C. Chen and J. Penzien - 1975 (PB 241 454)A09

EERC 75-5 "An Evaluation of Some Methods for Predicting Seismic Behavior of Reinforced Concrete Buildings," by S. A. Mahin and V. V. Bertero - 1975 (PB 246 306)A16

EERC 75-6 "Earthquake Simulator Story of a Steel Frame Structure, Vol. I: Experimental Results," by R. W. Clough and D. T. Tang - 1975 (PB 243 981)A13

EERC 75-7 "Dynamic Properties of San Bernardino Intake Tower," by D. Rea, C.-Y Liaw and A. K. Chopra - 1975 (AD/A 008 406)A05

EERC 75-8 "Seismic Studies of the Articulation for the Dumbarton Bridge Replacement Structure, Vol. 1: Description, Theory and Analytical Modeling of Bridge Components," by F. Baron and R. E. Hamati - 1975 (PB 251 539)A07

EERC 75-9 "Seismic Studies of the Articulation for the Dumbarton Bridge Replacement Structure, Vol. 2: Numerical Studies of Steel and Concrete Girder Alternates," by F. Baron and R. E. Hamati - 1975 (PB 251 540)A10

EERC 75-10 "Static and Dynamic Analysis of Nonlinear Structures," by D. P. Mondkar and G. H. Powell - 1975 (PB 242 434)A08

EERC 75-11 "Hysteretic Behavior of Steel Columns," by E. P. Popov, V. V. Bertero, and S. Chandramouli - 1975 (PB 252 365)A11

EERC 75-12 "Earthquake Engineering Research Center Library Printed Catalog " - 1975 (PB 243 711)A26

EERC 75-13 "Three Dimensional Analysis of Building Systems (Extended Version)," by E. L. Wilson, J. P. Hollings, and H. H. Dovey - 1975 (PB 243 989)A07

EERC 75-14 "Determination of Soil Liquefaction Characteristics by Large-Scale Laboratory Tests," by P. De Alba, C. K. Chan, and H. B. Seed - 1975 (NUREG 0027)A08

EERC 75-15 "A Literature Survey - Compressive, Tensile, Bond and Shear Strength of Masonry," by R. L. Mayes and R. W. Clough - 1975 (PB 246 292)A10

EERC 75-16 "Hysteretic Behavior of Ductile Moment-Resisting Reinforced Concrete Frame Components," by V. V. Bertero and E. P. Popov - 1975 (PB 246 388)A05

EERC 75-17 "Relationships Between Maximum Acceleration, Maximum Velocity, Distance from Source, Local Site Conditions for Moderately Strong Earthquakes," by H. B. Seed, R. Murarka, J. Lysmer, and I. M. Idriss - 1975 (PB 248 172)A03

EERC 75-18 "The Effects of Method of Sample Preparation on the Cyclic Stress-Strain Behavior of Sands," by J. Mulilis, C. K. Chan, and H. B. Seed - 1975 (Summarized in EERC 75-28)

EERC 75-19 "The Seismic Behavior of Critical Regions of Reinforced Concrete Components as Influenced by Moment, Shear and Axial Force," by M. B. Atalay and J. Penzien - 1975 (PB 258 842)A11

EERC 75-20 "Dynamic Properties of an Eleven Story Masonry Building," by R. M. Stephen, J. P. Hollings, J. G. Bouwkamp, and D. Jurukovski - 1975 (PB 246 945)A04

EERC 75-21 "State-of-the-Art in Seismic Strength of Masonry - An Evaluation and Review," by R. L. Mayes and R. W. Clough - 1975 (PB 249 040)A07

EERC 75-22 "Frequency Dependent Stiffness Matrices for Viscoelastic Half-Plane Foundations," by A. K. Chopra, P. Chakrabarti, and G. Dasgupta - 1975 (PB 248 121)A07

EERC 75-23 "Hysteretic Behavior of Reinforced Concrete Framed Walls," by T. Y. Wang, V. V. Bertero, and E. P. Popov - 1975

EERC 75-24 "Testing Facility for Subassemblages of Frame-Wall Structural Systems," by V. V. Bertero, E. P. Popov, and T. Endo - 1975

EERC 75-25 "Influence of Seismic History on the Liquefaction Characteristics of Sands," by H. B. Seed, K. Mori, and C. K. Chan - 1975 (Summarized in EERC 75-28)

EERC 75-26 "The Generation and Dissipation of Pore Water Pressures during Soil Liquefaction," by H. B. Seed, P. P. Martin, and J. Lysmer - 1975 (PB 252 648)A03

EERC 75-27 "Identification of Research Needs for Improving Aseismic Design of Building Structures," by V. V. Bertero - 1975 (PB 248 136)A05

EERC 75-28 "Evaluation of Soil Liquefaction Potential during Earthquakes," by H. B. Seed, I. Arango, and C. K. Chan - 1975 (NUREG 0026)A13

EERC 75-29 "Representation of Irregular Stress Time Histories by Equivalent Uniform Stress Series in Liquefaction Analyses," by H. B. Seed, I. M. Idriss, F. Makdisi, and N. Banerjee - 1975 (PB 252 635)A03

EERC 75-30 "FLUSH - A Computer Program for Approximate 3-D Analysis of Soil-Structure Interaction Problems," by J. Lysmer, T. Udaka, C.-F. Tsai, and H. B. Seed - 1975 (PB 259 332)A07

EERC 75-31 "ALUSH - A Computer Program for Seismic Response Analysis of Axisymmetric Soil-Structure Systems," by E. Berger, J. Lysmer, and H. B. Seed - 1975

EERC 75-32 "TRIP and TRAVEL - Computer Programs for Soil-Structure Interaction Analysis with Horizontally Travelling Waves," by T. Udaka, J. Lysmer, and H. B. Seed - 1975

EERC 75-33 "Predicting the Performance of Structures in Regions of High Seismicity," by J. Penzien - 1975 (PB 248 130)A03

EERC 75-34 "Efficient Finite Element Analysis of Seismic Structure-Soil-Direction," by J. Lysmer, H. B. Seed, T. Udaka, R. N. Hwang, and C.-F. Tsai - 1975 (PB 253 570)A03

EERC 75-35 "The Dynamic Behavior of a First Story Girder of a Three-Story Steel Frame Subjected to Earthquake Loading," by R. W. Clough and L.-Y. Li - 1975 (PB 248 841)A05

EERC 75-36 "Earthquake Simulator Story of a Steel Frame Structure, Volume II - Analytical Results," by D. T. Tang - 1975 (PB 252 926)A10

EERC 75-37 "ANSR-I General Purpose Computer Program for Analysis of Non-Linear Structural Response," by D. P. Mondkar and G. H. Powell - 1975 (PB 252 386)A08

EERC 75-38 "Nonlinear Response Spectra for Probabilistic Seismic Design and Damage Assessment of Reinforced Concrete Structures," by M. Murakami and J. Penzien - 1975 (PB 259 530)A05

EERC 75-39 "Study of a Method of Feasible Directions for Optimal Elastic Design of Frame Structures Subjected to Earthquake Loading," by N. D. Walker and K. S. Pister - 1975 (PB 247 781)A06

EERC 75-40 "An Alternative Representation of the Elastic-Viscoelastic Analogy," by G. Dasgupta and J. L. Sackman - 1975 (PB 252 173)A03

EERC 75-41 "Effect of Multi-Directional Shaking on Liquefaction of Sands," by H. B. Seed, R. Pyke, and G. R. Martin - 1975 (PB 258 781)A03

EERC 76-1 "Strength and Ductility Evaluation of Existing Low-Rise Reinforced Concrete Buildings - Screening Method," by T. Okada and B. Bresler - 1976 (PB 257 906)A11

EERC 76-2 "Experimental and Analytical Studies on the Hysteretic Behavior of Reinforced Concrete Rectangular and T-Beams," by S.-Y. M. Ma, E. P. Popov, and V. V. Bertero - 1976 (PB 260 843)A12

EERC 76-3 "Dynamic Behavior of a Multistory Triangular-Shaped Building," by J. Petrovski, R. M. Stephen, E. Gartenbaum, and J. G. Bouwkamp - 1976

EERC 76-4 "Earthquake Induced Deformations of Earth Dams," by N. Serff and H. B. Seed - 1976

EERC 76-5 "Analysis and Design of Tube-Type Tall Building Structures," by H. de Clercq and G. H. Powell - 1976 (PB 252 220)A10

EERC 76-6 "Time and Frequency Domain Analysis of Three-Dimensional Ground Motions,San Fernando Earthquake," by T. Kubo and J. Penzien - 1976 (PB 260 556)A11

EERC 76-7 "Expected Performance of Uniform Building Code Design Masonry Structures," by R. L. Mayes, Y. Omote, S. W. Chen, and R. W. Clough - 1976

EERC 76-8 "Cyclic Shear Tests on Concrete Masonry Piers, Part I - Test Results," by R. L. Mayes, Y. Omote, and R. W. Clough - 1976 (PB 264 424)A06

EERC 76-9 "A Substructure Method for Earthquake Analysis of Structure-Soil Interaction," by J. A. Gutierrez and A. K. Chopra - 1976 (PB 247 783)A08

EERC 76-10 "Stabilization of Potentially Liquefiable San Deposits using Gravel Drain Systems," by H. B. Seed and J. R. Booker - 1976 (PB 248 820)A04

EERC 76-11 "Influence of Design and Analysis Assumptions on Computed Inelastic Response of Moderately Tall Frames," by G. H. Powell and D. G. Row - 1976

EERC 76-12 "Sensitivity Analysis for Hysteretic Dynamic Systems: Theory and Applications," by D. Ray, K. S. Pister, and E. Polak - 1976 (PB 262 859)A04

EERC 76-13 "Coupled Lateral Torsional Response of Buildings to Ground Shaking," by C. L. Kan and A. K. Chopra - 1976 (PB 257 907)A09

EERC 76-14 "Seismic Analyses of the Banco de America," by V. V. Bertero, S. A. Mahin, and J. A. Hollings - 1976

EERC 76-15 "Reinforced Concrete Frame 2: Seismic Testing and Analytical Correlation," by R. W. Clough and J. Gidwani - 1976 (PB 261 323)A08

EERC 76-16 "Cyclic Shear Tests on Masonry Piers, Part II - Analysis of Test Results," by R. L. Mayes, Y. Omote, and R. W. Clough - 1976

EERC 76-17 "Structural Steel Bracing Systems: Behavior under Cyclic Loading," by E. P. Popov, K. Takanashi, and C. W. Roeder - 1976 (PB 260 715)A05

EERC 76-18 "Experimental Model Studies on Seismic Response of High Curved Overcrossings," by D. Williams and W. G. Godden - 1976

EERC 76-19 "Effects of Non-Uniform Seismic Disturbances on the Dumbarton Bridge Replacement Structure," by F. Baron and R. E. Hamati - 1976

EERC 76-20 "Investigation of the Inelastic Characteristics of a Single Story Steel Structure using System Identification and Shaking Table Experiments," by V. C. Matzen and H. D. McNiven - 1976 (PB 258 453)A07

EERC 76-21 "Capacity of Columns with Splice Imperfections," by E. P. Popov, R. M. Stephen and R. Philbrick - 1976 (PB 260 378)A04

EERC 76-22 "Response of the Olive View Hospital Main Building during the San Fernando Earthquake," by S. A. Mahin, V. V. Bertero, A. K. Chopra, and R. Collins," - 1976

EERC 76-23 "A Study on the Major Factors Influencing the Strength of Masonry Prisms," by N. M. Mostaghel, R. L. Mayes, R. W. Clough, and S. W. Chen - 1976

EERC 76-24 "GADFLEA - A Computer Program for the Analysis of Pore Pressure Generation and Dissipation during Cyclic or Earthquake Loading," by J. R. Booker, M. S. Rahman, and H. B. Seed - 1976 (PB 263 947)A04

EERC 76-25 "Rehabilitation of an Existing Building: A Case Study," by B. Bresler and J. Axley - 1976

EERC 76-26 "Correlative Investigations on Theoretical and Experimental Dynamic Behavior of a Model Bridge Structure," by K. Kawashima and J. Penzien - 1976 (PB 263 388)A11

EERC 76-27 "Earthquake Response of Coupled Shear Wall Buildings," by T. Srichatrapimuk - 1976 (PB 265 157)A07

EERC 76-28 "Tensile Capacity of Partial Penetration Welds," by E. P. Popov and R. M. Stephen - 1976 (PB 262 899)A03

EERC 76-29 "Analysis and Design of Numerical Integration Methods in Structural Dynamics," by H. M. Hilber - 1976 (PB 264 410)A06

EERC 76-30 "Contribution of a Floor System to the Dynamic Characteristics of Reinforced Concrete Buildings," by L. E. Malik and V. V. Bertero - 1976

EERC 76-31 "The Effects of Seismic Disturbances on the Golden Gate Bridge," by F. Baron, M. Arikan, R. E. Hamati - 1976

EERC 76-32 "Infilled Frames in Earthquake-Resistant Construction," by R. E. Klingner and V. V. Bertero - 1976 (PB 265 892)A13

UCB/EERC-77/01 "PLUSH - A Computer Program for Probabilistic Finite Element Analysis of Seismic Soil-Structure Interaction," by M. P. Romo Organista, J. Lysmer, and H. B. Seed - 1977

UCB/EERC-77/02 "Soil-Structure Interaction Effects at the Humboldt Bay Power Plant in the Ferndale Earthquake of June 7, 1975," by J. E. Valera, H. B. Seed, C.-F. Tsai, and J. Lysmer - 1977 (B 265 795)A04

UCB/EERC-77/03 "Influence of Sample Disturbance on Sand Response to Cyclic Loading," by K. Mori, H. B. Seed, and C. K. Chan - 1977 (PB 267 352)A04

UCB/EERC-77/04 "Seismological Studies of Strong Motion Records," by J. Shoja-Taheri - 1977 (PB 269 655)A10

UCB/EERC-77/05 "Testing Facility for Coupled Shear Walls," by L.-H. Lee, V. V. Bertero, and E. P. Popov - 1977

UCB/EERC-77/06 "Developing Methodologies for Evaluating the Earthquake Safety of Existing Buildings," No. 1 - B. Bresler; No. 2 - B. Bresler, T. Okada, and D. Zisling; No. 3 - T. Okada and B. Bresler; No. 4 - V. V. Bertero and B. Bresler - 1977 (PB 267 354)A08

UCB/EERC-77/07 "A Literature Survey - Transverse Strength of Masonry Walls," by Y. Omote, R. L. Mayes, S. W. Chen, and R. W. Clough - 1977

UCB/EERC-77/08 "DRAIN-TABS: A Computer Program for Inelastic Earthquake Response of Three Dimensional Buildings," by R. Guendelman-Israel and G. H. Powell - 1977

UCB/EERC-77/09 "SUBWALL: A Special Purpose Finite Element Computer Program for Practical Elastic Analysis and Design of Structural Walls with Substructure Option," by D. Q. Le, H. Petersson, and E. P. Popov - 1977

UCB/EERC-77/10 "Experimental Evaluation of Seismic Design Methods for Broad Cylindrical Tanks," by D. P. Clough - 1977

UCB/EERC-77/11 "Earthquake Engineering Research at Berkeley - 1976," - 1977

UCB/EERC-77/12 "Automated Design of Earthquake Resistant Multistory Steel Building Frames," by N. D. Walker, Jr. - 1977

UCB/EERC-77/13 "Concrete Confined by Rectangular Hoops and Subjected to Axial Loads," by J. Vallenas, V. V. Bertero, and E. P. Popov - 1977

UCB/EERC-77/14 "Seismic Strain Induced in the Ground during Earthquakes," by Y. Sugimura - 1977

UCB/EERC-77/15 "Bond Deterioration under Generalized Loading," by V. V. Bertero, E. P. Popov, and S. Viwathanatepa - 1977

UCB/EERC-77/16 "Computer-Aided Optimum Design of Ductile Reinforced Concrete Moment-Resisting Frames," by S. W. Zagajeski and V. V. Bertero - 1977

UCB/EERC-77/17 "Earthquake Simulation Testing of a Stepping Frame with Energy-Absorbing Devices," by J. M. Kelly and D. F. Tsztoo - 1977

UCB/EERC-77/18 "Inelastic Behavior of Eccentrically Braced Steel Frames under Cyclic Loadings," by C. W. Roeder and E. P. Popov - 1977

UCB/EERC-77/19 "A Simplified Procedure for Estimating Earthquake-Induced Deformation in Dams and Embankments," by F. I. Makdisi and H. B. Seed - 1977

UCB/EERC-77/20 "The Performance of Earth Dams during Earthquakes," by H. B. Seed, F. I. Makdisi, and P. de Alba - 1977

UCB/EERC-77/21 "Dynamic Plastic Analysis Using Stress Resultant Finite Element Formulation," by P. Lukkunapvasit and J.M. Kelly 1977

UCB/EERC-77/22 "Preliminary Experimental Study of Seismic Uplift of a Steel Frame," by R.W. Clough and A.A. Huckelbridge - 1977

UCB/EERC-77/23 "Earthquake Simulator Tests of a Nine-Story Steel Frame with Columns Allowed to Uplift," by A.A. Huckelbridge - 1977

UCB/EERC-77/24 "Nonlinear Soil-Structure Interaction of Skew Highway Bridges," by M.-C. Chen and Joseph Penzien - 1977

UCB/EERC-77/25 "Seismic Analysis of an Offshore Structure Supported on Pile Foundations," by D.D.-N. Liou - 1977

UCB/EERC-77/26 "Dynamic Stiffness Matrices for Homogeneous Viscoelastic Half-Planes," by G. Dasgupta and A.K. Chopra - 1977

UCB/EERC-77/27 "A Practical Soft Story Earthquake Isolation System," by J.M. Kelly and J.M. Eidinger - 1977